INTER-AMERICAN TROPICAL TUNA COMMISSION

SCIENTIFIC ADVISORY COMMITTEE

FOURTH MEETING

La Jolla, California (USA)
29 April - 3 May 2013

DOCUMENT SAC-04-05a

STATUS OF BIGEYE TUNA IN THE EASTERN PACIFIC OCEAN IN 2012 AND OUTLOOK FOR THE FUTURE

Alexandre Aires-da-Silva and Mark N. Maunder

CONTENTS

1. SUMMARY

This report presents the most current stock assessment of bigeye tuna (*Thunnus obesus*) in the eastern Pacific Ocean (EPO). An integrated statistical age-structured stock assessment model (Stock Synthesis 3) was used in the assessment.

Bigeye tuna are distributed across the Pacific Ocean, but the bulk of the catch is made to the east and to the west. The purse-seine catches of bigeye are substantially lower close to the western boundary (150ºW) of the EPO; the longline catches are more continuous, but relatively low between 160ºW and 180Wº. Bigeye are not often caught by purse seiners in the EPO north of 10ºN, but a substantial portion of the longline catches of bigeye in the EPO is made north of that parallel. It is likely that there is a continuous stock throughout the Pacific Ocean, with exchange of individuals at local levels. The assessment is conducted as if there were a single stock of bigeye in the EPO, and there is minimal net movement of fish between the EPO and the western and central Pacific Ocean. Its results are consistent with the results of other analyses of bigeye tuna on a Pacific-wide basis. Data from recent tagging programs, which will help to provide estimates of movement between the EPO and the western and central Pacific Ocean, are being collected and analyzed.

The assessment assumptions have been improved since the previous full assessment conducted in 2010, which had already been modified following the recommendations of the external review of the IATTC staff's assessment of bigeye tuna, held in May 2010. The current bigeye assessment includes several improvements. First of all, a new Richards growth curve estimated externally from an integrated analysis of otolith age-readings and tag-recapture observations was introduced. This curve reduced in particular the uncertainty about the average size of the oldest fish (L_2 parameter). In addition, the parameters which determine the variance of the length-at-age were also taken from the new externally-derived growth estimates. Diagnostic analyses with the previous base case model configuration indicated a dominant influence of the size-composition data in determining the productivity (the R_0 parameter) of the bigeye

stock, and conflicts among datasets were also found. As a result, improvements were made in the current assessment on the weighting assigned to the different datasets. Specifically, the size-composition data of all fisheries were down-weighted. In addition, the number of catch per unit of effort (CPUE) data series used as indices of abundance was reduced in order to minimize conflict trends among data sets. Rather than fitting to a total of ten CPUE series (two purse-seine indices and eight longline indices), a reduced set of indices of abundance was chosen to best represent the bigeye stock trends (the early and late periods of the Central and Southern longline fisheries).

The stock assessment requires a substantial amount of information. Data on retained catch, discards, CPUE, and size compositions of the catches from several different fisheries have been analyzed. Several assumptions regarding processes such as growth, recruitment, movement, natural mortality, and fishing mortality, have also been made. Catch and CPUE data for the surface fisheries have been updated, and include new data for 2012. New or updated longline catch data are available for China (2009 and 2011), Chinese Taipei (2009-2011), Japan (2009-2011), Korea (2011), the United States (2010-2011), and Vanuatu (2005-2011). Longline catch data for 2012 are available for China, Chinese Taipei, Japan, Korea, and Vanuatu from the monthly report statistics. New or updated CPUE data are available for the Japanese longline fleet (2009-2011). New purse-seine length-frequency data are available for 2012 and updates are available for 2011. New or updated length-frequency data are available for the Japanese longline fleet (2006-2011). A prominent feature in the time series of estimated bigeye recruitment is that the highest recruitment peaks of 1983 and 1998 coincide with the strongest El Niño events during the historic period of the assessment. There was a period of above-average annual recruitment during 1994-1998, followed by a period of below-average recruitment in 1999-2000. The recruitments were above average from 2001 to 2006, and were particularly strong in 2005. More recently, the recruitments were below average during 2007-2009, and have fluctuated around average during 2010-2012. The most recent annual recruitment estimate (2012) is slightly below average levels. However, this estimate is highly uncertain, and should be regarded with caution, due to the fact that recently-recruited bigeye are represented in only a few length-frequency data sets.

There have been important changes in the amount of fishing mortality caused by the fisheries that catch bigeye tuna in the EPO. On average, since 1993 the fishing mortality of bigeye less than about 15 quarters old has increased substantially, and that of fish more than about 15 quarters old has also increased, but to a lesser extent. The increase in the fishing mortality of the younger fish was caused by the expansion of the purse-seine fisheries that catch tuna in association with floating objects. It is clear that the longline fishery had the greatest impact on the stock prior to 1995, but with the decrease in longline effort and the expansion of the floating-object fishery, at present the impact of the purse-seine fishery on the bigeye stock is far greater than that of the longline fishery. The discarding of small bigeye has a small, but detectable, impact on the depletion of the stock.

Over the range of spawning biomasses estimated by the base case assessment, the abundance of bigeye recruits appears to be unrelated to the spawning potential of adult females at the time of hatching.

Since the start of 2005, the spawning biomass ratio (SBR; the ratio of the spawning biomass at that time to that of the unfished stock) gradually increased, to a level of 0.31 at the start of 2010. This may be attributed to a combined effect of a series of above-average recruitments since 2001, the IATTC tuna conservation resolutions during 2004-2009, and decreased longline fishing effort in the EPO. However, although the resolutions have continued to date, the rebuilding trend was not sustained, and the SBR gradually declined to a low historic level of 0.22 at the start of 2013. This decline could be related to a period dominated by below-average recruitments that began in late 2007 and coincides with a series of particularly strong la Niña events.

At the beginning of January 2013, the spawning biomass of bigeye tuna in the EPO appears to have been about 8% higher than S_{MSY}, and the recent catches are estimated to have been about 3% lower than the maximum sustainable yield (MSY). If fishing mortality is proportional to fishing effort, and the current patterns of age-specific selectivity are maintained, F_{MSY} is about 5% higher than the current level of effort.

According to the base case results, the most recent estimate indicates that the bigeye stock in the EPO is likely not overfished ($S>S_{MSY}$) and that overfishing is not taking place ($F<F_{MSY}$). In fact, the current exploitation is very close to the MSY target reference points. Likewise, interim limit reference points (0.5 S_{MSY} and 1.3 F_{MSY}) have not been exceeded under the current base case model. These interpretations, however, are subject to uncertainty, as indicated by the approximate confidence intervals around the most recent estimate in the phase plots. Also, they are strongly dependent on the assumptions made about the steepness parameter of the stock-recruitment relationship, the assumed levels of adult natural mortality, and the weighting assigned to the size-composition data.

The MSY of bigeye in the EPO could be maximized if the age-specific selectivity pattern were similar to that of the longline fisheries, because they catch larger individuals that are close to the critical weight. Before the expansion of the floating-object fishery that began in 1993, the MSY was greater than the current MSY and the fishing mortality was much less than F_{MSY}.

At current levels of fishing mortality, and if recent levels of effort and catchability continue and average recruitment levels persist, the SBR is predicted to further decline, to an historic low of 0.19 by 2015. After that, the SBR is predicted to gradually increase, and stabilize at about 0.21 around 2018, slightly above to the level corresponding to MSY (0.20). If a stock-recruitment relationship is assumed, it is estimated that catches will be lower in the future at current levels of fishing effort, particularly for the surface fisheries.

These simulations are based on the assumption that selectivity and catchability patterns will not change in the future. Changes in targeting practices or increased catchability of bigeye as abundance declines (*e.g.* density-dependent catchability) could result in differences from the outcomes predicted here.

Key Results

1. The results of this assessment indicate a recent recovery trend for bigeye tuna in the EPO (2005-2010), subsequent to IATTC tuna conservation resolutions initiated in 2004. However, a decline of the spawning biomass began at the start of 2011, persisted through 2012 and reduced both summary and spawning biomasses to their lowest historic levels at the start of 2013. This recent decline may be related to a series of recent below-average recruitments which coincide with a series of strong la Niña events. However, at current levels of fishing mortality, and if recent levels of effort and catchability continue and average recruitment levels persist, the SBR is predicted to stabilize at about 0.21, very close to the level corresponding to MSY.
2. There is uncertainty about recent and future recruitment and biomass levels.
3. The recent fishing mortality rates are estimated to be slightly below the level corresponding to MSY, and the recent levels of spawning biomass are estimated to slightly above that level. These interpretations are uncertain and highly sensitive to the assumptions made about the steepness parameter of the stock-recruitment relationship, the assumed rates of natural mortality for adult bigeye, and the weighting assigned to the size-composition data, in particular to the longline size-composition data. The results are more pessimistic if a stock-recruitment relationship is assumed, if lower rates of natural mortality are assumed for adult bigeye, and if a greater weight is assigned to the size-composition data, in particular the longline fisheries.

2. DATA

Catch, effort, and size-composition data for January 1975 through December 2012 were used to conduct the stock assessment of bigeye tuna, *Thunnus obesus*, in the eastern Pacific Ocean (EPO). The data for 2012, which are preliminary, include records that had been entered into the IATTC databases as of mid-March 2013. All data are summarized and analyzed on a quarterly basis.

2.1. Definitions of the fisheries

Twenty-three fisheries are defined for the stock assessment of bigeye tuna (Table 2.1); the spatial extent of each fishery and the boundaries of the length-frequency sampling areas are shown in Figure 2.1. They are defined on the basis of gear type (purse seine, pole and line, and longline), purse-seine set type (on floating objects, unassociated schools, and dolphins), time period, IATTC length-frequency sampling area or latitude, and unit of longline catch (in numbers or weight).

In general, the fisheries are defined so that, over time, there is little change in the average size composition of the catch. The fishery definitions for purse-seine sets on floating objects are also stratified to provide an approximate distinction among sets made mostly on flotsam (natural floating-objects) (Fishery 1), sets made mostly on fish-aggregating devices (FADs) (Fisheries 2-3, 5, 10-11, and 13), and sets made on a mixture of flotsam and FADs (Fisheries 4 and 12). Data on catches by pole-and-line gear and by purse-seine vessels setting on dolphins and unassociated schools (Fisheries 6 and 7) are pooled, since relatively few bigeye are captured by the first two methods, and the data from Fisheries 6 and 7 are dominated by information on catches from unassociated schools of bigeye. Given this latter fact, Fisheries 6 and 7 are referred to as fisheries that catch bigeye in unassociated schools throughout this report. This assessment considers four longline fisheries (Northern, Central, Southern and Inshore). The spatial definitions of the longline fishery are based on the results of a regression tree analysis using longline catch per unit of effort (CPUE) data and length-frequency data to investigate the stock structure of bigeye in the EPO (Lennert-Cody, Maunder and Aires-da-Silva 2010; Lennert-Cody, Maunder and Aires-da-Silva *et al*. 2012).

The previous full assessment of bigeye identified a major shift in residual patterns that occurred in the late 1980s in the bigeye longline size-composition distributions (Aires-da-Silva and Maunder 2010; Aires-da-Silva, Maunder and Lennert-Cody 2010), due apparently to important temporal changes in longline catchability and/or selectivity. A spatial analysis of trends in the numbers of hooks per basket, which determine the fishing depth of the longline gear, indicated a transition, around the late 1980s, from an early period of increasing and more variable numbers of hooks per basket, to a late period of more stable numbers of hooks per basket (Aires-da-Silva, Maunder and Lennert-Cody 2010). On the basis of these major changes in fishing technology, which occurred around 1990, all four longline fisheries (Fisheries 12-23) were subdivided into two time periods with different catchabilities and/or selectivities: early (1975-1989) and late (1990-2012).

The catch data reported by the longline fisheries are a mixture of catch in numbers and weight records. Since the Stock Synthesis model (see description in section 4) has the flexibility of including catch data in either numbers or weight, twelve longline fisheries are defined: eight fisheries with catch reported in numbers caught (Fisheries 12-19), and four additional longline fisheries that report catch in weight for the late period (Fisheries 20-23).

2.2. Catch

To conduct the stock assessment of bigeye tuna, the catch and effort data in the IATTC databases are stratified in accordance with the fishery definitions described in Section 2.1 and listed in Table 2.1. The three definitions relating to catch data used in previous reports (landings, discards, and catch) are described by Maunder and Watters (2001). The terminology in this report is consistent with the standard terminology used in other IATTC reports. Catches taken in a given year are assigned to that year even if they were not landed until the following year. Catches are assigned to two categories, retained catches and discards. Throughout this document, the term “catch” is used to reflect either total catch (retained catch plus discards) or retained catch; the appropriate definition is determined by the context.

Three types of catch data are used to assess the stock of bigeye tuna (Table 2.1): removals by Fisheries 1, 6, and 12-23 are simply retained catch; removals by Fisheries 2-5 and 7 are retained catch, plus some discards resulting from inefficiencies in the fishing process (Section 2.2.1); and removals by Fisheries 8-

11 are discards resulting only from sorting the catch taken by Fisheries 2-5 (Section 2.2.1).

Updated and new catch data for the surface fisheries (Fisheries 1-11) have been incorporated into the current assessment. The species-composition method (Tomlinson 2002) was used to estimate catches by the surface fisheries. Average scaling factors for 2000-2008 were calculated by dividing the total catch for all years and quarters for the species composition estimates by the total catch for all years and quarters for the standard estimates, and these were then applied to the cannery and unloading estimates for 1975-1999. For Fisheries 1, 6, and 7 we used the average of Fisheries 2-5, for Fisheries 2 and 3 we used the average of Fisheries 2 and 3, and for Fisheries 4 and 5 we used the average of Fisheries 4 and 5. Harley and Maunder (2005) provide a sensitivity analysis that compares the results from the stock assessment using the species composition estimates of purse-seine fishery landings with the results from the stock assessment using cannery unloading estimates.

Updated or new catch data for the longline fisheries (Fisheries 12-23) are available for China (2009 and 2011), Chinese Taipei (2009-2011), Japan (2009-2011), Korea (2011), the United States (2010-2011) and Vanuatu (2005-2011). Catch data for 2012 are available for China, Chinese Taipei, Japan, Korea, and Vanuatu from the monthly reporting statistics. Trends in the catches of bigeye taken by each fishery from the EPO during each year of the 1975-2012 period are shown in the upper panel of Figure 2.2. The annual catch trends for the combined surface fleet (Fisheries 1-11) and the longline fleet (Fisheries 12-23) are also shown (Figure 2.2, lower panel). There has been substantial annual variation in the catches of bigeye by all fisheries operating in the EPO (Figure 2.2, upper panel). Prior to 1996, the longline fleet removed more bigeye (in weight) from the EPO than did the surface fleet (Figure 2.2, lower panel). Since 1996, however, the catches by the surface fleet have mostly been greater than those by the longline fleet. It should be noted that the assessment presented in this report uses data starting from 1 January 1975, and substantial amounts of bigeye were already being removed from the EPO by that time.

2.2.1. Discards

For the purposes of the stock assessment, it is assumed that bigeye are discarded from the purse-seine catches for one of two reasons: inefficiencies in the fishing process (*e.g.* when the catch from a set exceeds the remaining storage capacity of the fishing vessel) or because the fishermen sort the catch to select fish that are larger than a certain size. In either case, the amount of discarded bigeye is estimated from information collected by observers from the IATTC or national programs, applying methods described by Maunder and Watters (2003). Regardless of why fish are discarded, it is assumed that they all die.

Estimates of discards resulting from inefficiencies in the fishing process are added to the retained purse-seine catches (Table 2.1). No observer data are available to estimate discards for surface fisheries that operated prior to 1993 (Fisheries 1 and 6), and it is assumed that there were no discards from these fisheries. For surface fisheries that have operated since 1993 (Fisheries 2-5 and 7), there are periods for which observer data are not sufficient to estimate the discards. For these periods, it is assumed that the discard rate (discards/retained catches) is equal to the average discard rate for the same quarter from adjacent years or, if not available, the following year.

Discards that result from the process of sorting the catch are treated as separate fisheries (Fisheries 8-11), and the catches taken by these fisheries are assumed to be composed only of fish that are 2-4 quarters old (Maunder and Hoyle 2007). Watters and Maunder (2001) provide a rationale for treating such discards as separate fisheries. Estimates of the amounts of fish discarded during sorting are made only for fisheries that take bigeye associated with floating objects (Fisheries 2-5), because sorting is thought to be infrequent in the other purse-seine fisheries.

Time series of annual discards as proportions of the total (retained plus discarded) catches for the surface fisheries that catch bigeye in association with floating objects are shown in Figure 2.3. For the four main floating-object fisheries (Fisheries 2-5) with corresponding discard fisheries (Fisheries 8-11), the proportions of the catches discarded have been low since the late 1990s relative to those observed during fishing on the strong cohorts produced in 1997-1998. There is strong evidence that some of this is due to year classes that were weaker than the 1997-1998 year classes. However, there have been several recruitments since 1998 which have been greater than the long-term average since 1998 (2001-2006; Figure 4.5b). It is possible that the regulations that have prohibited discarding of tuna since 2001 (Resolutions C-00-08 and C-05-04) have caused the proportion of discarded fish to decrease. However, the recent high proportions of discards observed in Fishery 10 (inshore) are an exception.

It is assumed that bigeye tuna are not discarded from longline fisheries (Fisheries 12-23).

2.3. Indices of abundance

Indices of abundance were derived from purse-seine and longline catch and effort data. Fishing effort data for the surface fisheries (Fisheries 1-7) have been updated and new data included for 2012. New or updated catch and effort data are available for the Japanese longline fisheries (2009-2011). Trends in the amount of fishing effort exerted by the fisheries defined for this assessment are shown in Figure 2.4. Purse-seine fishing effort (in days fished) has shown an overall increasing trend since the expansion of the floating-object fisheries in the mid-1990s (Fisheries 2, 3 and 5). With respect to longliners, the fishing effort went through a pronounced decline after 2002 (late longline Fisheries 13, 15, 17, and 19) which coincided with the sharp increase in the cost of fuel. However, an increasing trend in longline fishing effort has been observed in the EPO since the late 2000s, particularly in the central and southern areas (Fisheries 15 and 17).

Observer data are available only for purse-seine vessels with a fish-carrying capacity greater than 363 t (IATTC capacity class 6). The catch per unit of effort (CPUE) for such vessels was calculated as catch divided by number of days fished. The number of days fished by set type was estimated from the number of sets, using a multiple regression of total days fished against number of sets by set type (Maunder and Watters 2001).

Estimates of standardized CPUE (1975-2011) were obtained for the eight (early and late) longline fisheries (Fisheries 12-19). A delta-lognormal general linear model, in which the explanatory variables were latitude, longitude, and hooks per basket, was used (Hoyle and Maunder 2006).

The CPUE time series for the different fisheries are presented in Figure 2.5. The indices of abundance that were considered appropriate for model fitting in the assessment were the CPUE series from the early and late Central and Southern longline fisheries (Fisheries 14-15 and 16-17, respectively). The areas covered by these fisheries include the main longline fishing grounds for bigeye. Some of the fisheries excluded were considered inappropriate because the catch rates were extremely low (Fishery 1) or because they combined gears (purse seine and pole and line; Fisheries 6 and 7). In the previous assessment base case model configuration, the model was allowed to fit the indices of abundance from Fisheries 2, 3, and 5 (purse-seine sets on floating objects) and also Fisheries 12-13 and 18-19 (early and late Northern and Inshore longline fisheries). However, this was done while estimating the coefficients of variation (CVs) for these CPUE indices, which substantially down-weights their influence on the model fit. Considering their higher variability and lesser representativeness of the bigeye stock, these indices were excluded from the model fit in the current assessment, to avoid potential conflicts with other sources of data (see Section 4.3, Diagnostics).

2.4. Size composition data

New length-frequency data for 2012 are available for the surface fisheries. New or updated length-frequency data are available for the Japanese longline fleet (2006-2011). Size composition data for the other longline fleets are not used in the assessment.

The length-frequency data for the Chinese Taipei fleet include more smaller fish than those for the Japanese fleet. However, there is concern about the representativeness of the length-frequency samples from the Chinese Taipei fleet (Stocker 2005, Anonymous 2006), and therefore these data are not used in the base case assessment. Maunder and Hoyle (2007) conducted a sensitivity analysis in which the Chinese Taipei fleet was treated as a separate fishery. Also, Wang *et al.* (2009) carried out an investigation that treated the Chinese Taipei fishery as a separate entity, rather than combining data for that fishery with those for other longline fisheries, as in this assessment. The results from these studies revealed few differences with respect to the base case results.

The fisheries of the EPO catch bigeye tuna of various sizes. The average size compositions of the catches from each fishery defined in Table 2.1 have been described in previous assessments. The fisheries that catch bigeye associated with floating objects typically catch small (<75 cm) and medium-sized (75 to 125 cm) bigeye (Figures 2.6a-b, Fisheries 1-5). Prior to 1993, the catch of small bigeye was roughly equal to that of medium-sized bigeye (Figure 2.6a, Fishery 1); since 1993, however, small bigeye from the purse-seine fisheries that catch bigeye in association with floating objects have dominated the catches (Figures 2.6a-b, Fisheries 2-5). An exception is the 1999-2002 period, when a strong cohort moved through the fishery and medium-sized fish dominated the catch of the floating-object fisheries.

Prior to 1990, mostly medium-sized bigeye were captured in unassociated schools (Figure 2.6b, Fishery 6). Since 1990, more small and large (>125 cm) bigeye have been captured in unassociated schools (Figure 2.6c, Fishery 7).

As described above, there is high variability in the size composition data of the surface fisheries. This variability is particularly strong in the Central floating-object fishery (Fishery 3) when strong cohorts appear and are apparently targeted over the subsequent years (Figure 2.6a). This pattern has also been identified in the floating-object fisheries for yellowfin tuna, and indicates that selectivity is time-varying for these fisheries (External review of the yellowfin tuna assessment: Document YFT-01-06 and report). As described below, selectivities are assumed to be constant over time for the surface fisheries in the bigeye assessment (see Section 4, Stock Assessment). This potential model misspecification has been identified as a plausible cause for the strong retrospective pattern in recent recruitment estimates in previous assessments. For this reason, the size composition data of all surface fisheries has been down-weighted in the present base case model configuration (see Section 4, Stock Assessment).

The catches taken by longline fisheries 12-19 have distinctly different size compositions. In the area north of 10°N (Northern longline Fisheries 12 and 13), longliners catch mostly medium-sized fish, and the average size composition has two distinct peaks (Figure 2.6c: bands at 80 cm and 120 cm). In the Central and Southern longline areas (Fisheries 14-15 and 16-17, respectively), longliners catch substantial numbers of both medium-sized and large bigeye (Figures 2.6d and 2.6e). However, there appears to have been a transition from medium-sized fish to fish over 150 cm during the late 1980s. There also seems to be a shift to larger fish caught by longliners in the inshore area (Fisheries 18 and 19) around the late 1980s, but these fish are not as large as those caught in the central and southern areas in the late period (Fisheries 15 and 17). In order to better model these observed shifts in the size-composition data of bigeye caught by longliners, and deal with the associated residual pattern (see Section 4.3.1), the current assessment considers two time blocks with different catchabilities and/or selectivities for all longline fisheries (see Section 2.1).

Diagnostics identified the Japanese longline length-frequency data as the most influential component determining absolute scale (the R_0 parameter) in the previous base case model configuration (see Section 4.3, Diagnostics).This effect was minimized in the current assessment by down-weighting these data.

3. ASSUMPTIONS AND PARAMETERS

3.1. Biological and demographic information

3.1.1. Growth

As with many tuna species, specifying growth in the bigeye stock assessment for the EPO presents some challenges. Age-at-length data derived from readings of daily increments on otoliths are available for fish up to four years of age only (Schaefer and Fuller 2006), a narrow spectrum of ages for a species that is estimated from tagging studies to have a lifespan of at least 15-16 years (Langley *et al*. 2008). Otolith readings for large (older) fish are very difficult to interpret. Acquiring tag-recapture information for the older fish has been problematic since it is difficult to capture large bigeye for tagging, and few samples of tag recaptures from larger fish have been available from the longline fisheries.

The most recent study of the age and growth of bigeye in the EPO was done by Schaefer and Fuller (2006), who used tag-recapture data and otolith daily increments to estimate growth. The two data sources provided very similar estimates, but the asymptotic length of the von Bertalanffy growth curve is much greater than any length recorded. This is reasonable as long as no biological significance is given to the asymptotic parameter and the growth model is used only as a representation of the ages of fish that were sampled. The maximum age in their data set is around 4 years (16 quarters), and hence the resulting von Bertalanffy growth curve cannot be used to predict growth beyond this age.

An attempt has been made to estimate growth internally in previous EPO bigeye assessment models. The growth model is fitted to the age-at-length data from otolith readings (Schaefer and Fuller 2006) and the bigeye size-composition data sampled from different fisheries. Using the A-SCALA stock assessment model (Maunder and Watters 2003), a Richards growth curve was fitted while setting the asymptotic length parameter at about the size of the largest bigeye in the data (186.5 cm; Maunder and Hoyle 2006). This resulting curve has also been taken as a prior for all ages in the bigeye assessment (Maunder and Hoyle 2007).

Previous growth studies and stock assessments of tuna species (*e.g.* Harley and Maunder 2005; Maunder 2002a) indicate that rapid and almost linear growth of juvenile tuna is best fitted by a Richards growth model. In two early assessments of bigeye (Aires-da-Silva and Maunder 2007, 2009), a von Bertalanffy growth curve was used to predict the mean length-at-age, due mainly to a Richards function not being available then in Stock Synthesis (version 2; Methot 2005). In a subsequent bigeye assessment (Aires-da-Silva and Maunder 2010a), a sensitivity analysis was performed using the Richards growth model. There were substantial improvements in the model fit to the data, particularly to the bigeye age-at-length (otolith readings) and size-composition data.

Following the recommendations of the external review of the IATTC staff's assessment of bigeye tuna, held in May 2010, a transition was made in the previous full assessment from the traditional von Bertalanffy model to a more flexible Richards growth model (Aires-da-Silva and Maunder 2011). The choice of L_2 (average size of the oldest fish) for bigeye is somewhat arbitrary, and the parameter has generally been fixed at about the size of the largest fish in the data. As in previous assessments, and following the recommendation of the external review, L_2 is pre-specified rather than estimated in the present bigeye assessment; it was fixed at 185.5 cm, a value which is about the average size of the largest fish in the data. Previous sensitivity analyses have shown that the bigeye assessment results are highly sensitive to the assumed value for L_2 (Hampton and Maunder 2005; Aires-da-Silva and Maunder 2007; Aires da Silva and Maunder 2010c; Aires-da-Silva and Maunder 2011).

Another important component of growth used in age-structured statistical catch-at-length models is the variation in length-at-age, which can be just as influential as the mean length-at-age. Information on the variability of length-at-age can be obtained from age-at-length data, which is available for bigeye tuna (Schaefer and Fuller 2006). Unfortunately, the bigeye otolith samples were not collected randomly, but rather to cover a range of sizes to provide information on mean length-at-age. Therefore, these data do not provide a good measure of variation of length-at-age. In a previous assessment using A-SCALA (Maunder and Hoyle 2007), conditional probability was used to apply an appropriate likelihood to the data and estimate variation of length-at-age. These variability estimates have been used (fixed) in the latest assessments of bigeye that use Stock Synthesis. Following a recommendation of the external review, in the previous full assessment (Aires-da-Silva and Maunder 2011) the parameters that determine the variance of the length-at-age were estimated rather than set to the values estimated from A-SCALA.

Age-at-length data derived from otolith readings from fish caught in the floating-object fisheries (Schaefer and Fuller 2006) were integrated into the stock assessment model to provide information on variation in length at age.

Progress has been made in reducing the uncertainty regarding bigeye growth, in particular the average size of the older fish (L_2). A Richards growth model (Schnute 1981) was developed to fit simultaneously to the age-at-length (otolith readings) and tag-recapture data, following the Laslett-Eveson-Polacheck statistical framework (Laslett *et al*. 2002; Eveson *et al*. 2004). The age-at-length data consisted of age estimates from counts of daily increments on otoliths, and the lengths of 254 fish caught in 2002 in the floating-object fisheries (Schaefer and Fuller 2006). As noted above, these otolith readings are mostly from bigeye less than 4 years old and less than 150 cm in length. The available tag-recapture data are also dominated by young bigeye of less than 150 cm. However, some tag-recapture observations from larger (older) bigeye are also available, thanks to the recent recaptures of bigeye of up 190 cm after times at liberty up to almost 8 years.

The integrated aging and tagging data Richards growth model was parameterized following Schnute (1981). The variability of the length at age was estimated assuming a linear relationship between the standard deviation of the length at age and the mean length at age. The estimated Richards growth curve for bigeye, and the associated variability of the length at age and the model fit to the age-at-length and tag recapture data, are shown in Figure 3.1a. A comparison between the new Richards growth curve and that used in the last full assessment (Aires-da-Silva and Maunder 2011) is shown in Figure 3.1b. The value assumed for L_2 increased from 185 cm in the last assessment to 196 cm in the current assessment. In addition, the variability of the length-at-age increased slightly in the current assessment, particularly for older fish.

The following weight-length relationship, from Nakamura and Uchiyama (1966), was used to convert lengths to weights in the current stock assessment:

$$w = 3.661 \times 10^{-5} \cdot l^{2.90182}$$

where w = weight in kilograms and l = length in centimeters.

3.1.2. Natural mortality

Age-specific vectors of natural mortality (M) are assumed for bigeye. This assessment uses a sex-specific model, and therefore natural mortality schedules are provided for each sex (Figure 3.2). A higher level of natural mortality (M = 0.25) is assumed for fish of both sexes 0 quarters old, decreasing to 0.1 at 5 quarters of age. As in previous assessments, it is assumed that the natural mortality of females increases after they mature. These age-specific vectors of natural mortality are based on fitting to the estimates of age-specific proportions of females, maturity at age, and natural mortality of Hampton (2000).

The previous observation that different levels of natural mortality had a large influence on the absolute population size and the population size relative to that corresponding to the maximum sustainable yield (MSY; see definition in Section 5) (Watters and Maunder 2001) is retained. Harley and Maunder (2005) performed a sensitivity analysis to assess the effect of increasing natural mortality for bigeye younger than 10 quarters. In addition, the effect on the bigeye stock assessment of assuming alternative scenarios of juvenile natural mortality rates has been evaluated (Document SARM-9-INF-B[1]). The management quantities showed little sensitivity when higher levels of M were assumed for fish 0-5 quarters of age. In contrast, they showed a greater sensitivity to the assumption made about the oldest of the early ages (5-12 quarters old) included in the early high levels of M. However, the high levels of M assumed for bigeye 5-12 quarters (60-120 cm) old seem unrealistic. This report presents a sensitivity analysis to assuming lower and higher rates of adult natural mortality for bigeye (Appendix B).

[1] http://www.iattc.org/PDFFiles2/SARM-9-INF-B-Comments-on-Document-SARM-9-11d.pdf

An ongoing investigation of natural mortality rates for bigeye, based on an integrated analysis which includes tagging and sex ratio data, indicates levels of *M* for adult bigeye higher than those currently used (Maunder *et al.* 2010). However, these estimates are highly uncertain, and strongly dependent on the assumptions made about tag-reporting rates by longliners.

3.1.3. Recruitment and reproduction

It is assumed that bigeye tuna can be recruited to the fishable population during every quarter of the year. Recruitment may occur continuously throughout the year, because individual fish can spawn almost every day if the water temperatures are in the appropriate range (Kume 1967; Schaefer *et al*. 2005).

The Stock Synthesis model allows a Beverton-Holt (1957) stock-recruitment relationship to be specified. The Beverton-Holt curve is parameterized so that the relationship between spawning biomass (biomass of mature females) and recruitment is determined by estimating the average recruitment produced by an unexploited population (virgin recruitment), a parameter called steepness. Steepness controls how quickly recruitment decreases when the spawning biomass is reduced. It is defined as the fraction of virgin recruitment that is produced if the spawning biomass is reduced to 20% of its unexploited level. Steepness can vary between 0.2 (in which case recruitment is a linear function of spawning biomass) and 1.0 (in which case recruitment is independent of spawning biomass). In practice, it is often difficult to estimate steepness because of a lack of contrast in spawning biomass and because there are other factors (*e.g.* environmental influences) that can cause recruitment to be extremely variable. For the current assessment, recruitment is assumed to be independent of stock size (steepness = 1). There is no evidence that recruitment is related to spawning stock size for bigeye in the EPO and, if steepness is estimated as a free parameter, it is estimated to be close to 1. However, simulation analyses have shown that estimation of steepness is problematic, with large uncertainty and frequent estimates equal to 1 even if the true steepness is moderately less than 1 (Conn *et al*. 2010). A sensitivity analysis with steepness = 0.75 and a likelihood profile on this parameter are presented in Appendix A of this report. In addition to the assumptions required for the stock-recruitment relationship, a constraint on quarterly recruitment deviates with a standard deviation of 0.6 is applied. Recruitment is modeled at age-0 in Stock Synthesis.

Reproductive inputs are based on the results of Schaefer *et al*. (2005) and data provided by Dr. N. Miyabe of the National Research Institute of Far Seas Fisheries (NRIFSF) of Japan. Information on age at length (Schaefer and Fuller 2006) was used to convert proportion mature at length into an age-at-maturity schedule (Figure 3.3, Table 3.1). A maturity at length schedule following Schaefer and Fuller (2006) is incorporated in the assessment model. The corresponding age-at-maturity schedule is available (Figure 3.3 and Table 3.1).

3.1.4. Movement

The current assessment does not consider movement explicitly. Rather, it is assumed that the population is randomly mixed at the beginning of each quarter of the year. The IATTC staff is studying the movement of bigeye within the EPO, using data recently collected from conventional and archival tags, and these studies indicate substantial levels of regional fidelity of bigeye within the EPO. This implies that localized depletion patterns of bigeye may exist in the EPO. A preliminary evaluation of spatial structure in the bigeye stock assessment has been initiated (Aires-da-Silva and Maunder 2010b). A spatially-structured framework will be considered in future stock assessments. The spatial definition of the fisheries accommodates some forms of movement by means of different selectivity and catchability.

3.1.5. Stock structure

Schaefer and Fuller (2009) provide an overview of the stock structure of bigeye in the EPO. The results of tagging studies in the equatorial EPO, with releases restricted to around 95°W, indicate restricted movements and regional fidelity to the equatorial EPO, and suggest a very low level of mixing between the eastern and western Pacific (Schaefer and Fuller 2002, 2009). Accordingly, and for the purposes of the current assessment, it is assumed that there are two stocks, one in the EPO and the other in the western and central Pacific Ocean (WCPO), and that there is no net exchange of fish between these regions. The IATTC staff periodically conducts a Pacific-wide assessment of bigeye in collaboration with scientists of the Oceanic Fisheries Programme of the Secretariat of the Pacific Community and of the NRIFSF. This work may help indicate how the assumption of a single stock in the EPO is likely to affect interpretation of the results obtained from the Stock Synthesis model. Recent analyses (Hampton *et al*. 2003) that estimate movement rates within the Pacific Ocean provided biomass trends very similar to those estimated by Harley and Maunder (2004), and differences in absolute levels of biomass were mainly due to differences in growth rates between the two sides of the Pacific Ocean.

In order to investigate the sensitivity of the assessment results to the assumptions made about stock structure, a sensitivity analysis to extending the western limit of the bigeye stock distribution was conducted (Aires-da-Silva and Maunder 2010a). When the assumed western limit of the bigeye stock distribution was extended from 150°W to 170°E, and the additional catch taken from the WCPO was included in the model, the recruitments and biomasses were greater than those estimated by the base case model, but the relative trends are very similar. When the model was also fitted to the additional CPUE and size-composition data from the WCPO, the biomass estimates for most years became lower than the base case, but the relative trends were also similar. The stock status assessment for these sensitivity analyses was similar to that for the base case.

3.2. Environmental influences

Oceanographic conditions might influence the recruitment of bigeye tuna to fisheries in the EPO. In previous assessments (*e.g.* Watters and Maunder 2001, 2002), zonal-velocity anomalies (velocity anomalies in the east-west direction) at a depth of 240 m were used as the candidate environmental variable for affecting recruitment. The mechanism that is responsible for this relationship has not been identified, and correlations between recruitment and environmental indices are often spurious, so the relationship between zonal velocity and bigeye recruitment should be viewed with skepticism. Nevertheless, this relationship tends to indicate that bigeye recruitment is increased by strong El Niño events and decreased by strong La Niña events. In fact, two of the periods of greatest recruitment (1982-1983 and 1997-1998) coincide with the two strongest El Niño events of the 20th century. Maunder and Hoyle (2007) conducted a sensitivity analysis to investigate the relationship between recruitment and the El Niño index; this showed that there was a significant negative relationship, but it explained only a small proportion of the total variability in the recruitment.

Other sensitivity analyses in which environmental indices were incorporated into the stock assessment model have been conducted in previous assessments. It was assumed that oceanographic conditions might influence the efficiency of the fisheries that catch bigeye associated with floating objects (Fisheries 1-5) (Watters and Maunder 2001, 2002; Maunder and Harley 2002). In the assessment of Maunder and Harley (2002), an environmental influence on catchability was assumed for the Central floating-object fishery (Fishery 3) only. It was found that including this effect did not greatly affect the results.

In general, analyses in which no environmental indices were included produced estimates of recruitment similar to those that used zonal velocity (Harley and Maunder 2004). This suggests that there is sufficient information in the length-frequency data to estimate most historical year-class strengths, but the index may be useful for reducing uncertainty in estimates of the strengths of the most recent cohorts, for which few size-composition samples are available. A previous sensitivity analysis of the effect of including the environmental index showed that the index was not statistically significant (Maunder and Hoyle 2006), or explained only a small proportion of the total variation in recruitment (Maunder and Hoyle 2007). However, the “two-stanza” recruitment pattern for bigeye in the EPO identified in earlier assessments (Section 4.1.2), which consists of a period of lower recruitments (1975-1993) followed by a period of relatively large recruitments (1994-2009), may be preventing a significant correlation. Investigating environmental correlations for the late period only may be preferable. The time series of bigeye quarterly recruitments estimated in the current assessment (1975-2012) are compared with the Southern Oscillation

Index (SOI; Philander 1990) (see Section 4.1.2.). An evaluation of spatial structure in the bigeye assessment indicates that similar recruitment trends in different regions of the EPO may be driven by a similar large-scale environmental effect (*e.g.*, El Niño/La Niña events) (Aires-da-Silva and Maunder 2010b)

In view of the results from previous sensitivity analyses described above, no environmental index was incorporated into this assessment.

4. STOCK ASSESSMENT

The Stock Synthesis model (SS - Version 3.23b; Methot 2005, 2009; Methot and Wetzel 2013) was used to assess the status of bigeye tuna in the EPO. It consists of a size-based, age-structured, integrated (fitted to many different types of data) statistical stock assessment model.

The model is fitted to the observed data (indices of relative abundance and size compositions) by finding a set of population dynamics and fishing parameters that maximize a penalized likelihood, given the amount of catch taken by each fishery. Many aspects of the underlying assumptions of the model are described in Section 3. It also includes the following important assumptions:

1. Bigeye tuna are recruited to the discard fisheries (Fisheries 8-11) one quarter after hatching, and these discard fisheries catch only fish of the first few age classes (fully selected between 1 and 3 quarters of age).
2. The size-based selectivity curves for the late longline fisheries in the Central and Southern areas (Fisheries 15 and 17) are assumed to be asymptotic.
3. The data for fisheries that catch bigeye tuna in unassociated schools (Fisheries 6 and 7), the pre-1993 and Inshore floating-object fisheries (Fisheries 1 and 4), and fisheries whose catch is composed of discards from sorting (Fisheries 8-11), provide relatively little information about biomass levels, because these fisheries do not direct their effort at bigeye. For this reason, the CPUE time series for these fisheries were not used as indices of abundance. The CPUE time series for the Southern, Central and Northern floating-object fisheries (2-3) are highly variable. For this reason, and to avoid potential conflicts in the model fit with more reliable CPUE data, these CPUE time series were not used as indices of abundance. Likewise, the CPUE time series of the Northern and Inshore longline fisheries (12-13 and 18-19) were not used as indices of abundance. The former fishery is seasonal, and the catches of bigeye by both fisheries are minor.

The following parameters have been estimated in the current stock assessment of bigeye tuna from the EPO:

1. Recruitment in every quarter from the first quarter of 1975 through the fourth quarter of 2012 (includes estimation of virgin - or average - recruitment and temporal recruitment penalized anomalies);
2. Catchability coefficients for the four CPUE time series that are used as indices of abundance (the early and late periods of the Central and Southern longline fisheries (14-15 and 16-17, respectively). Following a recommendation by the external review, two time blocks (early and late fisheries, split at 1990, associated with a change in the mean length of the catch) with different catchability parameters are assumed for these longline fisheries.
3. Following a recommendation by the external review, the coefficients of variation (CVs) of the CPUE for the early and late Southern longline fisheries (16 and 17) were fixed at 0.15. The same fixed CV is applied in the current assessment to both periods (early and late) of the Central longline fisheries (14 and 15) which have shown similar CPUE trends to those observed in the Southern longline fisheries (16 and 17).
4. Selectivity curves for fifteen of the 23 fisheries (Fisheries 8-11 have an assumed selectivity curve,

and the selectivities of Fisheries 20 to 23 are the same as those of Fisheries 13, 15, 17, and 19, respectively). Except for the late Central and Southern longline fisheries (15 and 17), which catch larger bigeye, the selectivity curves of all fisheries that retain their catches are assumed to be dome-shaped (double normal).

5. Initial population size and age structure. Two initial fishing mortality parameters (for surface and combined longline fisheries, respectively) are estimated. In addition, the average recruitment used to estimate the initial conditions and deviates for the youngest 15 age classes are estimated.

The following parameters are assumed to be known for the current stock assessment of bigeye in the EPO:

1. Mean length-at-age and the variability of the length at age (Figure 3.1a);
2. Sex- and age-specific natural mortality rates (Figure 3.2);
3. Age-specific maturity curve (Table 3.1 and Figure 3.3);
4. Selectivity curves for the discard fisheries (Fisheries 8-11);
5. The steepness of the stock-recruitment relationship.

The estimates of management quantities and future projections were computed based on 3-year average fishing mortality rates, by gear, for 2010-2012. The sensitivity of estimates of key management quantities to including the last year (2012) in the 3-year average fishing mortality rate estimate was tested. For this purpose, a 2-year (2010-2011) average fishing mortality rate was used in the calculations.

There is uncertainty in the results of the current stock assessment. This uncertainty arises because the observed data do not perfectly represent the population of bigeye tuna in the EPO. Also, the stock assessment model may not perfectly represent the dynamics of the bigeye population or of the fisheries that operate in the EPO. Uncertainty is expressed as approximate confidence intervals and CVs. The confidence intervals and CVs have been estimated under the assumption that the stock assessment model does perfectly represent the dynamics of the system. Since it is unlikely that this assumption is satisfied, these values may underestimate the amount of uncertainty in the results of the current assessment. The model structure uncertainty is investigated in several sensitivity analyses.

The following summarizes the important aspects of the base case assessment (1) and the three sensitivity analyses (2-4):

1. **Base case assessment**: steepness of the stock-recruitment relationship = 1 (no relationship between stock and recruitment); the mean length-at-age, and the parameters that define the variability of the length-at-age, are fixed; fitted to CPUE time series for the early and late periods of the Central and Southern longline fisheries (14-17) (two time blocks of catchability separating the early and late periods of these fisheries); two time blocks of selectivity for longline Fisheries 12-19; asymptotic size-based selectivities for the late Central and Southern longline fisheries (15 and 17), which catch larger bigeye; and down-weighted size composition data for all fisheries (a multiplicative weighting factor – λ (lambda) - of 0.05 was applied to all size composition data; see Sections 2.4, Size composition data, and 4.3, Diagnostics, for rationale on this assumption).

2. **Sensitivity to the steepness of the stock-recruitment relationship**. The base case assessment includes the assumption that recruitment is independent of stock size, and a Beverton-Holt (1957) stock-recruitment relationship with a steepness of 0.75 was used for the sensitivity analysis. In addition, a likelihood profile for steepness was computed (steepness ranging from 0.5 to 1, with 0.1 increments).

3. **Sensitivity to assuming lower and higher values of adult natural mortality (*M*) for both females and males.** While defining the alternative *M* schedules for bigeye, and in order to maintain the age-specific absolute differences of natural mortality estimated from sex-ratio data

(Figure 3.2), the *M* values for adult (12+ quarters old) females and males assumed in the base case were decreased/increased by the same multiplicative factor (Figure B.1).

4. **Sensitivity to weighting assigned to the size composition data.** In the base case model, a multiplicative weighting factor (lambda, λ) of 0.05 was applied to the size composition data of all surface and longline fisheries. The following sensitivity analyses were done to explore the effect on the assessment results of assigning different weights to individual fisheries or groups of fisheries: 1) down-weighting (λ = 0.05) the size composition data for only the surface or the longline fisheries at a time, while keeping the original weighting (λ = 1) for the fisheries of the other gear type; 2) down-weighting (λ = 0.05) the size composition data for all fisheries except the Central and Southern longline fisheries (14-17) which were driving absolute scale (R_0) in the previous base case model configuration (see Section 4.3, Diagnostics); 3) down-weighting (λ = 0.05) the size composition data for all fisheries except the Southern floating-object fishery (2), which shows less variability and potentially less issues related to time-varying selectivity (see Figure 2.6a).

4.1. Assessment results

The results presented in the following sections are likely to change in future assessments because (1) future data may provide evidence contrary to these results, and (2) the assumptions and constraints used in the assessment model may change. Future changes are most likely to affect absolute estimates of biomass, recruitment, and fishing mortality.

4.1.1. Fishing mortality

There have been important changes in the amount of fishing mortality of bigeye in the EPO. On average, the fishing mortality of fish less than about 15 quarters old has increased greatly since 1993, and that of fish more than about 15 quarters old has increased to a much lesser extent since then (Figure 4.1). The increase in average fishing mortality of younger fish can be attributed to the expansion of the fisheries that catch bigeye in association with floating objects (Fisheries 2-5). These fisheries catch substantial amounts of bigeye (Figure 2.2), select fish that are generally less than about 100 cm in length (Figure 4.2), and have expended a relatively large amount of fishing effort since 1993 (Figure 2.4).

Temporal trends in the age-specific amounts of annual fishing mortality of bigeye are shown in Figure 4.3. These trends reflect the distribution of fishing effort among the various fisheries that catch bigeye (Figure 2.4) and changes in catchability. The trend in annual fishing mortality rate by time shows that fishing mortality has increased greatly for young fish (ages 1-12 quarters) since the early 1990s. This was due to the expansion of the purse-seine fisheries that catch juvenile bigeye on floating objects since 1993. Fishing mortality for older fish (13+ quarters) has also increased over the historic period of the assessment until the early 2000s. From 2002 to 2007-2008, fishing mortality of older fish declined by about 70%, which may be due to the combined effect of decreased longline fishing effort in the EPO (Figure 2.4) as well a strong cohort which entered the fishery in 1998 (see Section 4.1.2, Recruitment). Afterwards, fishing mortality rates for older fish increased again until 2012 (Figure 4.3). Fishing mortality rates for older fish (20+ quarters) increased greatly in the early 1990s, which is associated with the change in selectivity, as higher proportions of larger (>150 cm) fish became vulnerable to the longline fisheries, particularly in the Central and Southern areas (Fisheries 15 and 17, respectively; Figures 2.6d-e). The average levels of adult fishing mortality have remained nearly half of those for juvenile bigeye since the mid-1990s. An annual summary of the estimates of total fishing mortality is presented in Appendix E (Table E.1).

4.1.2. Recruitment

Over the range of estimated spawning biomasses shown in Figure 4.7, the abundance of bigeye recruits appears to be unrelated to the spawning biomass of adult females at the time of hatching (Figure 4.4). Previous assessments of bigeye in the EPO (*e.g.* Watters and Maunder 2001, 2002) also failed to show a relationship between adult biomass and recruitment over the estimated range of spawning biomasses. The base case estimate of steepness is fixed at 1, which corresponds to a model with an assumption that recruitment is independent of stock size. The consequences of overestimating steepness, in terms of lost equilibrium yield and potential for recruitment overfishing, are far worse than those of underestimating it (Zhu *et al*. 2012). A sensitivity analysis is presented in Appendix A that assumes that recruitment is related to stock size in varying degrees (steepness ranging from 0.5 to 1).

The time series of estimated quarterly recruitment (age-0 quarters fish) of bigeye produced by the current stock assessment is shown in Figure 4.5a, and the total recruitment estimated to occur during each year is shown in Figure 4.5b and Table 4.1. There was a period of above-average annual recruitment during 1994-1998, followed by a period of below-average recruitment in 1999-2000. The recruitments were above average from 2001 to 2006, and were particularly strong in 2005. More recently, the recruitments were below average during 2007-2009, and have fluctuated around average during 2010-2012. The most recent annual recruitment estimate (2012) is slightly below average levels. However, this estimate is highly uncertain, and should be regarded with caution, due to the fact that recently-recruited bigeye are represented in only a few length-frequency data sets.

There are two important features in the time series of estimated recruitment of bigeye which have been identified in previous assessments (Maunder and Hoyle 2007; Aires-da-Silva and Maunder 2011). In previous assessments, estimates of recruitment before 1993 were very uncertain, as the techniques for catching small bigeye associated with FADs were not in use. In addition, a "two-stanza" pattern was prominent in the time series of bigeye recruitments for the EPO (Figure 4.5 of Aires-da-Silva and Maunder 2011). This pattern was characterized by an early period of low recruitments (1975-1993) followed by a period of relatively large recruitments (1994-2009) which coincided with the expansion of the fisheries that catch bigeye in association with floating objects.

The "two-stanza" recruitment pattern has been greatly minimized under the current base case model configuration (Figure 4.19a in Section 4.4, Comparison to previous assessment). As explained in Sections 4.3, Diagnostics, and 5.3, Sensitivity Analyses, diagnostic analyses revealed that results from the previous bigeye assessment model configuration were highly driven by the model fit to the bigeye size-composition data. This dominant effect is not desirable, since there are unexplained inconsistencies with the longline size composition data and potential lack of the right modeling process to deal with time-varying selectivity of the surface fisheries (see Section 2.4, Size composition data, and Section 4.3, Diagnostics). Down-weighting the size composition data substantially reduced (about halved) the recruitment pattern; however, a shift towards higher average recruitment levels after 1994 is still apparent in the time series (Figure 4.19a). Any of the hypothesis previously presented to explain the recruitment pattern are still valid (Document SARM-9-INF-B; Aires-da-Silva, Maunder and Tomlinson 2010). The impact on the bigeye assessment results of potentially biased low recruitments prior to 1994 has been investigated as a sensitivity analysis in the previous full assessment (Aires-da-Silva and Maunder 2011). Adjustment of the spawning biomass ratios (SBRs, see definition in Section 5.1) and management quantities to using the recent period of the assessment only to calculate average recruitment would result in a more pessimistic stock evaluation (see Appendix A of SARM-9-INF-B). A sensitivity analysis was performed in the previous full assessment using fishery data covering the most recent period of the fishery only (1995-2009), which best reflects the current mix of tuna fisheries (surface and longline) and selectivities operating in the EPO (see Appendix D of Aires-da-Silva and Maunder 2011).

In Appendix D, the time series of estimated bigeye quarterly recruitments (1995-2009) are compared with the Southern Oscillation Index (SOI; Philander 1990). The strongest bigeye recruitments estimated within the historic period of the assessment (1975-2012) coincide with the strongest El Niño events, which were felt in 1983 and 1998. The relationship tends to indicate that the bigeye recruitment is increased by strong El Niño events and decreased by strong La Niña events (Figure D.1); however, the relationship often breaks down. The mainly below-average recruitments since 2007 coincide with a period dominated by particularly strong La Niña events.

4.1.3. Biomass

Trends in the biomass of 3+-quarter-old bigeye tuna in the EPO are shown in Figure 4.6, and estimates of the biomass at the beginning of each year are presented in Table 4.1. The biomass of 3+-quarter-old bigeye increased during 1983-1985, and reached the highest historic peak of about 1,378 thousand t in 1986, after which it gradually decreased to a historic low of about 428 thousand t at the beginning of 2013, with two intermediate peaks at 2000 and 2008. The trend in spawning biomass is also shown in Figure 4.7, and estimates of the spawning biomass at the beginning of each year are presented in Table 4.1. The spawning biomass has generally followed a trend similar to that of the biomass of 3+-quarter-old bigeye, but with a 1- to 2-year time lag. The biomasses of both 3+-quarter-old fish and spawners are estimated to have rebuilt during 2004-2010, after which they gradually declined to their lowest historic levels at the start of 2013. A simulation study indicates that the population increase may be attributed to the effect of the IATTC tuna conservation resolutions that started in 2004 (Section 6.2.3). Additional factors likely contributing to this increase are above-average recruitments and reduced longline effort in the EPO in the last decade. The most recent period dominated by below-average recruitments (2007-2012) could explain the declining trend observed since 2010.

There is uncertainty in the estimated biomasses of spawners. The average CV of the spawning biomass estimates is 0.30, which represents a slight decrease in precision when compared to previous assessments (CV at about 0.2). This results from the down-weighting of the size-composition data in the current assessment, which decreased the precision of the recruitment estimates and reduced information on abundance from the size-composition data, particularly for the two longline fisheries with asymptotic selectivity (Fisheries 15 and 17).

Given the amount of uncertainty in the estimates of both recruitment and biomass (Sections 4.1.2 and 4.1.3), it is difficult to determine whether trends in the biomass of bigeye have been influenced more by variation in recruitment or fishing mortality. Nevertheless, the assessment suggests two conclusions. First, the biomass of bigeye can be substantially increased by strong recruitment events. Both peaks in the biomass of 3+-quarter-old bigeye (1986 and 2001; Figure 4.6) were preceded by peak levels of recruitment (1982-1983 and 1997-1998, respectively; Figure 4.5). These strong recruitments coincide with the strongest El Niño events, which were felt in 1983 and 1998 (Figure D.1)

Second, it is apparent that fishing has reduced the total biomass of bigeye present in the EPO. This conclusion is drawn from the results of a simulation in which the biomass of bigeye tuna estimated to be present in the EPO if fishing had not occurred was projected over the historic period of the assessment (1975-2013), using the time series of estimated recruitment anomalies in the absence of fishing. To estimate the impact that different fisheries have had on the depletion of the stock, we ran simulations in which each gear was excluded and the model was run forward as in the no-fishing simulation (see Wang *et al*. 2009 for details of the simulation methodology). The results of this analysis are shown in Figure 4.8. It is clear that the longline fishery had the greatest impact on the stock prior to 1995, but with the decrease in effort by the longline fisheries, and the expansion of the floating-object fishery, at present the impact of the purse-seine fishery on the population is far greater than that of the longline fishery. The discarding of small bigeye has a small, but detectable, impact on the depletion of the stock. Overall, the current spawning biomass is estimated to be about 22% of that expected had no fishing occurred.

4.1.4. Average weights of fish in the catch

Trends in the average weights of bigeye caught by the fisheries that operate in the EPO are shown in Figure 4.9. The fisheries that catch bigeye in association with floating objects (Fisheries 1-5) have taken mostly small fish that, on average, weigh less than the critical weight, which indicates that these fisheries do not maximize the yield per recruit (Maunder and Hoyle 2007). The average weight of bigeye taken by the longline fisheries (Fisheries 12 and 19) has been around the critical weight, which indicates that these fisheries tend to maximize the yield per recruit. The average weight for all fisheries combined declined substantially after 1993 as the catch of bigeye in purse-seine sets on floating objects increased and that of bigeye by longline decreased.

The average weight in both the surface and longline fisheries declined around 1997-2000 as a strong cohort entered the fishery. The average weights then increased as the fish in that cohort increased in size. The average weight then declined again as that cohort was removed from the population.

The average weights for the surface fishery predicted by the model differ from the observed mean weights, particularly before 1984 (Figure 4.9, middle panel). The observed average weights are estimated by scaling up the length-frequency samples to the total catch, which differs from the method used in the stock assessment model, which uses the selectivity curves and estimated fishing mortality rates for each fishery to estimate the average weight. There was an apparent shift around 1985 from higher proportions of smaller (<75 cm) bigeye caught to higher proportions of medium-sized (75-125 cm) bigeye caught by the early floating-object fishery (Fishery 1; Figure 2.6a). Therefore, assuming two time blocks of selectivity (pre- and post-1985) in future assessments may help to minimize the differences between observed and predicted average weights for this early fishery.

Improvement was made in the previous full assessment (Aires-da-Silva and Maunder 2011) with regard to the differences identified in previous assessments between the observed weights of bigeye caught by Japanese longliners and the estimates predicted by the stock assessment model (Figure 4.9, bottom panel). This better correspondence between the observed and predicted average weights of bigeye results from the new assumption of two blocks of catchability and selectivity for the longline fisheries, split at 1990 (recommendation by the External Review). There are some exceptions, particularly in the late 1990s and early 2000s, which coincide with the expansion of the Chinese Taipei fishery in the EPO. The correspondence between the observed and predicted average weights of bigeye for the longline fishery has deteriorated for the late period (post-1990) under the current base case model configuration. Specifically, the model overestimates the average weight of bigeye caught by the longline fisheries. This result can be explained by the down-weighting of the size-composition data as well as the higher assumed value for the average size of the oldest fish (L_2).

4.2. Comparisons to external data sources

No comparisons to external data were made in this assessment.

4.3. Diagnostics

Diagnostics are discussed in the next four sections: data diagnostics, R_0 profile, residual analysis, and retrospective analysis.

4.3.1. R_0 profile

A new method for diagnosing over-weighting of size-composition data and misspecification of selectivity based on likelihood profiling of virgin recruitment is applied to the bigeye tuna assessment. Virgin recruitment (R_0; the equilibrium recruitment in the absence of fishing) is a common parameter in stock assessment that scales the population size. Information on population size comes from two main sources: 1) how catch changes indices of relative abundance; and 2) how the relative abundance changes in consecutive ages of age composition data (or appropriately adjusted size-composition data). Francis (2011) argues that abundance information should primarily come from indices of abundance and not from composition data. This is particularly true if the selectivity curve is not asymptotic. The diagnostic indicates over-weighting of composition data or misspecification in selectivity when the associated composition component of the likelihood profile for R_0 provides too much information about how low or how high R_0 can be. The selectivity curve for the fishery or survey related to that composition data should be modified, or the weighting of the composition data reduced, so that the composition data has little information on R_0. These features are indicative of model misspecification and should be minimized (Francis 2011).

The following aspects are revealed from the R_0 likelihood profile diagnostic applied to the results from the previous base case model configuration (Figure 4.10a). First, the R_0 maximum likelihood estimate at about 8.6 (in log space) is strongly driven by the dominant gradient provided by the size-composition data of Fishery 17, which consists of the late period of the Southern longline fishery, which assumes logistic selectivity (top panel, Figure 4.10a). The change in the negative log-likelihood is about 30 units higher compared to that of other data components. Second, there is a conflicting trend between the CPUE data fitted in the model as indices of abundance (bottom panel 4.10a). While the CPUE data of longline Fisheries 14, 16, and 17 are signaling the model for a low R_0 estimate, Fishery 15 is dominating among the CPUE data components towards a higher R_0 value.

The issues above were minimized through down-weighting of the size-composition data (4.10b). A multiplicative weighting factor of 0.05 (~1/30=0.03) was applied equally to all size-composition data.

4.3.2. Residual analysis

The model fits to the CPUE data from different fisheries are shown in Figure 4.11a-c. The model fits the longline CPUE observations of the early and late Central and Southern longline fisheries closely (Fisheries 14-15 and 16-17, respectively). The model fits particularly well to the CPUE data of the early and late Southern longline fishery (Fisheries 16 and 17). When compared to model fits from previous assessments (Figure 4.10 of Aires-da-Silva and Maunder 2011), the new assumption of two time blocks (early and late) for longline catchability and selectivity greatly improved the model fit to the CPUE increases observed around the mid-1980s (Fishery 16) and early 2000s (Fishery 17). The fits to the surface fisheries CPUE data series are less satisfactory.

Pearson residual plots are presented for the model fits to the size-composition data (Figures 4.12a-f). The gray and black circles represent observations that are, respectively, less than and greater than the model predictions. The areas of the circles are proportional to the absolute values of the residuals. There are several notable characteristics of the residuals. The model underestimates (black circles) the proportions of medium and small fish for the post-1993 floating-object fisheries. In particular, it underestimates the proportions of large fish during 1999-2002, when a strong cohort moved through the fishery.

No prominent residual pattern is identifiable in the model fit to size-composition data collected for both periods of the Northern (Fisheries 12 and 13) and Inshore (Fisheries 18 and 19) longline fisheries. However, there is still prominent residual pattern in the model fit to the Central (Fisheries 14 and 15), and the Southern (Fisheries 16 and 17) longline size-composition data. The residual pattern is particularly strong in the model fit to the length data from the late period of the Southern and Central longline fisheries (Fisheries 15 and 17; Figure 4.12d-e). Specifically, the proportions of medium-sized fish are systematically underestimated around two distinct length modes centered at about 100 and 150 cm. Possible reasons for the remaining pattern are further spatial misspecification issues, time-varying selectivity, and dome-shaped rather than logistic selectivity as specified for this fishery. The average fits to the observed size-compositions of the catches taken by the surface and longline fisheries defined in the stock assessment model are shown in Figure 4.12g. The model fits to the size-compositions of the recent catches of bigeye are also shown for different selected fisheries (Figures 4.12h-k). The model estimates more larger fish in the two longline fisheries with asymptotic selectivity than were observed.

The fit to the data, as measured by root mean square error, indicates that the model fits the CPUE index for the early and late Southern longline fisheries (Fisheries 16 and 17) better (CV = 0.11 and 0.13, respectively) than the CPUE index for the early and late Central longline fisheries (CV = 0.19 and 0.12, respectively). Although the model is not fitting to the CPUE series of the other fisheries, the root mean square error provides an indication of how well the model corresponds with these data. Disregarding the CPUE series of floating-object Fisheries 1 and 4 (early and Inshore) which are not considered reliable, the worst correspondence to the CPUE data are those for floating-object fisheries 3 and 5 (both with CV = 0.57), followed by the late Northern longline fishery (Fishery 13; CV = 0.43). These results are very similar to those obtained in the previous full assessment (Aires-da-Silva and Maunder 2011) in which the CPUE series of the floating-object fisheries were fitted in the model while estimating their CVs. With respect to the length-frequency data, the model fits the data better (as indicated by the estimated effective sample size) than is reflected by the assumed sample sizes in the likelihood functions. In an earlier assessment (Aires-da-Silva and Maunder 2007), a sensitivity analysis, using iterative reweighting, was conducted to investigate the weighting of the data sets. Specifically, the appropriate standard deviations and sample sizes for the likelihood functions were determined iteratively, based on the fit to the data. When iterative reweighting was applied, more weight was given to the length-frequency data, and the biomasses were estimated to be lower in the earlier and later segments of the historical period. However, increasing the weight on the size-composition data causes the composition data to have an even larger influence on the estimates of absolute abundance and abundance trends relative to the indices of abundance, which is not desirable.

4.3.3. Retrospective analysis

Retrospective analysis is useful for determining how consistent a stock assessment method is from one year to the next. Inconsistencies can often highlight inadequacies in the method. This approach is different from the comparison of recent assessments (Section 4.4), in which the model assumptions differ among these assessments, and differences would be expected. Retrospective analyses are usually carried out by repeatedly eliminating one year of data from the analysis while using the same method and assumptions. This allows the analyst to determine the change in estimated quantities as more data are included in the model. Estimates for the most recent years are often uncertain and biased. Retrospective bias does not necessarily indicate the magnitude and direction of the bias in the current assessment, only that the model may be misspecified.

Retrospective analyses were conducted by removing one year 2012), two years (2012 and 2011), three years (2012, 2011, 2010) and four years (2012, 2011, 2010, 2009) of data (Figures 4.13-4.15). Previous bigeye assessments showed strong retrospective patterns in the recent recruitment estimates, which propagated into the recent biomass levels. Specifically, the recruitment and biomass estimates from the base case model were lower than those estimated when the last years of data were not incorporated into the model. Retrospective bias in recent recruitment estimates was greatly minimized with the current base case model configuration (Figure 4.13) when compared to retrospective analyses presented in previous assessments. This improvement resulted from down-weighting the size-composition data, which indicates some model mis-specification in previous assessments (*e.g*., constant selectivity curves for the floating-object fisheries). Likewise, a retrospective pattern is not found in the recent estimates of the summary biomass produced by the current assessment (Figure 4.14). The exception is the run dropping the longest period of terminal years (four years), which resulted in a slight change of absolute scale. However, there is no retrospective bias in the time series of the spawning biomass ratios (SBR, see definition in Section 5.1) even when the last four years of data are dropped from the model (Figure 4.15).

4.3.4. Sensitivity analyses

The results of the three sensitivity analyses are presented in the appendices: sensitivity to (a) the stock–recruitment relationship (Appendix A); (b) assuming higher rates of adult natural mortality (M) for bigeye (Appendix B); and (c) assigning different weighting to the size-composition data (Appendix C). Here we describe differences in model fit and model prediction, and defer our discussion of differences in stock status until Section 5. A comparison of the likelihoods for the base case and sensitivity analyses is provided in Table 4.3a. In addition, a comparison of the average effective sample sizes estimated for the base case and the sensitivity analyses is given in Table 4.3b.

The steepness of the Beverton-Holt (1957) stock-recruitment relationship was set at 0.75. The estimates of the summary biomass (Figure A.1) are greater than those estimated in the base case assessment, but the trends are similar. Absolute recruitment estimates are slightly greater than those estimated in the base case (Figure A.2a), but the relative recruitment time series is similar to that of the base case (Figure A.2b). The trends in the SBR are very similar between the base case and the model that assumes a stock-recruitment relationship (Figure A.3). The estimated stock-recruitment relationship is shown in Figure A.4. A likelihood profile on the steepness parameter indicates that the model fits the data better for higher values of steepness, and that the base case (steepness = 1) produced the best fit. In addition, different data components all support a steepness of 1.

A sensitivity analysis was conducted to assuming several scenarios of adult natural mortality (*M*) for bigeye tuna of both sexes (Figure B.1). To be consistent with the absolute differences in *M* between females and males estimated from sex-ratio data, the absolute difference in *M* between sexes was kept the same in all sensitivity analyses. The biomass and recruitment estimates are very sensitive to adult *M* (Figures B.2 and B.3): they are greater for higher levels of adult *M*. As expected, absolute recruitment estimates increase in order to explain observed catches with higher natural mortality rates (Figure B.3a). As described in Aires-da-Silva, Maunder and Tomlinson (2010), assuming higher rates of adult *M* contributes to minimizing the "two-stanza" bigeye recruitment pattern (Section 4.1.2). A likelihood profile on adult *M* indicates that the model fits better for higher values of *M* than those assumed in the base case (Figure B.5). However, these rates seem unreasonably high for bigeye.

A sensitivity analysis was conducted to investigate the effect on assessment results from assigning different weights to the size-composition data. The absolute scale of the summary biomass was found to be strongly determined by the weighting assigned to the size-composition data, in particular the data from the Central and Southern longline fisheries (14-17) which include a late period that assumes logistic selectivity (Figure C.1a). The absolute scale of the biomasses is much less affected by the weighting assigned to the size-composition data of the floating-object fisheries (Figure C.1b). This results from the impact that different weighting assigned to the size-composition data has on virgin recruitment (R_0) which drives the absolute scale of the recruitment estimates (Figure C.2a and C.2b), and corresponding biomasses. Down-weighting the size-composition data of the longline fisheries greatly minimized the "two-stanza" recruitment pattern identified in previous assessments (Figure C.3a). The effect of down-weighting the size-composition data of the floating-object fisheries contributed little to minimizing this pattern (Figure C.3b).

Other sensitivity analyses, including investigation of growth estimation, environmental effects on recruitment and catchability, natural mortality, use of iterative reweighting, and use of two time blocks for selectivity and catchability for the southern longline fishery, were conducted by Watters and Maunder (2002), Harley and Maunder (2004, 2005), Maunder and Hoyle (2007), and Aires-da-Silva and Maunder (2007, 2009, 2010a, b, c).

4.4. Comparison to previous assessment

There are substantial differences between the summary and the spawning biomasses (Figures 4.15 and 4.16, respectively) estimated by the current and the previous stock assessment models (Aires-da-Silva and Maunder 2010). These differences are mainly due to reduced size-composition data weighting, in particular to down-weighting of the size-composition data. As explained early in Section 4.3,.Diagnostics, the size-composition data of longline Fisheries 15 and 17 were found to be dominating over other data components in the previous base case model configuration. Down-weighting all size-composition data minimized this dominance and balanced out the contribution of all data components, in particular the longline CPUE data which are believed to provide the most reliable information on absolute scale (the virgin recruitment parameter, R_0). R_0 increased in the current assessment, which explains its higher biomass levels when compared to those produced by the previous assessment (Figures 4.16 and 4.17). However, relative trend is very similar between the two assessments, except in the earliest and the later years of the assessment. The absolute and relative differences in the biomasses in the early years are due to higher uncertainty in the estimates for the initial conditions (Figure 4.7) resulting from the down-weighting of the size compositions. Those differences in the recent years are more likely due to the new data available for those years, in particular the recent declines observed in the longline CPUE data. The relative trends in the SBRs are also very similar, with final SBR levels being very similar (at about 0.24 at the start of 2012; Figure 4.18). The recruitments estimated by the current assessment are generally higher than the estimates from the previous assessment prior to 1994 when the floating-object fisheries expanded, and lower after that year (Figure 4.19). This reflects a reduction in the magnitude of the "two-stanza" recruitment pattern reported in previous assessments (see Section 4.1.2. Recruitment). In fact, the difference in average recruitment estimates between the early and late period have been greatly minimized under the current base case model configuration (Figure 4.19a). In addition, the recent recruitments estimated in the current assessment are generally lower than those from the previous assessment (Figure 4.19b). This result is explained by improvements made in the current assessment on the retrospective pattern of recent recruitments (see Section 4.3.3, Retrospective analysis)

4.5. Summary of results from the assessment model

There have been important changes in the amount of fishing mortality caused by the fisheries that catch bigeye tuna in the EPO. On average, the fishing mortality of bigeye less than about 15 quarters old has increased substantially since 1993, and that of fish more than about 15 quarters old has increased to a much lesser extent. The increase in fishing mortality of the younger fish was caused by the expansion of the fisheries that catch bigeye in association with floating objects.

Over the range of spawning biomasses estimated by the base case assessment, the abundance of bigeye recruits appears to be unrelated to the spawning potential of adult females at the time of hatching.

There are two important features in the estimated time series of bigeye recruitment which have been identified under the previous assessment model configuration. In previous assessments, estimates of recruitment before 1993 were very uncertain, as the floating-object fisheries were not catching significant amounts of small bigeye. In addition, a "two-stanza" pattern was prominent in the time series of bigeye recruitments for the EPO. This pattern was characterized by an early period of low recruitments (1975-1993) followed by a period of relatively large recruitments (1994-2009) which coincided with the expansion of the fisheries that catch bigeye in association with floating objects. The "two-stanza" recruitment pattern has been greatly reduced under the current base case model configuration.

A prominent feature in the time series of estimated bigeye recruitment is that the highest recruitment peaks of 1983 and 1998 coincide with the strongest El Niño events during the historic period of the assessment. Recently, the recruitments were below average during 2007-2009, and have fluctuated around average during 2010-2012.

The biomass of 3+-quarter-old bigeye increased during 1983-1985, and reached its highest historic peak of about 1,378 thousand t in 1986, after which it gradually decreased to a historic low of about 428 thousand t at the beginning of 2013, with two intermediate peaks at 2001 and 2009. The spawning biomass has generally followed a trend similar to that of the biomass of 3+-quarter-old bigeye, but with a 1- to 2-year time lag. There is uncertainty in the estimated biomasses of both 3+-quarter-old bigeye and spawners. Nevertheless, it is apparent that fishing has reduced the total biomass of bigeye in the EPO. The biomasses of both 3+-quarter-old fish and spawners are estimated to have rebuilt during 2004-2010, after which they gradually declined to their lowest historical levels at the start of 2013. A simulation study indicates that the population increase may be attributed to the effect of the IATTC tuna conservation resolutions which started in 2004 (see Section 6.2.3). Additional factors likely contributing to this increase are above-average recruitments and reduced longline effort in the EPO in the last decade. The most recent period dominated by below-average recruitments (2007-2012) could explain the declining trend observed since 2010.

The estimates of summary biomass are moderately sensitive to the steepness of the stock-recruitment relationship. Specifically, the estimates of biomass are greater than those estimated in the base case assessment, but the trends are similar. The relative trend in recruitment is similar to the base case.

The estimated biomass and recruitment time series are very sensitive to the assumed rate of adult natural mortality for bigeye. Biomass and recruitment estimates increase with higher levels of adult M. A likelihood profile on adult M indicates that the model fits better to all data components for higher values of adult *M*, which indicates higher productivity for the bigeye stock than is estimated by the base case model. However, the higher rates of natural mortality seem unreasonably high for bigeye.

The estimated biomass and recruitment time series are very sensitivity to the weighting assigned to the size composition data, in particular the data from the Central and Southern longline fisheries (14-17), which include a later period assuming logistic selectivity. Higher biomasses and recruitments are obtained if these data are down-weighted in the model.

5. STOCK STATUS

The status of the stock of bigeye tuna in the EPO is assessed by considering calculations based on the spawning biomass and the maximum sustainable yield (MSY). MSY is defined as the largest long-term average catch or yield that can be taken from a stock or stock complex with constant fishing mortality under prevailing ecological and environmental conditions.

Maintaining tuna stocks at levels that produce the MSY is the management objective specified by the IATTC Convention. The IATTC has not adopted any target or limit reference points for the stocks that it manages, but some possible reference points are described in the following subsections.

5.1. Assessment of stock status based on spawning biomass

The spawning biomass ratio (the ratio of the current spawning biomass to that of the unfished stock; SBR), described by Watters and Maunder (2001), has been used to define reference points in many fisheries. It has a lower bound of zero. If it is near zero, the population has been severely depleted, and is probably overexploited. If the SBR is one, or slightly less than that, the fishery has probably not reduced the spawning stock. If the SBR is greater than one, it is possible that the stock has entered a regime of increased production.

Various studies (*e.g.* Clark 1991, Francis 1993, Thompson 1993, Mace 1994) suggest that some fish populations are capable of producing the MSY when the SBR is about 0.3 to 0.5, and that some fish populations are not capable of producing the MSY if the spawning biomass (*S*) during a period of exploitation is less than about 0.2. Unfortunately, the types of population dynamics that characterize tuna populations have generally not been considered in these studies, and their conclusions are sensitive to assumptions about the relationship between adult biomass and recruitment, natural mortality, and growth rates. In the absence of simulation studies that are designed specifically to determine appropriate SBR-based reference points for tunas, estimates of SBR can be compared to an estimate of SBR corresponding to the MSY ($SBR_{MSY} = S_{MSY}/S_{F=0}$).

Estimates of SBR for bigeye tuna in the EPO have been computed from the base case assessment. Estimates of the spawning biomass during the study period (1975-2012) are presented in Section 4.1.3. The SBR corresponding to the MSY (SBR_{MSY}) is estimated to be about 0.20.

At the beginning of January 2013, the spawning biomass of bigeye tuna in the EPO was at about 115 thousand tons (Figure 4.7). At that time the SBR was about 0.22, 7% higher than the level corresponding to the MSY (Figure 5.1). The SBR trend follows that observed for the spawning biomass (see Section 4.1.3)

5.2. Assessment of stock status based on MSY

Maintaining tuna stocks at levels that permit the MSY to be taken is the management objective specified by the IATTC Convention. Watters and Maunder (2001) describe how the MSY and its related quantities are calculated. These calculations have, however, been modified to include, where applicable, the Beverton-Holt (1957) stock-recruitment relationship (see Maunder and Watters (2003) for details). It is important to note that estimates of the MSY and its associated quantities are sensitive to the steepness of the stock-recruitment relationship (Section 5.4), and, for the base case assessment, steepness was fixed at 1 (an assumption that recruitment is independent of stock size); however, a sensitivity analysis (steepness = 0.75) is provided to investigate the effect of a stock-recruitment relationship.

The MSY-based estimates were computed with the parameter estimates from the base case assessment and estimated fishing mortality patterns averaged over 2010 and 2012. Therefore, while these MSY-based results are currently presented as point estimates, there are uncertainties in the results.

At the beginning of January 2013, the spawning biomass of bigeye tuna in the EPO appears to have been about 8% higher than S_{MSY}, and the recent catches are estimated to have been about 3% lower than the MSY (Table 5.1).

If fishing mortality is proportional to fishing effort, and the current patterns of age-specific selectivity (Figure 4.2) are maintained, F_{MSY} is about 5% higher than the current level of effort.

The MSY-based quantities are estimated by assuming that the stock is at equilibrium with fishing and ecological conditions. However, the catch of bigeye by the surface fleet may be determined largely by the strength of cohorts recruited to the fishery. For example, the catches of bigeye taken by the surface fleet declined when the large cohorts recruited during 1995-1998 were no longer vulnerable to those fisheries.

Estimates of the MSY, and its associated quantities, are sensitive to the age-specific pattern of selectivity that is used in the calculations. The MSY-based quantities described previously were based on an average selectivity pattern for all fisheries combined (estimated from the current allocation of effort among fisheries). Different allocations of fishing effort among fisheries would change this combined selectivity pattern. To illustrate how the MSY might change if the effort is reallocated among the various fisheries that catch bigeye in the EPO, the previously-described calculations were repeated, using the age-specific selectivity pattern estimated for each group of fisheries (Table 5.2). If only the purse-seine fishery were operating, the MSY would be about 27% less. If bigeye were caught only by the longline fishery, the MSY would about 139% greater than that estimated for all gears combined. To achieve this MSY level, longline effort would need to be increased by 857%.

The MSY-related quantities vary with the size composition of the catch. The evolution of four of these quantities during 1975-2012 is shown in Figure 5.2. Before the expansion of the floating-object fishery that began in 1993, MSY was greater than the current MSY, and the fishing mortality was less than that corresponding to MSY (Figure 5.2). The MSY increased about 24,000 tons with respect to the previous assessment estimate (Aires-da-Silva and Maunder 2012). This is explained by an increase in R_0 after down-weighting the size-composition data in the current base case.

When MSY is estimated using the average fishing mortality rates for 2010-2011, it is about 1,575 t (1%) higher than that of the base case.

The historical time series of exploitation rates, spawning biomass, and summary biomasses relative to potential MSY-based target and interim limit reference points (0.5 S_{MSY} and 1.3 F_{MSY}) are shown in Figures 5.3a and 5.3b, respectively. Overall, results from the current base case model indicate that the target reference points were not exceeded during the historic period of the assessment (1975-2012). According to the base case results, the most recent estimate indicates that the bigeye stock in the EPO is likely not overfished ($S>S_{MSY}$) and that overfishing is not taking place ($F<F_{MSY}$). In fact, current exploitation is very close to the MSY target reference points. Likewise, limit reference points have not been exceeded under the current base case model. These interpretations, however, are subject to uncertainty, as indicated by the approximate confidence intervals around the most recent estimate in the phase plots (model precision). Also, they are strongly dependent on the assumptions made about the steepness parameter of the stock-recruitment relationship, the assumed levels of adult natural mortality, and the weighting assigned to the size-composition data (model uncertainty) (Figure 5.3c). A simulation was conducted to evaluate the effects of the IATTC tuna conservation resolutions implemented during 2004-2012 (see Section 6.2.3) on potential MSY-based target reference points, particularly in recent years. Without the management actions established by the resolutions since 2004, the base case model predicts that the bigeye stock would have been currently overfished ($S<S_{MSY}$) and overfishing ($F>F_{MSY}$) would have been occurring (Figure 5.3d).

5.3. Sensitivity to alternative parameterizations and data

Yields and reference points are highly sensitive to alternative model assumptions, input data, and the periods assumed for fishing mortality (Tables 5.1 and 5.2).

The sensitivity analysis that included a stock-recruitment relationship with a steepness of 0.75 estimated the SBR required to support the MSY to be at 0.30, compared to 0.20 for the base case assessment (Table 5.1). The sensitivity analysis for steepness = 0.75 estimated an *F* multiplier of 0.82, considerably lower than that for the base case assessment (1.05). Assuming lower values of steepness results in much lower *F* multipliers (Table A.1, Figure A.6). Although the base case model results indicate that the recent spawning biomass level is above that corresponding to MSY (S_{recent}/S_{MSY} = 1.08), this ratio is estimated to be less than 1 for assumed steepness values lower than 1.

When lower rates of adult natural mortality are assumed for both sexes of bigeye, the stock status is more pessimistic than the base case results (lower *F* multiplier). Assuming higher adult natural mortality rates produces the opposite effect (higher *F* multiplier). However, the highest rates considered in this sensitivity analysis seem biologically unrealistic for bigeye. Likewise, the S_{recent}/S_{MSY} ratio is highly sensitive to the assumed rates of adult natural mortality: specifically, it decreases and increases towards, respectively, lower and higher assumed values of *M*,.

Finally, the management quantities estimated in the bigeye stock assessment are highly sensitive to the weighting of the size-composition data (Table C.1). In particular, the weighting factors (λ) assigned to the size-composition data of the Central and Southern longline fisheries (Fisheries 14 to 17) strongly determine the bigeye stock status. If the original sample sizes input in the model for these fisheries are not down-weighted (λ = 1), the management quantities produced are pessimistic (*F* multiplier = 0.51; S_{recent}/S_{MSY} = 0.32). This result is due to the dominance of the size-composition data of longline Fisheries 15 and 17 (with assumed logistic selectivities) in determining absolute scale (the R_0 parameter) in the model. Once this dominance is balanced out by down-weighting these data (λ = 0.05), other data components (mainly the longline CPUE) are allowed to also inform the model on absolute scale (R_0). As a result, management quantities are less pessimistic (see R_0 profile in Section 4.3, Diagnostics). The effect on the *F* multiplier of assigning different weight factors (λ) equally applied to the size-composition data for all fisheries is shown on Figure C.5.

5.4. Summary of stock status

At the beginning of January 2013, the SBR of bigeye tuna in the EPO was at about 0.22, about 8% higher than the level corresponding to the MSY.

Recent catches are estimated to have been 3% lower than the MSY level (Table 5.1). If fishing mortality is proportional to fishing effort, and the current patterns of age-specific selectivity are maintained, the level of fishing effort corresponding to the MSY is about 5% higher than the current (2010-2012) level of effort. The MSY of bigeye in the EPO could be maximized if the age-specific selectivity pattern were similar to that for the longline fishery, because it catches larger individuals that are close to the critical weight. Before the expansion of the floating-object fishery that began in 1993, the MSY was greater than the current MSY, and the fishing mortality was less than F_{MSY} (Figure 5.2).

The management quantities are sensitive to how the assessment model is parameterized and the data that are included in the assessment. In particular, the *F* multiplier and S_{recent}/S_{MSY} are highly sensitive to the assumptions made about the steepness parameter of the stock-recruitment relationship, the rates of adult natural mortality assumed for both sexes of bigeye, and the weighting assigned to the size composition data in the model.

6. SIMULATED EFFECTS OF TUNA CONSERVATION RESOLUTIONS AND FUTURE FISHING OPERATIONS

A simulation study was conducted to gain further understanding on the effects of the IATTC tuna conservation resolutions implemented during 2004-2012 (C-04-09, C-06-02, C-09-01, C-10-01, and C-11-01), and of how changes in the amount of fishing effort exerted by the tuna fisheries in the EPO in the future might simultaneously affect the stock of bigeye tuna in the EPO and the catches of bigeye by the various fisheries.

In order to evaluate the effects of the resolutions, a model was constructed in which the fishing effort (fishing mortality) of different fisheries was increased to simulate a scenario in which no resolutions were in force during 2004-2012. Beginning in 2004, this model was then projected into the future, using the time series of historic recruitment anomalies estimated by the base case model.

With respect to future fishing operations, different scenarios were constructed to define how the various fisheries that catch bigeye in the EPO would operate in the future, and also to define the future dynamics of the bigeye stock. The assumptions that underlie these scenarios are outlined in Sections 6.1 and 6.2. The method is implemented by extending the assessment model an additional 10 years (40 quarters), with exploitation rates equal to 1) the average for 2010-2012 and 2) F_{MSY}. No catch or length-frequency data are included for these future years. The recruitments for the 10 years are estimated as in the assessment model, with a lognormal penalty with a standard deviation of 0.6. The uncertainty in the projected recruitment is implemented following Maunder *et al*. (2006).

6.1. Assumptions about fishing operations

6.1.1. Fishing effort

Projection studies were carried out to investigate the influence of different levels of fishing effort (fishing mortality rates) on the stock biomass and catch.

The analyses carried out were:

1. Quarterly fishing effort (fishing mortality rates) during 2004-2012 was increased to simulate a scenario in which IATTC tuna conservation resolutions C-04-09, C-06-02, C-09-01 and C-11-01 had not been in force.
    a. Resolutions C-04-09 and C-06-02 call for restrictions on purse-seine effort and longline catches during 2004-2007: a six-week closure during the third or fourth quarter of the year for purse-seine fisheries, and longline catches not to exceed 2001 levels. For 2004-2007, fishing mortality rates were increased by 86% for the purse-seine fisheries in the third quarter.
    b. Resolution C-09-01, adopted in 2009, establishes more restrictive measures than previous resolutions: purse-seine vessels must stop fishing for a period of 59 days in 2009, 62 days in 2010, and 73 days (12 weeks) in 2011 in the entire EPO, and in the area from 96° to 110°W between 4°N and 3°S from 29 September to 29 October. The "no resolution" scenario results in a 212% increase in fishing mortality by purse-seine fisheries in the third quarter of 2009..
    c. Resolution C-11-01 establishes a 62-day closure of the EPO for purse-seine vessels during each of the years 2010-2013, plus the closure of the high-seas area, as in C-09-01. The "no resolution" scenario results in a 248% increase in fishing mortality by purse-seine fisheries in the third quarter of 2009.
    d. Longline fishing mortality for 2004 and later is set to the actual fishing mortality or the fishing mortality, by quarter, averaged over 2001-2003, whichever is larger.
2. Quarterly fishing mortality rates for each year in the future were set equal to the average rates during 2010-2012, to simulate that fishing mortality rates are maintained at current levels (F_{cur}) – a *status quo* exploitation strategy. An additional analysis was carried out that estimates the population status if fishing effort is approximated to the levels corresponding to MSY (F_{MSY}).

6.2. Simulation results

The simulations were used to predict future levels of the spawning biomass, SBR, the total annual catch taken by the primary surface fisheries that would presumably continue to operate in the EPO (Fisheries 2-5 and 7), and the total annual catch taken by the longline fleet (Fisheries 12-23). There is probably more uncertainty in the future levels of these outcome variables than is suggested by the results presented in Figures 6.1-6.6. The amount of uncertainty is probably underestimated, because the simulations were conducted under the assumption that the stock assessment model accurately describes the dynamics of the system, with no account taken of variation in catchability.

6.2.1. Current fishing mortality rates (F_{cur}) – *status quo*

Projections were undertaken, assuming that fishing mortality rates would remain at the average 2010-2012 levels.

SBR is estimated to have gradually increased since 2005 and attained a level of 0.31 at the start of 2010 (Figure 5.1). This increase may be attributed to the combined effect of three consecutive years of above-average annual recruitments (2004-2006; Figure 4.5b), IATTC tuna conservation resolutions during 2004-2009, and decreased longline fishing effort in the EPO (Section 6.2.3). Regardless of continuing IATTC conservation resolutions throughout 2010-2012, the rebuilding trend was not sustained after 2010, and the SBR gradually declined to its lowest historic level of 0.22 at the start of 2013. This decline may be explained by a series of predominantly below-average recruitments in recent years (2007-2012; Figure 4.5b). In fact, a simulation run assuming average recruitments since 2004, when the IATTC resolutions began, shows that the SBR decline after its 2010 peak would have been much less, and that the SBR would have stabilized above the level corresponding to MSY (Figure 6.5).

Under current levels of fishing mortality, and if recent levels of effort and catchability continue and average recruitment levels persist, the SBR is predicted to further decline and reach a historic low of 0.19 by 2015 (Figure 6.1a). After that, the SBR is predicted to gradually increase and stabilize at about 0.21 around 2018, very close to the level corresponding to MSY. Under the *status quo* scenario and the assumption of no stock-recruitment relationship, purse-seine catches are predicted to increase from 2013-2015 and then stabilize at around 71,000 t in 2016 (Figure 6.3a, upper panel). At current effort, longline catches are predicted to slightly decrease to around 32,000 t in 2015 and then increase and stabilize at about 35,000 t in 2020 (Figure 6.3a, lower panel). If a stock-recruitment relationship is included, the catches of the surface and longline fisheries would stabilize at lower levels, at around 66,000 and 33,000 t. respectively (Figure 6.3a). Predicted catches for both gears are based on the assumption that the selectivity of each fleet will remain the same and that catchability will not increase as abundance declines. If the catchability of bigeye increases at low abundance, catches will, in the short term, be greater than those predicted here.

6.2.2. Fishing mortality rates at MSY (F_{MSY})

Maintaining tuna stocks at levels that permit MSY to be taken is the management objective specified by the IATTC Convention. To assess the impact on the bigeye stock of an exploitation strategy targeting MSY, we projected the population forward 10 years, assuming the fishing mortality rates (fishing effort) corresponding to MSY (F_{MSY}). Projected catches for both surface and longline fisheries at F_{MSY} stabilize at about the same levels obtained at F_{cur} (less than 1,000 t difference; Figure 6.3a). The long-term SBR levels which would be attained if the current fishing mortalities persist in the future (0.22) are only slightly higher than those corresponding to the MSY (0.20) (Figure 6.4).

6.2.3. Effect of IATTC tuna conservation resolutions

A comparison of the spawning biomass predicted with and without the restrictions of the resolutions shows substantial differences (Figures 6.4 and 6.6). Without the effect of the resolutions from 2004 to 2012, the SBR would have declined well below the level corresponding to MSY (0.2). Future projections assuming the "no resolution" scenario and average recruitment conditions indicate that the SBR would decline and stabilize at around 0.08, a level that would not support MSY. Simulations using average recruitment since 2004 show that recruitment contributed to the increase in spawning biomass in the late 2000s, but it was minor compared to the management actions (Figure 6.5). The simulations also showed that the recent decline in spawning biomass is partly due to lower recruitment.

6.2.4. Sensitivity analysis

The analysis that includes a stock-recruitment relationship indicates that the population is substantially below SBR_{MSY} and will remain at this level at current effort levels (Figure 6.1b).

6.3. Summary of the simulation results

At current effort levels, the population is likely to remain above the level corresponding to MSY.

These simulations are based on the assumption that selectivity and catchability patterns will not change in the future. Changes in targeting practices or increasing catchability of bigeye as abundance declines (*e.g.* density-dependent catchability) could result in differences from the outcomes predicted here.

7. FUTURE DIRECTIONS

7.1. Collection of new and updated information

The IATTC staff intends to continue its collection of catch, effort, and size-composition data from the fisheries that catch bigeye tuna in the EPO. Updated and new data will be incorporated into the next stock assessment.

The IATTC staff will continue to compile catch, effort and size-composition data for the longline fisheries operating in the EPO. In particular, it will attempt to obtain data for recently-developed and growing fisheries.

7.2. Refinements to the assessment model and methods

The IATTC staff will continue developing the Stock Synthesis (Version 3) assessment model for bigeye tuna in EPO. Much of the progress will depend on how the Stock Synthesis software is modified in the future. The following changes would be desirable for future assessments:

1. Determine appropriate weighting of the different data sets;
2. Include available tagging data in the assessment;
3. Explore alternative assumptions on stock structure (spatial analysis);
4. Investigate the need for logistic selectivities;
5. Improve growth estimates as more large tagged bigeye tuna are recovered;
6. Investigate possible discrepancies in some of the size-composition data.

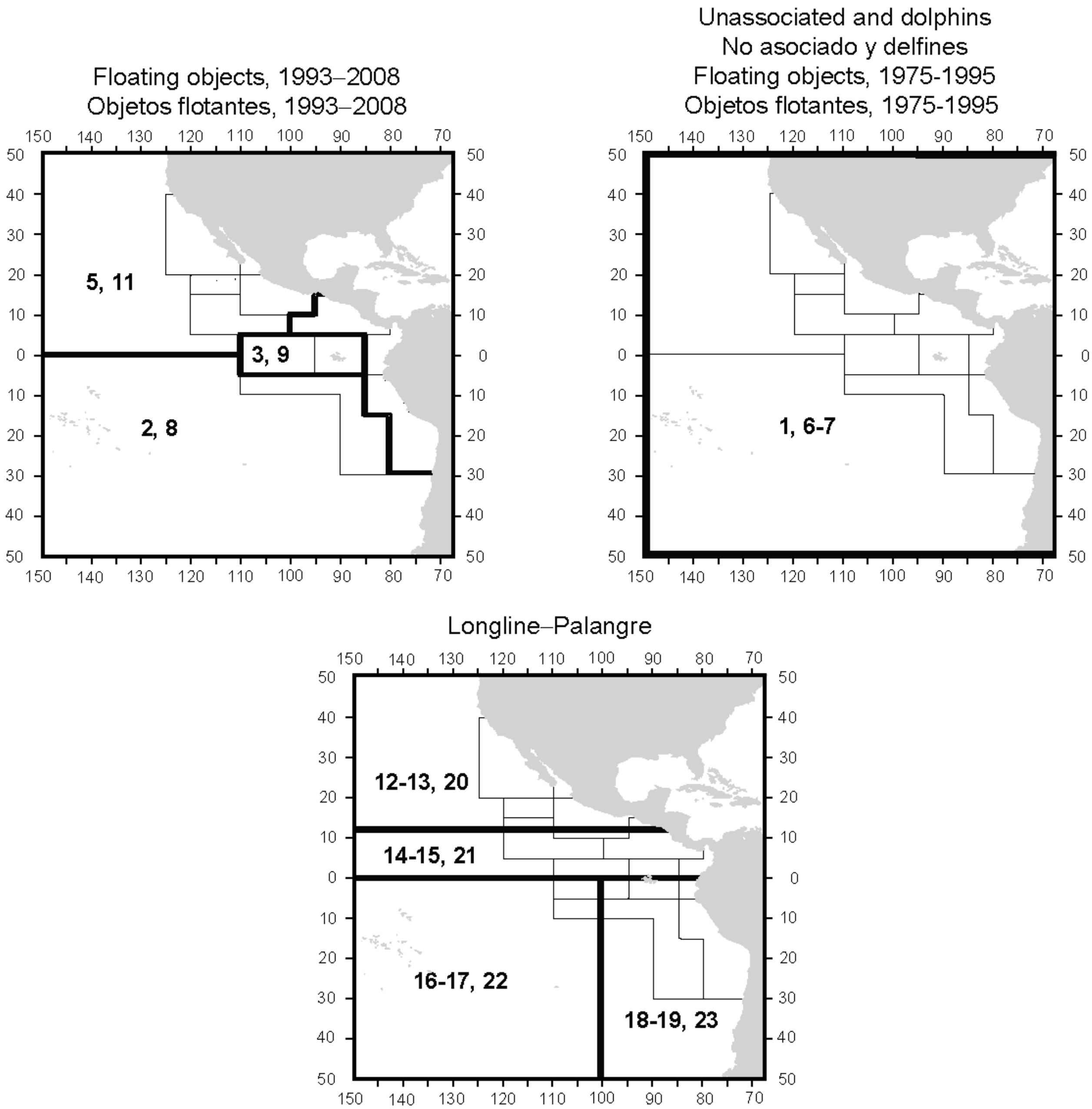

FIGURE 2.1. Spatial extents of the fisheries defined for the stock assessment of bigeye tuna in the EPO. The thin lines indicate the boundaries of 13 length-frequency sampling areas, the bold lines the boundaries of each fishery defined for the stock assessment, and the bold numbers the fisheries to which the latter boundaries apply. The fisheries are described in Table 2.1.

FIGURA 2.1. Extensión espacial de las pesquerías definidas para la evaluación de la población de atún patudo en el OPO. Las líneas delgadas indican los límites de 13 zonas de muestreo de frecuencia de tallas, las líneas gruesas los límites de cada pesquería definida para la evaluación de la población, y los números en negritas las pesquerías correspondientes a estos últimos límites. En la Tabla 2.1 se describen las pesquerías.

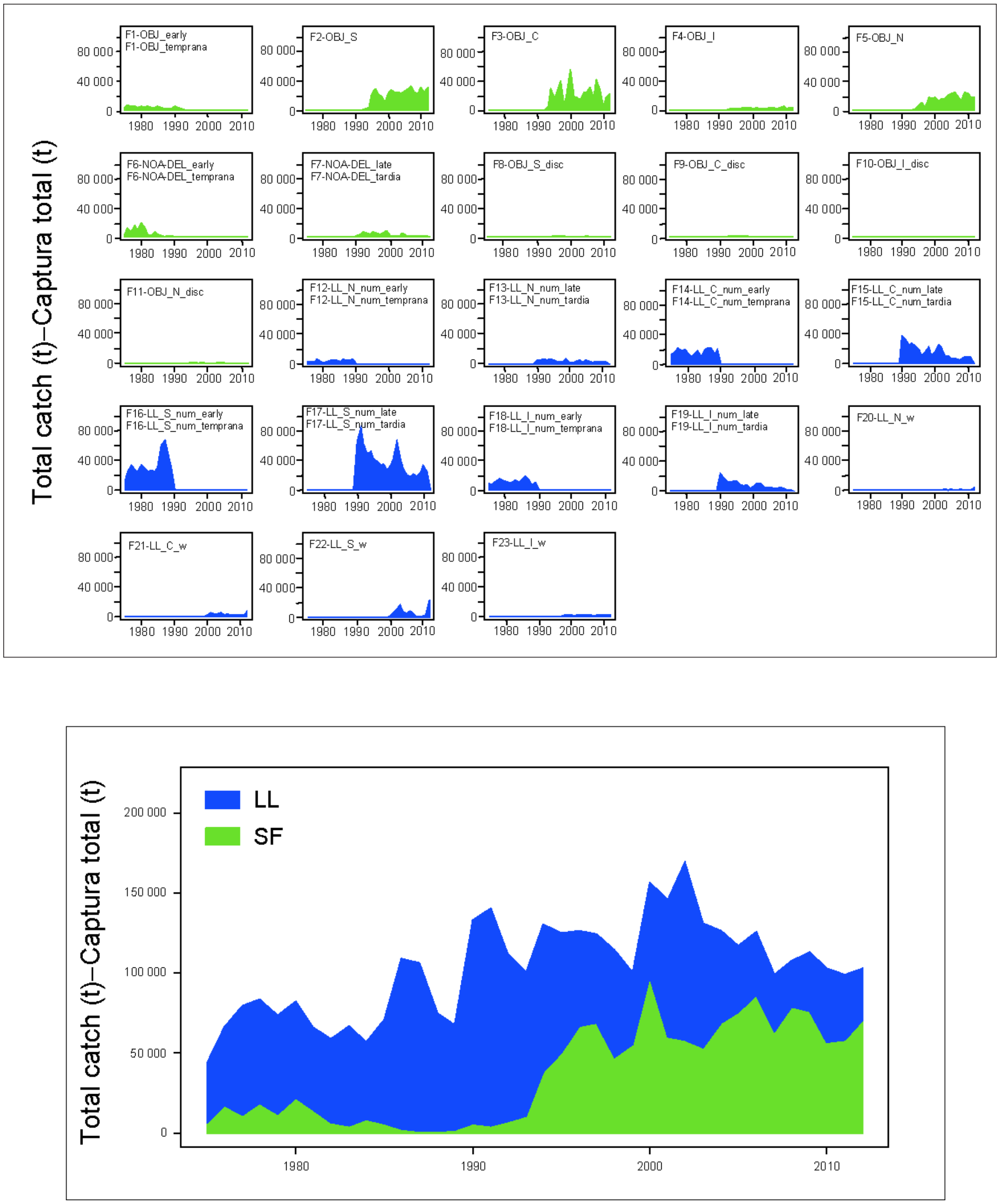

FIGURE 2.2. Upper panel: Annual catches of bigeye tuna taken by the fisheries defined for the stock assessment of that species in the EPO (Table 2.1). The stock assessment model uses catches in numbers of fish for longline Fisheries 12-19, but the figure shows catches in weight estimated by the model for those fisheries. The numbers in the panels correspond to the numbers designating the fisheries in Table 2.1. Lower panel: Annual catches of bigeye tuna pooled by longline and surface fisheries in the EPO. LL = longline; SF = surface fisheries; t = metric tons.

FIGURA 2.2. Panel superior: Capturas anuales de atún patudo por las pesquerías definidas para la evaluación de la población de esa especie en el OPO (Tabla 2.1). El modelo de evaluación usa capturas en número de peces para las Pesquerías 12 a 19, pero en la figura se presentan capturas en peso estimadas por el modelo para esas pesquerías. El número en cada panel corresponde a los números que designan las pesquerías en la Tabla 2.1. Panel inferior: Capturas anuales de atún patudo en el OPO de las pesquerías de palangre y de superficie combinadas. LL = palangre; SF = pesquerías de superficie; t = toneladas métricas.

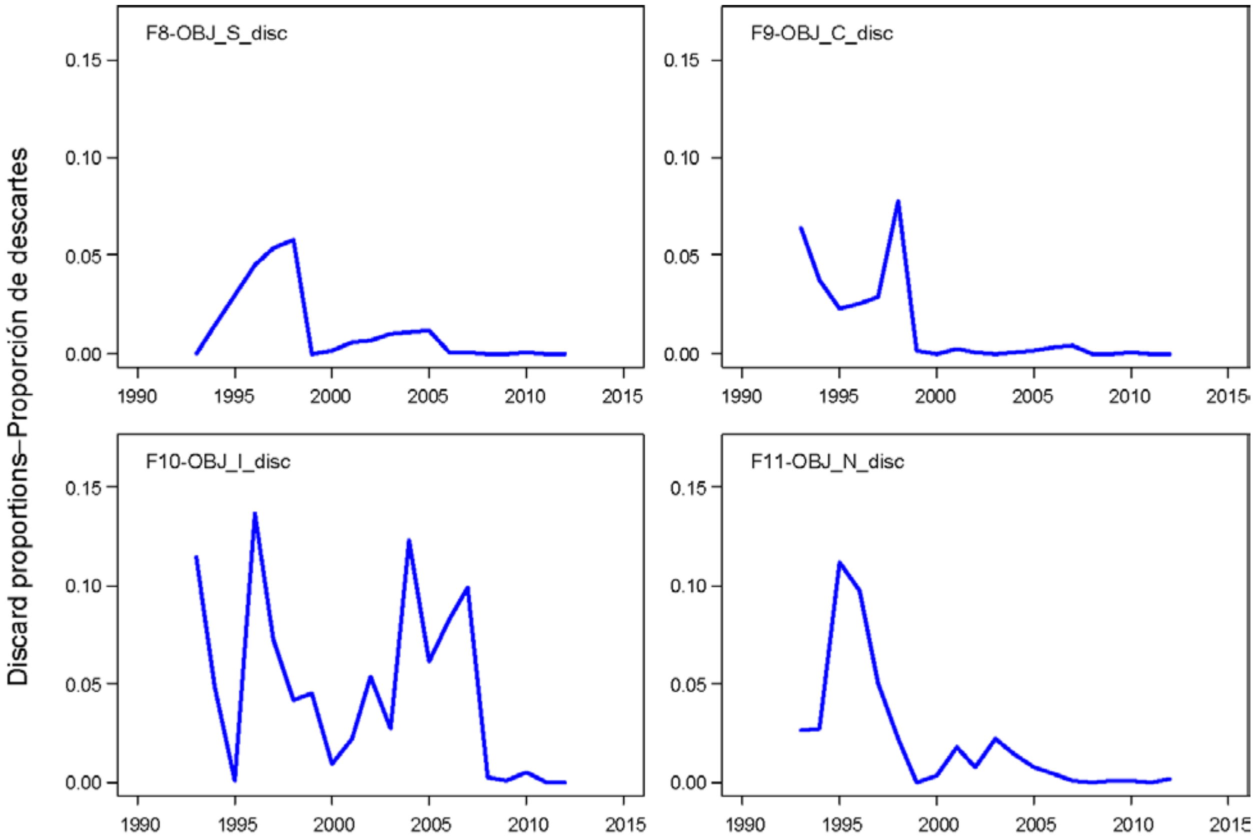

FIGURE 2.3. Weights of discarded bigeye tuna as proportions of the total (retained plus discarded) annual catches for the four floating-object fisheries. Fisheries 2-5 are the "real" fisheries, and Fisheries 8-11 are the corresponding discard fisheries. The numbers in the panels correspond to the numbers designating the fisheries in Table 2.1.

FIGURA 2.3. Pesos de atún patudo descartado como proporción de las capturas anuales totales (retenidas más descartadas) de las cuatro pesquerías sobre objetos flotantes. Las Pesquerías 2-5 son las pesquerías "reales", y las Pesquerías 8-11 las pesquerías de descarte correspondientes. El número en cada panel corresponde a los números que designan las pesquerías en la Tabla 2.1.

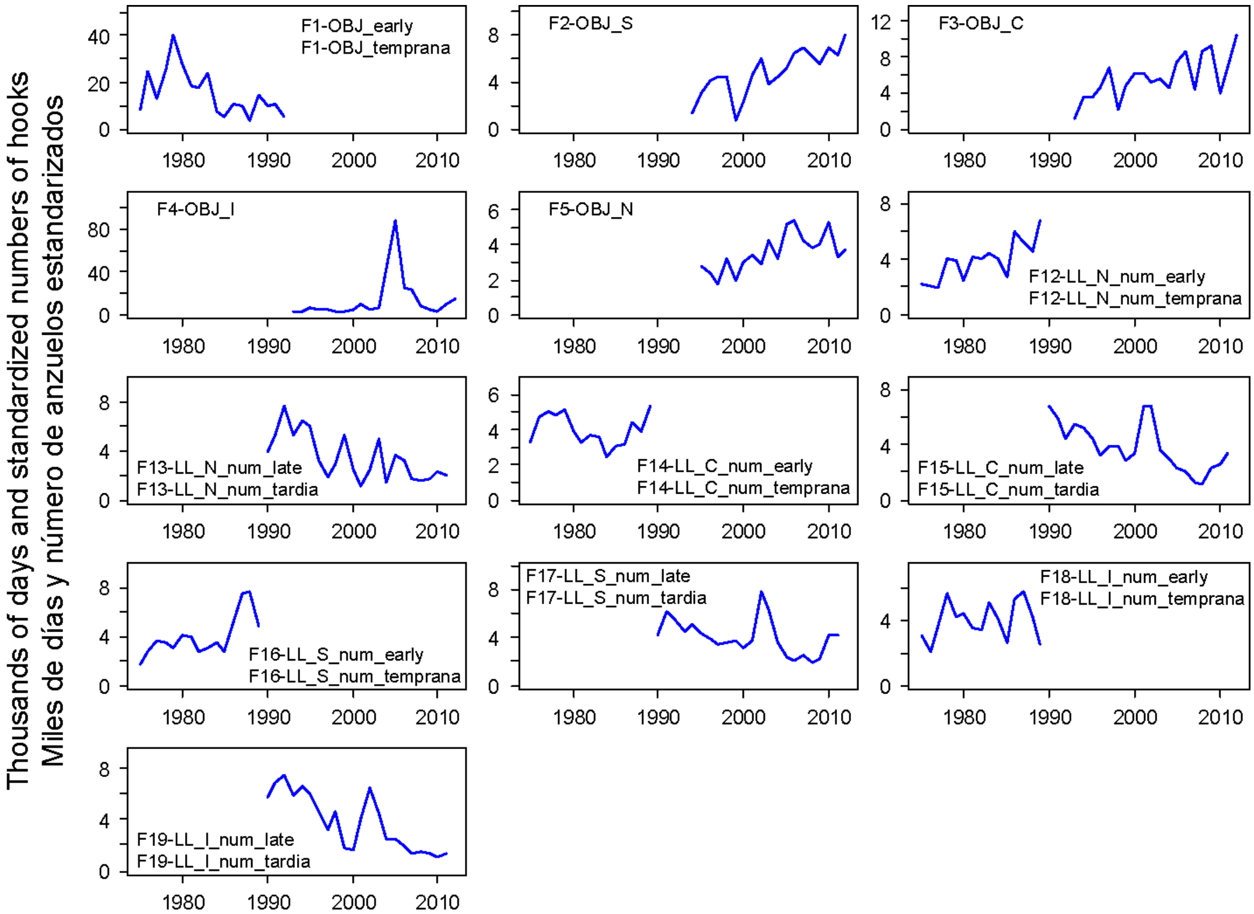

FIGURE 2.4. Annual fishing effort by purse-seine vessels of more than 363 metric tons carrying capacity and longline vessels in the fisheries defined for the stock assessment of bigeye tuna in the EPO (Table 2.1). The effort for Fisheries 1-5 is in days fished, and that for Fisheries 12-19 in standardized numbers of hooks. Fishing effort is not shown for Fisheries 6 and 7, since two gears (purse seine and pole-and-line) were combined for these fisheries. Fishing effort for the discard fisheries (8-11) is that of their corresponding 'real' fisheries (2-5). Note that the vertical scales of the panels are different. The numbers in the panels correspond to the numbers designating the fisheries in Table 2.1.

FIGURA 2.4. Esfuerzo de pesca anual por buques de cerco de más de 363 toneladas métricas de capacidad de acarreo y buques de palangre en las pesquerías definidas para la evaluación de la población de atún patudo en el OPO (Tabla 2.1). Se expresa el esfuerzo de las Pesquerías 1-5 en días de pesca, el de las Pesquerías 12-19 en número estandarizado de anzuelos. No se ilustra el esfuerzo de pesca de las Pesquerías 6 y 7, ya que se combinaron dos artes (red de cerco y caña) en las mismas. El esfuerzo de pesca de las pesquerías de descarte (8-11) es aquél de sus pesquerías 'reales' correspondientes (2-5). Nótese que las escalas verticales de los recuadros son diferentes. El número en cada panel corresponde a los números que designan las pesquerías en la Tabla 2.1.

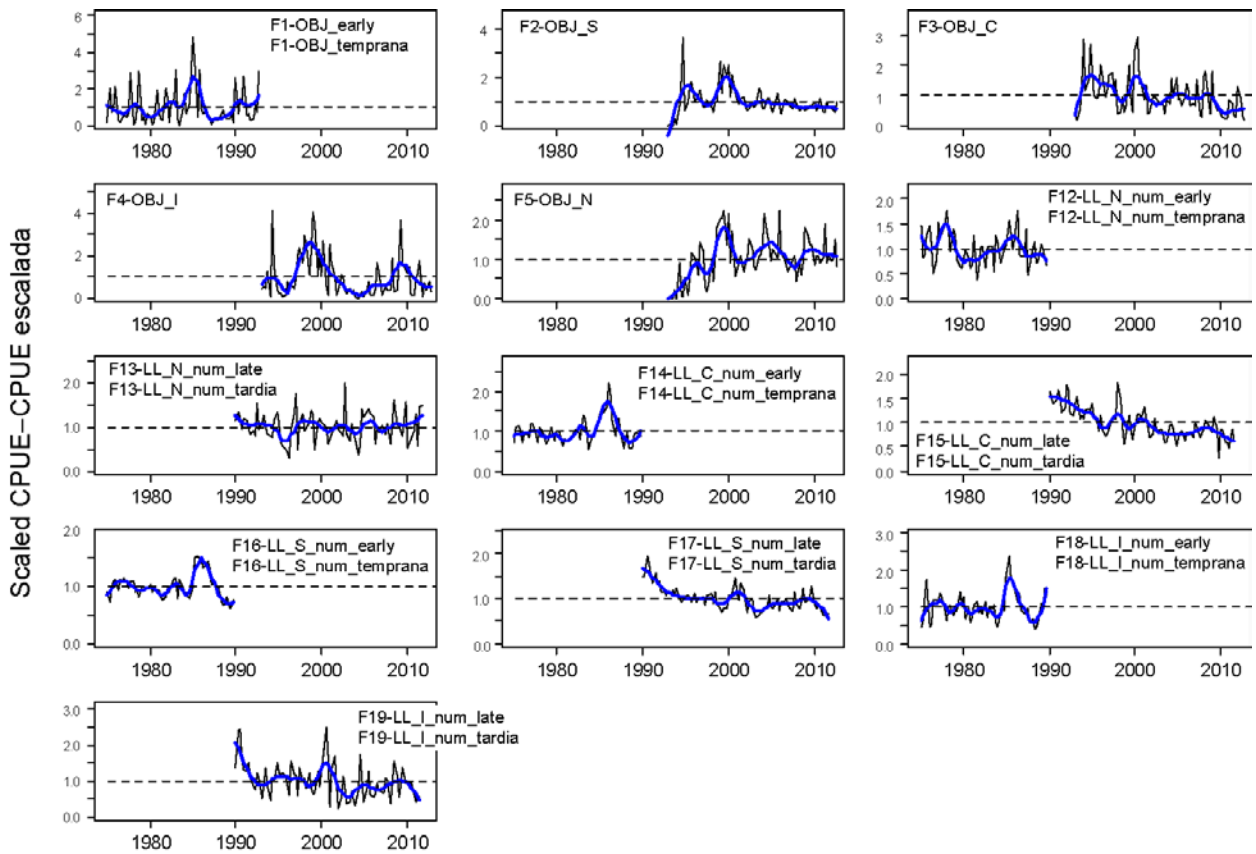

FIGURE 2.5. Quarterly CPUE and four-quarterly running average CPUEs of the fisheries defined for the stock assessment of bigeye tuna in the EPO (Table 2.1). The CPUEs for the floating-object fisheries (1-5) are in kilograms per day fished, and those for the longline fisheries (12-19) are standardized CPUE. The data are adjusted so that the mean of each time series is equal to 1.0. Note that the vertical scales of the panels are different. The numbers in the panels correspond to the numbers designating the fisheries in Table 2.1.

FIGURA 2.5. CPUE trimestral y promedio móvil de cuatro trimestres de CPUE de las pesquerías definidas para la evaluación de la población de atún patudo en el OPO (Tabla 2.1). Se expresan las CPUE de las pesquerías de superficie (1-5) en kilogramos por día de pesca, y las de las pesquerías de palangre (12-19) en CPUE estandarizada. Se ajustaron los datos para que el promedio de cada serie de tiempo equivalga a 1,0. Nótese que las escalas verticales de los recuadros son diferentes. El número en cada panel corresponde a los números que designan las pesquerías en la Tabla 2.1.

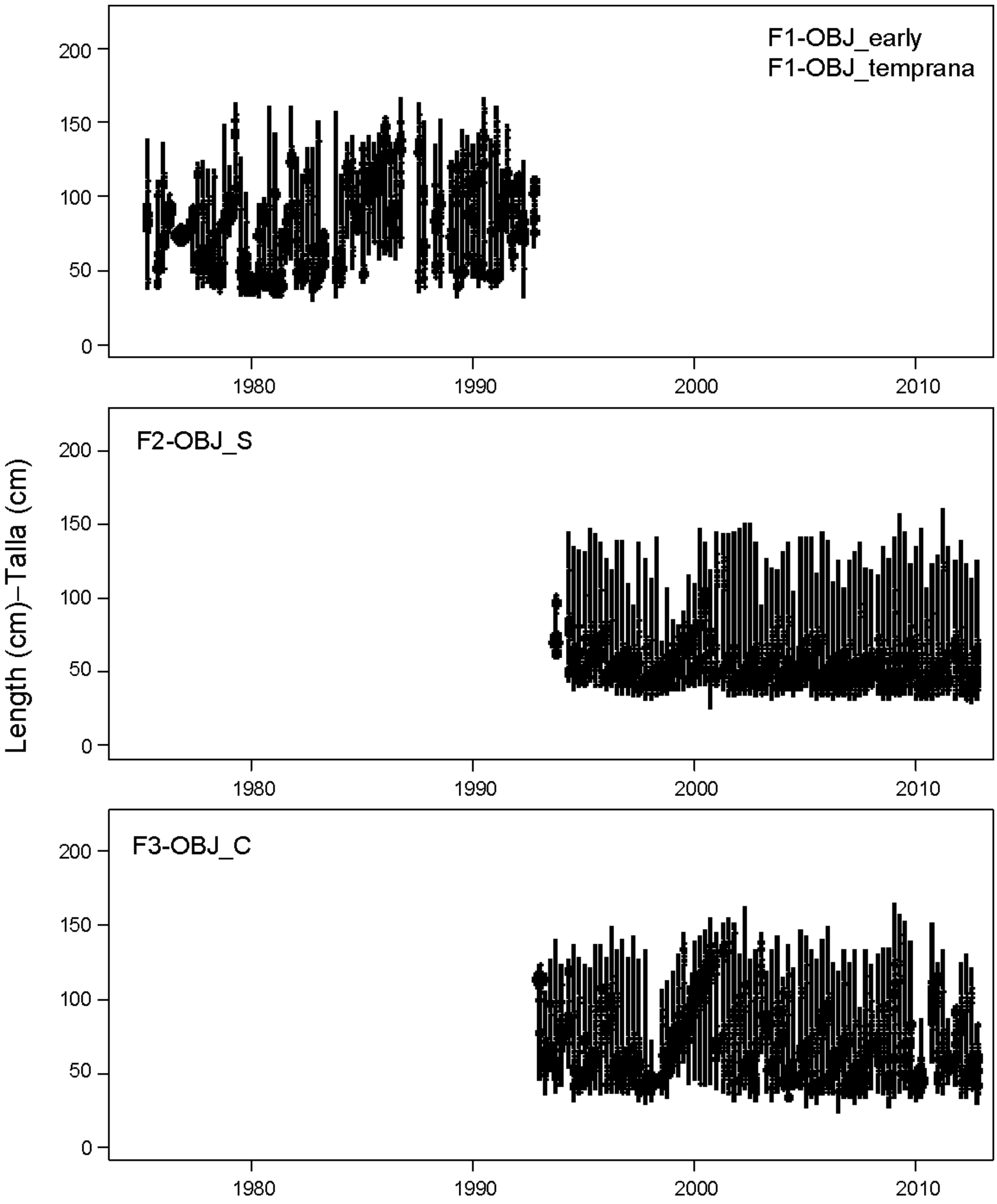

FIGURE 2.6a. Size compositions of the catches of bigeye tuna taken by Fisheries 1, 2 and 3, by quarter. The areas of the circles are proportional to the catches. The numbers in the panels correspond to the numbers designating the fisheries in Table 2.1.

FIGURA 2.6a. Composición por talla de las capturas de patudo de las Pesquerías 1, 2 y 3, por trimestre. El área de los círculos es proporcional a la captura. El número en cada panel corresponde a los números que designan las pesquerías en la Tabla 2.1.

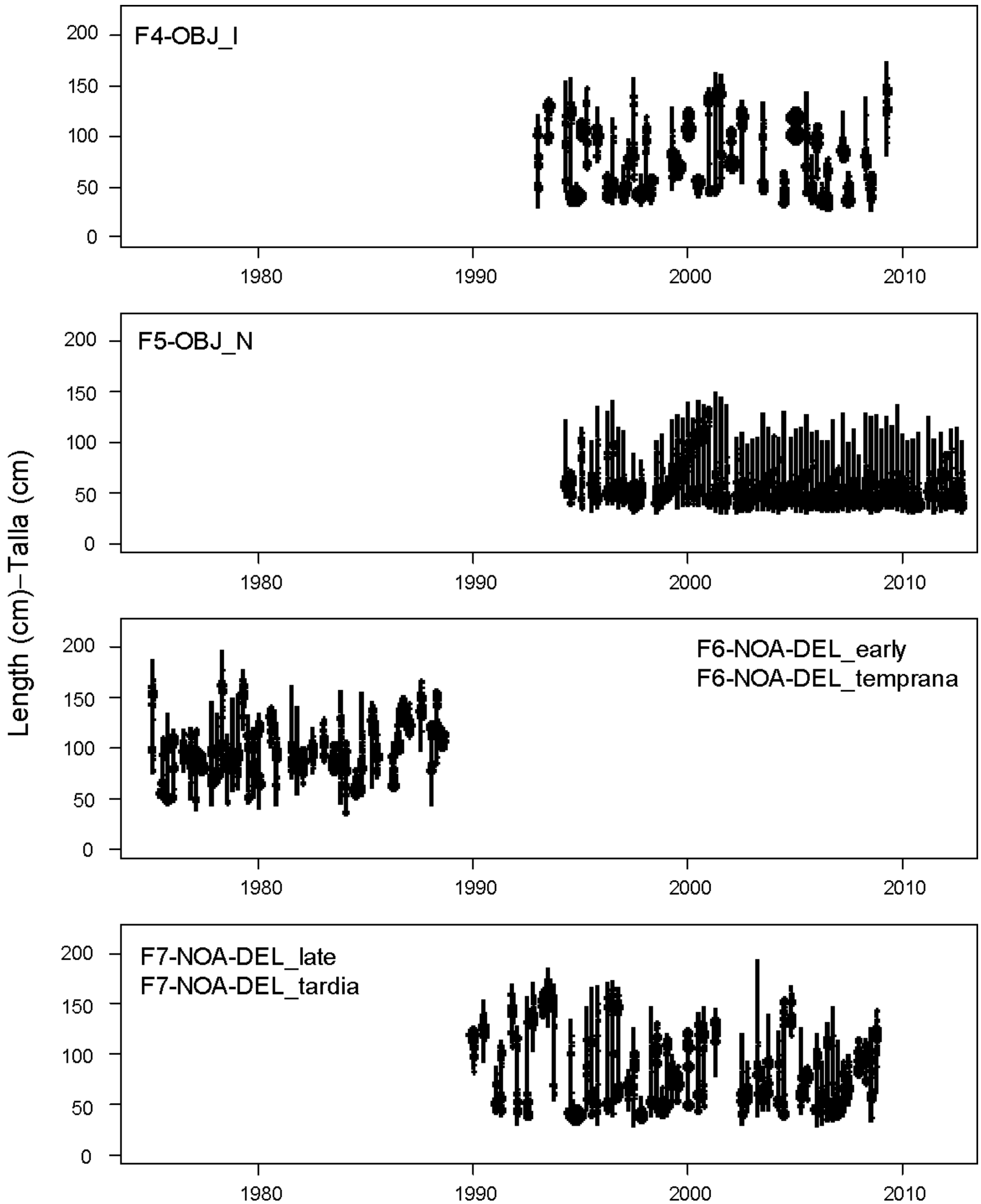

FIGURE 2.6b. Size compositions of the catches of bigeye tuna taken by Fisheries 4, 5, 6, and 7, by quarter. The areas of the circles are proportional to the catches. The numbers in the panels correspond to the numbers designating the fisheries in Table 2.1.

FIGURA 2.6b. Composición por talla de las capturas de patudo de las Pesquerías 4, 5, 6, y 7, por trimestre. El área de los círculos es proporcional a la captura. El número en cada panel corresponde a los números que designan las pesquerías en la Tabla 2.1.

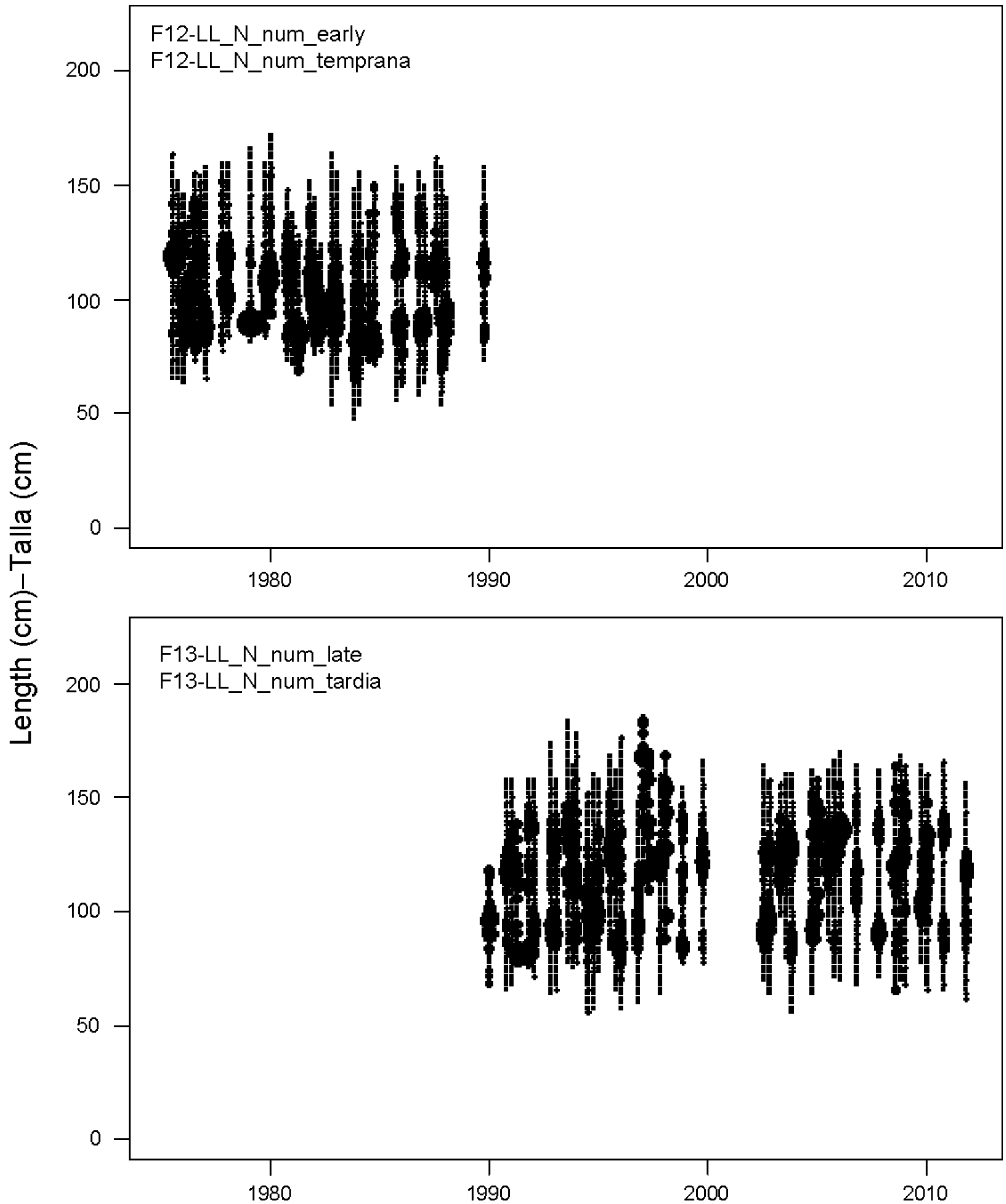

FIGURE 2.6c. Size compositions of the catches of bigeye tuna taken by the northern longline fishery (Fisheries 12 and 13), by quarter. The areas of the circles are proportional to the catches. The numbers in the panels correspond to the numbers designating the fisheries in Table 2.1.

FIGURA 2.6c. Composición por talla de las capturas de patudo de la pesquería de palangre del norte (Pesquerías 12 y 13), por trimestre. El área de los círculos es proporcional a la captura. El número en cada panel corresponde a los números que designan las pesquerías en la Tabla 2.1.

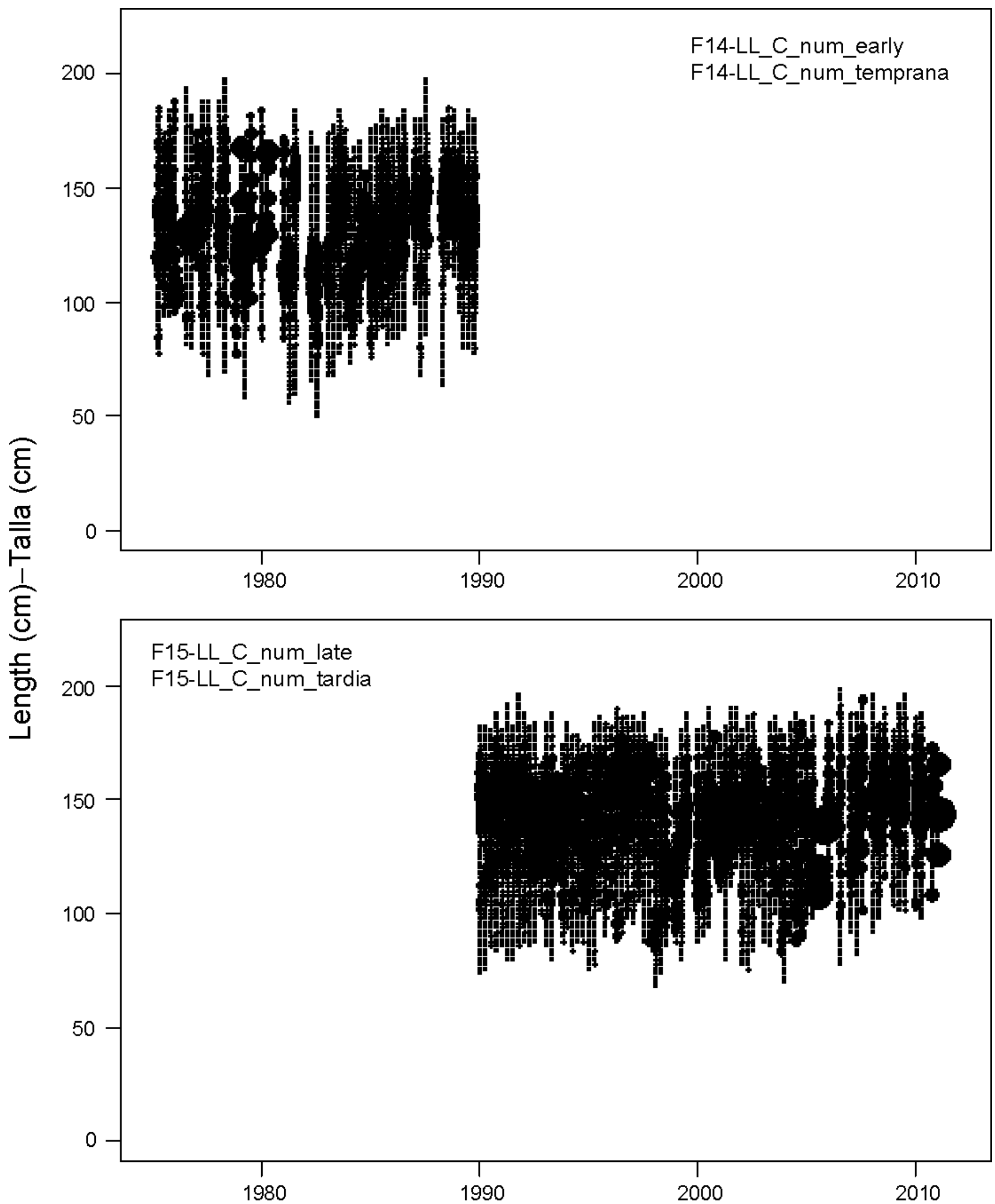

FIGURE 2.6d. Size compositions of the catches of bigeye tuna taken by the central longline fisheries (Fisheries 14 and 15), by quarter. The areas of the circles are proportional to the catches. The numbers in the panels correspond to the numbers designating the fisheries in Table 2.1.

FIGURA 2.6d. Composición por talla de las capturas de patudo de las pesquerías de palangre centrales (Pesquerías 14 y 15), por trimestre. El área de los círculos es proporcional a la captura. El número en cada panel corresponde a los números que designan las pesquerías en la Tabla 2.1.

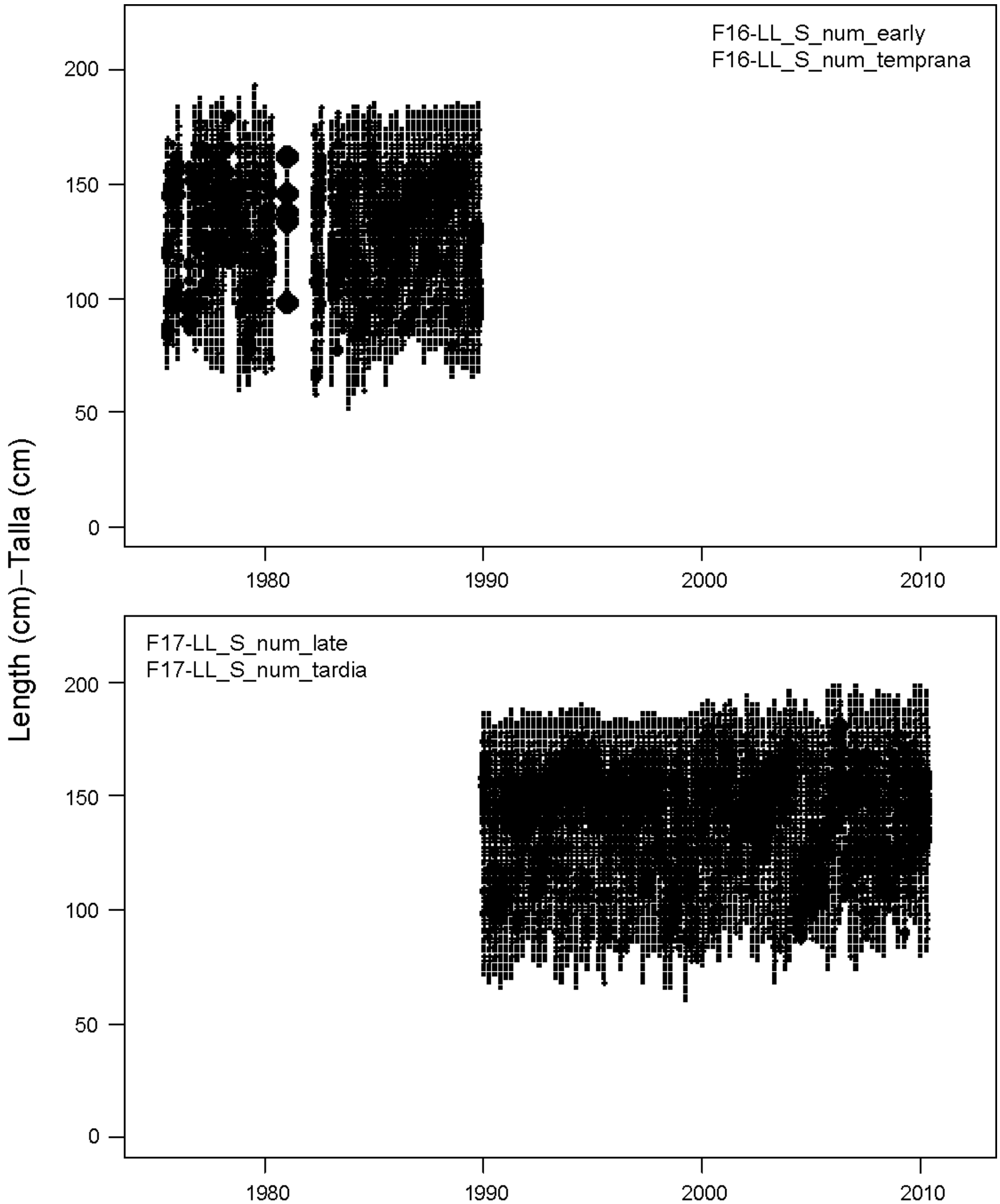

FIGURE 2.6e. Size compositions of the catches of bigeye tuna taken by the southern longline fisheries (Fisheries 16 and 17), by quarter. The areas of the circles are proportional to the catches. The numbers in the panels correspond to the numbers designating the fisheries in Table 2.1.

FIGURA 2.6e. Composición por talla de las capturas de patudo de las pesquerías de palangre del sur (Pesquerías 16 y 17), por trimestre. El área de los círculos es proporcional a la captura. El número en cada panel corresponde a los números que designan las pesquerías en la Tabla 2.1.

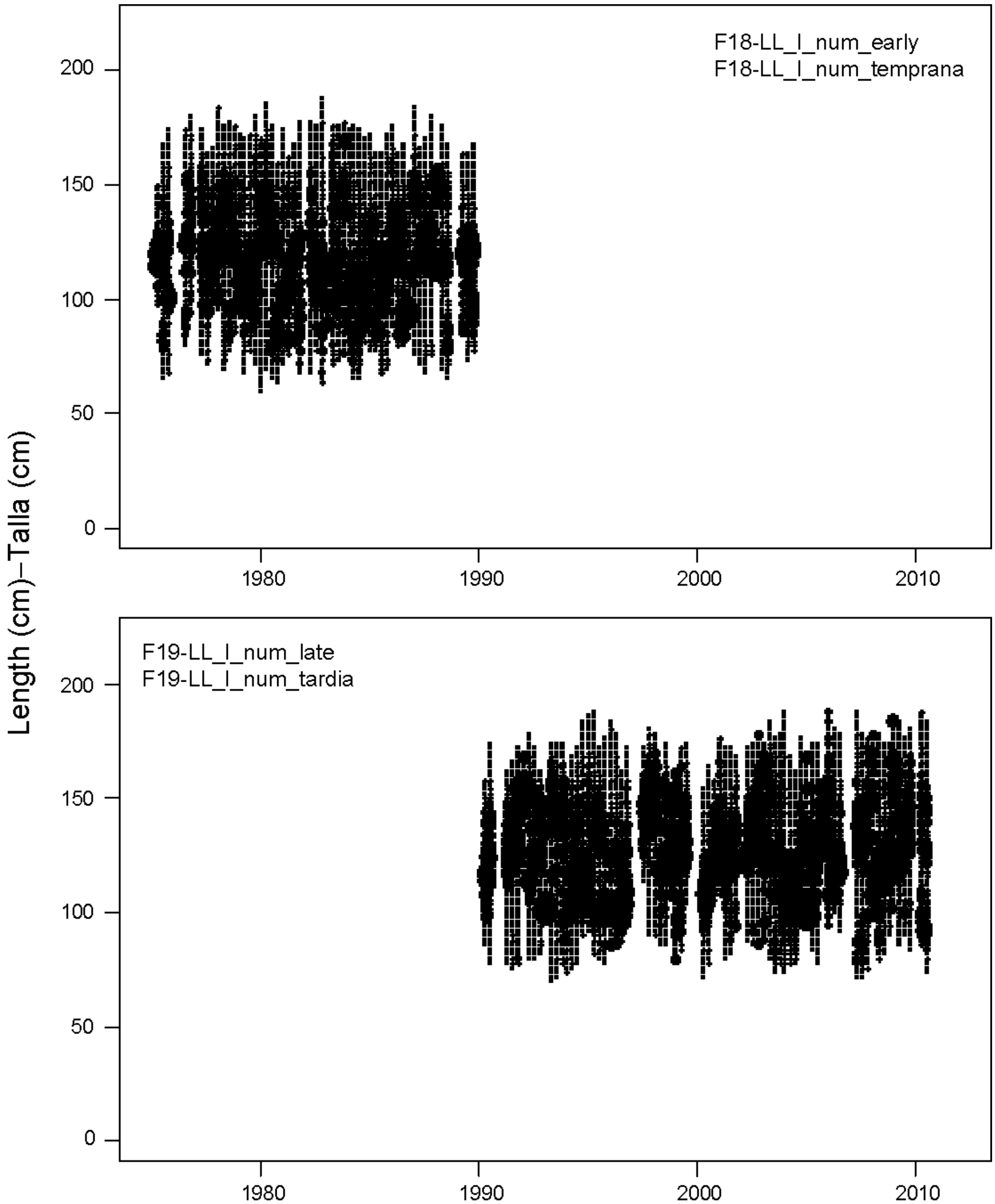

FIGURE 2.6f. Size compositions of the catches of bigeye tuna taken by the inshore longline fisheries (Fisheries 18 and 19), by quarter. The areas of the circles are proportional to the catches. The numbers in the panels correspond to the numbers designating the fisheries in Table 2.1.

FIGURA 2.6f. Composición por talla de las capturas de patudo de las pesquerías de palangre costeras (Pesquerías 18 y 19), por trimestre. El área de los círculos es proporcional a la captura. El número en cada panel corresponde a los números que designan las pesquerías en la Tabla 2.1.

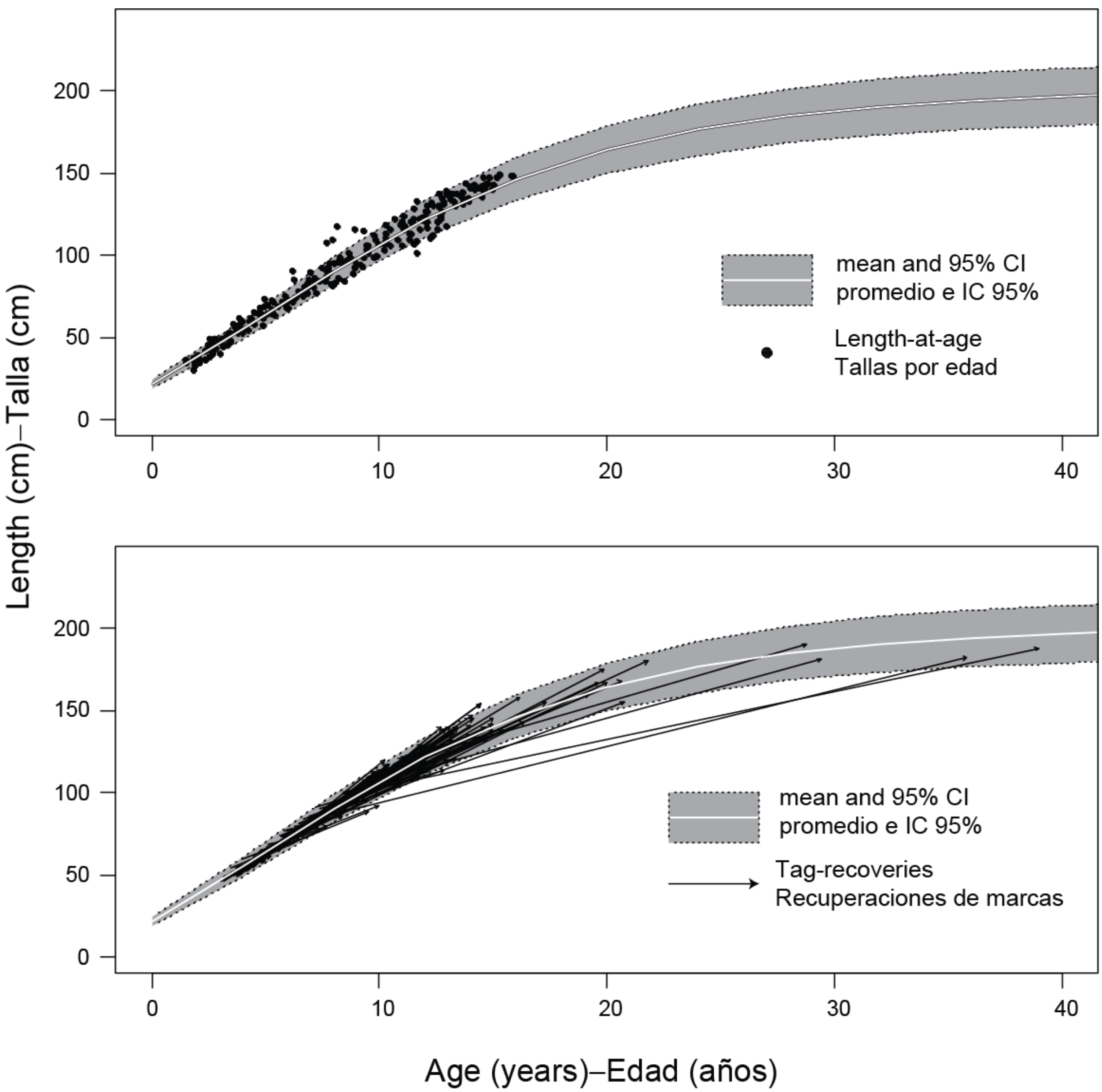

FIGURE 3.1a. Richards growth curve estimated for bigeye tuna in the EPO from an integrated age-at-length and tagging data model. Top panel: model fit to the otolith age-at-length data (dots); bottom panel: model fit to the tag-recapture data (vectors). The shaded area indicates the estimated variation (95% confidence intervals) of the mean lengths at age.

FIGURA 3.1a. Curva de crecimiento de Richards estimada para el atún patudo en el OPO con un modelo que integra datos de talla por edad y marcado. El Panel superior: ajuste del modelo a los datos de otolitos de talla por edad (puntos); panel inferior: ajuste del modelo a los datos de marcado (vectores). La zona sombreada indica la variación estimada (intervalos de confianza de 95%) de las tallas medias por edad.

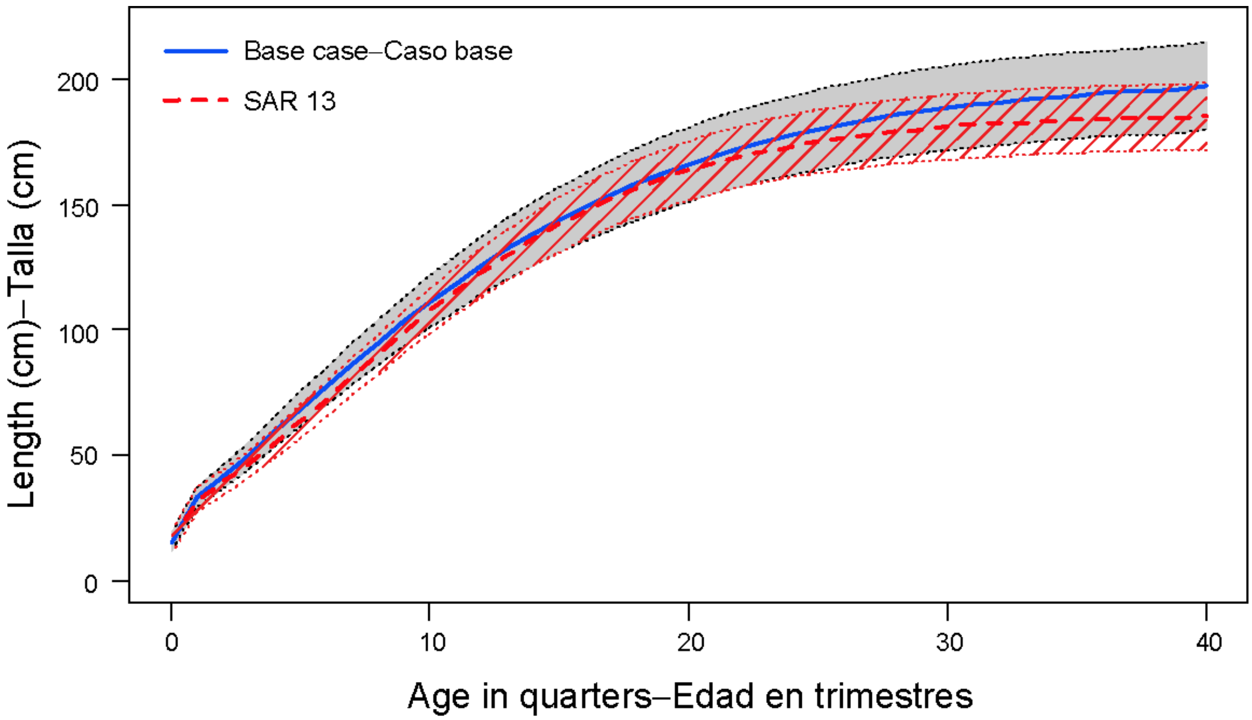

FIGURE 3.1b. Comparison between the Richards growth curve for bigeye from the integrated age-at-length and tagging data model and the growth curve estimated in the previous assessment (SAR 13; Aires-da-Silva and Maunder 2012).

FIGURA 3.1b. Comparación de la curva de crecimiento de Richards para el patudo del modelo que integra los datos de talla por edad y marcado y la curva de crecimiento estimada en la evaluación previa (SAR 13; Aires-da-Silva y Maunder 2012).

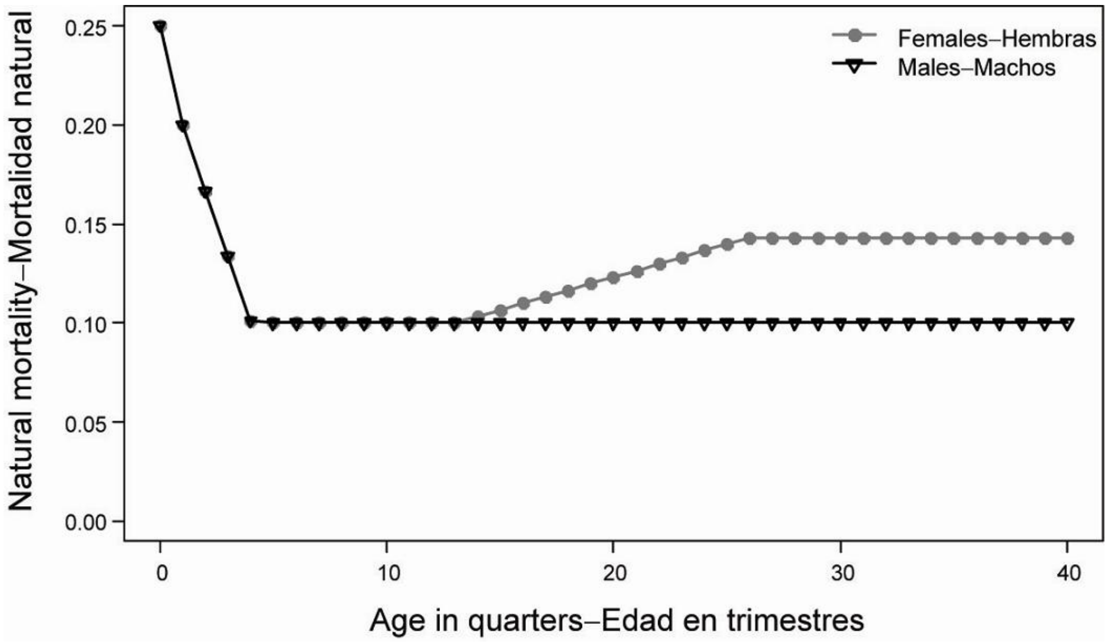

FIGURE 3.2. Quarterly natural mortality (*M*) rates used for the base case assessment of bigeye tuna in the EPO.
FIGURA 3.2. Tasas trimestrales de mortalidad natural (*M*) usadas en la evaluación del caso base del atún patudo en el OPO.

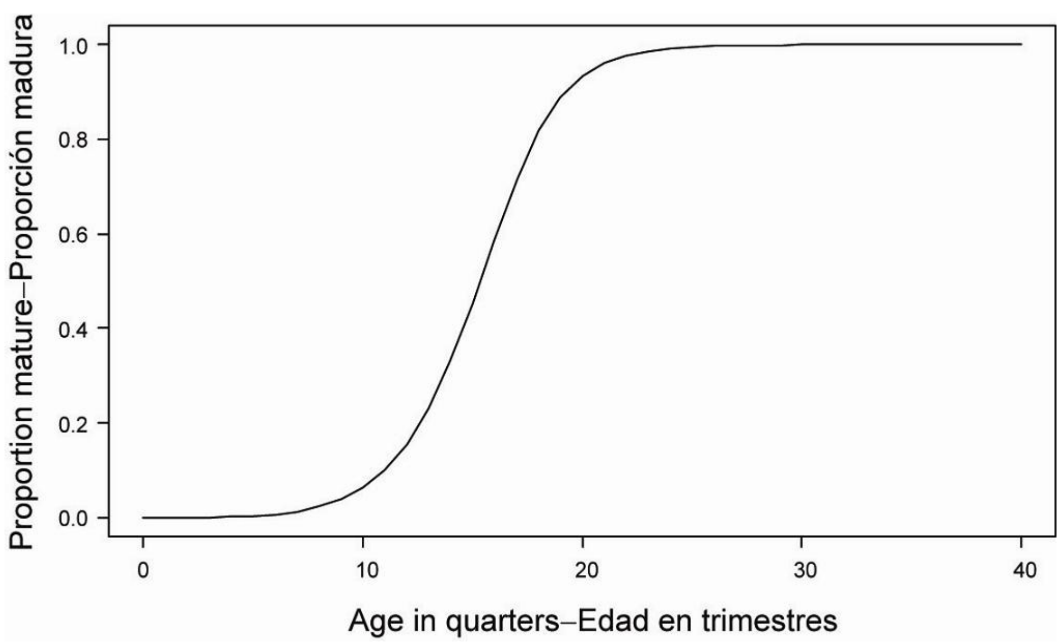

FIGURE 3.3. Age-specific maturity schedule (proportions of mature females) of bigeye tuna as assumed in the base case model.
FIGURA 3.3. Relación de madurez por edad (proporción de hembras maduras) de atún patudo, supuesto en el modelo del caso base.

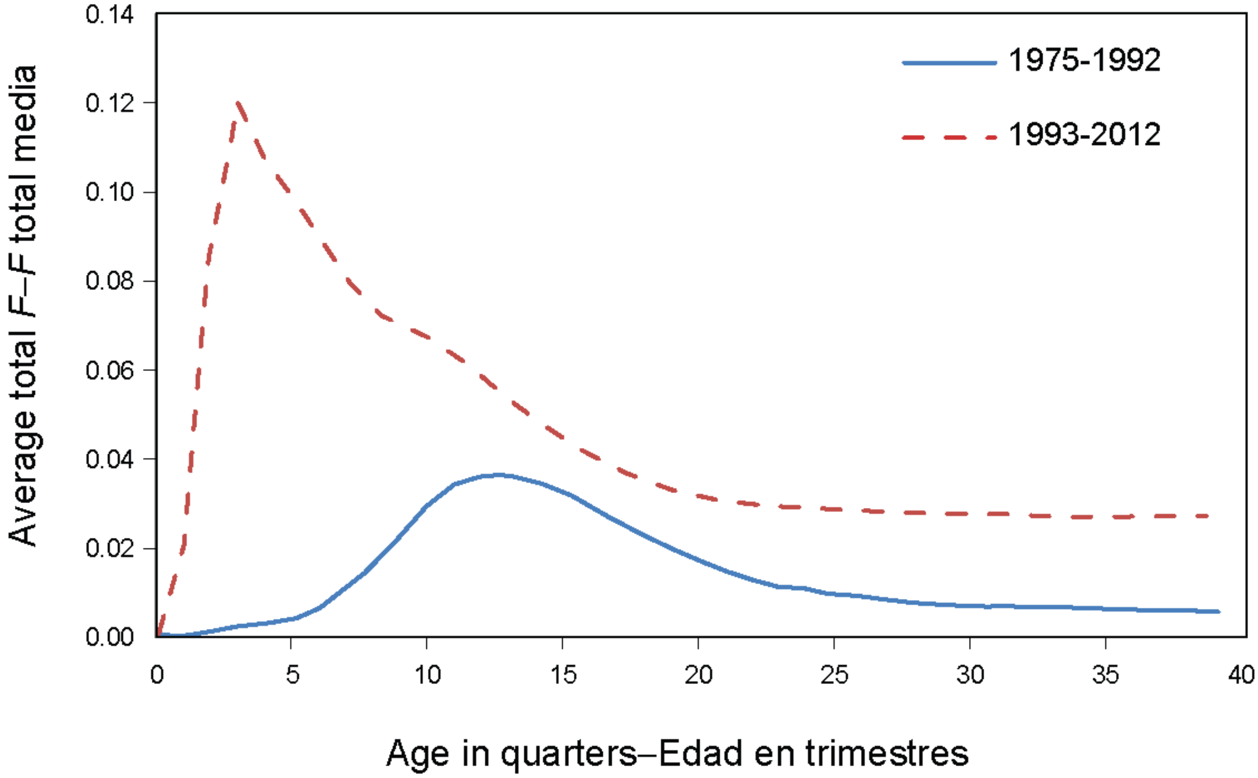

FIGURE 4.1. Average quarterly fishing mortality at age of bigeye tuna, by all gears, in the EPO. The curves for 1975-1992 and 1993-2012 display the averages for the periods before and after the expansion of the floating-object fisheries, respectively.

FIGURA 4.1. Mortalidad por pesca trimestral media por edad de atún patudo en el OPO, por todas las artes. Las curvas de 1975-1992 y 1993-2012 indican los promedios de los períodos antes y después de la expansión de las pesquerías sobre objetos flotantes, respectivamente.

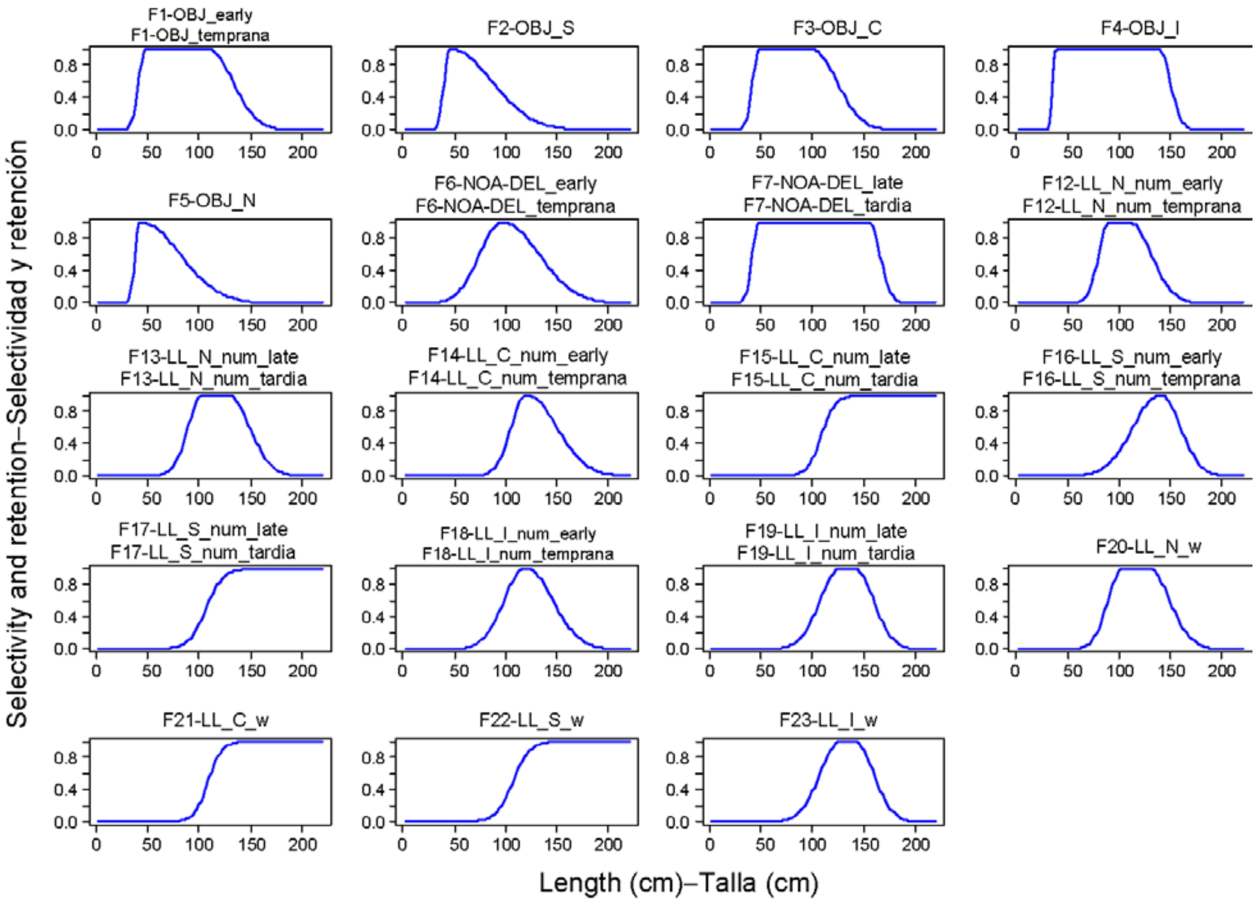

FIGURE 4.2. Size selectivity curves for surface Fisheries 1-7 and longline Fisheries 12-23 estimated with Stock Synthesis. Age 1-3 quarter fish are assumed to be fully selected for the discard fisheries (8-11). The selectivity curves for Fisheries 20-23 are the same as those for Fisheries 13, 15, 17, and 19, respectively. The numbers in the panels correspond to the numbers designating the fisheries in Table 2.1.

FIGURA 4.2. Curvas de selectividad por talla correspondientes a las pesquerías de superficie 1-7 y las pesquerías de palangre 12-23 estimadas con *Stock Synthesis*. En el caso de las pesquerías de descarte (8-11), se supone que los peces de 1 a 3 trimestres de edad son plenamente seleccionados. Las curvas de selectividad de las pesquerías 20-23 son iguales que las de las pesquerías 13, 15, 17, y 19, respectivamente. El número en cada panel corresponde a los números que designan las pesquerías en la Tabla 2.1.

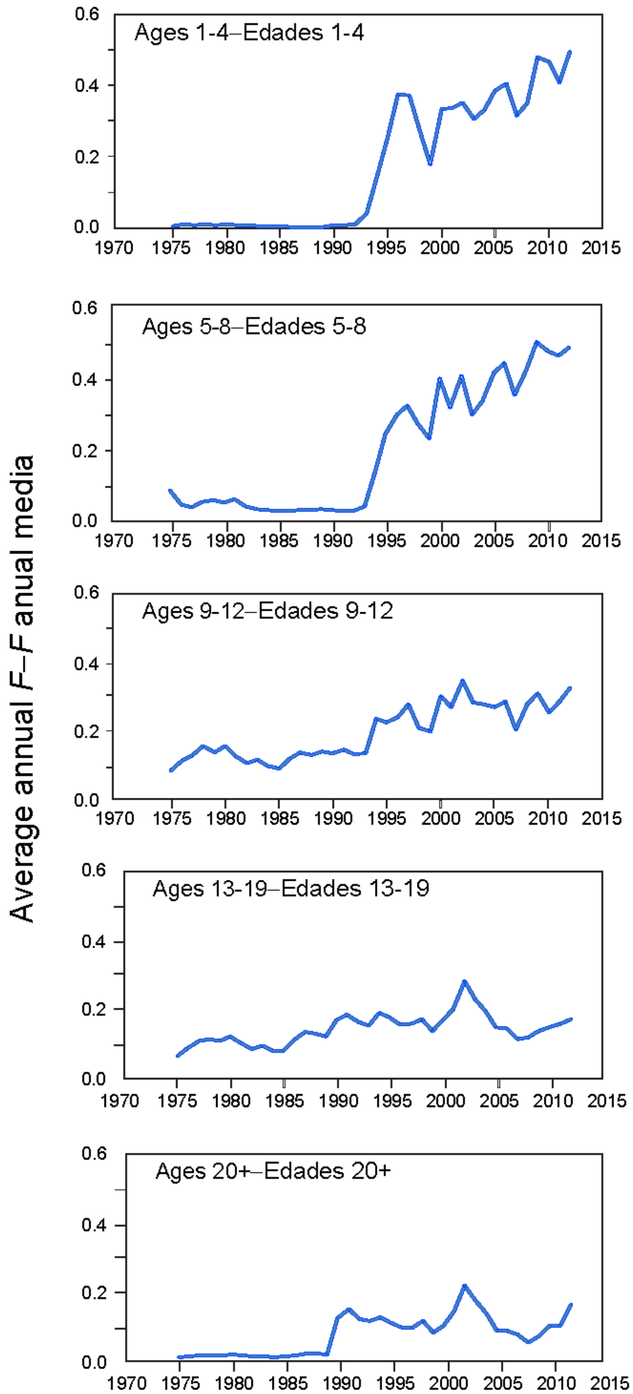

FIGURE 4.3. Average annual fishing mortality, by all gears, of bigeye tuna recruited to the fisheries of the EPO. Each panel illustrates the average fishing mortality rates that affected the fish within the range of ages indicated in the title of each panel. For example, the trend illustrated in the top panel is an average of the fishing mortalities that affected the fish that were 1-4 quarters old.

FIGURA 4.3. Mortalidad por pesca anual media, por todas las artes, de atún patudo reclutado a las pesquerías del OPO. Cada recuadro ilustra las tasas medias de mortalidad por pesca que afectaron a los peces de la edad indicada en el título de cada recuadro. Por ejemplo, la tendencia ilustrada en el recuadro superior es un promedio de las mortalidades por pesca que afectaron a los peces de entre 1 y 4 trimestres de edad.

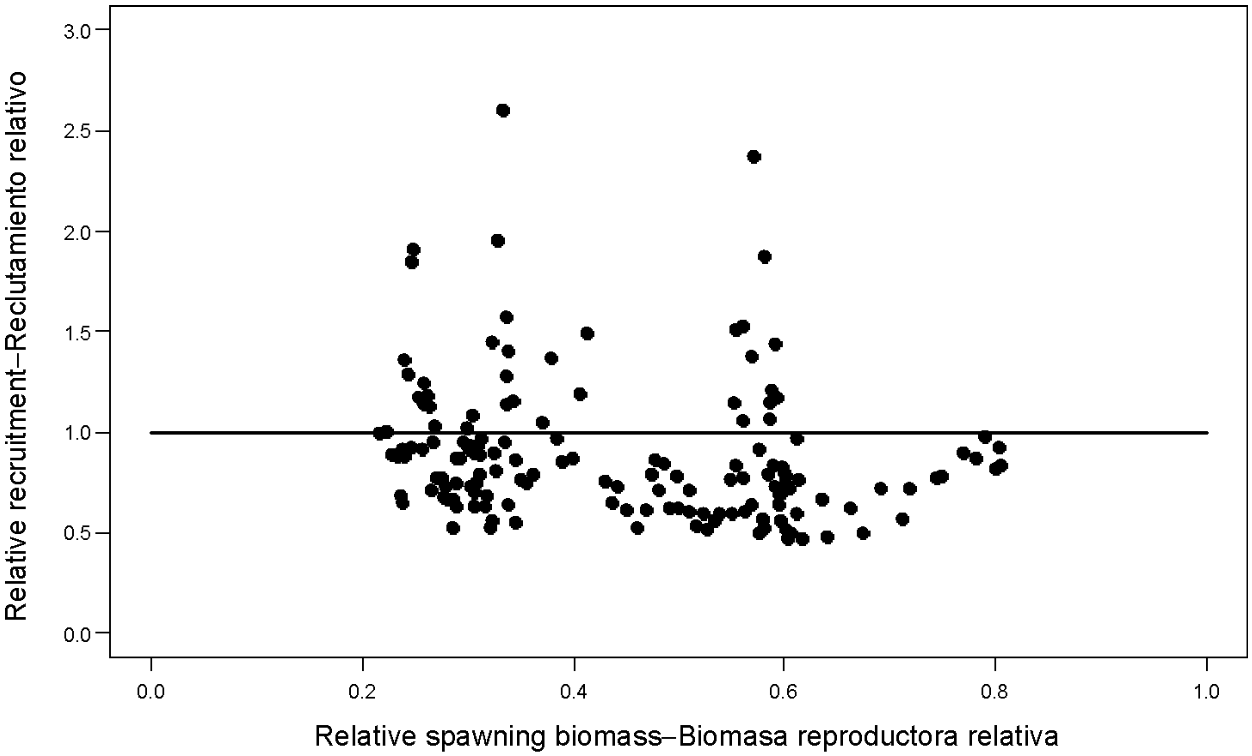

FIGURE 4.4. Estimated relationship between the recruitment and spawning biomass of bigeye tuna. The recruitment is scaled so that the estimate of virgin recruitment is equal to 1.0. Likewise, the spawning biomass is scaled so that the estimate of virgin spawning biomass is equal to 1.0. The horizontal line represents the assumed stock-recruitment relationship.

FIGURA 4.4. Relación estimada entre el reclutamiento y la biomasa reproductora del atún patudo. Se escala el reclutamiento para que la estimación de reclutamiento virgen equivalga a 1,0, y la biomasa reproductora para que la estimación de biomasa reproductora virgen equivalga a 1,0. La línea horizontal representa la relación población-reclutamiento supuesta.

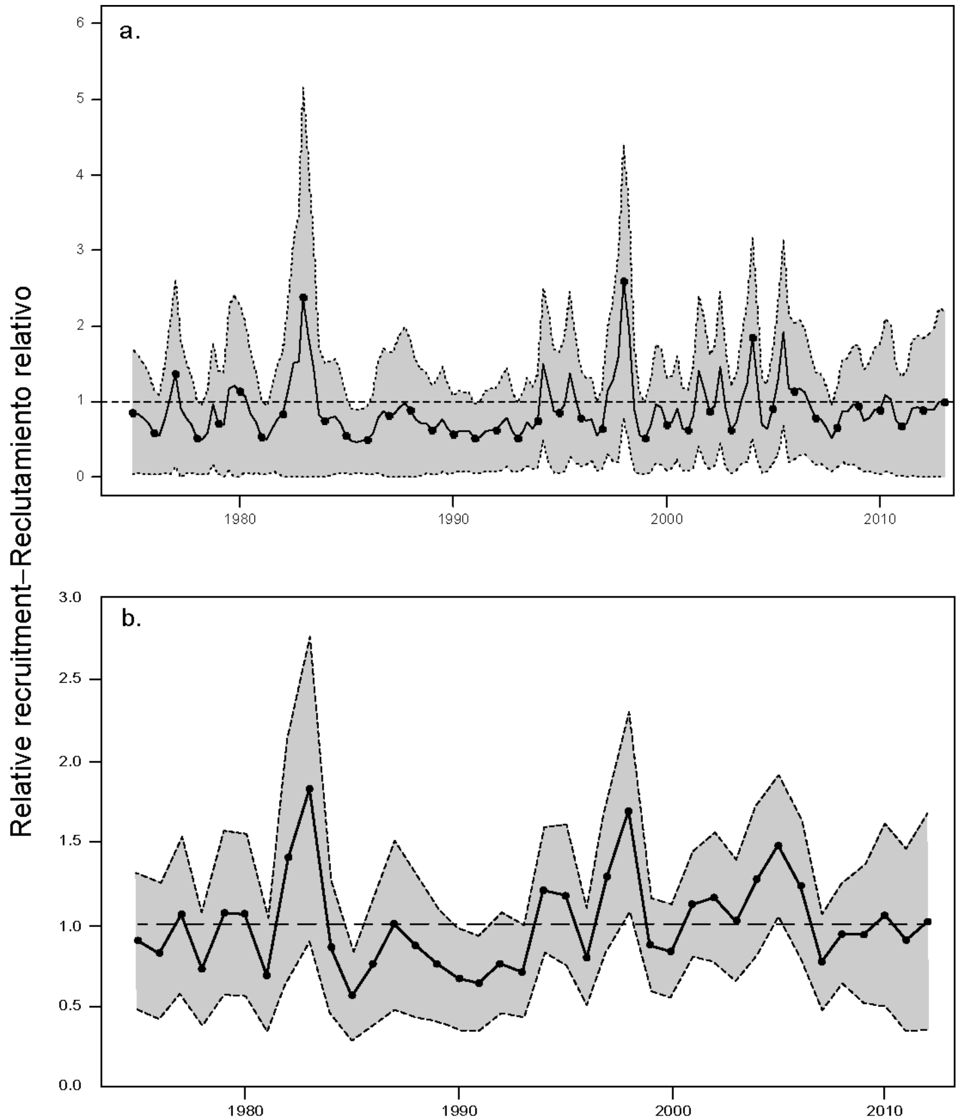

FIGURE 4.5. Estimated recruitment of bigeye tuna to the fisheries of the EPO: a) quarterly recruitment; b) annual recruitment. The estimates are scaled so that the estimate of virgin recruitment is equal to 1.0 (dashed horizontal line). The bold line illustrates the maximum likelihood estimates of recruitment, and the thin dashed lines the confidence intervals (±2 standard deviations) around those estimates.. The labels on the time axis are drawn at the beginning of each year, but, since the assessment model represents time on a quarterly basis, there are four estimates of recruitment for each year.

FIGURA 4.5. Reclutamiento estimado de atún patudo a las pesquerías del OPO: a) reclutamiento trimestral; b) reclutamiento anual. Se escalan las estimaciones para que la estimación de reclutamiento virgen equivalga a 1,0 (línea horizontal de trazos). La línea gruesa ilustra las estimaciones de reclutamiento de verosimilitud máxima, y las líneas delgadas de trazos los intervalos de confianza (±2 desviaciones estándar) alrededor de esas estimaciones. Se dibujan las leyendas en el eje de tiempo al principio de cada año, pero, ya que el modelo de evaluación representa el tiempo por trimestres, hay cuatro estimaciones de reclutamiento para cada año.

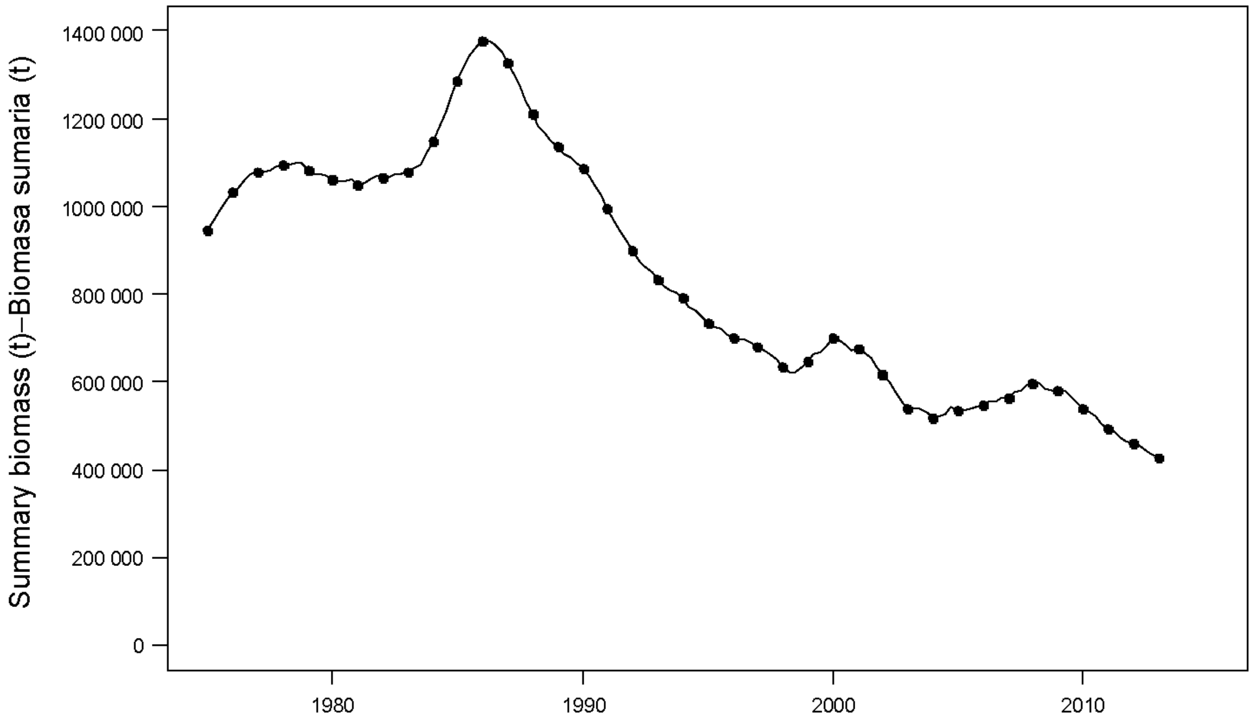

FIGURE 4.6. Maximum likelihood estimates of the biomass of bigeye tuna 3+ quarters old in the EPO (summary biomass). Since the assessment model represents time on a quarterly basis, there are four estimates of biomass for each year. t = metric tons.

FIGURA 4.6. Estimaciones de verosimilitud máxima de la biomasa de atún patudo de 3+ trimestres de edad en el OPO (biomasa sumaria). Ya que el modelo de evaluación representa el tiempo por trimestre, hay cuatro estimaciones de biomasa para cada año. t = toneladas métricas.

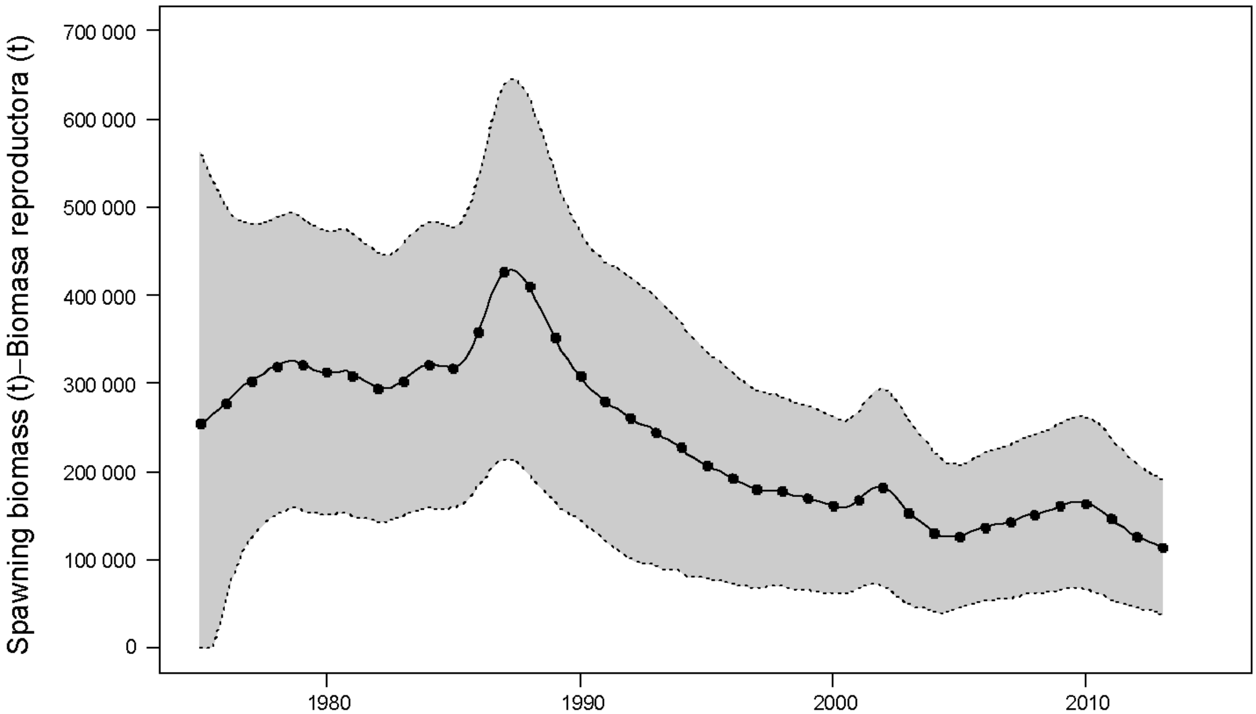

FIGURE 4.7. Maximum likelihood estimates of the spawning biomass (Section 4.1.3) of bigeye tuna in the EPO. The solid line illustrates the maximum likelihood estimates of the biomasses, and the dashed lines the confidence intervals (±2 standard deviations) around those estimates. Since the assessment model represents time on a quarterly basis, there are four estimates of the index for each year. t = metric tons.

FIGURA 4.7. Estimaciones de verosimilitud máxima del índice de biomasa reproductora (Sección 4.1.3) de atún patudo en el OPO. La línea sólida ilustra las estimaciones de verosimilitud máxima de la biomasa, y las líneas de trazos los intervalos de confianza (±2 desviaciones estándar) alrededor de estas estimaciones. Ya que el modelo de evaluación representa el tiempo por trimestre, hay cuatro estimaciones del índice para cada año. t = toneladas métricas.

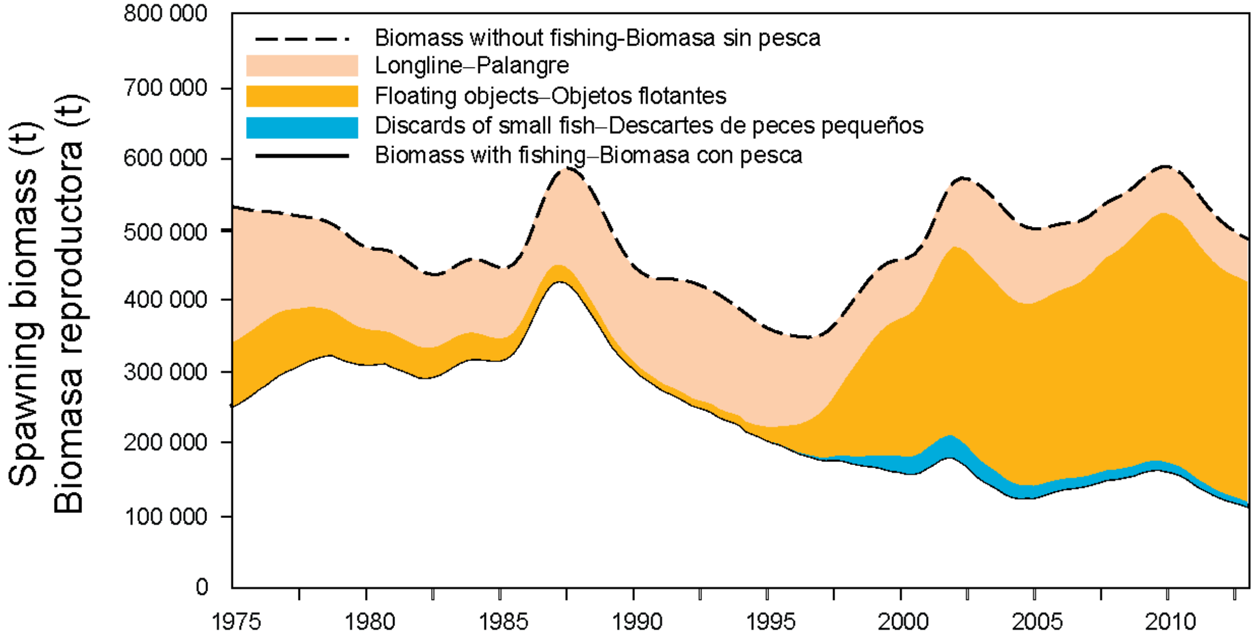

FIGURE 4.8. Trajectory of the spawning biomass of a simulated population of bigeye tuna that was not exploited (top line) and that predicted by the stock assessment model (bottom line). The shaded areas between the two lines show the portions of the impact attributed to each fishing method. t = metric tons.

FIGURA 4.8. Trayectoria de la biomasa reproductora de una población simulada de atún patudo no explotada (línea superior) y la que predice el modelo de evaluación (línea inferior). Las áreas sombreadas entre las dos líneas señalan la porción del efecto atribuida a cada método de pesca. t = toneladas métricas.

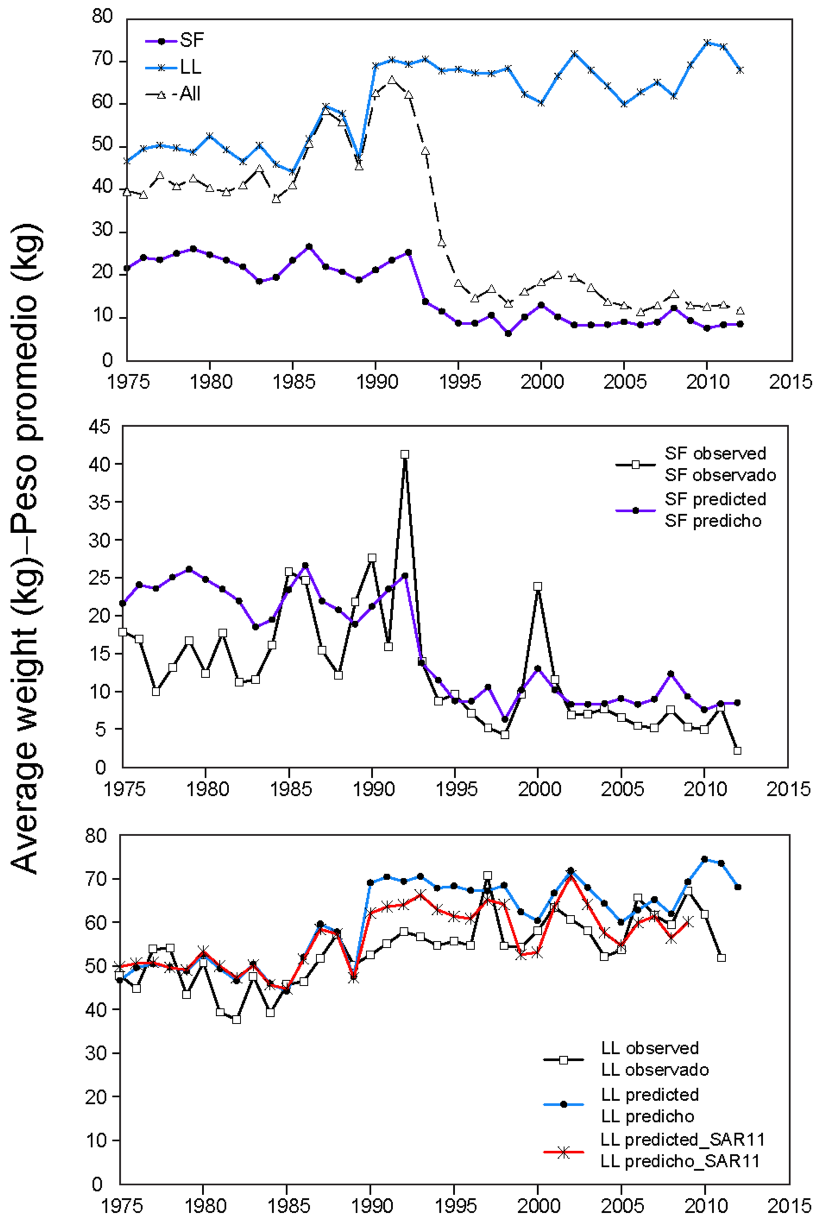

FIGURE 4.9. Average weights of bigeye tuna caught in the EPO, 1975-2012, by the surface fisheries (SF, Fisheries 1-7), longline fisheries (LL, Fisheries 12-23), and all fisheries combined (All). Upper panel: predicted average weights; middle panel: predicted and observed average weights for the surface fisheries; lower panel: predicted (present and previous full assessments, SAR11) and observed (Japanese data) average weights for the longline fisheries.

FIGURA 4.9. Peso promedio de atún patudo capturado en el OPO, 1975-2012, por las pesquerías de superficie (SF, pesquerías 1-7), de palangre (LL, pesquerías 12-23), y todas las pesquerías combinadas (All). Recuadro superior: pesos promedio predichos; recuadro medio: pesos promedio predichos y observados de las pesquerías de superficie; recuadro inferior: pesos promedio predichos (evaluaciones actual y completa previa, SAR 11) y observados (datos japoneses) de las pesquerías de palangre.

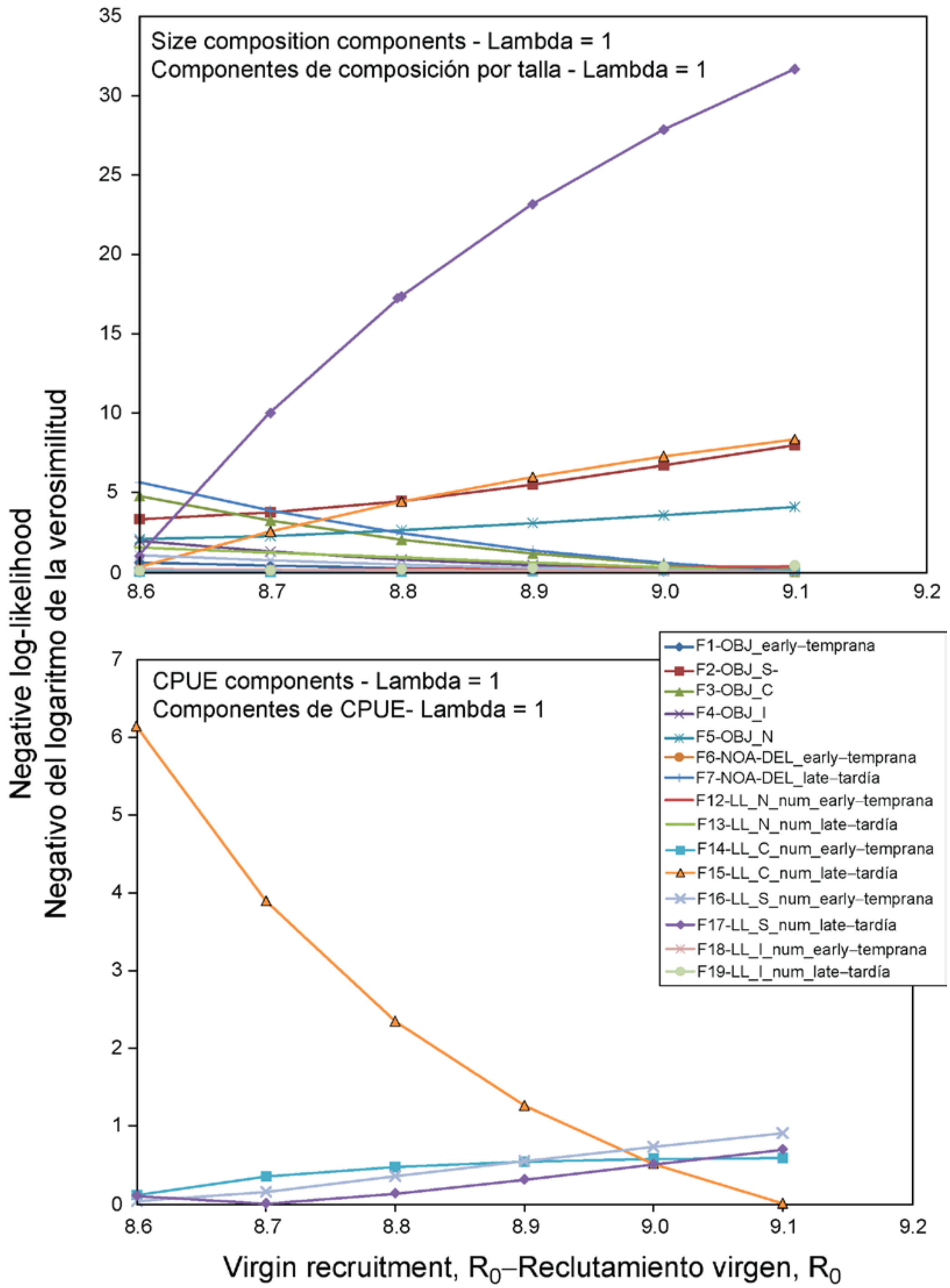

FIGURE 4.10a. Likelihood profile for the virgin recruitment (R_0) parameter estimated under the previous base case model configuration (Aires-da-Silva and Maunder 2011), which assumed the original input sample sizes of the size composition data ($\lambda = 1$). Each line represents the profile for each data component included in the model fit.

FIGURA 4.10a. Perfil de verosimilitud del parámetro de reclutamiento virgen (R_0) estimado con la configuración del modelo de caso base previo (Aires-da-Silva y Maunder 2011), que supuso los tamaños de muestra de los insumos originales de los datos de composición por talla ($\lambda = 1$). Cada línea representa el perfil correspondiente a cada componente de datos incluido en el ajuste del modelo.

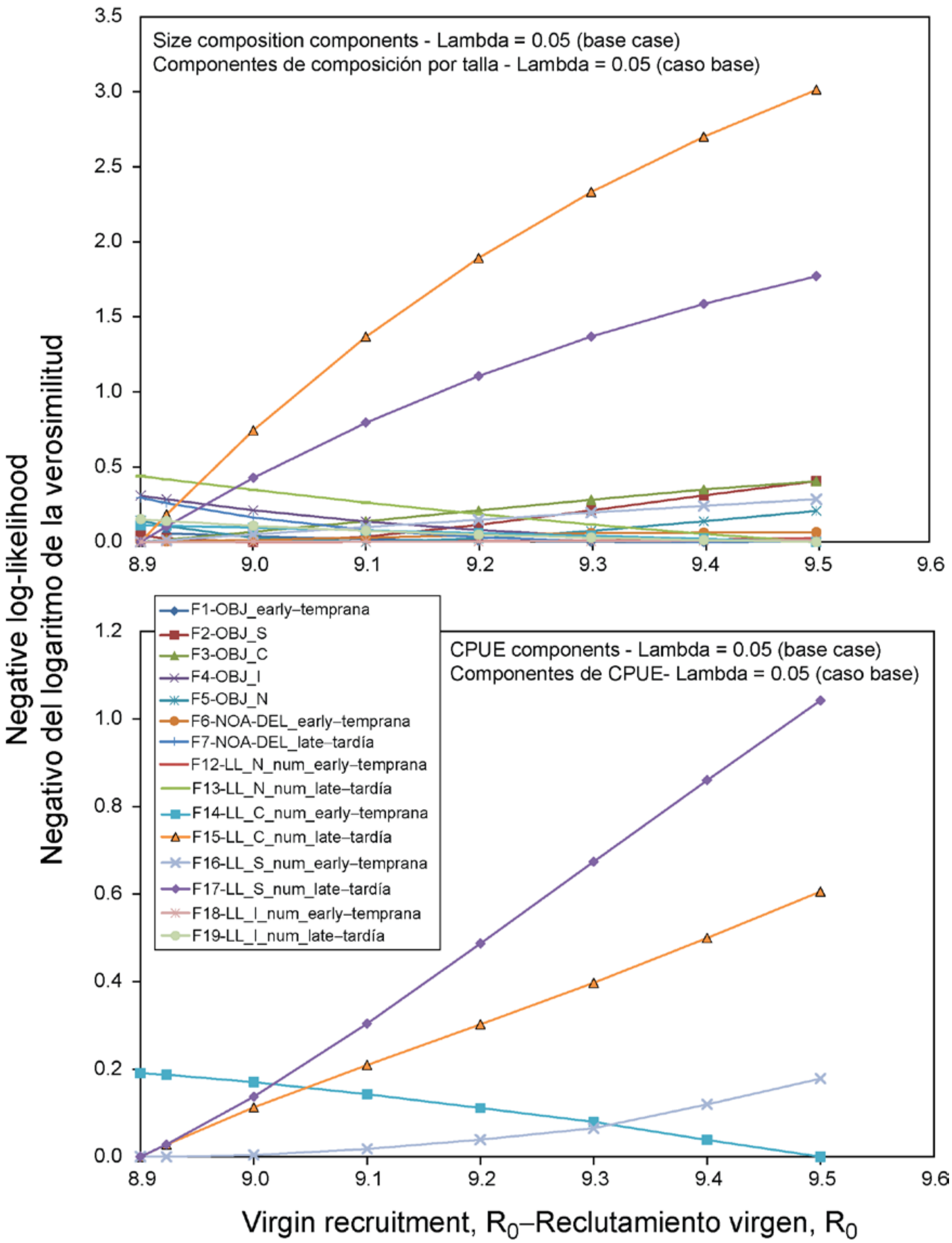

FIGURE 4.10b. Likelihood profile for the virgin recruitment (R_0) parameter estimated under the current base case model in which the size composition data was downweighted for all fisheries (λ = 0.05). Each line represents the profile for each data component included in the model fit.

FIGURA 4.10b. Perfil de verosimilitud del parámetro de reclutamiento virgen (R_0) estimado con el modelo de caso base actual en el cual se redujo la ponderación de los datos de composición por talla para todas las pesquerías (λ = 0,05). Cada línea representa el perfil correspondiente a cada componente de datos incluido en el ajuste del modelo.

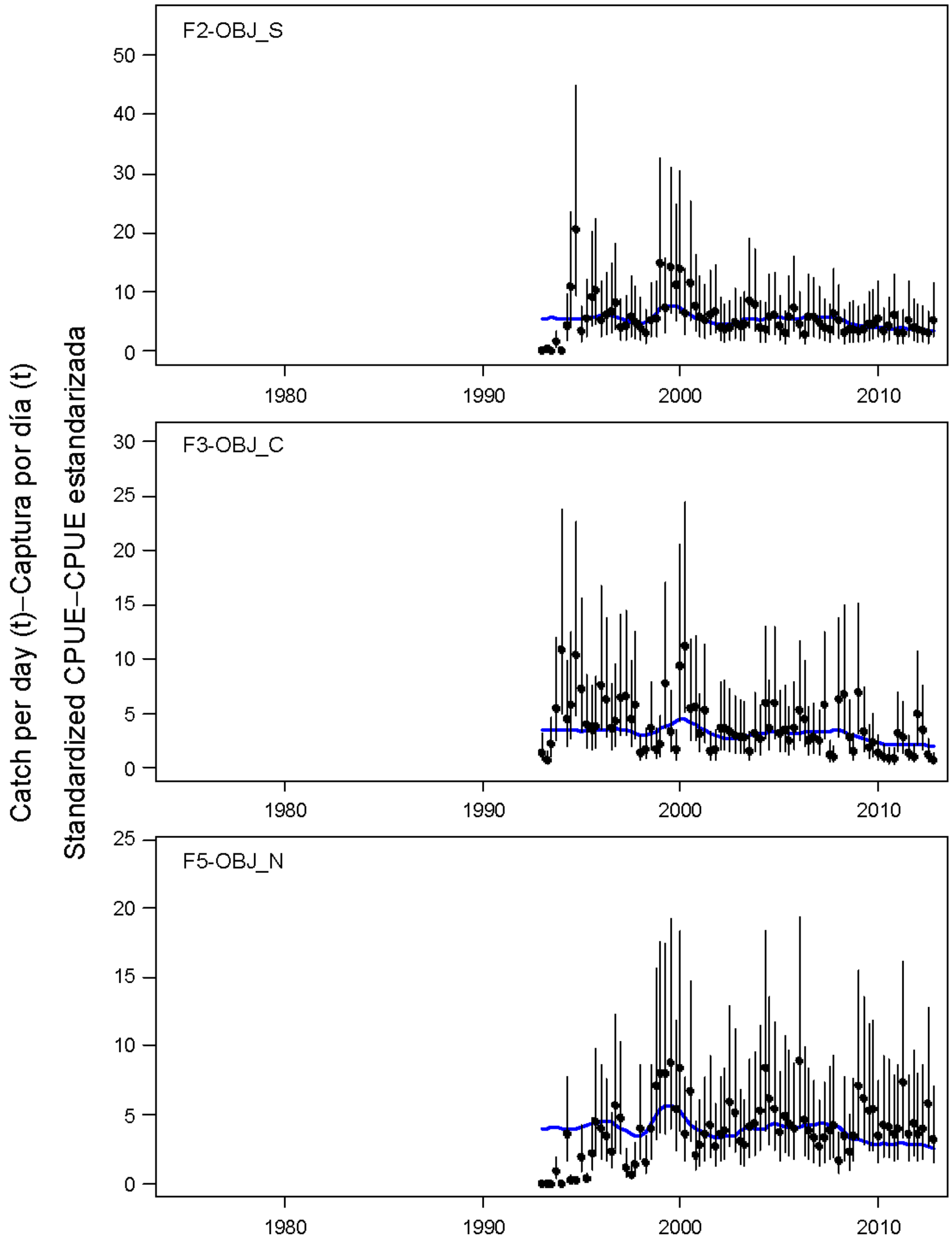

FIGURE 4.11a. Model fit to the CPUE data from different surface fisheries. The CPUEs for surface fisheries 2, 3, and 5 are in tons per day fished. The vertical lines represent the fixed confidence intervals (±2 standard deviations) around the observed CPUE values. The numbers in the panels correspond to the numbers designating the fisheries in Table 2.1. t = metric tons.

FIGURA 4.11a. Ajuste del modelo a los datos de CPUE de distintas pesquerías de superficie. Se expresan las CPUE de las pesquerías de superficie 2, 3, y 5 en toneladas por día de pesca. Las líneas verticales representan los intervalos de confianza fijos (±2 desviaciones estándar) alrededor de los valores de CPUE observados. El número en cada panel corresponde a los números que designan las pesquerías en la Tabla 2.1. t = toneladas métricas.

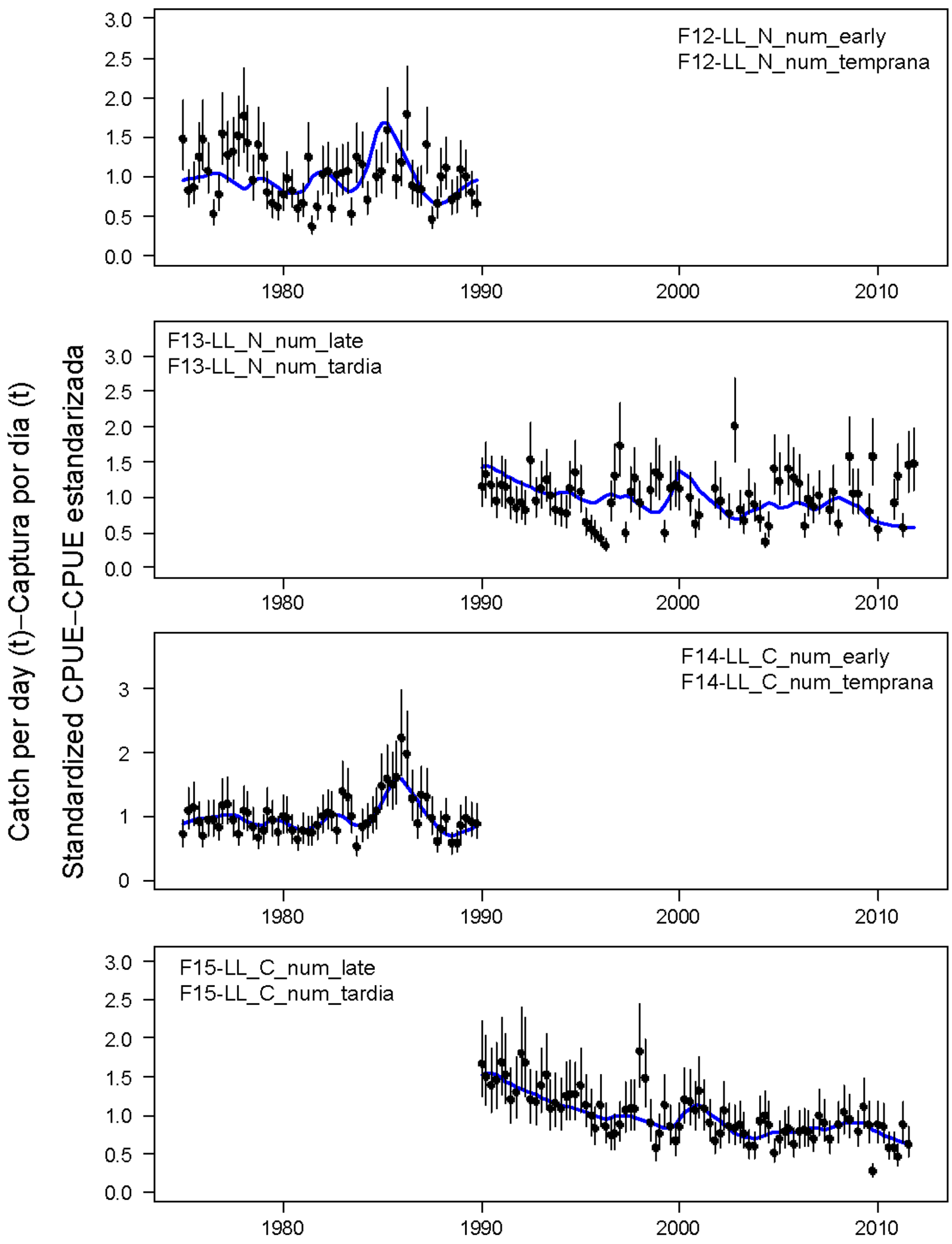

FIGURE 4.11b. Model fit to the CPUE data from different longline fisheries. The CPUEs for longline Fisheries 12-15 are standardized CPUE. The vertical lines represent the fixed confidence intervals (±2 standard deviations) around the CPUE values. The numbers in the panels correspond to the numbers designating the fisheries in Table 2.1.

FIGURA 4.11b. Ajuste del modelo a los datos de CPUE de distintas pesquerías de palangre. Las CPUE de las pesquerías de palangre 12-15 son CPUE estandarizadas. Las líneas verticales representan los intervalos de confianza fijos (±2 desviaciones estándar) alrededor de los valores de CPUE observados. El número en cada panel corresponde a los números que designan las pesquerías en la Tabla 2.1.

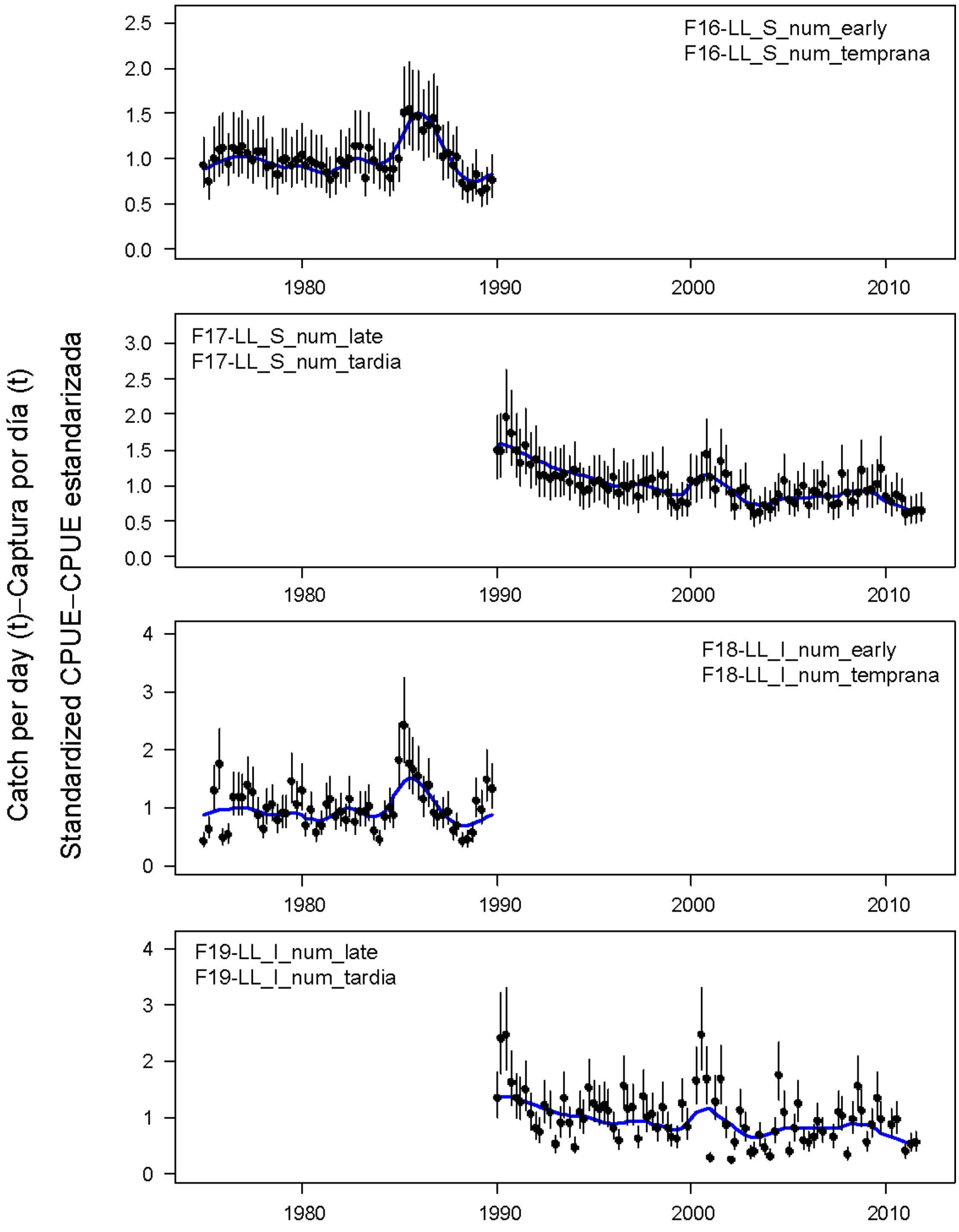

FIGURE 4.11c. Model fit to the CPUE data from different longline fisheries. The CPUEs for longline Fisheries 16-19 are standardized CPUE. The vertical lines represent the fixed confidence intervals (±2 standard deviations) around the CPUE values. The numbers in the panels correspond to the numbers designating the fisheries in Table 2.1.

FIGURA 4.11c. Ajuste del modelo a los datos de CPUE de distintas pesquerías de palangre. Las CPUE de las pesquerías de palangre 16-19 son CPUE estandarizada. Las líneas verticales representan los intervalos de confianza fijos (±2 desviaciones estándar) alrededor de los valores de CPUE observados. El número en cada panel corresponde a los números que designan las pesquerías en la Tabla 2.1.

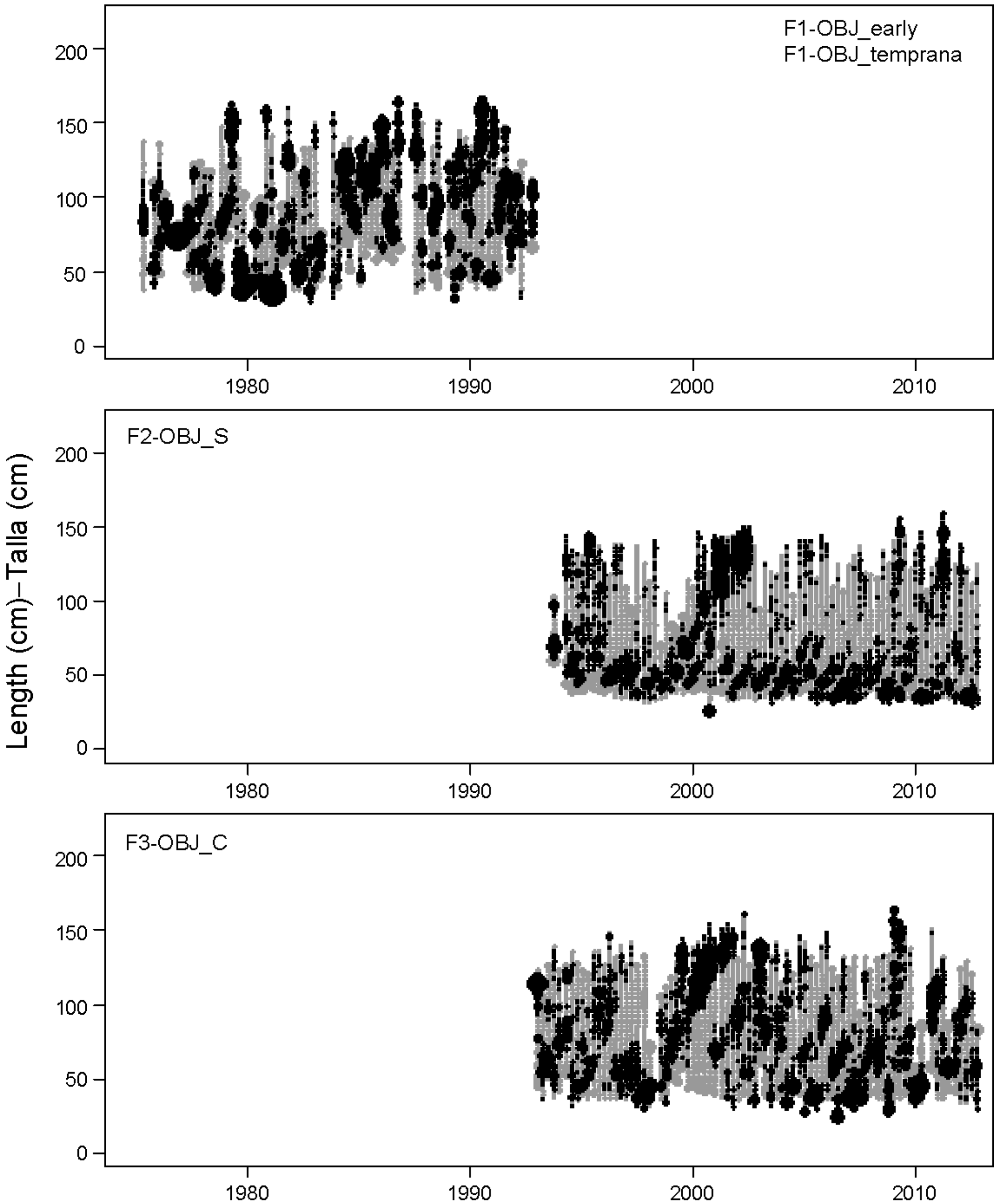

FIGURE 4.12a. Pearson residual plots for the model fits to the length-composition data for Fisheries 1, 2, and 3. The gray and black circles represent observations that are higher and lower, respectively, than the model predictions. The areas of the circles are proportional to the absolute values of the residuals. The numbers in the panels correspond to the numbers designating the fisheries in Table 2.1.

FIGURA 4.12a. Gráficas de residuales de Pearson para los ajustes del modelo a los datos de composición por talla de las pesquerías 1, 2, y 3. Los círculos grises y negros representan observaciones mayores y menores, respectivamente, que las predicciones del modelo. El área de los círculos es proporcional al valor absoluto de los residuales. El número en cada panel corresponde a los números que designan las pesquerías en la Tabla 2.1.

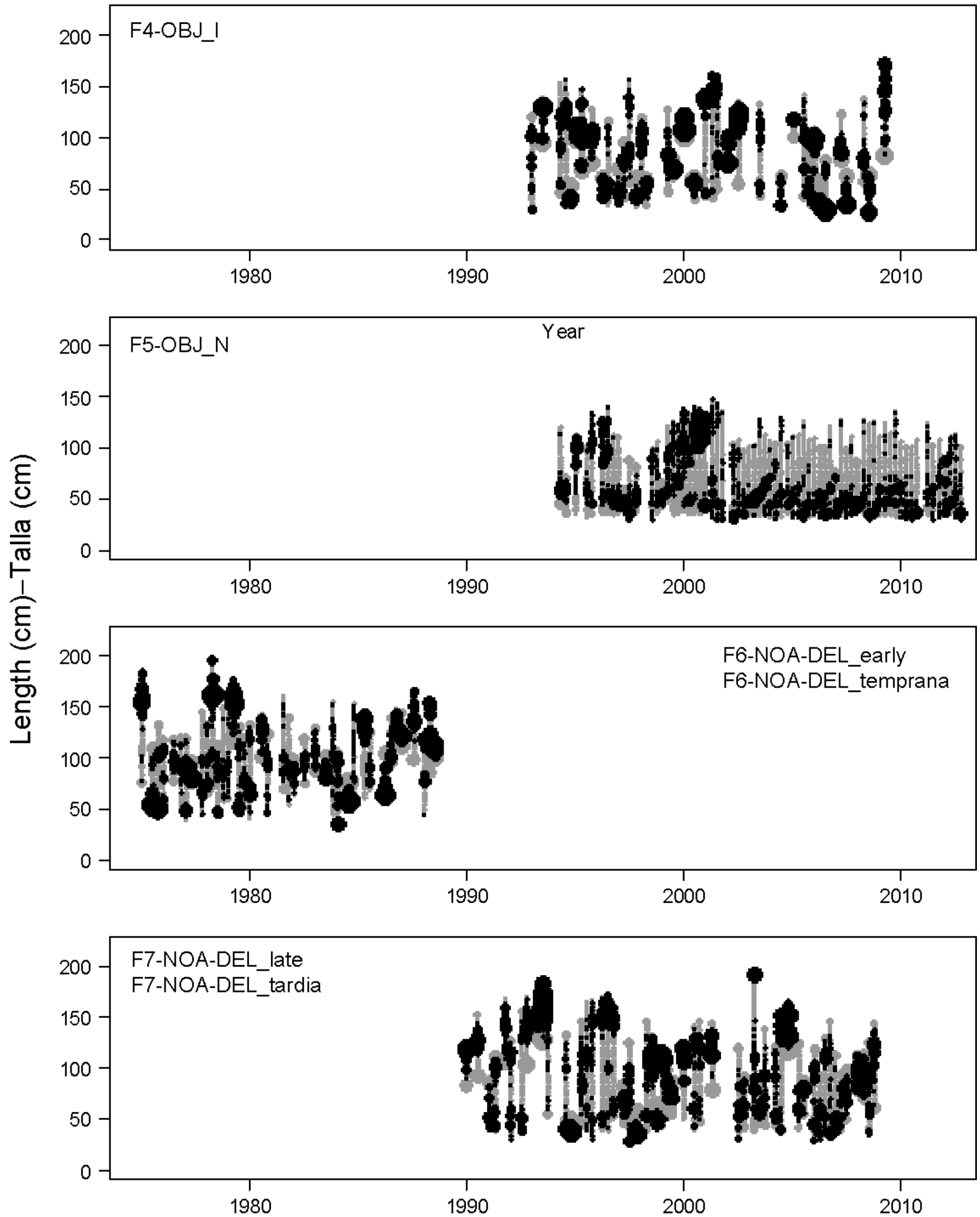

FIGURE 4.12b. Pearson residual plots for the model fits to the length-composition data for Fisheries 4-7. The gray and black circles represent observations that are higher and lower, respectively, than the model predictions. The areas of the circles are proportional to the absolute values of the residuals. The numbers in the panels correspond to the numbers designating the fisheries in Table 2.1.

FIGURA 4.12b. Gráficas de residuales de Pearson para los ajustes del modelo a los datos de composición por talla de las pesquerías 4-7. Los círculos abiertos y sólidos representan observaciones mayores y menores, respectivamente, que las predicciones del modelo. El área de los círculos es proporcional al valor absoluto de los residuales. El número en cada panel corresponde a los números que designan las pesquerías en la Tabla 2.1.

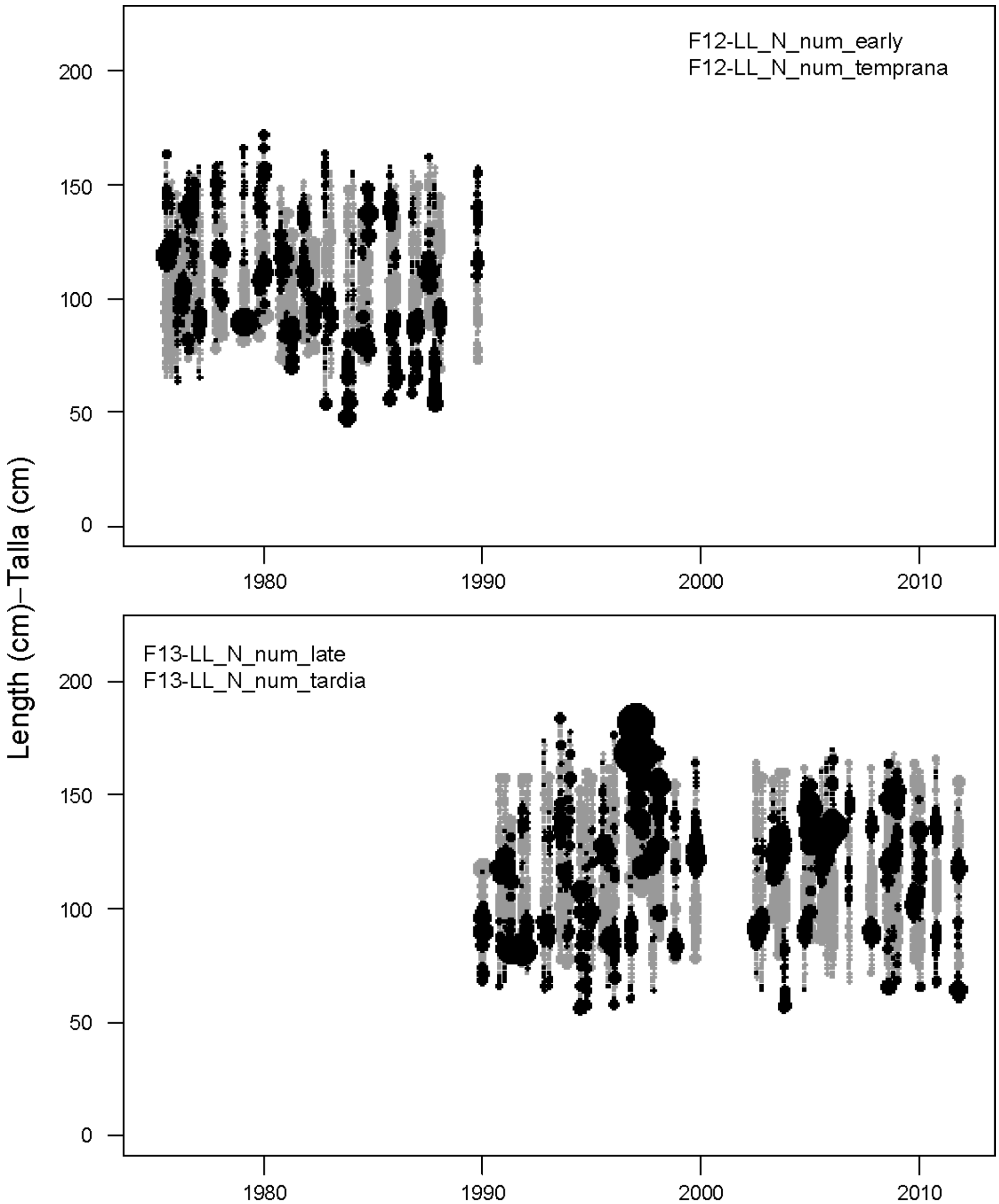

FIGURE 4.12c. Pearson residual plots for the model fits to the length-composition data for Fisheries 12 and 13. The gray and black circles represent observations that are higher and lower, respectively, than the model predictions. The areas of the circles are proportional to the absolute values of the residuals. The numbers in the panels correspond to the numbers designating the fisheries in Table 2.1.

FIGURA 4.12c. Gráficas de residuales de Pearson para los ajustes del modelo a los datos de composición por talla de las pesquerías 12 y 13. Los círculos abiertos y sólidos representan observaciones mayores y menores, respectivamente, que las predicciones del modelo. El área de los círculos es proporcional al valor absoluto de los residuales. El número en cada panel corresponde a los números que designan las pesquerías en la Tabla 2.1.

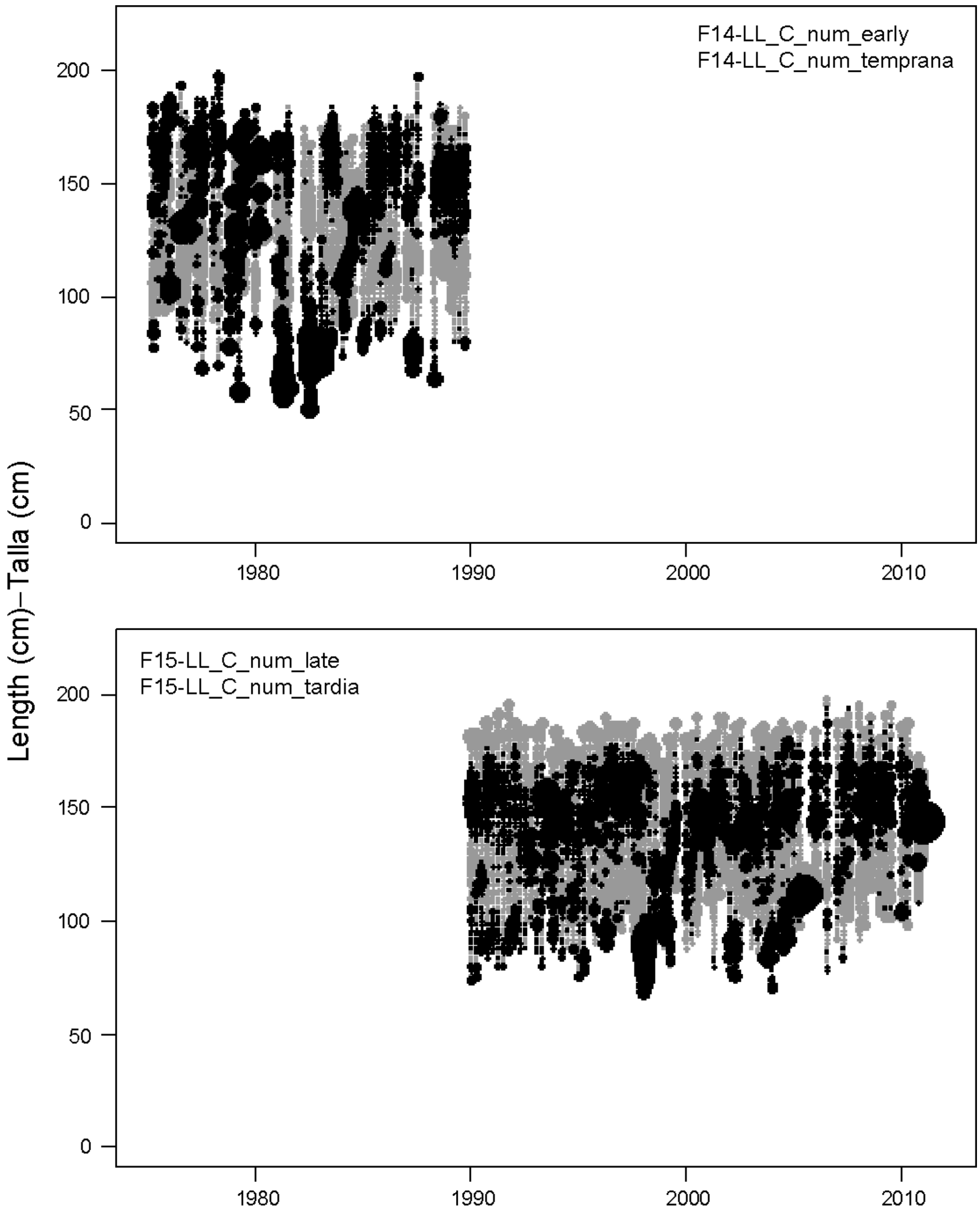

FIGURE 4.12d. Pearson residual plots for the model fits to the length-composition data for Fisheries 14 and 15. The gray and black circles represent observations that are higher and lower, respectively, than the model predictions. The areas of the circles are proportional to the absolute values of the residuals. The numbers in the panels correspond to the numbers designating the fisheries in Table 2.1.

FIGURA 4.12d. Gráficas de residuales de Pearson para los ajustes del modelo a los datos de composición por talla de las pesquerías 14 y 15. Los círculos abiertos y sólidos representan observaciones mayores y menores, respectivamente, que las predicciones del modelo. El área de los círculos es proporcional al valor absoluto de los residuales. El número en cada panel corresponde a los números que designan las pesquerías en la Tabla 2.1.

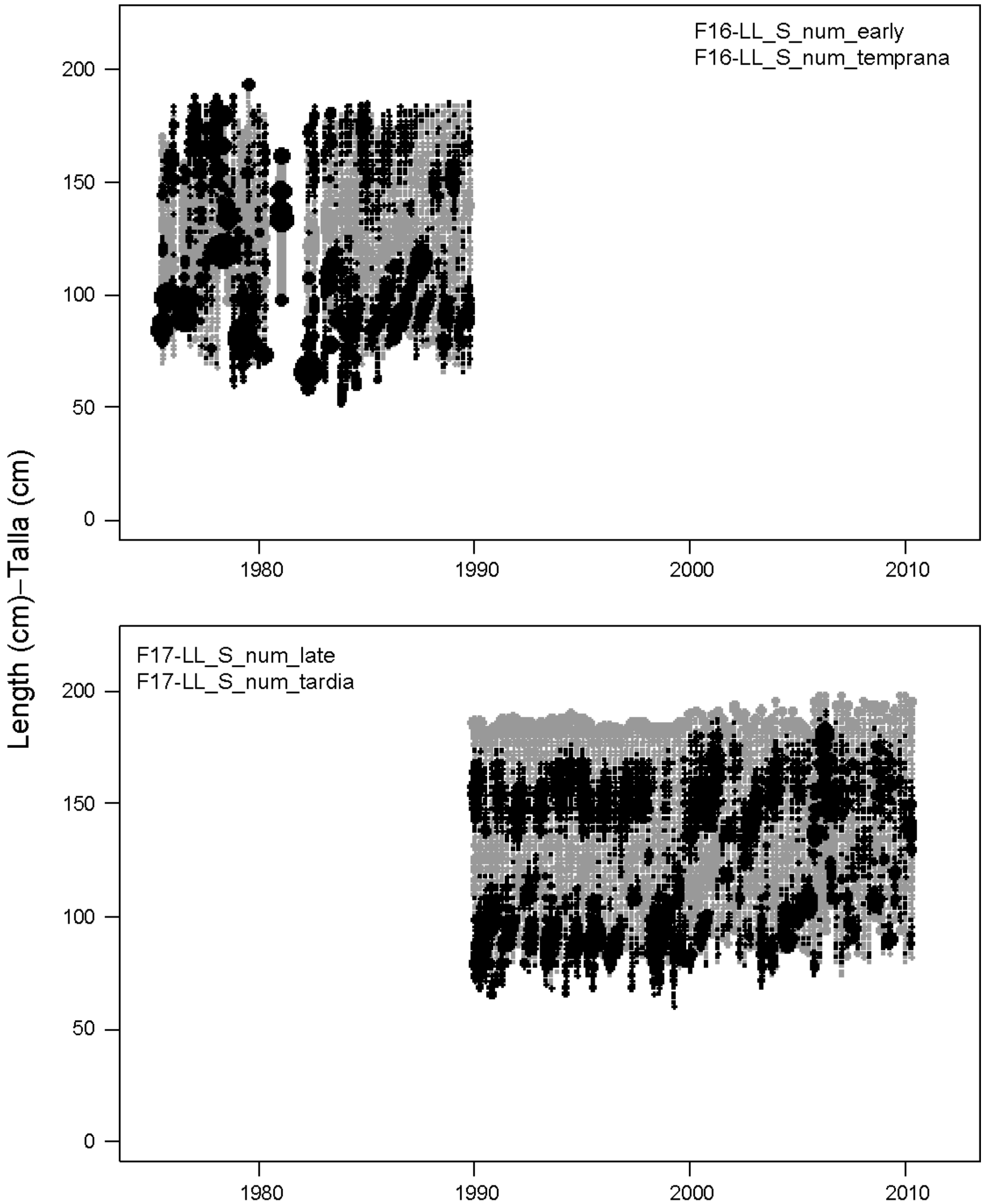

FIGURE 4.12e. Pearson residual plots for the model fits to the length-composition data for Fisheries 16 and 17. The gray and black circles represent observations that are higher and lower, respectively, than the model predictions. The areas of the circles are proportional to the absolute values of the residuals. The numbers in the panels correspond to the numbers designating the fisheries in Table 2.1.

FIGURA 4.12e. Gráficas de residuales de Pearson para los ajustes del modelo a los datos de composición por talla de las pesquerías 16 and 17. Los círculos abiertos y sólidos representan observaciones mayores y menores, respectivamente, que las predicciones del modelo. El área de los círculos es proporcional al valor absoluto de los residuales. El número en cada panel corresponde a los números que designan las pesquerías en la Tabla 2.1.

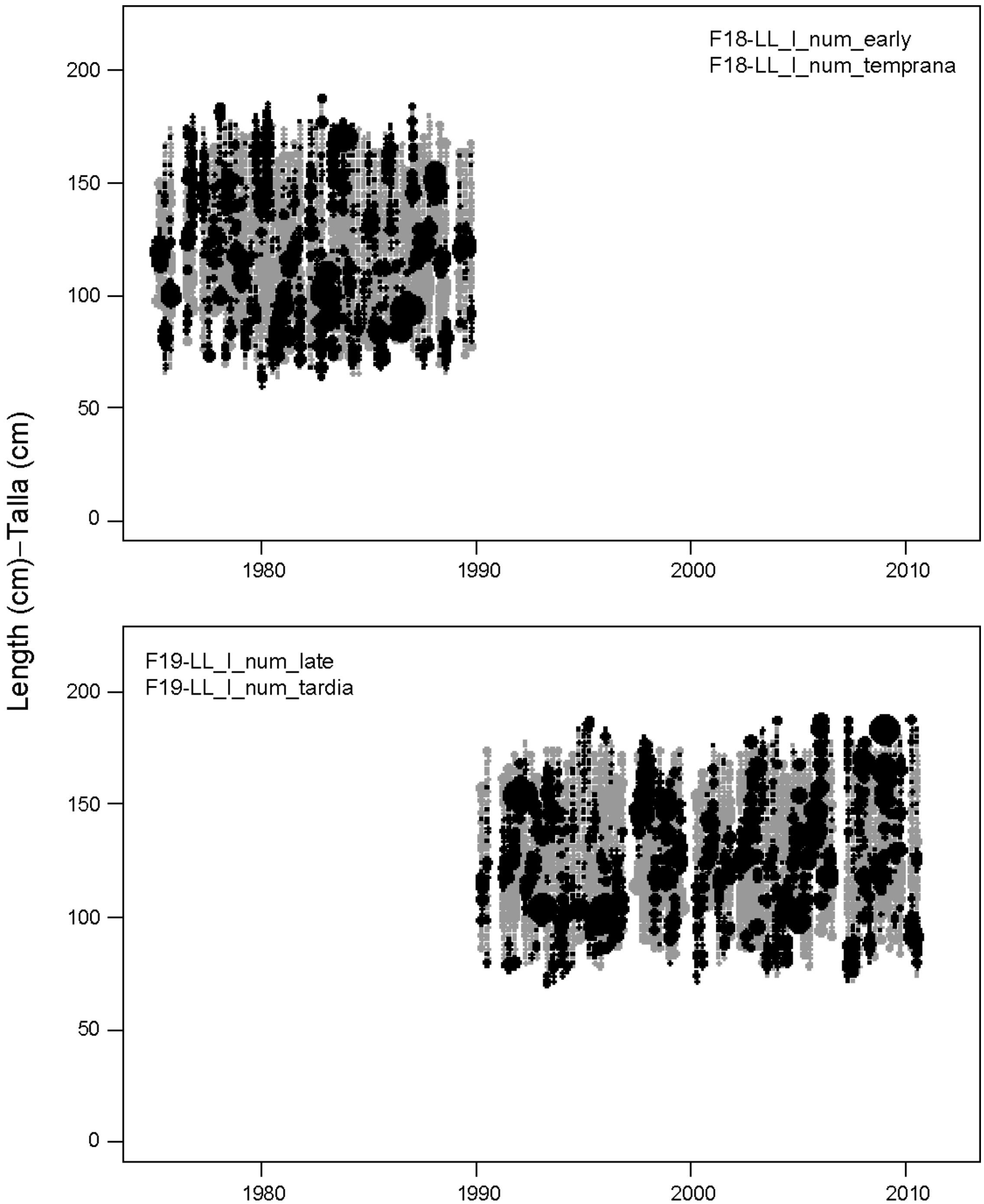

FIGURE 4.12f. Pearson residual plots for the model fits to the length-composition data for Fisheries 18 and 19. The gray and black circles represent observations that are higher and lower, respectively, than the model predictions. The areas of the circles are proportional to the absolute values of the residuals. The numbers in the panels correspond to the numbers designating the fisheries in Table 2.1.

FIGURA 4.12f. Gráficas de residuales de Pearson para los ajustes del modelo a los datos de composición por talla de las pesquerías 18 y 19. Los círculos abiertos y sólidos representan observaciones mayores y menores, respectivamente, que las predicciones del modelo. El área de los círculos es proporcional al valor absoluto de los residuales. El número en cada panel corresponde a los números que designan las pesquerías en la Tabla 2.1.

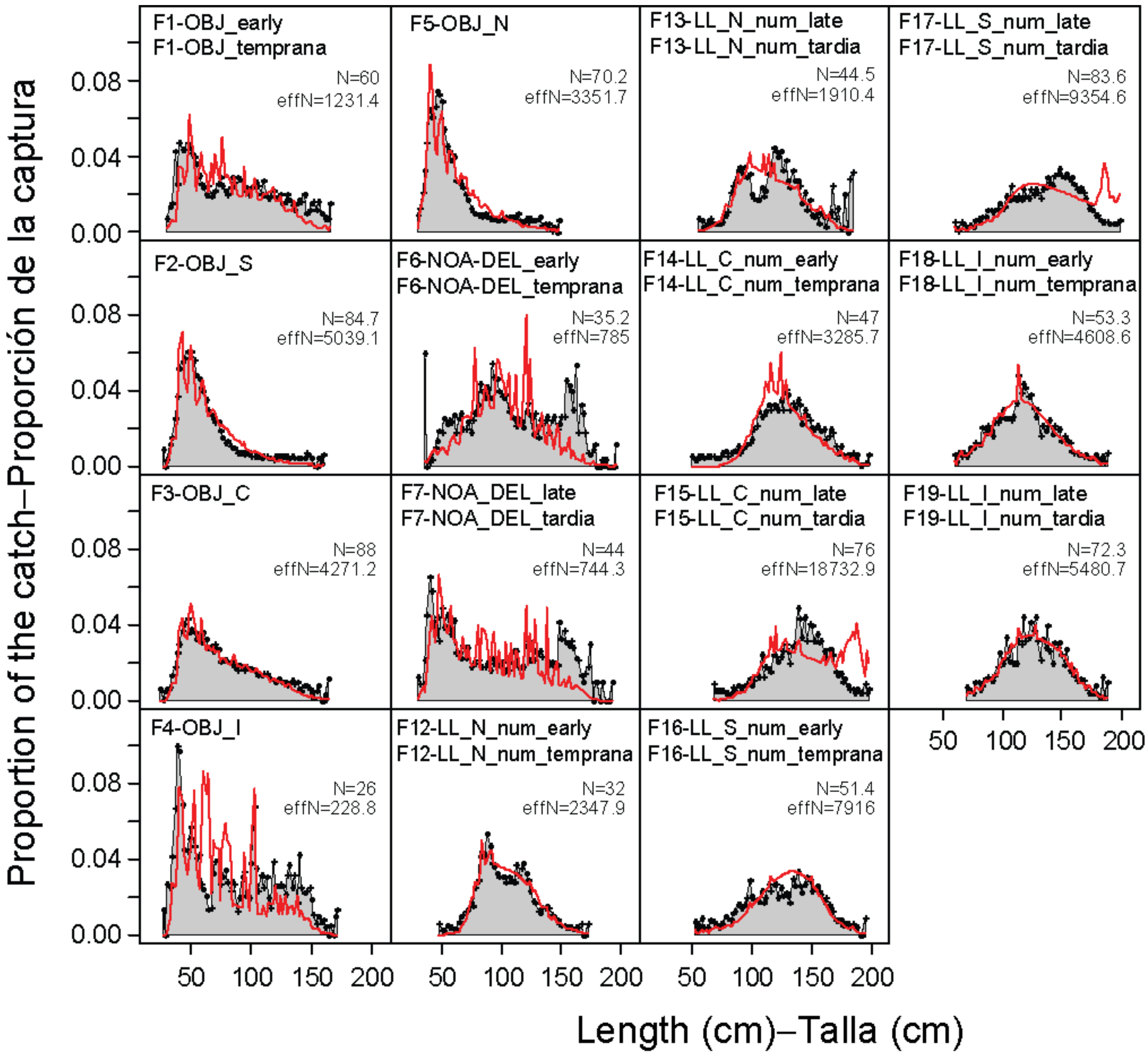

FIGURE 4.12g. Average observed (dots) and predicted (curves) length compositions of the catches taken by surface Fisheries 1-7 and longline Fisheries 12-19 defined for the stock assessment of bigeye tuna in the EPO. The numbers in the panels correspond to the numbers designating the fisheries in Table 2.1.

FIGURA 4.12g. Composición por talla media observada (puntos) y predicha (curvas) de las capturas realizadas por las pesquerías de superficie 1-7 y las pesquerías de palangre 12-19 definidas para la evaluación de la población de atún patudo en el OPO. El número en cada panel corresponde a los números que designan las pesquerías en la Tabla 2.1.

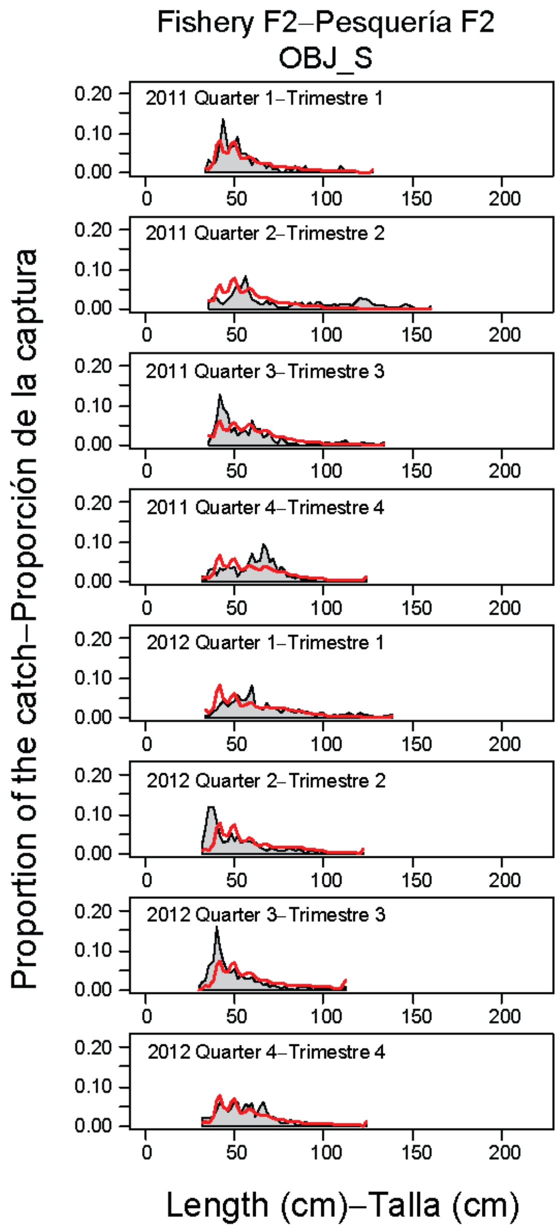

FIGURE 4.12h. Observed (dots) and predicted (curves) length compositions of the recent catches of bigeye tuna by Fishery 2. The tails of the predicted length compositions are accumulated at the length intervals corresponding to the lowest and highest observations.

FIGURA 4.12h. Composición por talla observada (puntos) y predicha (curvas) de las capturas recientes de atún patudo por la Pesquería 2. Las colas de las composiciones por talla predichas se acumulan en los intervalos de talla que corresponden a las observaciones mínimas y máximas.

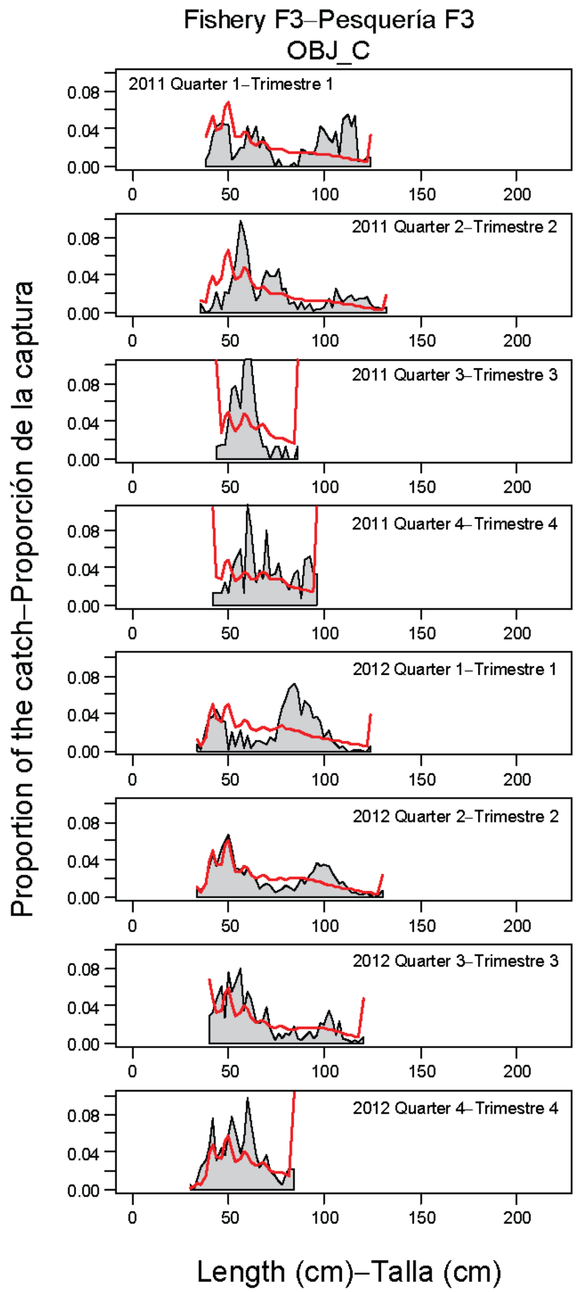

FIGURE 4.12i. Observed (dots) and predicted (curves) length compositions of the recent catches of bigeye tuna by Fishery 3. The tails of the predicted length compositions are accumulated at the length intervals corresponding to the lowest and highest observations.

FIGURA 4.12i. Composición por talla observada (puntos) y predicha (curvas) de las capturas recientes de atún patudo por la Pesquería 3. Las colas de las composiciones por talla predichas se acumulan en los intervalos de talla que corresponden a las observaciones mínimas y máximas.

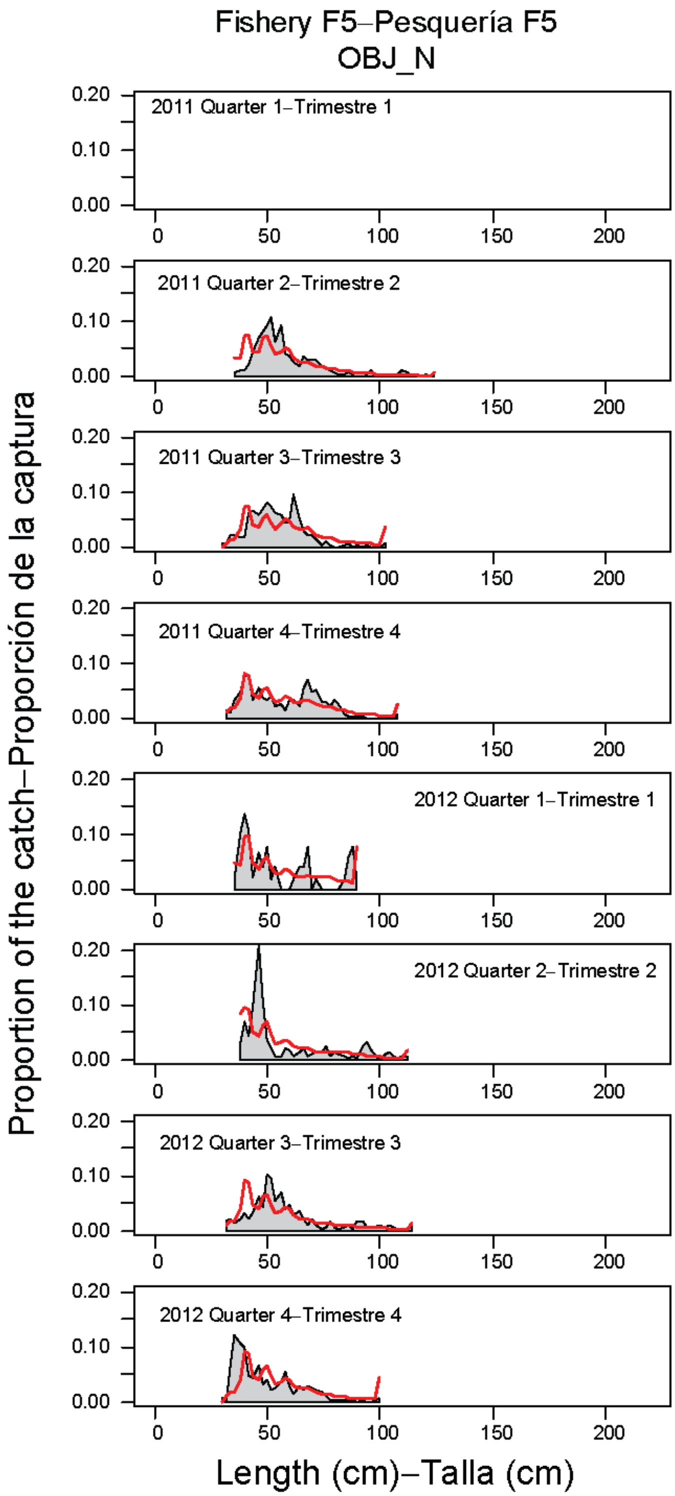

FIGURE 4.12j. Observed (dots) and predicted (curves) length compositions of the recent catches of bigeye tuna by Fishery 5. The tails of the predicted length compositions are accumulated at the length intervals corresponding to the lowest and highest observations.

FIGURA 4.12j. Composición por talla observada (puntos) y predicha (curvas) de las capturas recientes de atún patudo por la Pesquería 5. Las colas de las composiciones por talla predichas se acumulan en los intervalos de talla que corresponden a las observaciones mínimas y máximas.

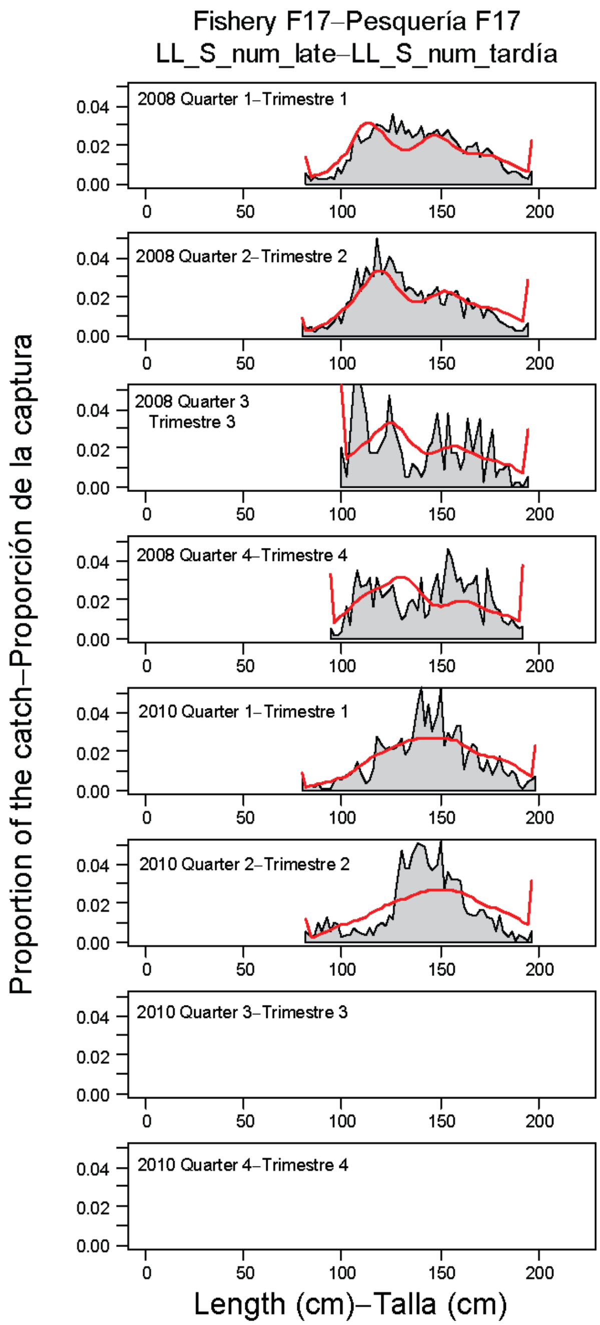

FIGURE 4.12k. Observed (dots) and predicted (curves) length compositions of the recent catches of bigeye tuna by Fishery 17. The tails of the predicted length compositions are accumulated at the length intervals corresponding to the lowest and highest observations.

FIGURA 4.12k. Composición por talla observada (puntos) y predicha (curvas) de las capturas recientes de atún patudo por la pesquería 17. Las colas de las composiciones por talla predichas se acumulan en los intervalos de talla que corresponden a las observaciones mínimas y máximas.

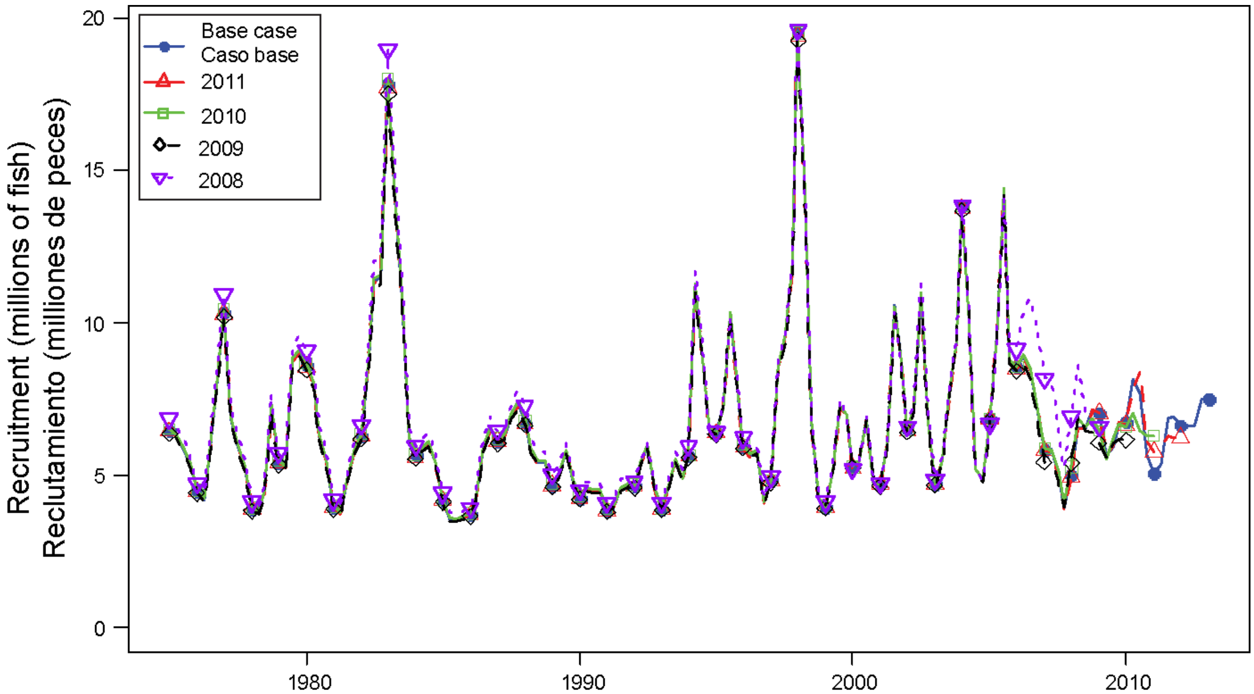

FIGURE 4.13. Retrospective comparisons of estimates of the recruitment of bigeye tuna in the EPO. The estimates from the base case model are compared with the estimates obtained when the most recent year (2012), two years (2012 and 2011), three years (2012, 2011, and 2010) or four years (2012, 2011, 2010, and 2009) of data were excluded.

FIGURA 4.13. Comparaciones retrospectivas de las estimaciones de reclutamiento de atún patudo en el OPO. Se comparan las estimaciones del modelo del caso base con aquellas obtenidas cuando se excluyeron los datos del año más reciente (2012), o de los dos años (2012 y 2011), tres años (2012, 2011, y 2010), o cuatro años (2012, 2011, 2010, y 2011) más recientes.

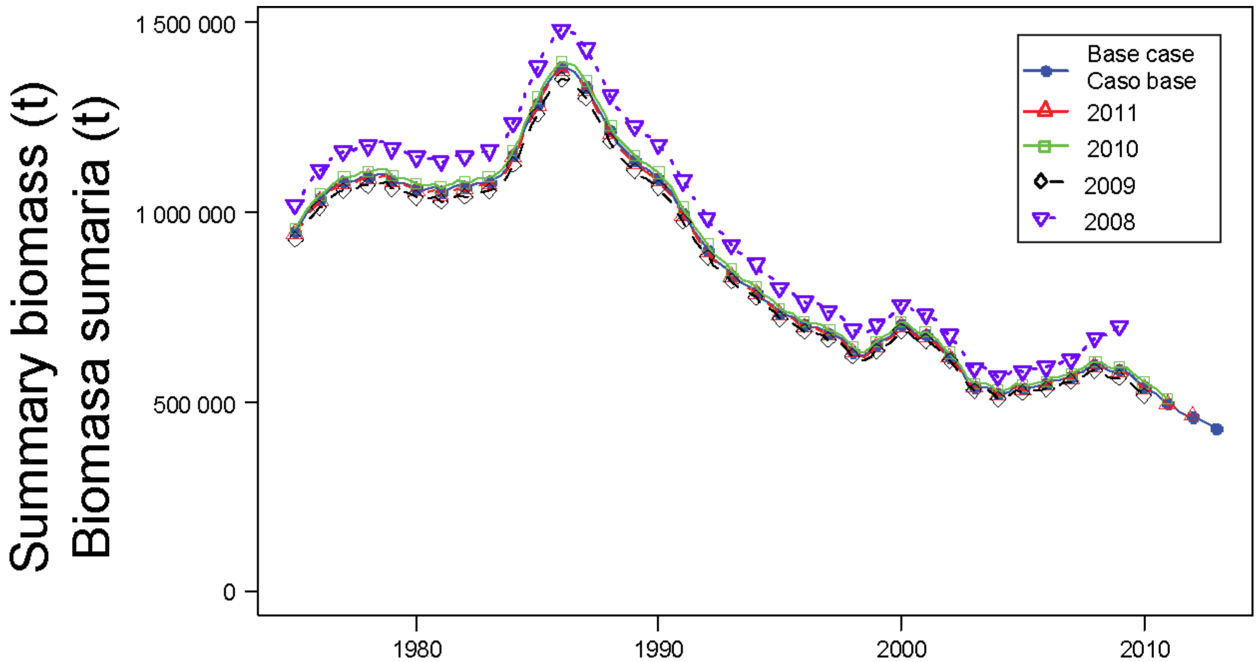

FIGURE 4.14. Retrospective comparisons of estimates of biomass of bigeye tuna 3+ quarters old in the EPO (summary biomass). The estimates from the base case model are compared to the estimates obtained when the most recent year (2012), two years (2012 and 2011), three years (2012, 2011, and 2010) or four years (2012, 2011, 2010, and 2009) of data were excluded. t = metric tons.

FIGURA 4.14. Comparaciones retrospectivas de las estimaciones de la biomasa de atún patudo de 3+ trimestres de edad en el OPO (biomasa sumaria). Se comparan las estimaciones del modelo del caso base con aquellas obtenidas cuando se excluyeron los datos del año más reciente (2012), o de los dos años (2012 y 2011), tres años (2012, 2011, y 2010), o cuatro años (2012, 2011, 2010, y 2011) más recientes. t = toneladas métricas.

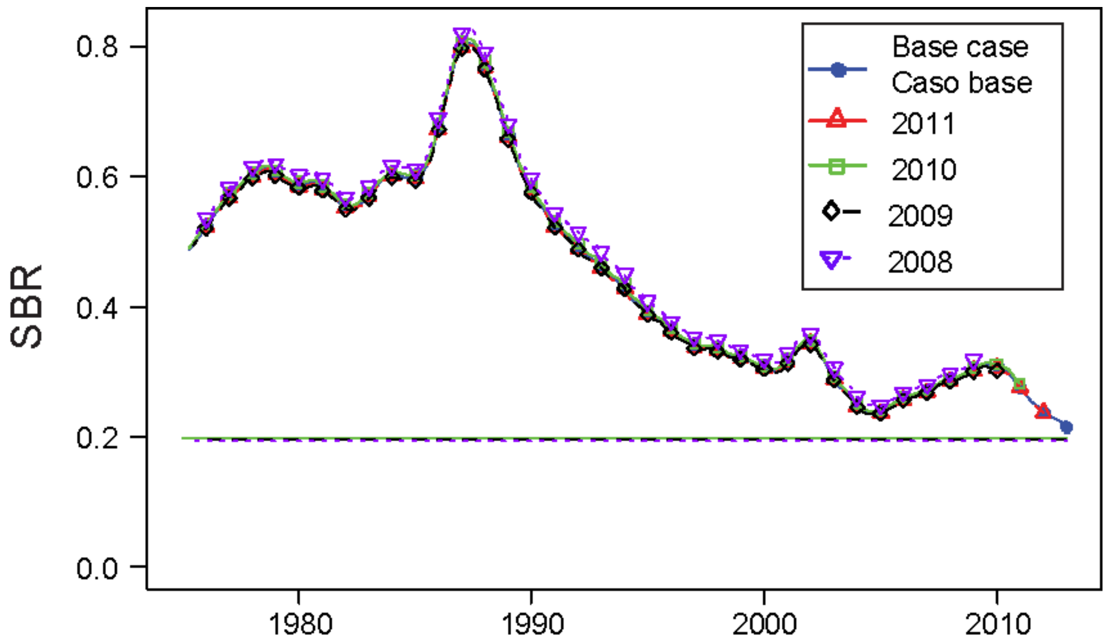

FIGURE 4.15. Retrospective comparisons of estimates of the spawning biomass ratio (SBR) of bigeye tuna in the EPO. The estimates from the base case model are compared with the estimates obtained when the most recent year (2012), two years (2012 and 2011), three years (2012, 2011, and 2010) or four years (2012, 2011, 2010, and 2009) of data were excluded. The horizontal line indicates the SBR at MSY.
FIGURA 4.15. Comparaciones retrospectivas de las estimaciones del cociente de biomasa reproductora (SBR) de atún patudo en el OPO. Se comparan las estimaciones del modelo del caso base con aquéllas obtenidas cuando se excluyeron los datos del año más reciente (2012), o de los dos años (2012 y 2011), tres años (2012, 2011, y 2010), o cuatro años (2012, 2011, 2010, y 2011) más recientes. La línea horizontal indica el SBR en RMS.

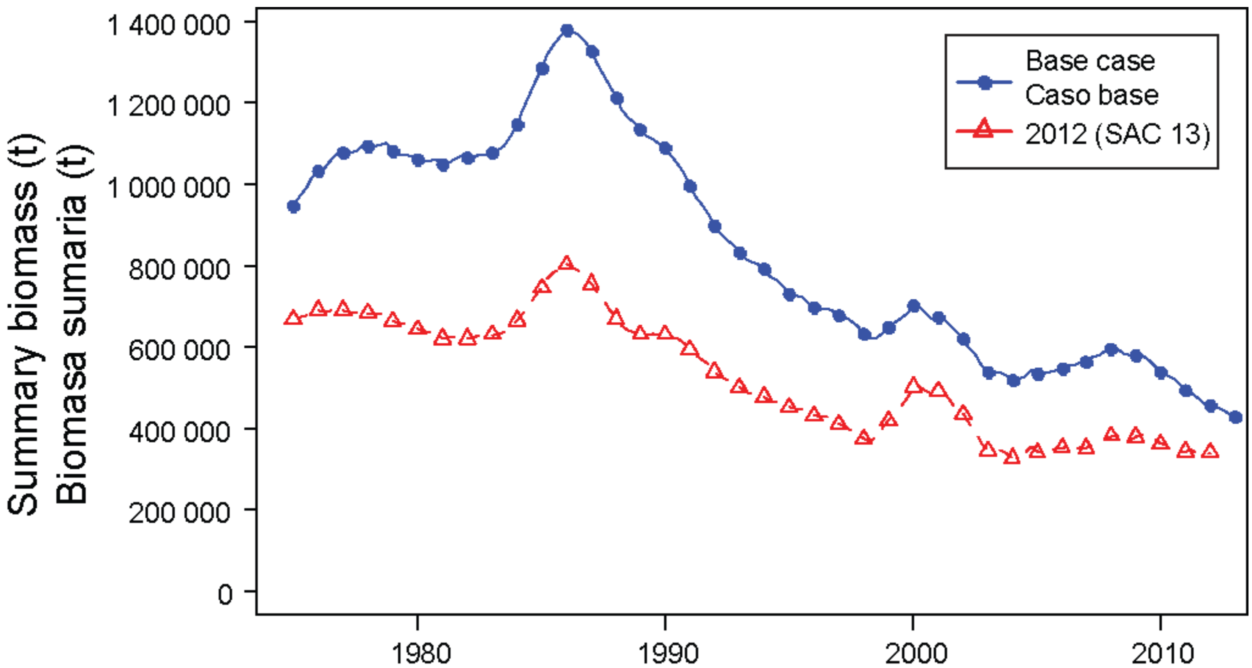

FIGURE 4.16. Comparison of estimates of the biomass of bigeye tuna 3+ quarters old (summary biomass) from the most recent assessment (Aires-da-Silva and Maunder 2012) and the base case model of the current assessment. t = metric tons.

FIGURA 4.16. Comparación de las estimaciones de la biomasa de atún patudo de 3+ trimestres de edad (biomasa sumaria) de la evaluación más reciente (Aires-da-Silva and Maunder 2012) y el modelo de caso base de la evaluación actual. t = toneladas métricas.

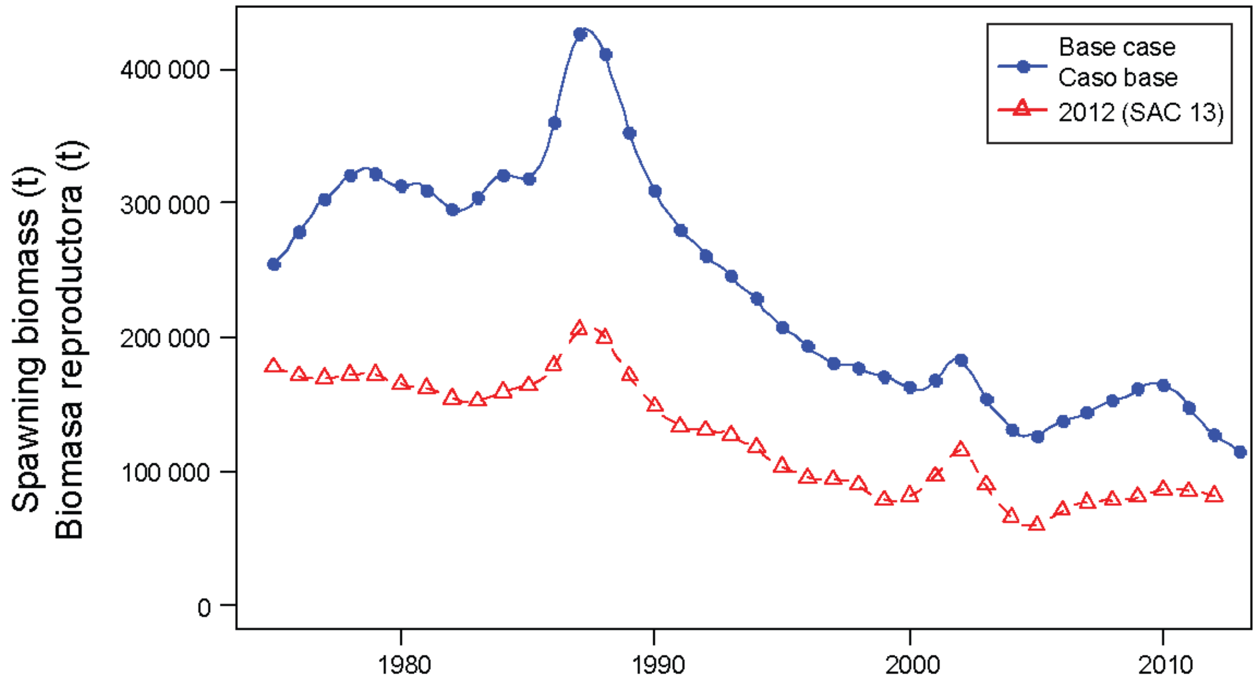

FIGURE 4.17. Comparison of estimates of the spawning biomass of bigeye tuna in the EPO from the most recent assessment (Aires-da-Silva and Maunder 2012) and the base case model of the current assessment. t = metric tons.
FIGURA 4.17. Comparación de la biomasa reproductora estimada de atún patudo en el OPO de la evaluación más reciente (Aires-da-Silva and Maunder 2012) y el modelo de caso base de la evaluación actual. t = toneladas métricas.

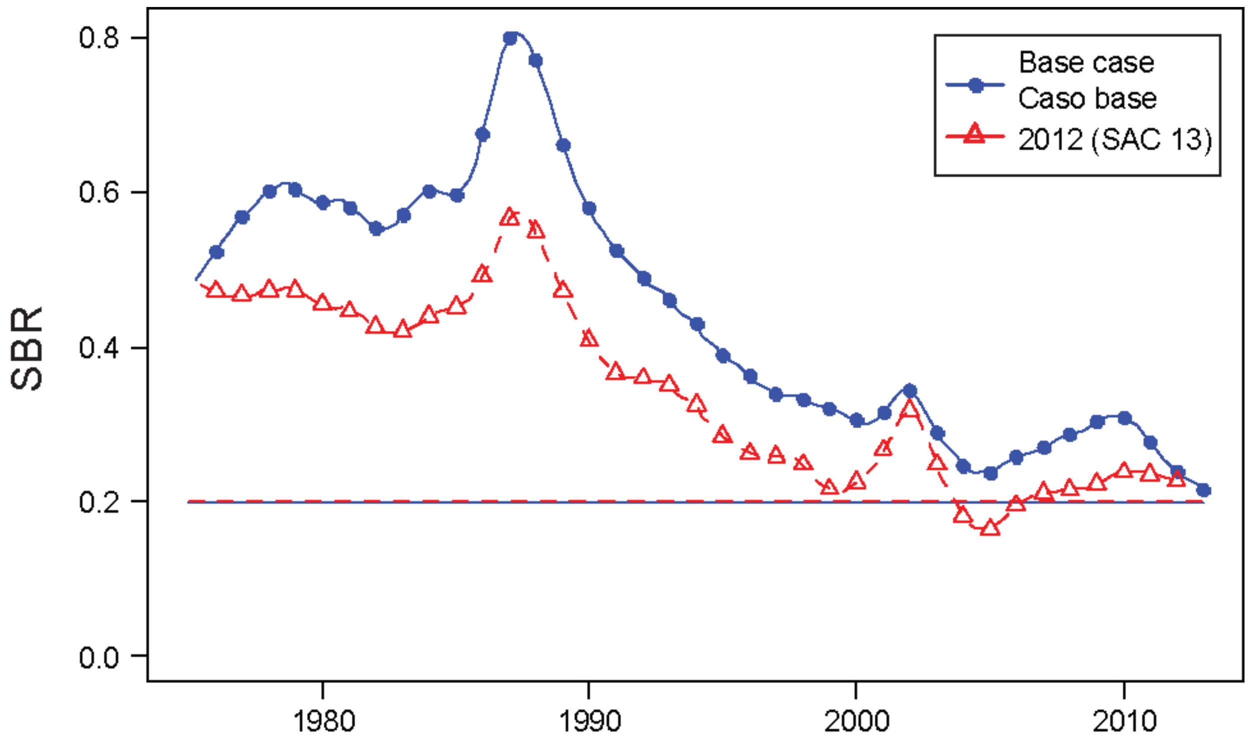

FIGURE 4.18. Comparison of estimated spawning biomass ratios (SBRs) for bigeye tuna in the EPO from the most recent assessment (Aires-da-Silva and Maunder 2012) and the base case model of the current assessment, both using Stock Synthesis. The horizontal lines indicate the SBR at MSY.

FIGURA 4.18. Comparación del cociente de biomasa reproductora (SBR) estimado de atún patudo en el OPO de la evaluación más reciente (Aires-da-Silva and Maunder 2012) y el modelo de caso base de la evaluación actual, ambos con *Stock Synthesis*. Las líneas horizontales indican el SBR en RMS.

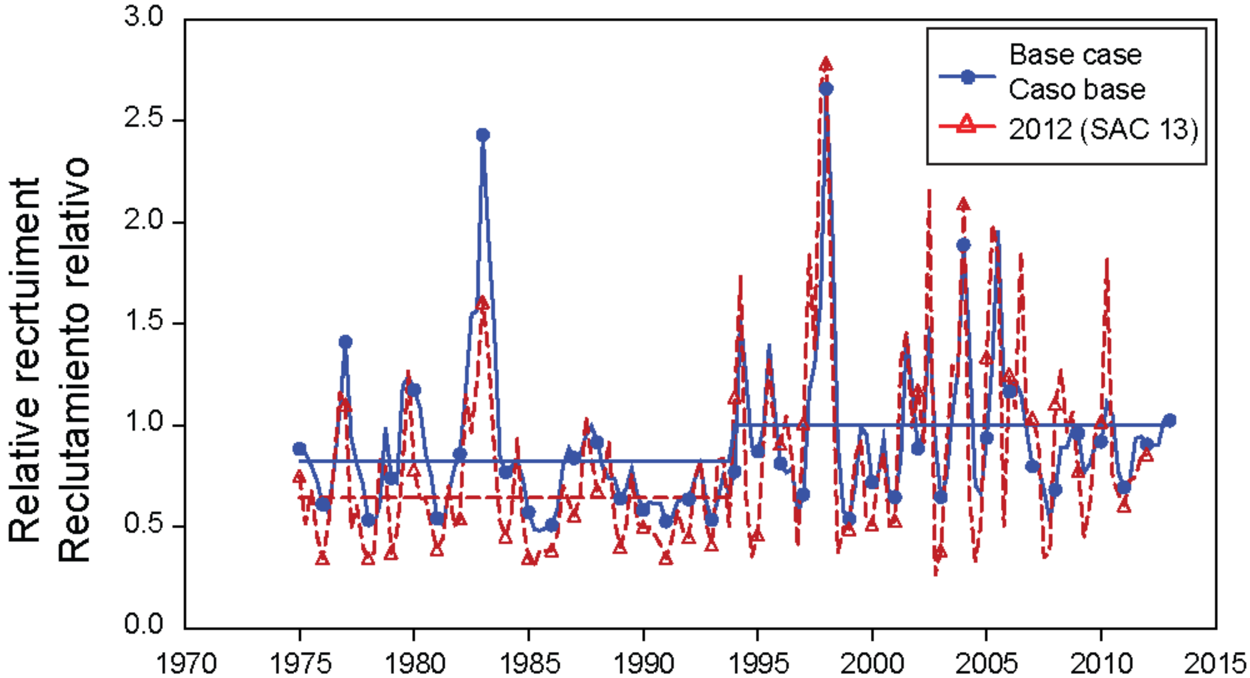

FIGURE 4.19a. Comparison of estimated relative recruitment of bigeye tuna in the EPO from the most recent assessment (Aires-da-Silva and Maunder 2012) and the base case model of the current assessment, both using Stock Synthesis. The horizontal solid and dashed lines represent average recruitment (relative to the post-1994 average recruitment) to visualize the "two-stanza" recruitment pattern in both assessments.

FIGURA 4.19a. Comparación del reclutamiento relativo estimado de atún patudo en el OPO de la evaluación más reciente (Aires-da-Silva y Maunder 2012) y del modelo de caso base de la evaluación actual, ambos con *Stock Synthesis*. Las líneas horizontales sólida y de trazos representan el reclutamiento promedio (relativo al reclutamiento promedio posterior a 1994) para visualizar el patrón de reclutamiento de dos stanzas en ambas evaluaciones.

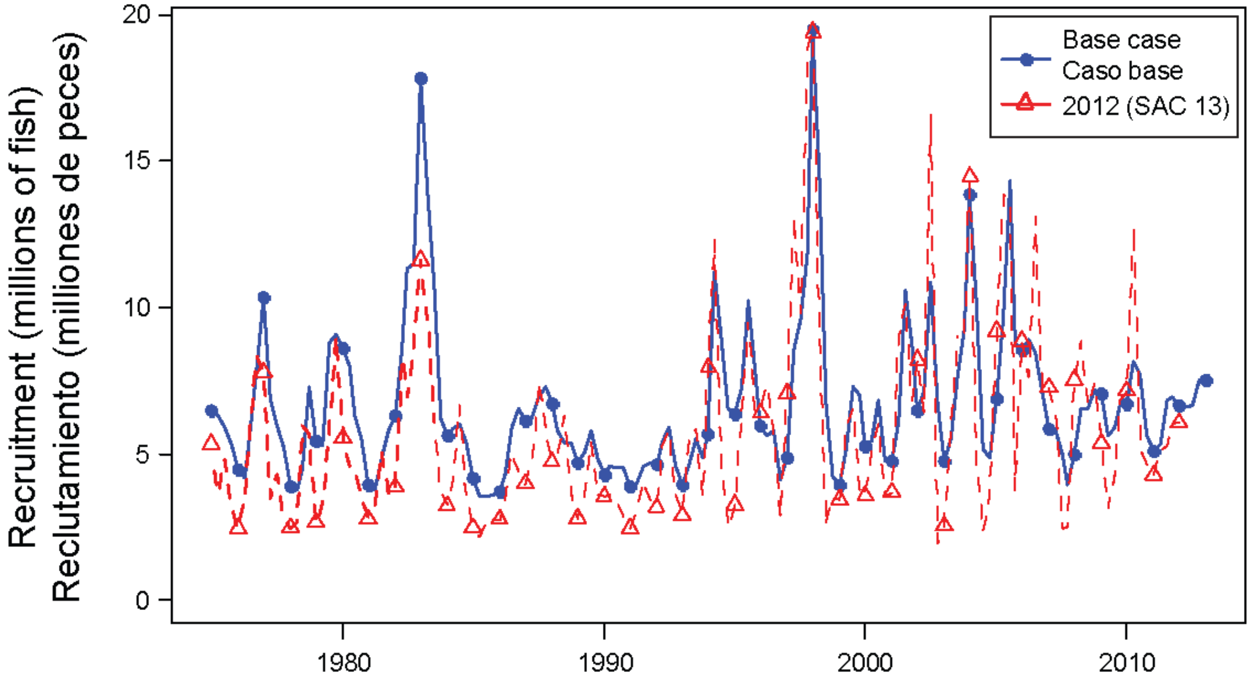

FIGURE 4.19b. Comparison of estimated absolute recruitment of bigeye tuna in the EPO from the most recent assessment (Aires-da-Silva and Maunder 2012) and the base case model of the current assessment, both using Stock Synthesis.

FIGURA 4.19b. Comparación del reclutamiento absoluto estimado de atún patudo en el OPO de la evaluación más reciente (Aires-da-Silva y Maunder 2012) y del modelo de caso base de la evaluación actual, ambos con *Stock Synthesis*.

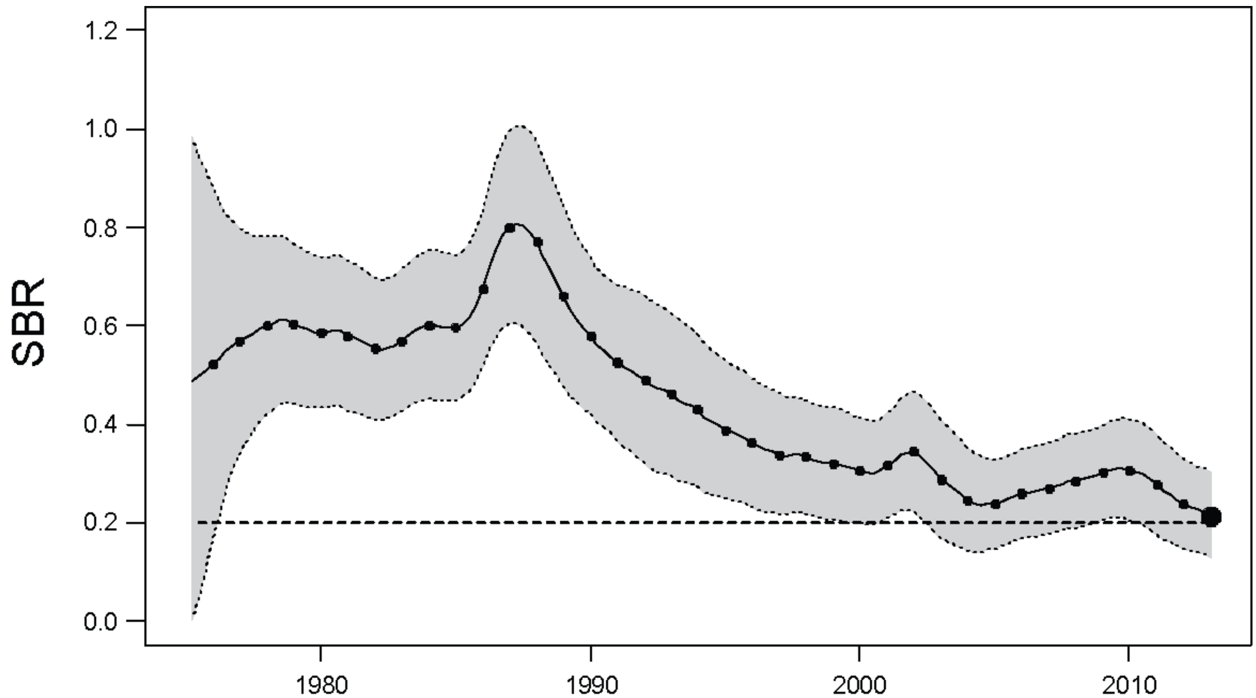

FIGURE 5.1. Estimated spawning biomass ratios (SBRs) for bigeye tuna in the EPO. The dashed horizontal line (at about 0.20) identifies the SBR at MSY. The solid line illustrates the maximum likelihood estimates, and the shaded area represents the confidence intervals (±2 standard deviations) around those estimates.

FIGURA 5.1. Cocientes de biomasa reproductora (SBR) estimados para el atún patudo en el OPO. La línea de trazos horizontal (en aproximadamente 0,20) identifica el SBR en RMS. La línea sólida ilustra las estimaciones de verosimilitud máxima, y el área sombreada representa los intervalos de confianza (±2 desviaciones estándar) alrededor de esas estimaciones.

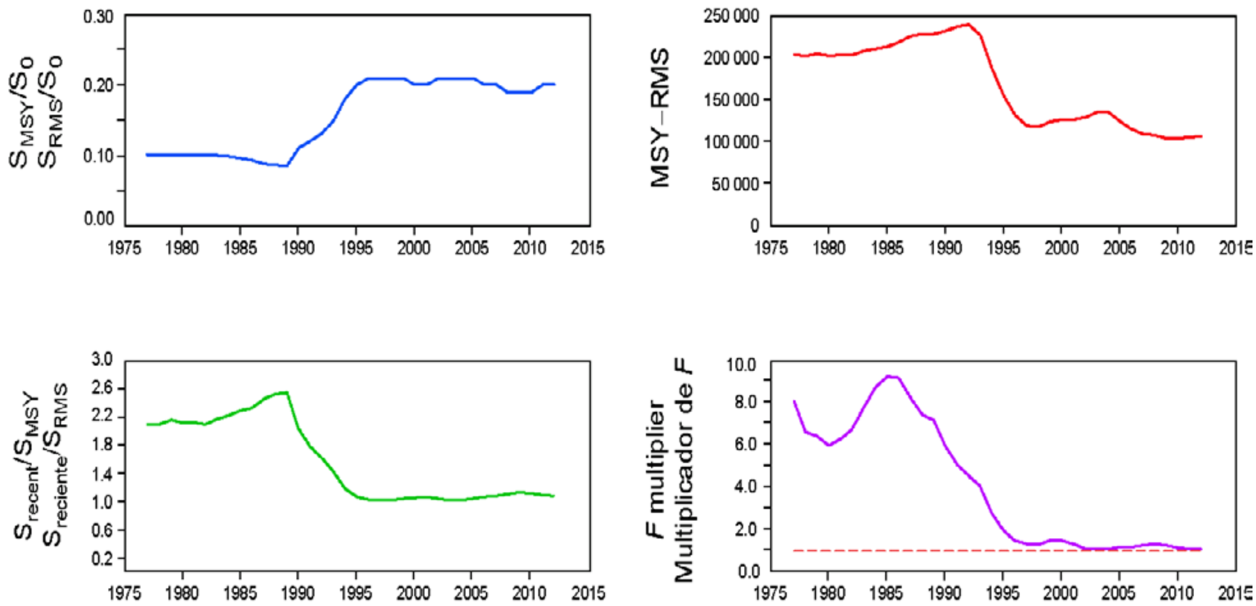

FIGURE 5.2. Estimates of MSY-related quantities calculated using the average age-specific fishing mortality for each year. (S_{recent} is the spawning biomass at the beginning of 2013.)

FIGURA 5.2. Estimaciones de cantidades relacionadas con el RMS calculadas usando la mortalidad por pesca por edad para cada año. ($S_{reciente}$ es la biomasa reproductora al principio de 2013.)

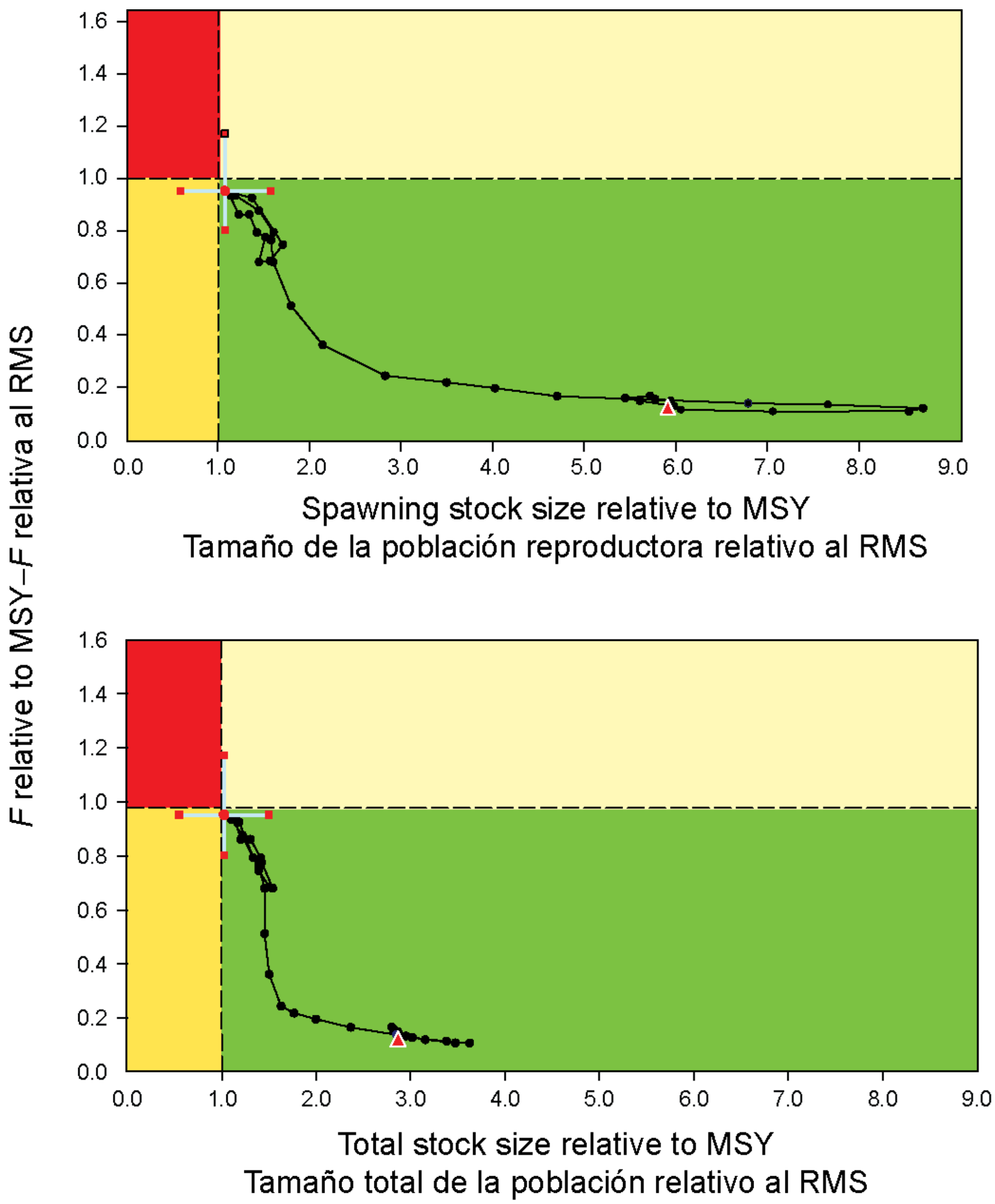

FIGURE 5.3a. Target Kobe (phase) plot of the time series of estimates of stock size (top: spawning biomass; bottom: total biomass) and fishing mortality relative to their MSY reference points. The panels represent proposed target reference points (S_{MSY} and F_{MSY}). Each dot is based on the average fishing mortality rate over three years; the large dot indicates the most recent estimate. The squares around the most recent estimate represent its approximate 95% confidence interval. The triangle is the first estimate (1975).

FIGURA 5.3a. Gráfica de Kobe (fase) objetivo de la serie de tiempo de las estimaciones del tamaño de la población (arriba: biomasa reproductora; abajo: biomasa total) y la mortalidad por pesca en relación con sus puntos de referencia de RMS. Los recuadros representan puntos de referencia objetivo propuestos (S_{RMS} and F_{RMS}). Cada punto se basa en la tasa de explotación media de un trienio; el punto grande indica la estimación más reciente. Los cuadros alrededor de la estimación más reciente representan el intervalo de confianza de 95% aproximado. El triángulo es la primera estimación (1975).

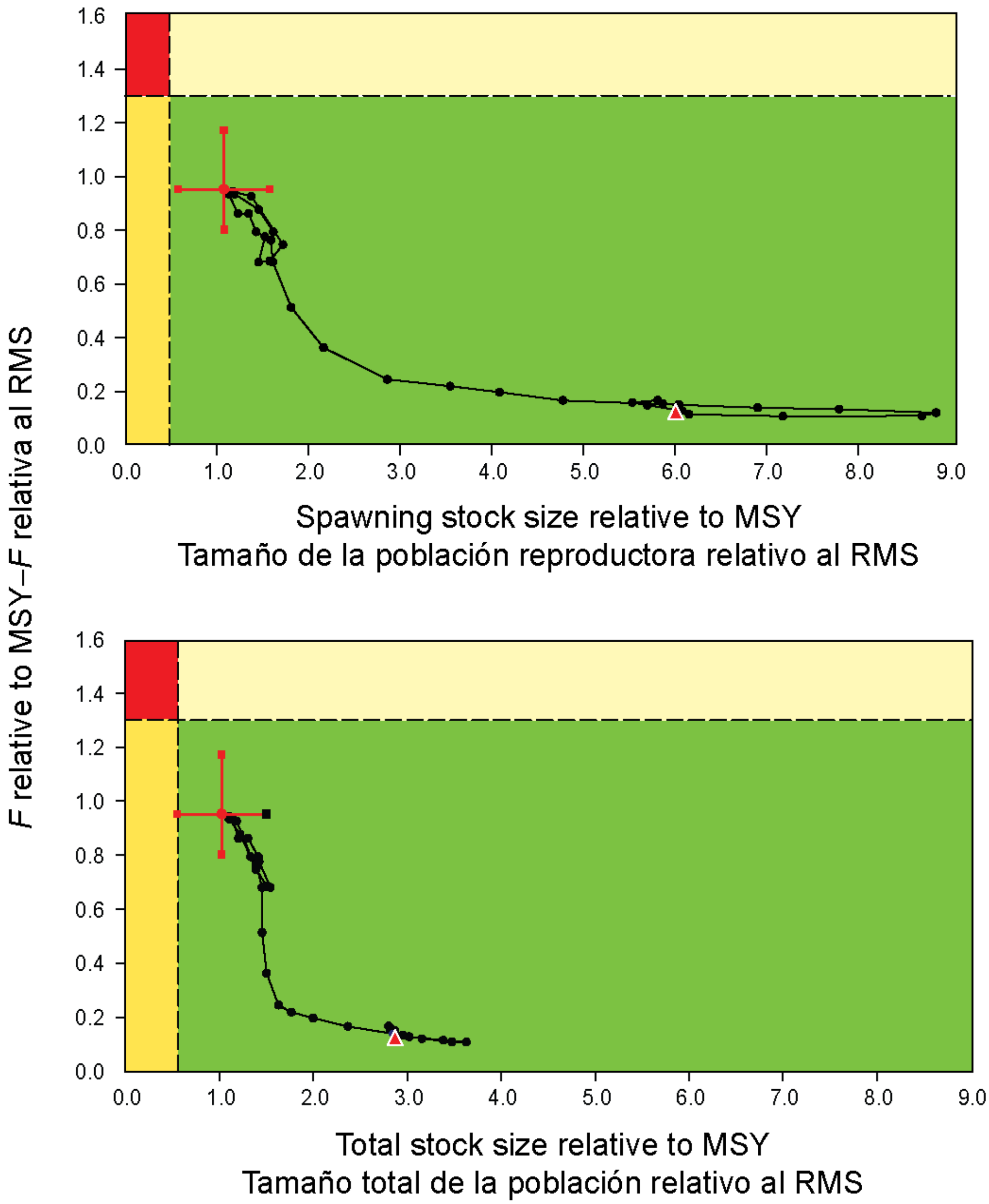

FIGURE 5.3b. Limit Kobe (phase) plot of the time series of estimates of stock size (top: spawning biomass; bottom: total biomass) and fishing mortality relative to their MSY reference points. The panels represent proposed limit reference points (0.5 S_{MSY} and 1.3 F_{MSY}). Each dot is based on the average fishing mortality rate over three years; the large dot indicates the most recent estimate. The squares around the most recent estimate represent its approximate 95% confidence interval. The triangle is the first estimate (1975).

FIGURA 5.3b. Gráfica de Kobe (fase) límite de la serie de tiempo de las estimaciones del tamaño de la población (arriba: biomasa reproductora; abajo: biomasa total) y la mortalidad por pesca en relación con sus puntos de referencia de RMS. Los recuadros representan puntos de referencia límite propuestos (0,5 S_{RMS} and 1,3 F_{RMS}). Cada punto se basa en la tasa de explotación media de un trienio; el punto grande indica la estimación más reciente. Los cuadros alrededor de la estimación más reciente representan el intervalo de confianza de 95% aproximado. El triángulo es la primera estimación (1975).

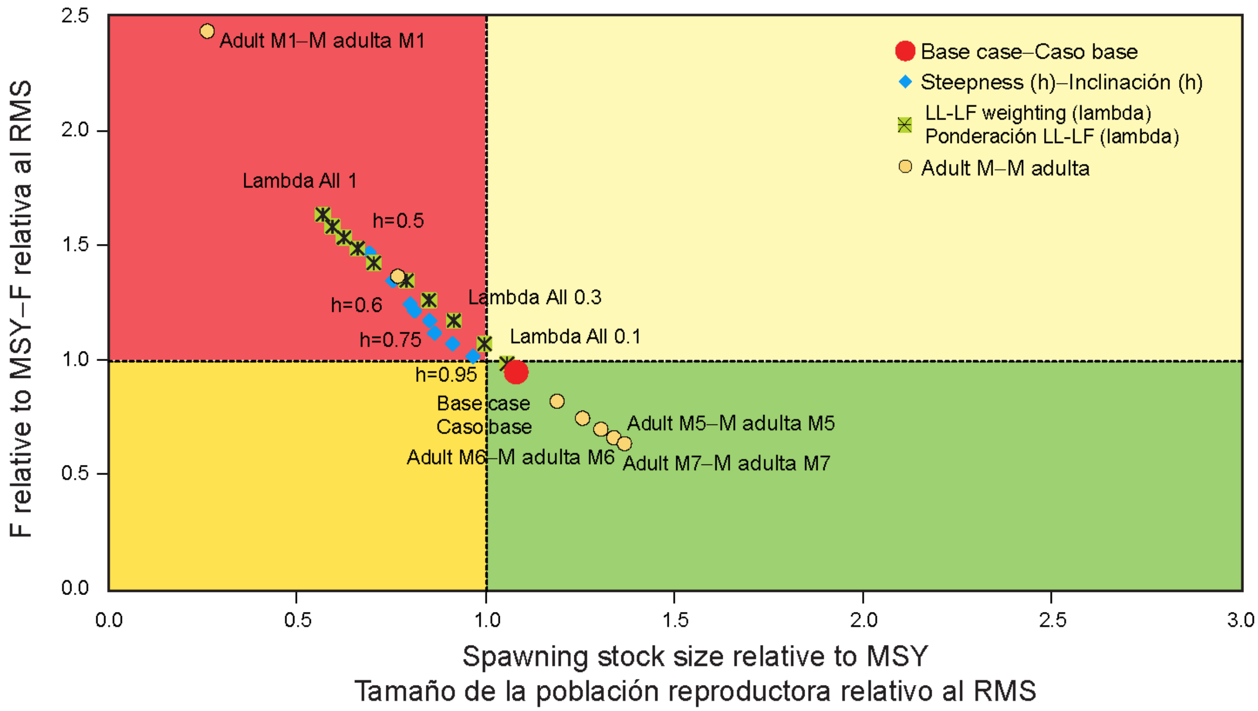

FIGURE 5.3c. Phase plot of the most recent estimate of spawning biomass stock size and fishing mortality relative to their MSY reference points. Each point is based on the average fishing mortality rate over the most recent three years.

FIGURA 5.3c. Gráfica de fase de la estimación más reciente del tamaño de la biomasa reproductora y la mortalidad por pesca en relación con sus puntos de referencia de RMS. Cada punto se basa en la tasa de explotación media de los tres años más recientes.

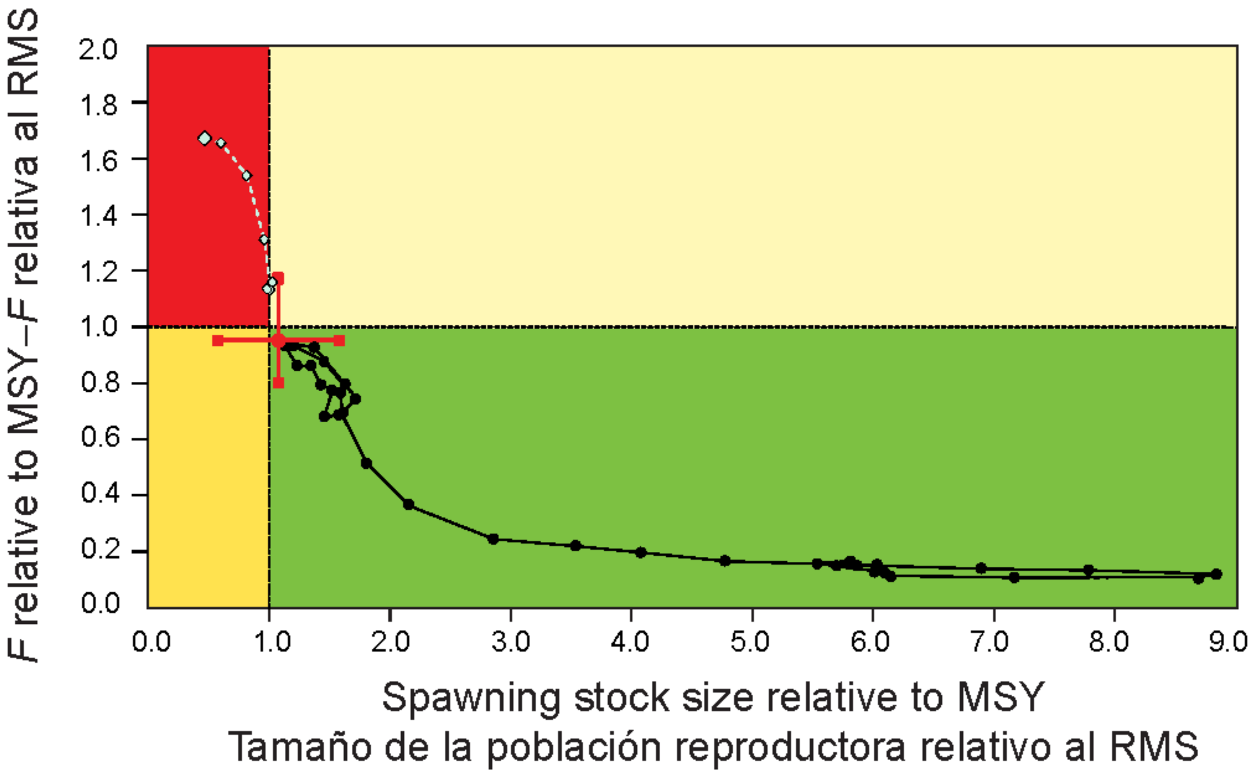

FIGURE 5.3d. Target Kobe (phase) plot of the time series of estimates of spawning biomass and fishing mortality relative to their MSY reference points, with (dots and solid line) and without (squares and dashed line) IATTC conservation resolutions. The panels represent proposed target reference points (S_{MSY} and F_{MSY}). Each dot (square) is based on the average fishing mortality rate over three years; the large dot (square) indicates the most recent estimate. The squares around the most recent estimate represent its approximate 95% confidence interval. The triangle is the first estimate (1975). .

FIGURA 5.3a. Gráfica de Kobe (fase) objetivo de la serie de tiempo de las estimaciones de biomasa reproductora y mortalidad por pesca en relación con sus puntos de referencia de RMS, con (puntos y línea sólida) y sin (cuadros y línea de trazos) resoluciones de conservación de la CIAT. Los recuadros representan puntos de referencia objetivo propuestos (S_{RMS} y F_{RMS}). Cada punto se basa en la tasa de explotación media de un trienio; el punto (cuadro) grande indica la estimación más reciente. Los cuadros alrededor de la estimación más reciente representan su intervalo de confianza de 95% aproximado. El triángulo es la primera estimación (1975).

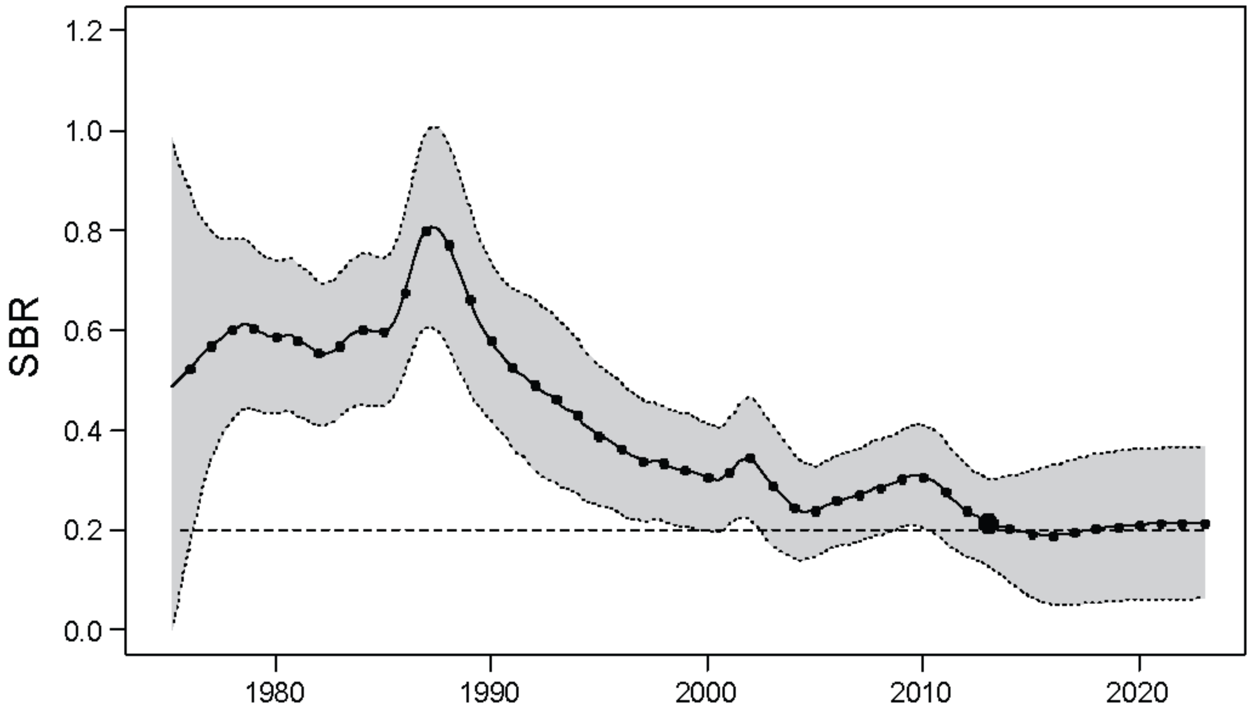

FIGURE 6.1a. Spawning biomass ratios (SBRs) of bigeye tuna in the EPO, including projections for 2013-2022 based on average fishing mortality rates during 2010-2012. The dashed horizontal line (at about 0.20) identifies the SBR at MSY. The solid line illustrates the maximum likelihood estimates, and the estimates after 2013 (the large dot) indicate the SBR predicted to occur if fishing mortality rates continue at the average of that observed during 2010-2012. The dashed lines are the 95-percent confidence intervals around these estimates.

FIGURA 6.1a. Cocientes de biomasa reproductora (SBR) del atún patudo en el OPO, incluyendo proyecciones para 2011-2020 basadas en las tasas medias de mortalidad por pesca durante 2010-2012. La línea sólida ilustra las estimaciones de verosimilitud máxima, y las estimaciones a partir de 2013 (el punto grande) señalan el SBR predicho si las tasas de mortalidad por pesca continúan en el promedio observado durante 2012-2013. Las líneas de trazos representan los intervalos de confianza de 95% alrededor de esas estimaciones.

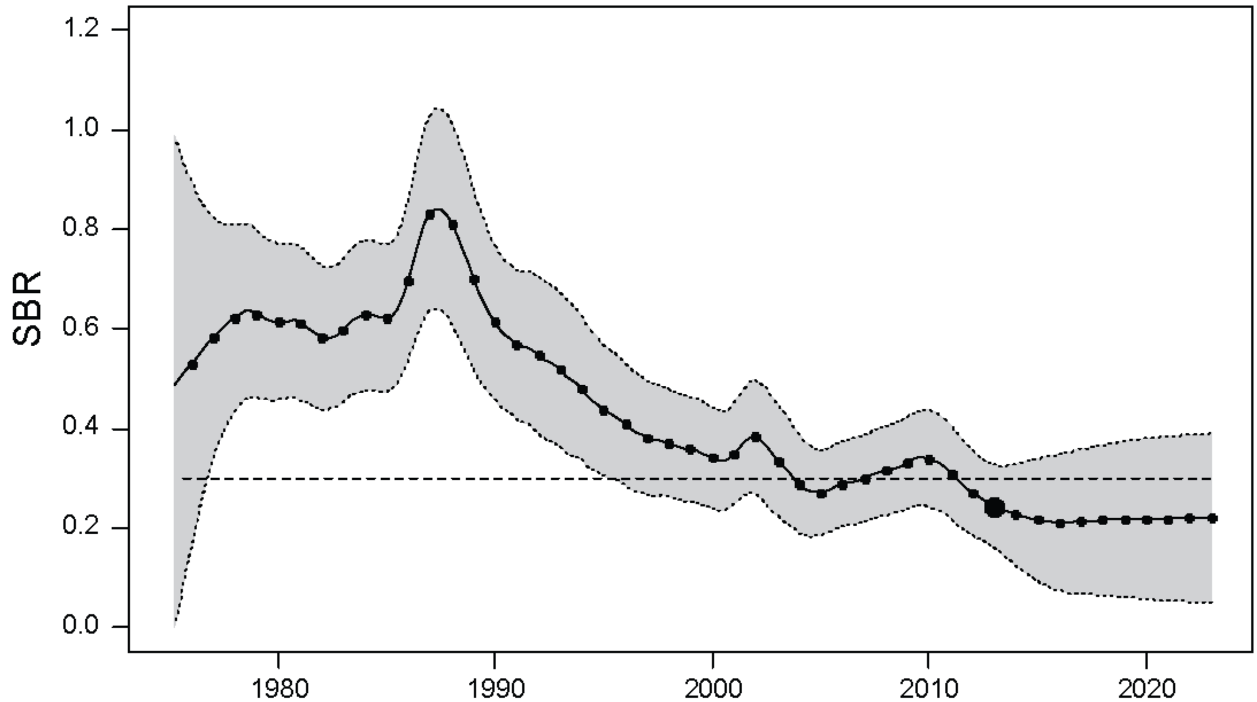

FIGURE 6.1b. Projected spawning biomass ratios (SBRs) of bigeye tuna in the EPO from the stock-recruitment sensitivity analysis based on average fishing mortality rates during 2010-2012. The dashed horizontal line (at about 0.30) identifies the SBR at MSY. The solid line illustrates the maximum likelihood estimates, and the estimates after 2013 (the large dot) indicate the SBR predicted to occur if fishing mortality rates continue at the average of that observed during 2012-2013. The dashed lines are the 95-percent confidence intervals around these estimates.

FIGURA 6.1b. Cocientes de biomasa reproductora (SBR) para el atún patudo en el OPO del análisis de sensibilidad de población-reclutamiento basadas en las tasas medias de mortalidad por pesca durante 2010-2012. La línea de trazos horizontal (en aproximadamente 0,30) identifica el SBR en RMS. La línea sólida ilustra las estimaciones de verosimilitud máxima, y las estimaciones a partir de 2013 (el punto grande) señalan el SBR predicho si las tasas de mortalidad por pesca continúa en el promedio observado durante 2010-2012. Las líneas de trazos representan los intervalos de confianza de 95% alrededor de esas estimaciones.

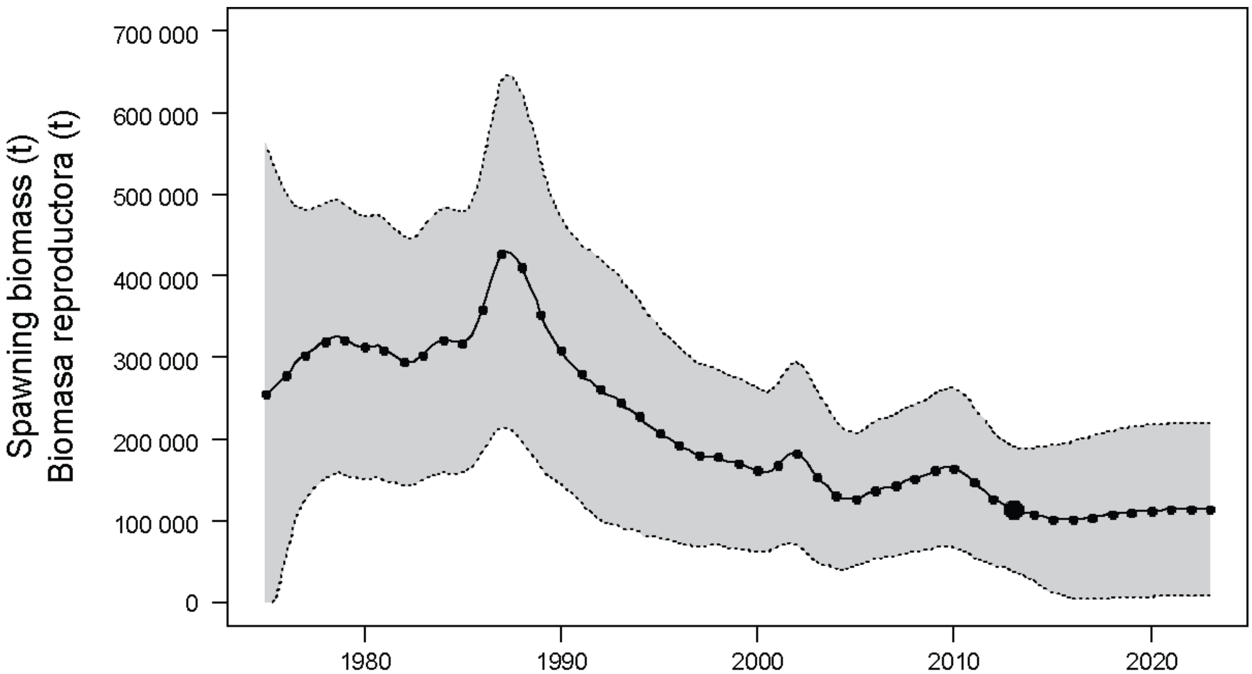

FIGURE 6.2. Spawning biomass of bigeye tuna, including projections for 2013-2022 based on average fishing mortality rates during 2010-2012. The solid line illustrates the maximum likelihood estimates, and the estimates after 2013 (the large dot) indicate the spawning biomass predicted to occur if fishing mortality rates continue at the average of that observed during 2010-2012. The areas between the dashed lines indicate the 95-percent confidence intervals. t = metric tons.

FIGURE 6.2. Biomasa reproductora de atún patudo, incluyendo proyecciones para 2013-2022 basadas en las tasas de mortalidad por pesca media durante 2010-2012. La línea sólida ilustra las estimaciones de verosimilitud máxima, y las estimaciones a partir de 2013 (el punto grande) señalan la biomasa reproductora predicha si las tasas de mortalidad por pesca continúan en el promedio observado durante 2010-2012. La zona sombreada entre las líneas de trazos representa los intervalos de confianza de 95%. t = toneladas métricas.

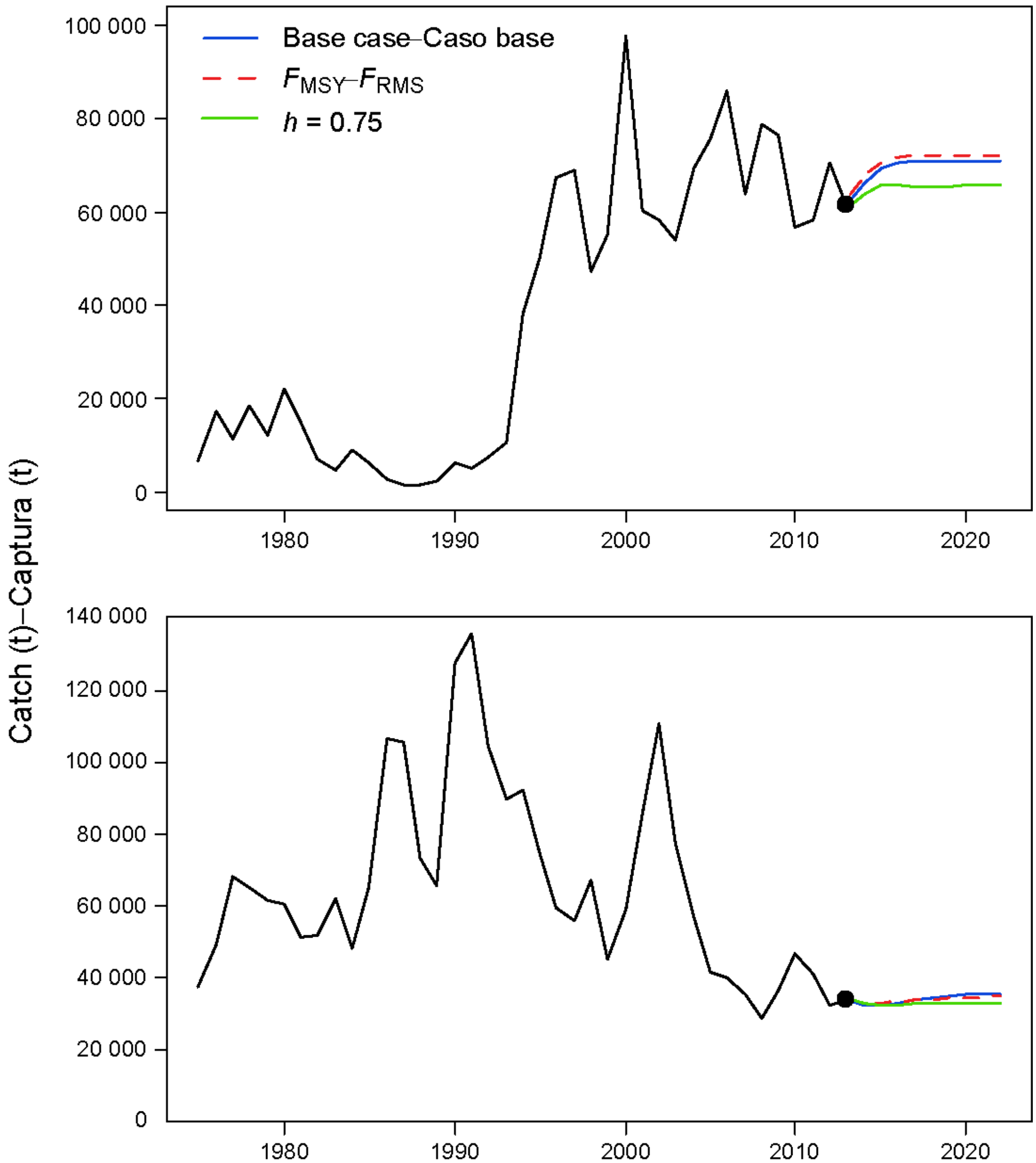

FIGURE 6.3. Historic and predicted annual catches of bigeye tuna during 2013-2022 for the surface (top panel) and longline (bottom panel) fisheries, based on fishing mortality rates during 2010-2012. Predicted catches are compared between the base case, the analysis assuming F_{MSY} and the analysis in which a stock-recruitment relationship (h = 0.75) was used. t = metric tons.

FIGURA 6.3. Capturas anuales históricas y predichas de atún patudo durante 2013-2022 en las pesquerías de superficie (recuadro superior) y de palangre (recuadro inferior), basadas en las tasas de mortalidad por pesca durante 2010-2012. Se comparan las capturas predichas entre el caso base, el análisis que supone F_{MSY} y el análisis en el que se usa una relación población-reclutamiento (h = 0.75). t = toneladas métricas.

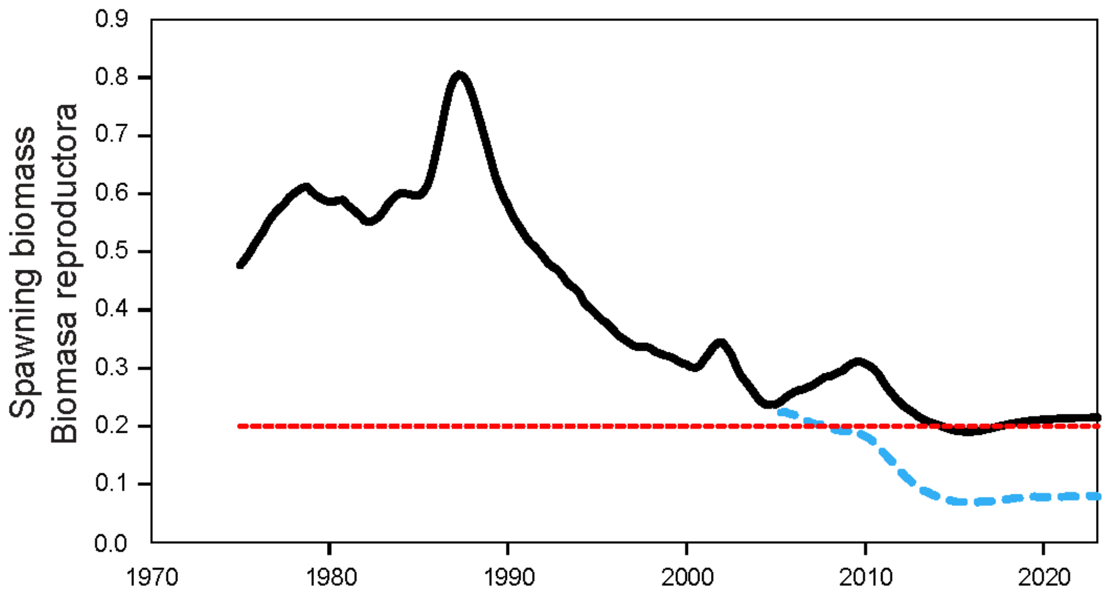

FIGURE 6.4. Projected spawning biomass ratio (SBR) from the base case model assuming a harvesting strategy targeting current fishing mortality rates (solid), the fishing mortality rate corresponding to MSY (long dash), and the fishing mortality corresponding to a no conservation resolution scenario (short dash).
FIGURA 6.4. Cociente de biomasa reproductora (SBR) proyectado a partir del modelo de caso base suponiendo una estrategia de extracción que apunta a las tasas de mortalidad por pesca actuales (sólida), la tasa de mortalidad por pesca correspondiente al RMS (trazos largos), y la mortalidad por pesca correspondiente a un escenario sin resoluciones de conservación (trazos cortos).

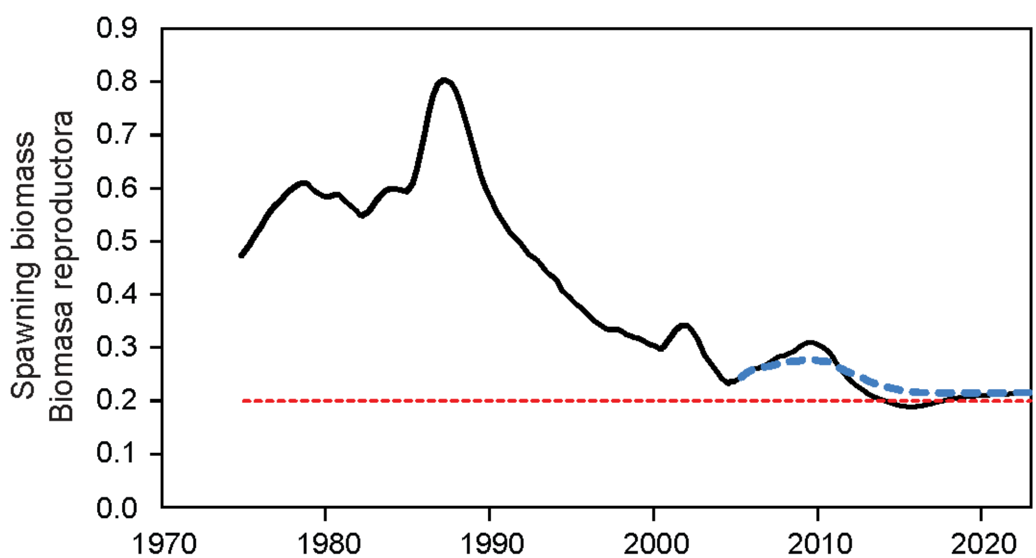

FIGURE 6.5. Projected spawning biomass ratio (SBR) from the base case model assuming a harvesting strategy targeting current fishing mortality rates (solid) and from a model assuming average recruitment starting in 2004 (dashed).
FIGURA 6.5. Cociente de biomasa reproductora (SBR) proyectado a partir del modelo de caso base suponiendo una estrategia de extracción que apunta a las tasas de mortalidad por pesca actuales (sólida) y de un modelo que supone que la reclutamiento medio a partir de 2004 (trazos).

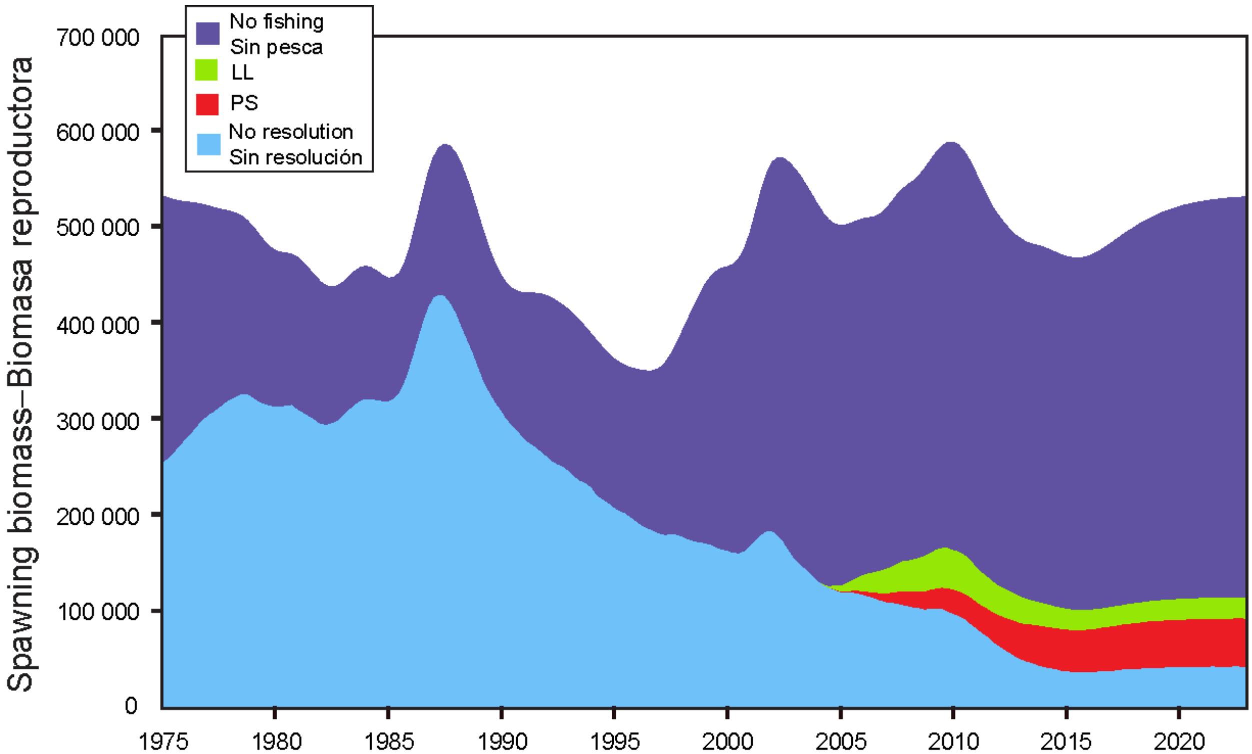

FIGURE 6.6 Trajectory of the spawning biomass of a simulated population of bigeye tuna that was not exploited (top line) and that predicted by the stock assessment model without the resolution management actions in place (bottom line). The shaded areas between the two lines show the portions of the impact of the resolution management action attributed to each fishing method. t = metric tons.

FIGURA 6.6 Trayectoria de la biomasa reproductora de una población simulada de atún patudo que no fue explotada (línea superior) y aquella predicha por el modelo de evaluación sin las acciones de ordenación en vigor (línea inferior). Las zonas sombreadas entre las dos líneas señalan las porciones del impacto de la acción de ordenación atribuida a cada método de pesca. t = toneladas métricas.

TABLE 2.1. Fisheries defined for the stock assessment of bigeye tuna in the EPO. PS = purse-seine; LP = pole and line; LL = longline; OBJ = sets on floating objects; NOA = sets on unassociated fish; DEL = sets on dolphins. The sampling areas are shown in Figure 2.1, and the discards are described in Section 2.2.1.
TABLA 2.1. Pesquerías definidas para la evaluación de la población de atún patudo en el OPO. PS = red de cerco; LP = caña; LL = palangre; OBJ = lances sobre objetos flotantes; NOA = lances sobre atunes no asociados; DEL = lances sobre delfines. En la Figura 2.1 se ilustran las zonas de muestreo, y en la Sección 2.2.1 se describen los descartes.

Fishery	Gear	Set type	Years	Sampling areas	Catch data
Pesquería	**Arte**	**Tipo de lance**	**Años**	**Zonas de muestreo**	**Datos de captura**
1	PS	OBJ	1975-1992	1-13	retained catch only–captura retenida solamente
2	PS	OBJ	1993-2008	11-12	retained catch + discards from inefficiencies in fishing process–captura retenida + descartes de ineficacias en el proceso de pesca
3	PS	OBJ	1993-2008	7, 9	
4	PS	OBJ	1993-2008	5-6, 13	
5	PS	OBJ	1993-2008	1-4, 8, 10	
6	PS LP	NOA DEL	1975-1989	1-13	retained catch only–captura retenida solamente
7	PS LP	NOA DEL	1990-2008	1-13	retained catch + discards from inefficiencies in fishing process–captura retenida + descartes de ineficacias en el proceso de pesca
8	PS	OBJ	1993-2008	11-12	discards of small fish from size-sorting the catch by Fishery 2 – descartes de peces pequeños de clasificación por tamaño en la Pesquería 2
9	PS	OBJ	1993-2008	7, 9	discards of small fish from size-sorting the catch by Fishery 3 – descartes de peces pequeños de clasificación por tamaño en la Pesquería 3
10	PS	OBJ	1993-2008	5-6, 13	discards of small fish from size-sorting the catch by Fishery 4 – descartes de peces pequeños de clasificación por tamaño en la Pesquería 4
11	PS	OBJ	1993-2008	1-4, 8, 10	discards of small fish from size-sorting the catch by Fishery 5 – descartes de peces pequeños de clasificación por tamaño en la Pesquería 5
12	LL	-	1975-1989	N of–de 10°N	retained catch only (in numbers)–captura retenida solamente (en número)
13	LL	-	1990-2009	N of–de 10°N	
14	LL	-	1975-1989	N of–de 0° and S of–de 10°N	retained catch only (in numbers)–captura retenida solamente (en número)
15	LL	-	1990-2009	N of–de 0° and S of–de 10°N	
16	LL	-	1975-1989	S of–de 0° and W of–de 100°W	retained catch only (in numbers)–captura retenida solamente (en número)
17	LL	-	1990-2009	S of–de 0° and W of–de 100°W	
18	LL	-	1975-1989	S of–de 0° and E of–de 100°W	retained catch only (in numbers)–captura retenida solamente (en número)
19	LL	-	1990-2009	S of–de 0° and E of–de 100°W	
20	LL	-	1990-2009	N of–de 10°N	retained catch only (in weight) –captura retenida solamente (en peso)
21	LL	-	1990-2009	N of–de 0° and S of–de 10°N	retained catch only (in weight) –captura retenida solamente (en peso)
22	LL	-	1990-2009	S of–de 0° and W of–de 100°W	retained catch only (in weight) –captura retenida solamente (en peso)
23	LL	-	1990-2009	S of–de 0° and E of–de 100°W	retained catch only (in weight) –captura retenida solamente (en peso)

TABLE 3.1. Age-specific maturity schedule (proportion of mature female fish) used to define the spawning biomass.

TABLA 3.1. Relación de madurez por edad (proporción de peces hembra maduros) usada para definir la biomasa reproductora.

Age (quarters)	**Proportion mature**	**Age (quarters)**	**Proportion mature**
Edad (trimestres)	**Proporción madura**	**Edad (trimestres)**	**Proporción madura**
1	0.00	21	0.96
2	0.00	22	0.98
3	0.00	23	0.98
4	0.00	24	0.99
5	0.00	25	0.99
6	0.01	26	1.00
7	0.01	27	1.00
8	0.02	28	1.00
9	0.04	29	1.00
10	0.06	30	1.00
11	0.10	31	1.00
12	0.16	32	1.00
13	0.23	33	1.00
14	0.33	34	1.00
15	0.45	35	1.00
16	0.59	36	1.00
17	0.71	37	1.00
18	0.82	38	1.00
19	0.89	39	1.00
20	0.93	40	1.00

TABLE 4.1. Estimated total annual recruitment (thousands of age-0 quarters fish), summary biomass (fish of age 3+ quarters), spawning biomass (metric tons), and spawning biomass ratio (SBR) of bigeye tuna in the EPO.

TABLA 4.1. Reclutamiento anual total estimado (miles de peces de edad 0), biomasa sumaria (peces de edad 3+ trimestres), biomasa reproductora (toneladas métricas), y cociente de biomasa reproductora (SBR) de atún patudo en el OPO.

Year Año	Total recruitment Reclutamiento total	Summary biomass Biomasa sumaria	Spawning biomass Biomasa reproductora	SBR SBR
1975	24,035	947,749	254,379	0.48
1976	22,301	1,034,370	279,099	0.52
1977	28,390	1,078,330	303,633	0.57
1978	19,400	1,092,950	320,361	0.60
1979	28,528	1,083,840	322,321	0.60
1980	28,374	1,061,810	312,798	0.59
1981	18,336	1,050,340	309,876	0.58
1982	37,744	1,064,230	295,137	0.55
1983	48,890	1,079,340	303,875	0.57
1984	22,912	1,147,710	320,770	0.60
1985	14,893	1,284,510	318,268	0.60
1986	20,404	1,378,340	359,784	0.67
1987	26,663	1,328,090	426,686	0.80
1988	23,296	1,212,010	410,653	0.77
1989	20,273	1,134,370	353,195	0.66
1990	17,820	1,088,420	309,173	0.58
1991	17,109	995,346	280,239	0.53
1992	20,534	899,447	261,416	0.49
1993	18,909	834,681	245,798	0.46
1994	32,365	790,916	228,842	0.43
1995	31,734	732,782	207,689	0.39
1996	21,443	699,779	193,121	0.36
1997	34,811	678,499	180,547	0.34
1998	45,117	633,369	177,663	0.33
1999	23,341	649,349	170,774	0.32
2000	22,334	701,734	163,029	0.31
2001	30,032	674,610	168,355	0.32
2002	31,269	620,272	183,541	0.34
2003	27,243	540,494	154,163	0.29
2004	34,091	520,057	131,609	0.25
2005	39,668	534,673	126,477	0.24
2006	33,006	546,266	137,760	0.26
2007	20,549	565,529	143,732	0.27
2008	25,245	596,815	152,453	0.29
2009	25,232	581,421	161,345	0.30
2010	28,205	539,092	163,903	0.31
2011	24,185	495,623	147,287	0.28
2012	27,420	459,772	127,277	0.24
2013	-	428,325	114,919	0.22

TABLE 4.2. Estimates of the average sizes and weights of bigeye tuna derived from the base case model. The ages are quarters after hatching.
TABLA 4.2. Estimaciones del tamaño y peso promedio del atún patudo derivados del modelo de caso base. Se expresa la edad en trimestres desde la cría.

Age (quarters)	Average length (cm)	Average weight (kg)	Age (quarters)	Average length (cm)	Average weight (kg)
Edad (trimestres)	**Talla media (cm)**	**Peso medio (kg)**	**Edad (trimestres)**	**Talla media (cm)**	**Peso medio (kg)**
1	33.2	1.0	21	169.4	108.1
2	41.5	1.8	22	172.4	113.8
3	50.3	3.2	23	175.2	119.2
4	59.4	5.2	24	177.7	124.2
5	68.5	7.8	25	180.0	128.9
6	77.6	11.2	26	182.0	133.3
7	86.4	15.4	27	183.9	137.3
8	95.1	20.2	28	185.6	140.9
9	103.3	25.8	29	187.1	144.3
10	111.2	31.9	30	188.5	147.4
11	118.6	38.5	31	189.7	150.3
12	125.6	45.4	32	190.8	152.8
13	132.2	52.7	33	191.9	155.2
14	138.3	60.0	34	192.8	157.3
15	143.9	67.4	35	193.6	159.2
16	149.1	74.7	36	194.3	161.0
17	153.9	81.9	37	195.0	162.6
18	158.3	88.9	38	195.6	164.0
19	162.3	95.6	39	196.1	165.3
20	166.0	102.0	40	197.0	167.6

TABLE 4.3a. Likelihood components obtained for the base case and the sensitivity analyses.
TABLA 4.3a. Componentes de verosimilitud obtenidos para el caso base y los análisis de sensibilidad.

		Appendix-Anexo							
		A	B		C				
Data Datos	Base case Caso base	h = 0.75	Adult M-M adulto		λ = 1				
			Sens $M1$	Sens $M5$	LL All-Todas	LL 14-17	PS All-Todas	LL 2
CPUE								
1	195.84	195.156	191.852	196.099	192.452	192.688	193.958	195.94
2	-44.5238	-44.2195	-42.9116	-44.1636	-45.0213	-44.6798	-42.2471	-44.3206
3	6.13	6.06965	7.26421	8.30431	8.73637	6.91472	8.30835	4.91525
4	212.75	211.7	217.657	212.022	217.036	216.482	213.66	216.769
5	6.90	7.96826	12.2763	5.51157	8.96672	10.0219	11.433	11.0729
12	56.04	57.3324	51.7447	57.1805	57.0969	50.7934	65.1018	56.0167
13	164.45	168.757	150.042	161.369	148.791	154.081	267.705	216.091
14	-67.60	-67.6281	-67.34	-67.6288	-63.3868	-63.202	-66.7725	-67.5925
15	-66.62	-66.4128	-66.01	-66.8958	-57.2769	-58.7199	-50.6992	-55.2851
16	-98.09	-98.1472	-97.67	-98.0399	-94.6007	-94.6036	-97.8979	-98.0853
17	-131.43	-131.139	-131.43	-131.505	-128.296	-128.197	-123.58	-130.666
18	17.80	17.2513	16.25	17.6372	16.9751	20.9719	13.4457	17.5684
19	172.00	169.689	191.80	169.001	197.656	186.622	172.701	174.137
Total	**-363.751**	**-363.327**	**-362.444**	**-364.070**	**-343.560**	**-344.723**	**-338.950**	**-351.629**
Size compositions – Composición por talla								
1	55.0732	55.05	55.1812	54.93	56.4414	56.27	159.095	55.0937
2	25.1443	25.12	28.3671	25.47	27.8636	26.52	299.884	279.032
3	41.7469	41.79	43.5306	41.62	45.6855	43.25	328.801	43.2651
4	43.3528	43.16	43.30	43.19	45.5335	45.08	77.3006	44.1171
5	27.8305	27.76	32.00	27.87	32.7235	29.78	203.996	26.8177
6	38.1199	38.17	38.25	38.17	38.4488	38.24	124.149	38.1183
7	55.7242	55.43	55.61	55.68	59.8478	59.14	131.071	55.7707
12	12.6024	12.61	12.66	12.60	31.5795	13.01	13.7197	12.6066
13	25.8381	25.70	26.01	25.60	61.4318	25.51	27.8317	27.3964
14	24.6072	24.60	24.82	24.62	34.0475	33.27	23.2526	24.6
15	35.8985	37.19	37.69	31.21	49.2388	48.95	41.4491	36.1078
16	16.233	16.34	16.03	16.34	40.5502	40.44	16.7004	16.2187
17	19.8067	20.57	22.31	16.08	120.932	122.08	23.0363	19.4529
18	19.6126	19.61	19.65	19.60	53.4593	19.26	19.5067	19.6119
19	29.5176	29.44	29.77	29.54	60.7296	30.62	30.1652	28.936
Total	471.108	472.529	485.188	462.523	758.513	631.422	1519.958	727.145
Recruitment-Reclutamiento								
	-55.0666	-54.7508	-37.4801	-56.6466	-42.2957	-42.2957	-27.6621	-43.0154
Total	52.290	54.451	85.264	41.807	372.657	244.404	1153.347	332.501

TABLE 4.3b. Average effective sample sizes estimated for the base case and the sensitivity analyses.
TABLA 4.3b. Tamaños de muestra efectiva promedio estimados para el caso base y los análisis de sensibilidad.

		Appendix-Anexo						
		A	B		C			
Data Datos	Base case Caso base	*h* = 0.75	Adult *M*-*M* adulto		λ = 1			
			Sens *M*1	Sens *M*5	LL All-Todas	LL 14-17	PS All-Todas	LL 2
1	19.91	19.92	20.00	19.97	19.16	19.25	21.42	19.93
2	66.30	66.44	54.63	66.79	56.13	60.93	77.24	78.29
3	54.77	55.11	47.20	55.27	50.31	54.92	67.06	58.23
4	6.49	6.61	6.44	6.53	5.99	6.11	6.98	6.59
5	49.29	49.74	35.29	50.46	37.23	40.26	59.25	52.68
6	19.84	19.86	20.20	19.78	19.47	19.12	30.15	19.84
7	14.25	14.03	14.38	14.06	14.55	14.65	14.08	14.06
12	73.37	73.58	73.04	73.65	71.75	68.71	67.02	73.27
13	44.43	44.96	41.65	44.97	48.67	42.11	40.52	42.21
14	69.91	69.82	70.95	70.22	101.13	112.09	76.22	70.00
15	243.30	109.62	58.02	85.04	97.40	103.80	34.35	156.76
16	158.32	157.29	165.03	156.23	197.21	198.38	157.77	158.88
17	114.08	100.90	101.35	183.07	173.96	173.52	86.95	114.40
18	86.96	86.84	86.86	87.34	90.48	87.57	86.07	86.95
19	76.12	76.48	74.56	76.01	81.95	66.08	74.32	78.48
Average-Promedio	73.16	63.41	57.97	67.29	71.03	71.17	59.96	68.70

TABLE 5.1. Estimates of the MSY and its associated quantities for bigeye tuna for the base case assessment and the sensitivity analyses. All analyses are based on average fishing mortality during 2010-2012. B_{recent} and B_{MSY} are defined as the biomass of fish 3+ quarters old (in metric tons) at the beginning of 2013 and at MSY, respectively. S_{recent} and S_{MSY} are in metric tons. C_{recent} is the estimated total catch in 2012. The F multiplier indicates how many times effort would have to be effectively increased to achieve the MSY in relation to the average fishing mortality during 2010-2012.

TABLA 5.1. Estimaciones del RMS y sus cantidades asociadas para el atún patudo para la evaluación del caso base y los análisis de sensibilidad. Todos los análisis se basan en la mortalidad por pesca promedio de 2010-2012. Se definen B_{recent} y B_{RMS} como la biomasa de peces de 3+ trimestres de edad (en toneladas métricas) al principio de 2013 y en RMS, respectivamente. Se expresan S_{recent} y S_{MSY} en toneladas métricas. C_{recent} es la captura total estimada en 2012. El multiplicador de F indica cuántas veces se tendría que incrementar el esfuerzo para lograr el RMS en relación con la mortalidad por pesca media durante 2010-2012.

		Appendix-Anexo							
		A	**B**		**C**				
	Base case-Caso base	**h = 0.75**	**Adult *M*-*M* adulto**		**λ = 1**				
			Sens *M*1	**Sens *M*5**	**LL All-Todas**	**LL 14-17**	**PS All-Todas**	**LL 2**
MSY-RMS	106,706	101,994	100,282	121,804	99,124	98,180	97,018	95,334
B_{MSY}- B_{RMS}	418,468	754,430	561,929	413,296	312,484	313,793	409,722	388,362
S_{MSY}- S_{RMS}	105,969	210,470	168,599	95,869	71,818	72,708	106,472	99,877
B_{MSY}/B_0- B_{RMS}/B_0	0.24	0.33	0.27	0.25	0.29	0.29	0.24	0.24
S_{MSY}/S_0- S_{RMS}/S_0	0.20	0.30	0.26	0.20	0.22	0.22	0.20	0.20
C_{recent}/MSY- C_{recent}/RMS	0.97	1.01	1.03	0.85	1.04	1.05	1.06	1.08
$B_{\text{recent}}/B_{\text{MSY}}$- $B_{\text{recent}}/B_{\text{RMS}}$	1.02	0.80	0.29	1.25	0.47	0.41	1.01	0.86
$S_{\text{recent}}/S_{\text{MSY}}$-$S_{\text{recent}}/S_{\text{RMS}}$	1.08	0.81	0.26	1.33	0.36	0.32	1.12	0.97
F multiplier-Multiplicador de F	1.05	0.82	0.41	1.42	0.54	0.51	0.95	0.85

TABLE 5.2. Estimates of the MSY and its associated quantities for bigeye tuna, obtained by assuming that there is no stock-recruitment relationship (base case), that each fishery maintains its current pattern of age-specific selectivity (Figure 4.5), and that each fishery is the only one operating in the EPO. The estimates of the MSY and B_{MSY} are in metric tons. The F multiplier indicates how many times effort would have to be effectively increased to achieve the MSY in relation to the average fishing mortality during 2010-2012. An analysis of the sensitivity of the management quantities estimates to using the average fishing mortality rates for 2010-2011 is also presented. PS: purse seine; LL: longline; "only" means that only that gear is used and the fishing mortality for the other gears is set to zero.

TABLA 5.2. Estimaciones del RMS y sus cantidades asociadas para el atún patudo, obtenidas suponiendo que no existe una relación población-reclutamiento (caso base), que cada pesquería mantiene su patrón actual de selectividad por edad (Figura 4.5), y que cada pesquería es la única que opera en el OPO. Se expresan las estimaciones del RMS y B_{RMS} en toneladas métricas. El multiplicador de F indica cuántas veces el esfuerzo necesitaría ser incrementado efectivamente para obtener el RMS en relación con la mortalidad por pesca promedio durante 2010-2012. Se presenta también un análisis de sensibilidad a las estimaciones de las cantidades de ordenación al uso de las tasas medias de mortalidad de pesca durante 2010-2011 PS: red de cerco; LL: palangre; « solamente » significa que se usa solamente ese arte, y se fija la mortalidad por pesca de las otras artes en cero.

	Base case-Caso base	**PS only-solamente**	**LL only-solamente**	**2010-2011**
MSY-RMS	106,706	77,766	254,983	108,281
B_{MSY}- B_{RMS}	418,468	323,018	464,742	426,310
S_{MSY}- S_{RMS}	105,969	84,446	61,676	108,054
B_{MSY}/B_0- B_{RMS}/B_0	0.24	0.19	0.27	0.25
S_{MSY}/S_0- S_{RMS}/S_0	0.20	0.16	0.12	0.20
C_{recent}/MSY- C_{recent}/RMS	0.97	1.32	0.40	0.95
B_{recent}/B_{MSY}- B_{recent}/B_{RMS}	1.02	1.33	0.92	1.00
S_{recent}/S_{MSY}-S_{recent}/S_{RMS}	1.08	1.36	1.86	1.06
F multiplier-Multiplicador de F	1.05	1.54	8.57	1.09

APPENDIX A: SENSITIVITY ANALYSIS FOR STEEPNESS
ANEXO A: ANÁLISIS DE SENSIBILIDAD A LA INCLINACIÓN

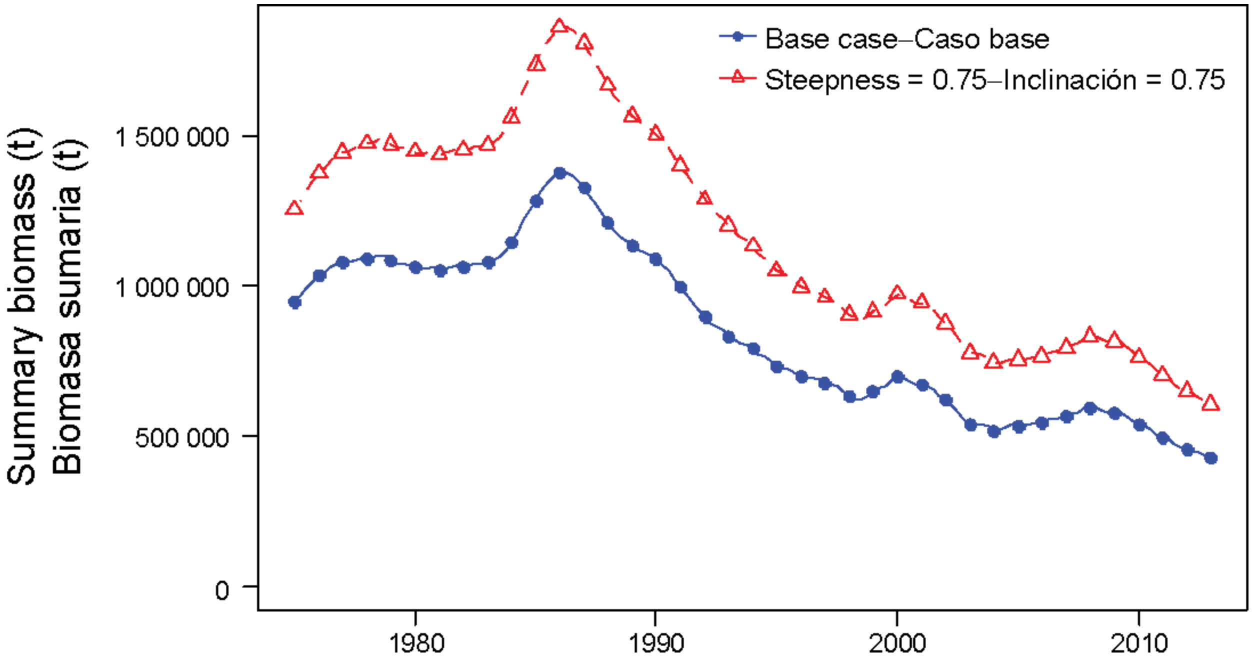

FIGURE A.1. Comparison of estimates of biomass of bigeye tuna 3+ quarters old (summary biomass) from the analysis without a stock-recruitment relationship (base case) and with a stock-recruitment relationship (steepness = 0.75). t = metric tons.

FIGURA A.1. Comparación de las estimaciones de la biomasa de atún patudo de 3+ trimestres de edad (biomasa sumaria) del análisis sin una relación población-reclutamiento (caso base) y con dicha relación (inclinación = 0.75). t = toneladas métricas.

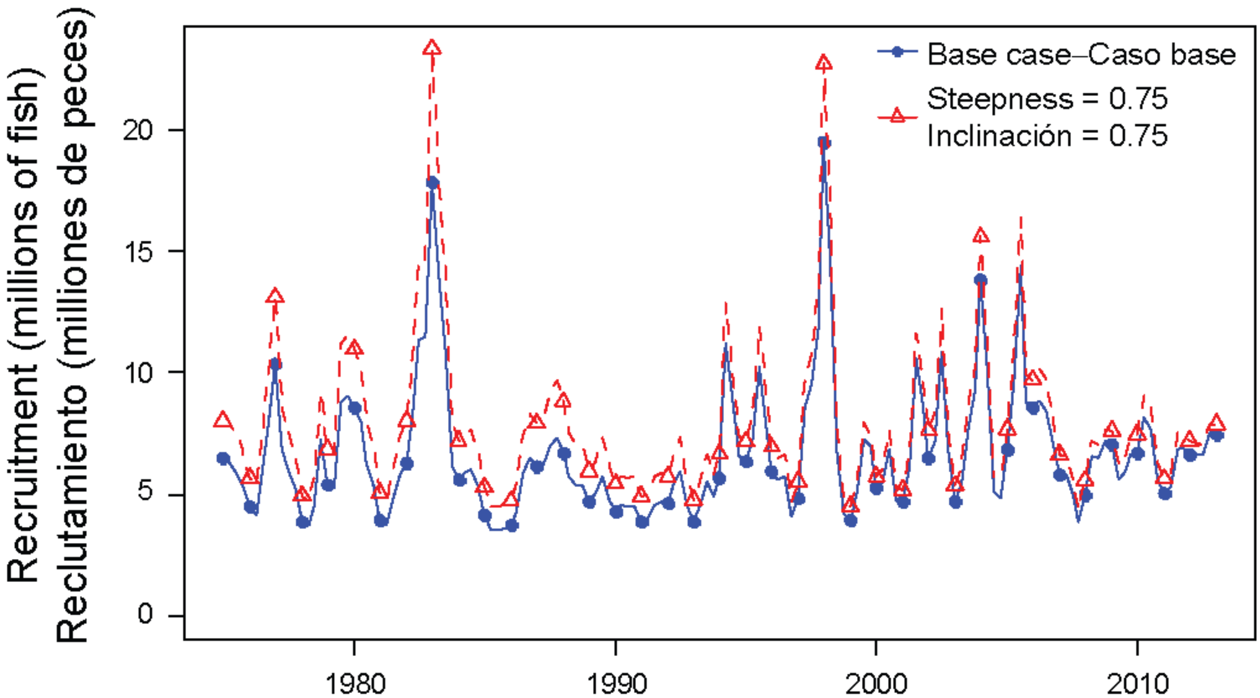

FIGURE A.2a. Comparison of estimates of absolute recruitment for bigeye tuna from the analysis without a stock-recruitment relationship (base case) and with a stock-recruitment relationship (steepness = 0.75).

FIGURA A.2a. Comparación de las estimaciones de reclutamiento absoluto de atún patudo del análisis sin una relación población-reclutamiento (caso base) y con dicha relación (inclinación = 0.75).

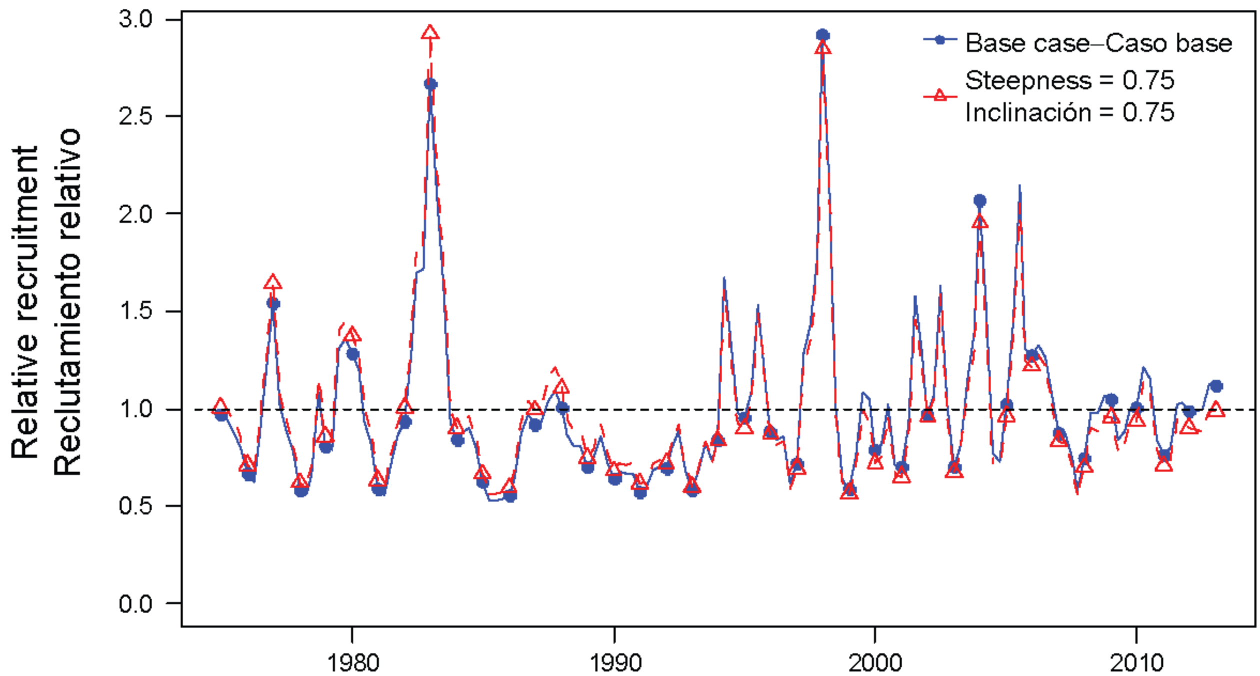

FIGURE A.2b. Comparison of estimates of relative recruitment for bigeye tuna from the analysis without a stock-recruitment relationship (base case) and with a stock-recruitment relationship (steepness = 0.75). The estimates are scaled so that the estimate of average recruitment is equal to 1.0 (dashed horizontal line).

FIGURA A.2b. Comparación de las estimaciones de reclutamiento relativo de atún patudo del análisis sin una relación población-reclutamiento (caso base) y con dicha relación (inclinación = 0.75). Se escalan las estimaciones para que la estimación de reclutamiento medio equivalga a 1,0 (línea de trazos horizontal).

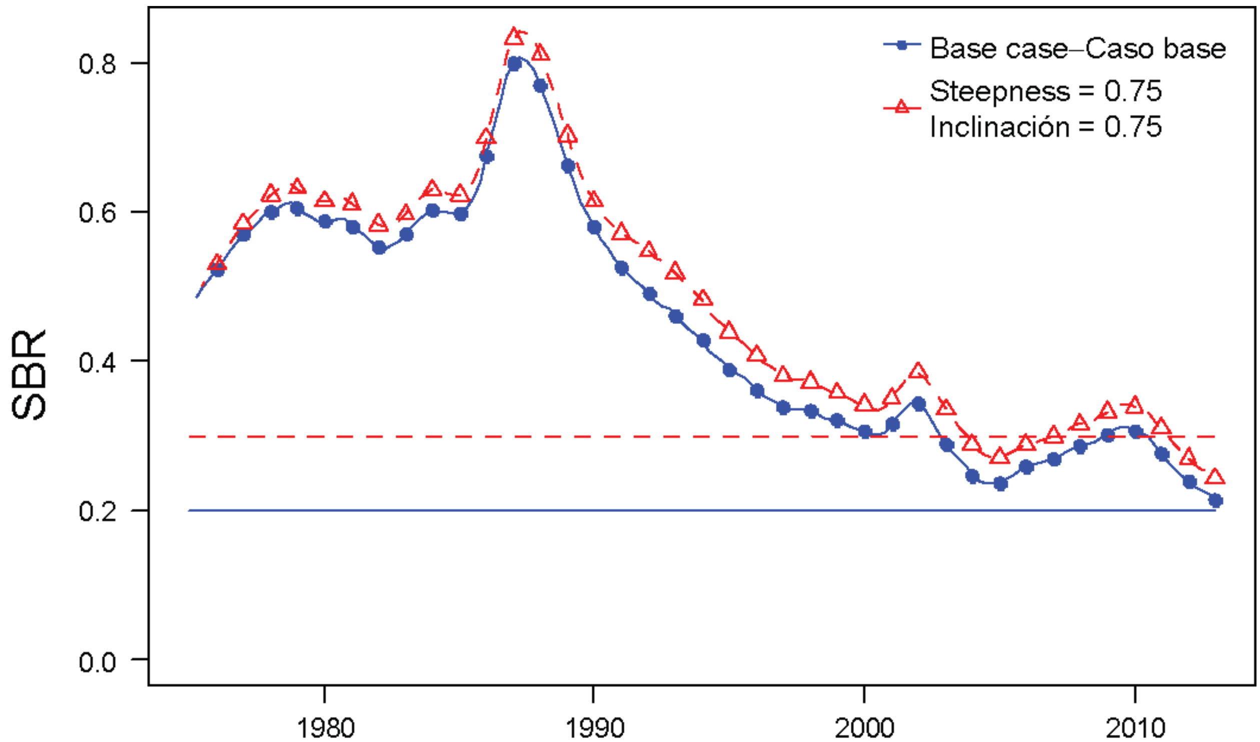

FIGURE A.3. Comparison of estimates of the spawning biomass ratio (SBR) of bigeye tuna from the analysis without a stock-recruitment relationship (base case) and with a stock-recruitment relationship (steepness = 0.75). The horizontal lines represent the SBRs associated with MSY under the two scenarios.
FIGURA A.3. Comparación de las estimaciones del cociente de biomasa reproductora (SBR) de atún patudo del análisis sin una relación población-reclutamiento (caso base) y con dicha relación (inclinación = 0.75). Las líneas horizontales representan los SBR asociados con el RMS en los dos escenarios.

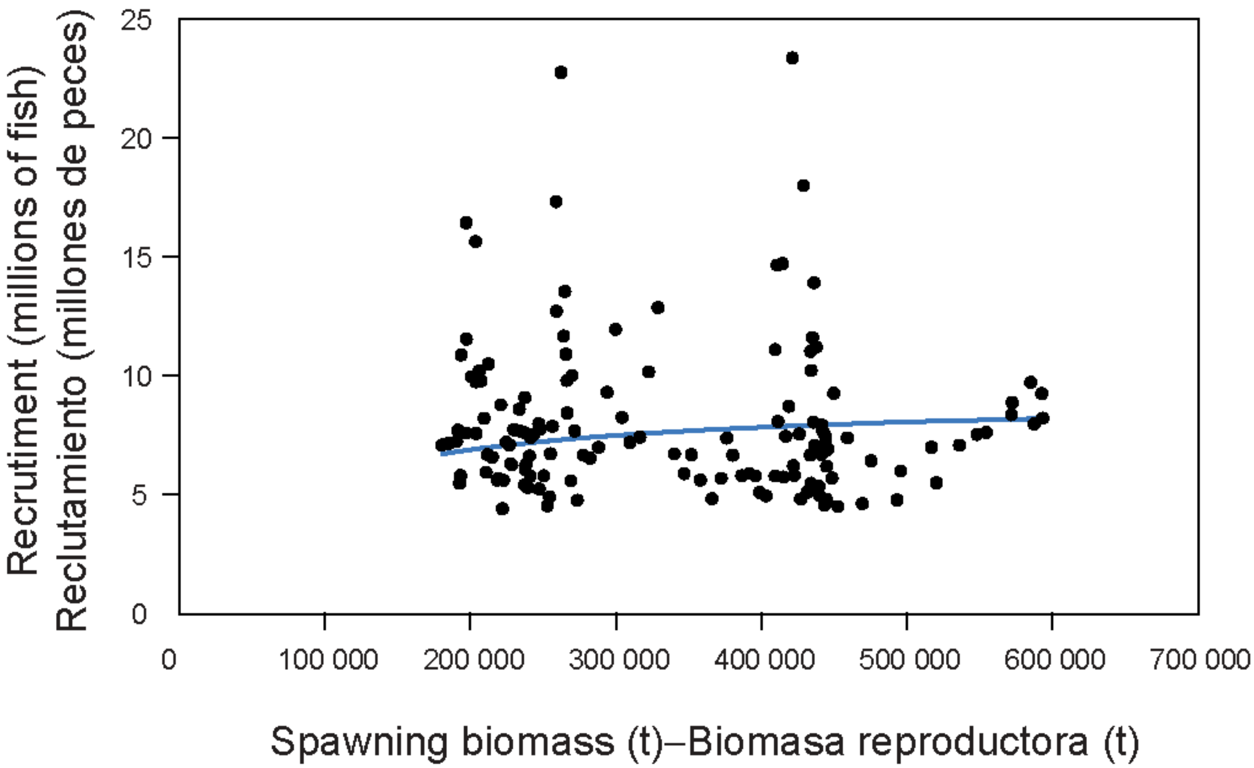

FIGURE A.4. Recruitment of bigeye tuna plotted against spawning biomass when the analysis has a stock-recruitment relationship (steepness = 0.75).
FIGURA A.4. Reclutamiento de atún patudo graficado como función de la biomasa reproductora cuando el análisis incluye una relación población-reclutamiento (inclinación = 0.75).

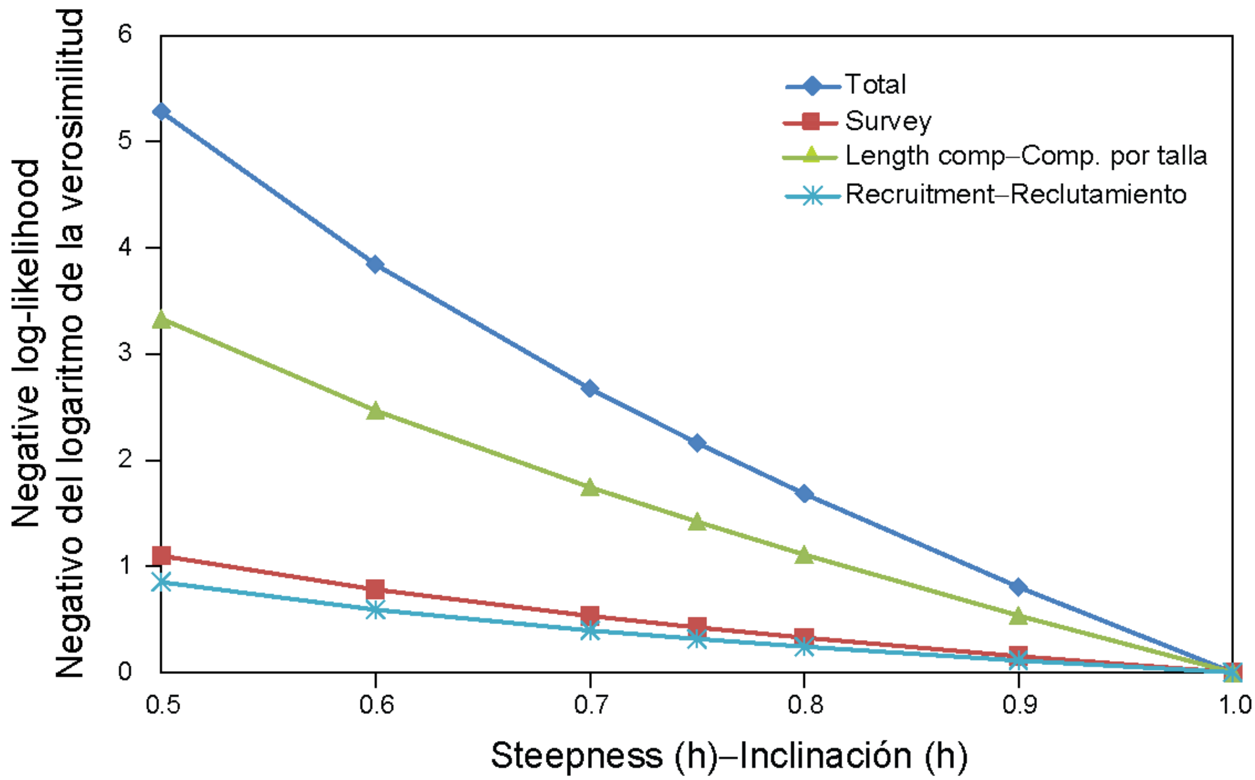

FIGURE A.5. Likelihood profile on steepness.
FIGURA A.5. Perfil de verosimilitud en inclinación.

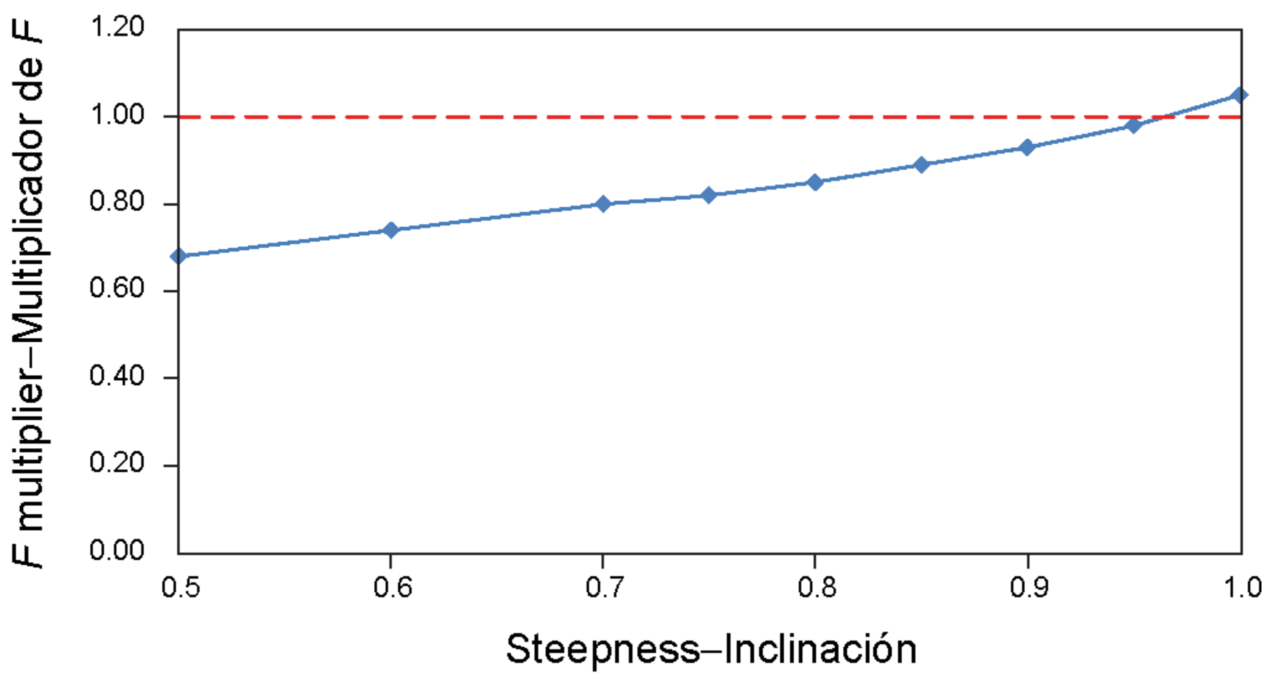

FIGURE A.6. *F* multiplier as a function of steepness.
FIGURA A.6. Multiplicador de *F* como función de la inclinación.

TABLE A.1. Estimates of the MSY and its associated quantities for bigeye tuna, for different assumptions on steepness (*h*).

TABLA A.1. Estimaciones de RMS y sus cantidades asociadas para el atún patudo, correspondientes a distintos supuestos sobre la inclinación (*h*).

	Base case–Caso base (*h*=1)	***h* = 0.9**	***h* = 0.8**	***h* = 0.75**	***h* = 0.7**	***h* = 0.6**	***h* = 0.5**
MSY-RMS	106,706	104,468	102,782	101,994	101,199	99,483	97,415
B_{MSY}- B_{RMS}	418,468	547,941	679,829	754,430	838,483	1,051,330	1,375,260
S_{MSY}- S_{RMS}	105,969	146,270	187,294	210,470	236,561	302,550	402,818
B_{MSY}/B_0- B_{RMS}/B_0	0.24	0.28	0.32	0.33	0.34	0.37	0.39
S_{MSY}/S_0- S_{RMS}/S_0	0.20	0.25	0.28	0.30	0.31	0.34	0.38
C_{recent}/MSY- C_{recent}/RMS	0.97	0.99	1.00	1.01	1.02	1.04	1.06
B_{recent}/B_{MSY}- B_{recent}/B_{RMS}	1.02	0.90	0.83	0.80	0.78	0.74	0.70
S_{recent}/S_{MSY}-S_{recent}/S_{RMS}	1.08	0.92	0.84	0.81	0.79	0.74	0.70
F multiplier- Multiplicador de *F*	1.05	0.93	0.85	0.82	0.80	0.74	0.68

APPENDIX B: SENSITIVITY ANALYSIS TO HIGHER RATES OF ADULT NATURAL MORTALITY
ANEXO B: ANÁLISIS DE SENSIBILIDAD A TASAS MAYORES DE MORTALIDAD NATURAL DE ADULTOS

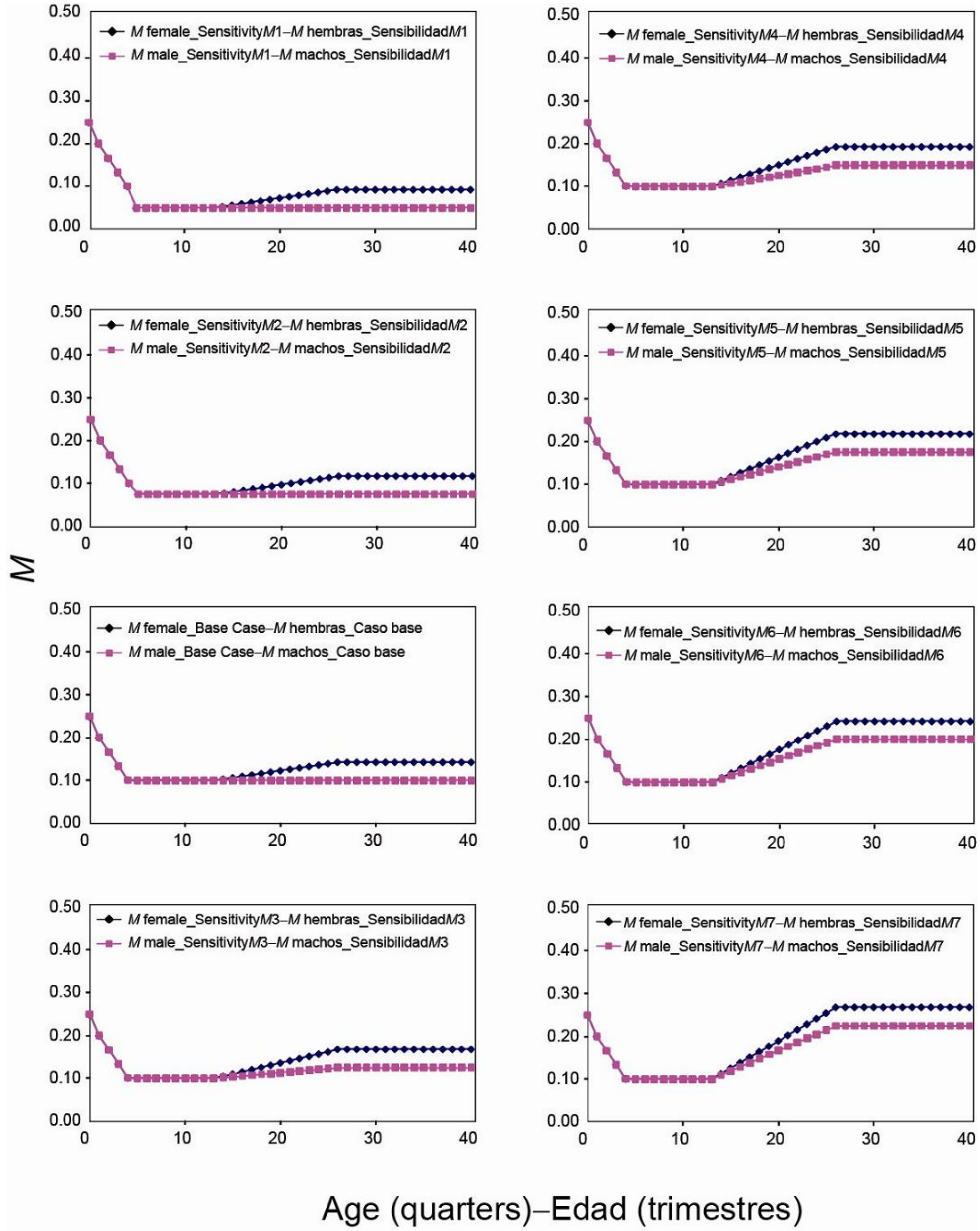

FIGURE B.1. Natural mortality (*M*) schedules for female and male bigeye investigated in the sensitivity analysis to higher *M* values for adults.
FIGURA B.1. Vectores de mortalidad natural (*M*) de patudos hembra y macho investigados en el análisis de sensibilidad a valores mayores de *M* para los adultos.

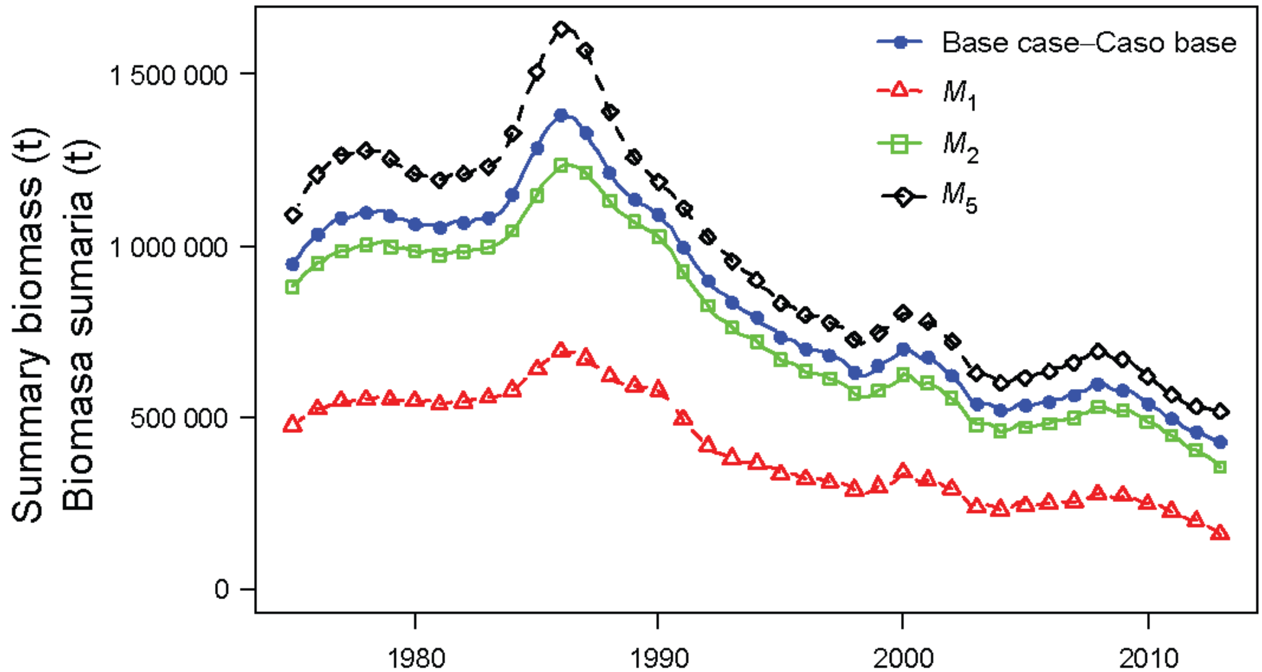

FIGURE B.2. Comparison of estimates of biomass of bigeye tuna 3+ quarters old (summary biomass) from the base case analysis and two sensitivity analyses assuming lower (Sensitivity *M*1) and higher (Sensitivity *M*5) rates of adult natural mortality (*M*), respectively (see Figure B.1 to compare *M* schedules). t = metric tons.

FIGURA B.2. Comparación de las estimaciones de biomasa de atún patudo de 3+ trimestres de edad (biomasa sumaria) del análisis de caso base y de dos análisis de sensibilidad que suponen tasas de mortalidad natural (*M*) de adultos menores (Sensibilidad *M*1) y mayores (Sensibilidad *M*5), respectivamente (ver Figura B.1 para comparar vectores de *M*). t = toneladas métricas.

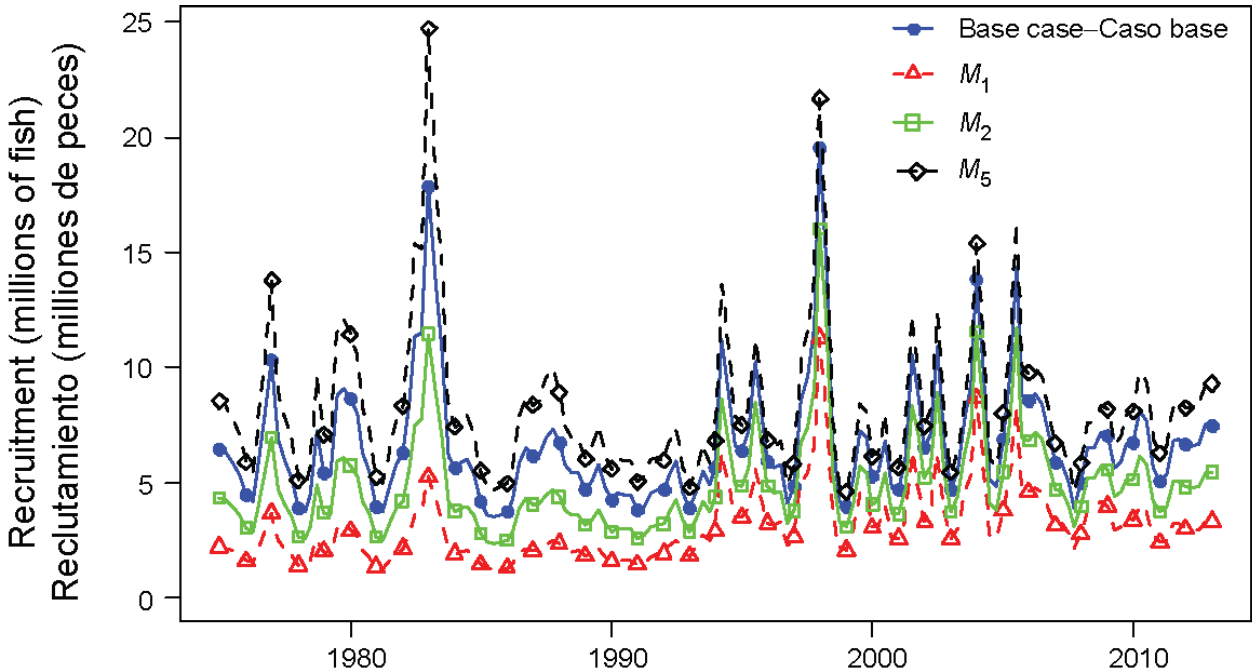

FIGURE B.3a. Comparison of estimates of absolute recruitment (in millions of fish) for bigeye tuna from the base case analysis and two sensitivity analyses assuming lower (Sensitivity *M*1) and higher (Sensitivity *M*5) rates of adult natural mortality (*M*), respectively (see Figure B.1 to compare *M* schedules).

FIGURA B.3a. Comparación de las estimaciones de reclutamiento absoluto (en millones de peces) de atún patudo del análisis de caso base y de dos análisis de sensibilidad que suponen tasas de mortalidad natural (*M*) de adultos menores (Sensibilidad *M*1) y mayores (Sensibilidad *M*5), respectivamente (ver Figura B.1 para comparar vectores de *M*).

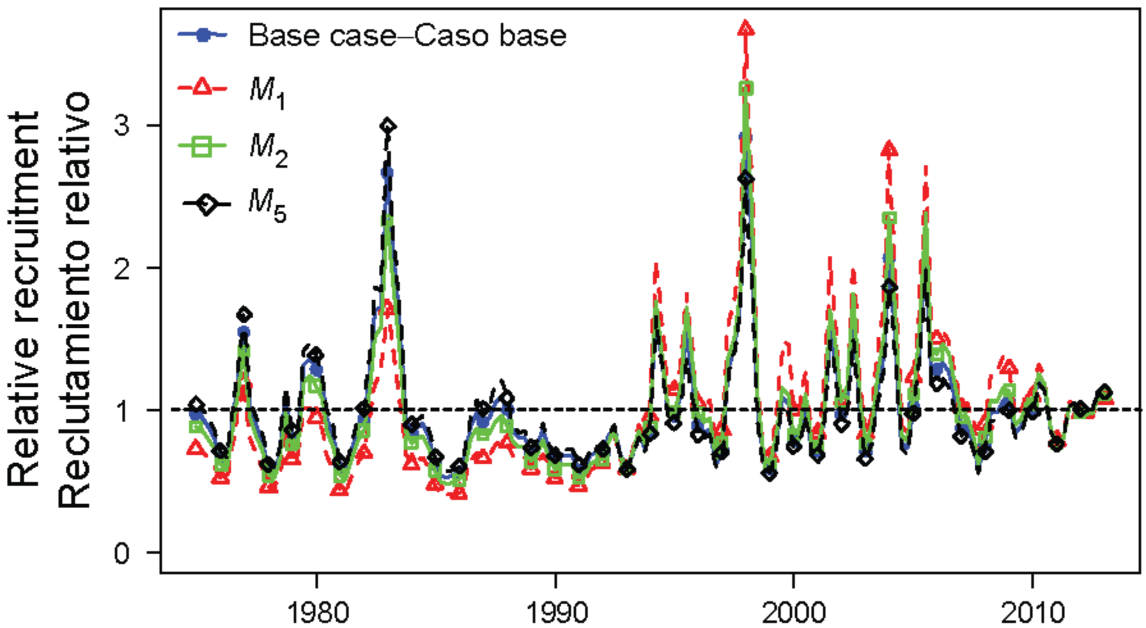

FIGURE B.3b. Comparison of estimates of relative recruitment for bigeye tuna from the base case analysis and from two sensitivity analyses assuming lower (Sensitivity *M*1) and higher (Sensitivity *M*5) rates of adult natural mortality (*M*), respectively (see Figure B.1 to compare *M* schedules). The estimates are scaled so that the estimate of average recruitment is equal to 1.0 (dashed horizontal line).
FIGURA B.3b. Comparación de las estimaciones de reclutamiento relativo de atún patudo del análisis de caso base y de dos análisis de sensibilidad que suponen tasas de mortalidad natural (*M*) de adultos menores (Sensibilidad *M*1) y mayores (Sensibilidad *M*5), respectivamente (ver Figura B.1 para comparar vectores de *M*). Se escala el reclutamiento para que la estimación de reclutamiento medio equivalga a 1,0 (línea de trazos horizontal).

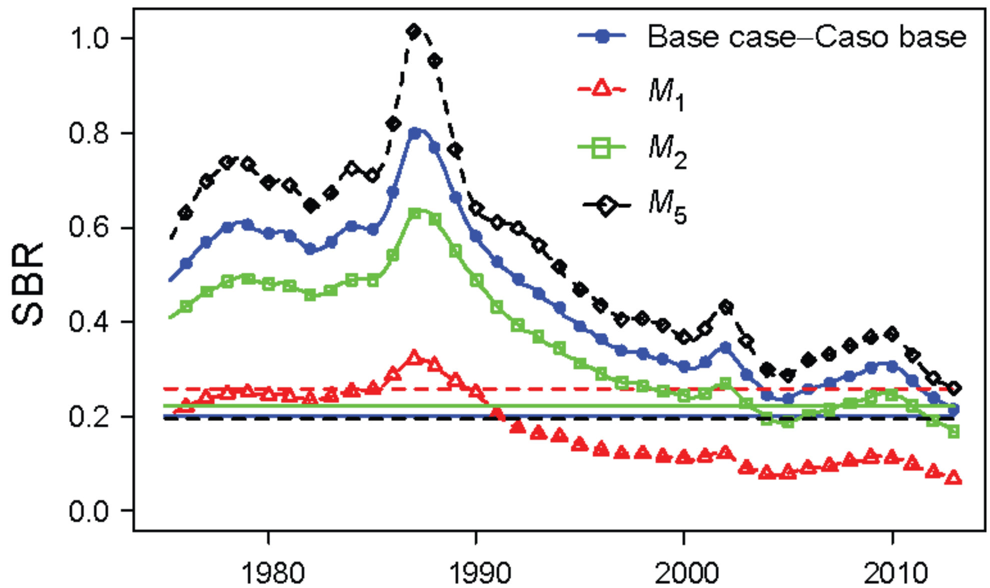

FIGURE B.4. Comparison of estimates of the spawning biomass ratio (SBR) of bigeye tuna from the base case analysis and from two sensitivity analyses assuming lower (Sensitivity *M*1) and higher (Sensitivity *M*5) rates of adult natural mortality (*M*), respectively (see Figure B.1 to compare *M* schedules). The horizontal lines represent the SBRs associated with MSY under the two scenarios.

FIGURA B.4. Comparación de las estimaciones del cociente de biomasa reproductora (SBR) de atún patudo del análisis de caso base y de dos análisis de sensibilidad que suponen tasas de mortalidad natural (*M*) de adultos menores (Sensibilidad *M*1) y mayores (Sensibilidad *M*5), respectivamente (ver Figura B.1 para comparar vectores de *M*). Las líneas horizontales representan los SBR asociados con el RMS bajo los dos escenarios.

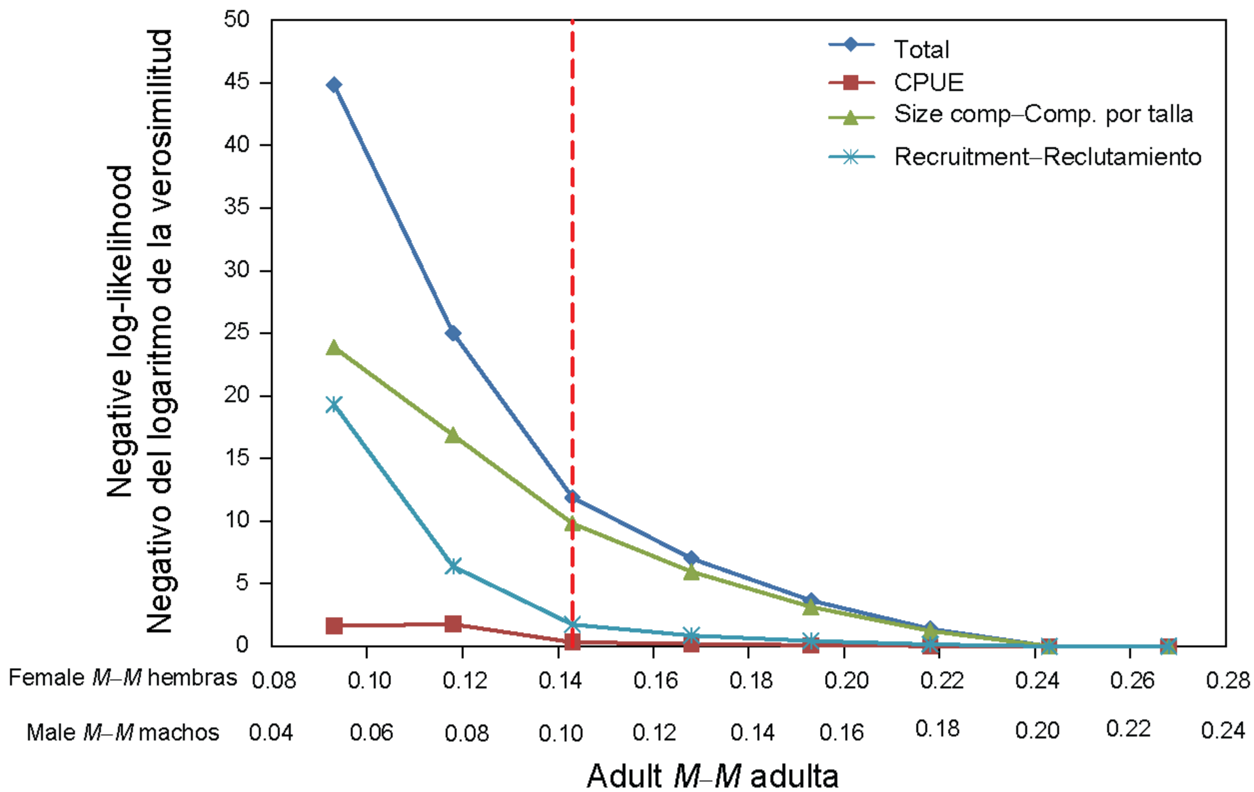

FIGURE B.5. Negative log-likelihood for adult natural mortality (*M*). Profiles are shown for total likelihood and different data components (subtracted to their respective minimum negative log-likelihood). The vertical dashed line represents the *M* values assumed in the base case model.

FIGURA B.5. Negativo del logaritmo de la verosimilitud correspondiente a la mortalidad natural (*M*) de los adultos. Se ilustran los perfiles de verosimilitud total y de distintos componentes de los datos (restados a su negativo mínimo respectivo del logaritmo de la verosimilitud). La línea de trazos vertical representa los supuestos de *M* usados en el modelo de caso base .

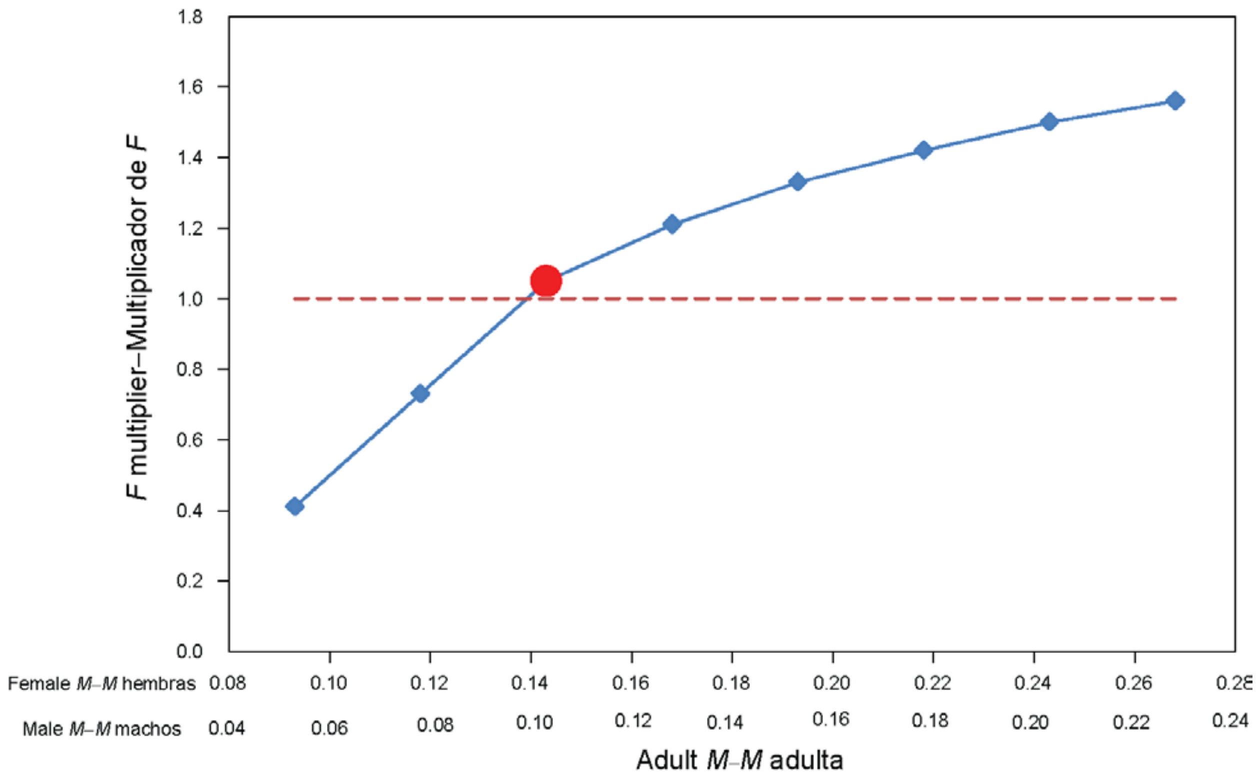

FIGURE B.6. Relationship between the *F* multiplier and the assumed levels of adult natural mortality (*M*) for females and males. The large dot indicates the *M* assumed in the base case model. The horizontal dashed line indicates F_{MSY}.

FIGURA B.6. Relación entre el multiplicador de *F* y los niveles supuestos de mortalidad natural (*M*) de hembras y machos adultos. El punto grande indica la *M* supuesta en el modelo de caso base. La línea de trazos horizontal indica F_{RMS}.

TABLE B.1. Estimates of management-related quantities for bigeye tuna for the base case and adult natural mortality (*M*) sensitivity analysis (see Figure B.1 to compare *M* schedules).
TABLA B.1. Estimaciones de las cantidades relacionadas con la ordenación para el atún patudo del caso base y del análisis de sensibilidad a la mortalidad natural (*M*) de adultos (ver Figura B.1 para comparar vectores de *M*).

	M1	**M2**	**Base case**	**M3**	**M4**	**M5**	**M6**	**M7**
Female M	0.09	0.12	0.14	0.17	0.19	0.22	0.24	0.27
Male M	0.05	0.08	0.10	0.13	0.15	0.18	0.20	0.23
MSY-RMS	100,282	94,542	106,706	112,840	117,782	121,804	124,890	127,458
B_{MSY}- B_{RMS}	561,929	487,368	418,468	419,145	416,585	413,296	410,355	407,473
S_{MSY}- S_{RMS}	168,599	138,347	105,969	103,381	99,086	95,869	92,700	89,789
B_{MSY}/B_0- B_{RMS}/B_0	0.27	0.25	0.24	0.24	0.25	0.25	0.25	0.25
S_{MSY}/S_0- S_{RMS}/S_0	0.26	0.22	0.2	0.2	0.2	0.2	0.2	0.2
C_{recent}/MSY- C_{recent}/RMS	1.03	1.09	0.97	0.91	0.87	0.85	0.82	0.81
B_{recent}/B_{MSY}- B_{recent}/B_{RMS}	0.29	0.73	1.02	1.13	1.2	1.25	1.29	1.31
S_{recent}/S_{MSY}-S_{recent}/S_{RMS}	0.26	0.76	1.08	1.2	1.28	1.33	1.37	1.4
F multiplier- Multiplicador de *F*	0.41	0.73	1.05	1.21	1.33	1.42	1.5	1.56

APPENDIX C: SENSITIVITY ANALYSIS TO THE WEIGHTING ASSIGNED TO THE SIZE COMPOSITION DATA

ANEXO C: ANÁLISIS DE SENSIBILIDAD A LA PONDERACIÓN ASIGNADA A LOS DATOS DE COMPOSICIÓN POR TALLA

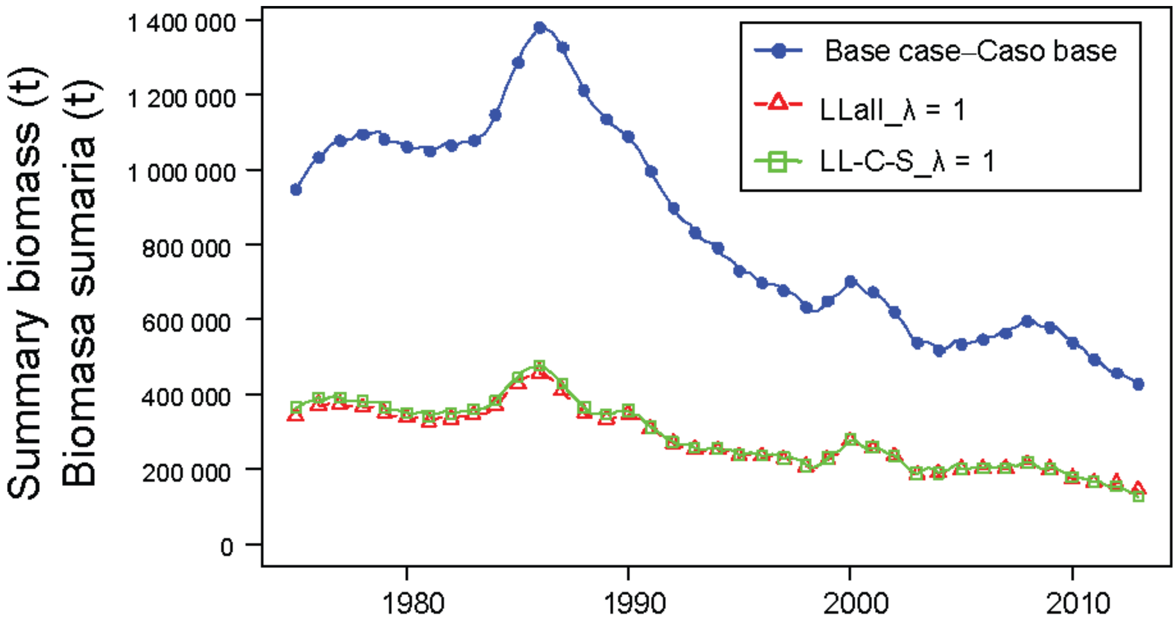

FIGURE C.1a. Comparison of estimates of biomass of bigeye tuna 3+ quarters old (summary biomass) from the base case analysis (blue dots; size-composition λ for all fisheries = 0.05) and two sensitivity analyses which up-weight (λ = 1) the size-composition data of all the longline fisheries (Fisheries 12-19; green squares), or the Central and Southern longline fisheries only (Fisheries 14-17; red triangles). t = metric tons.

FIGURA C.1a. Comparación de las estimaciones de la biomasa de atún patudo de 3+ trimestres de edad (biomasa sumaria) del análisis de caso base (puntos azules; λ de composición por talla de todas las pesquerías = 0,05) y de dos análisis de sensibilidad que incrementan la ponderación (λ = 1) de los datos de composición por talla de todas las pesquerías palangreras (Pesquerías 12-19, cuadros verdes), o de las pesquerías palangreras central y del sur solamente (Pesquerías 14-17; triángulos rojos). t = toneladas métricas.

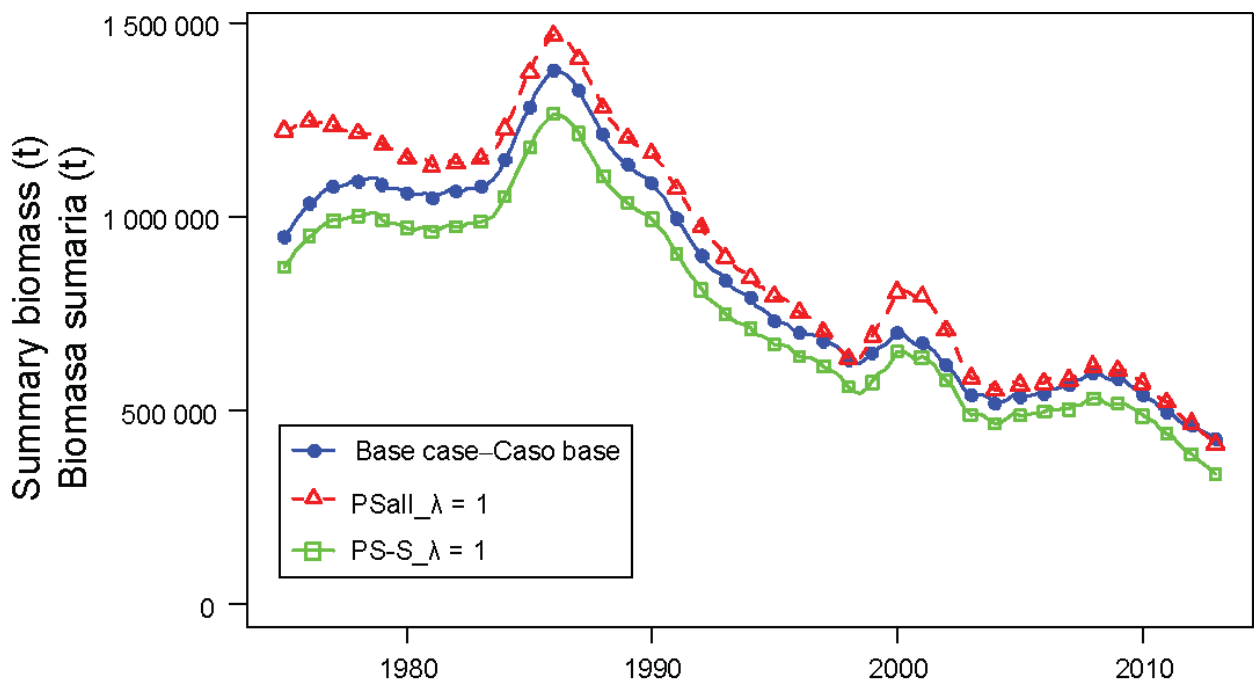

FIGURE C.1b. Comparison of estimates of biomass of bigeye tuna 3+ quarters old (summary biomass) from the base case analysis (blue dots; size composition λ for all fisheries = 0.05) and two sensitivity analyses which up-weight (λ = 1) the size-composition data of all the purse-seine fisheries (Fisheries 1-11; red triangles), or the southern purse-seine fishery only (Fishery 2; green squares). t = metric tons.

FIGURA C.1b. Comparación de las estimaciones de la biomasa de atún patudo de 3+ trimestres de edad (biomasa sumaria) del análisis de caso base (puntos azules; λ de composición por talla de todas las pesquerías = 0,05) y de dos análisis de sensibilidad que incrementan la ponderación (λ = 1) de los datos de composición por talla de todas las pesquerías cerqueras (Pesquerías 1-11, triángulos rojos), o de la pesquería cerquera del sur solamente (Pesquería 2; cuadros verdes). t = toneladas métricas.

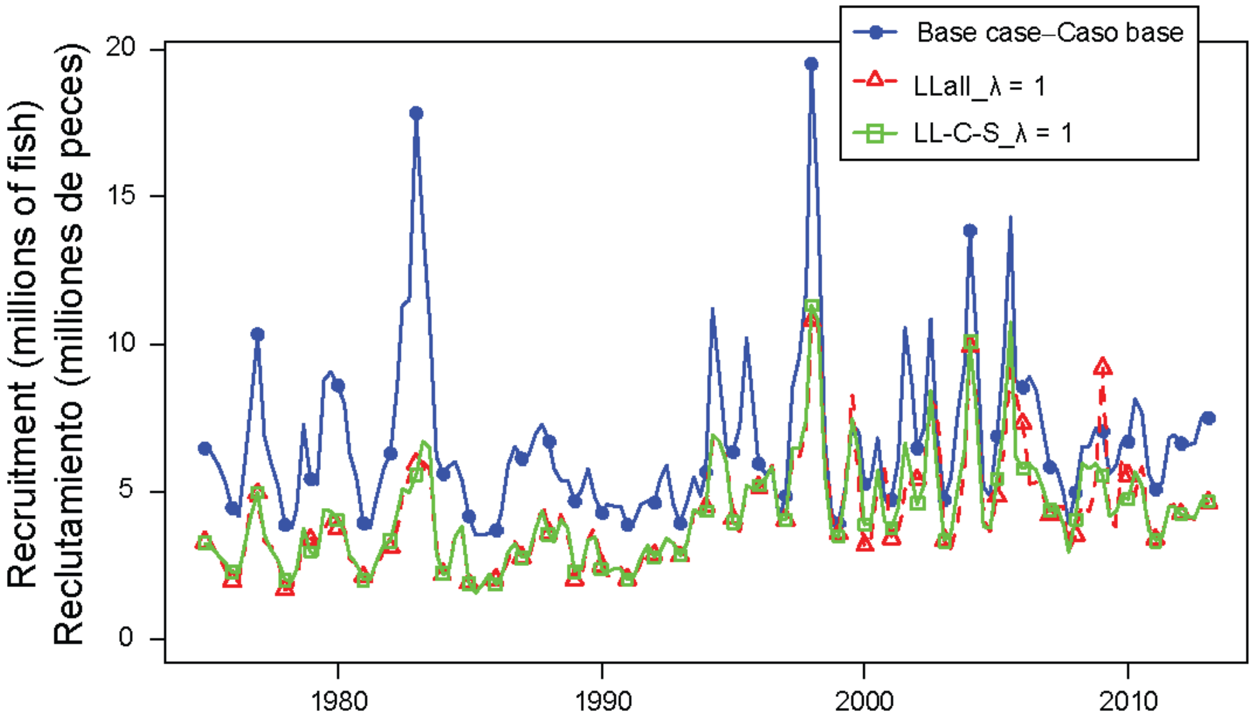

FIGURE C.2a. Comparison of estimates of absolute recruitment (in millions of fish) of bigeye tuna from the base case analysis (blue dots; size composition λ for all fisheries = 0.05) and two sensitivity analyses which up-weight (λ = 1) the size-composition data of all longline fisheries (Fisheries 12-19; red triangles), or the central and southern longline fisheries only (Fisheries 14-17; green squares). t = metric tons.

FIGURA C.2a. Comparación de las estimaciones del reclutamiento absoluto (en millones de peces) de atún patudo del análisis de caso base (puntos azules; λ de composición por talla de todas las pesquerías = 0,05) y de dos análisis de sensibilidad que incrementan la ponderación (λ = 1) de los datos de composición por talla de todas las pesquerías palangreras (Pesquerías 12-19, triángulos rojos), o de las pesquerías palangreras central y del sur solamente (Pesquerías 14-17; cuadros verdes). t = toneladas métricas.

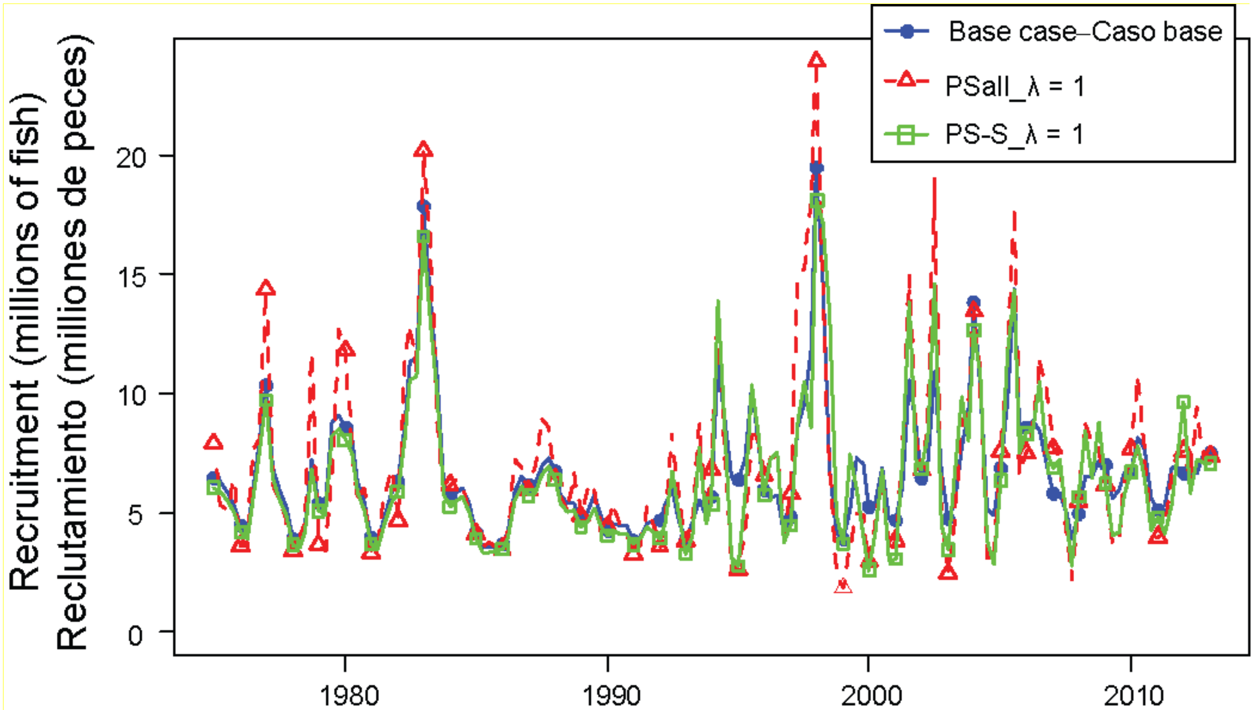

FIGURE C.2b. Comparison of estimates of absolute recruitment (in millions of fish) of bigeye tuna from the base case analysis (blue dots; size composition λ for all fisheries = 0.05) and two sensitivity analyses which up-weight (λ = 1) the size-composition data of all purse-seine fisheries (Fisheries 1-11; red triangles), or the southern purse-seine fishery only (Fishery 2; green squares). t = metric tons.

FIGURA C.2b. Comparación de las estimaciones del reclutamiento absoluto (en millones de peces) de atún patudo del análisis de caso base (puntos azules; λ de composición por talla de todas las pesquerías = 0,05) y de dos análisis de sensibilidad que incrementan la ponderación (λ = 1) de los datos de composición por talla de todas las pesquerías cerqueras (Pesquerías 1-11, triángulos rojos), o de la pesquería cerquera del sur solamente (Pesquería 2; cuadros verdes). t = toneladas métricas.

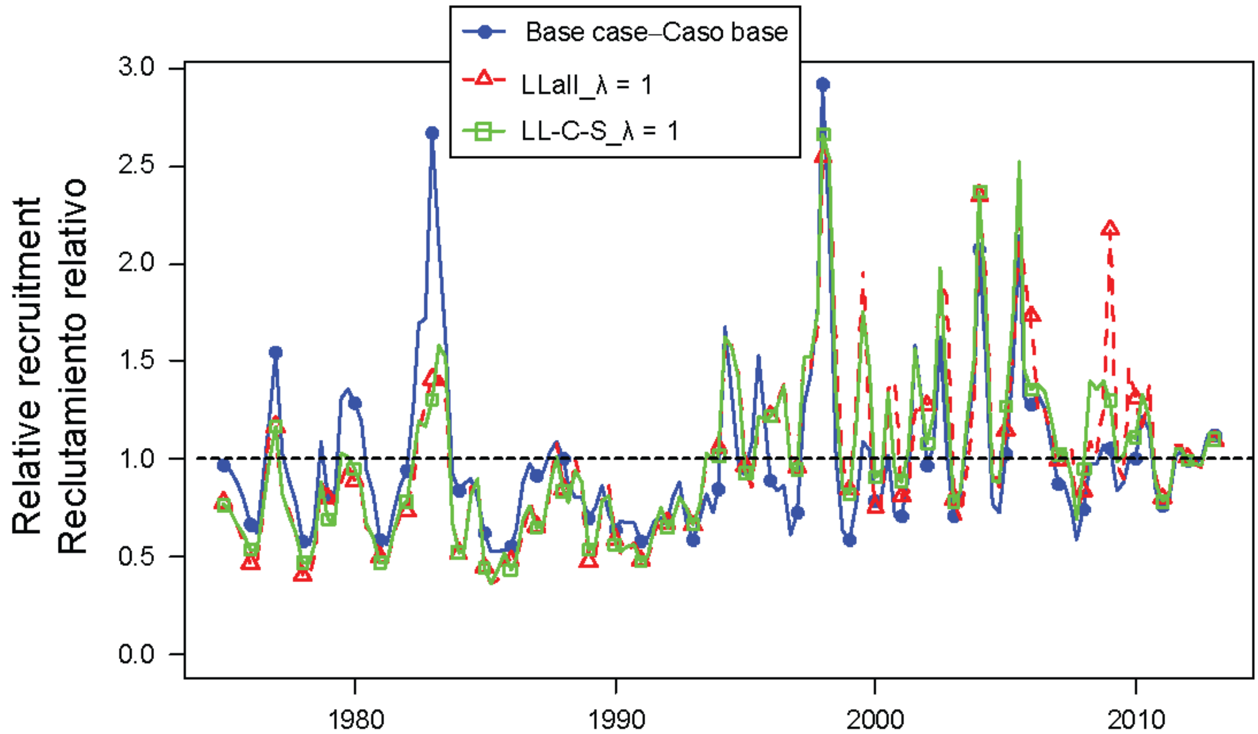

FIGURE C.3a. Comparison of estimates of relative recruitment of bigeye tuna from the base case analysis (blue dots; size composition λ for all fisheries = 0.05) and two sensitivity analyses which up-weight (λ = 1) the size-composition data of all longline fisheries (Fisheries 12-19; red triangles), or the central and southern longline fisheries only (Fisheries 14-17; green squares). t = metric tons.
FIGURA C.3a. Comparación de las estimaciones del reclutamiento relativo de atún patudo del análisis de caso base (puntos azules; λ de composición por talla de todas las pesquerías = 0,05) y de dos análisis de sensibilidad que incrementan la ponderación (λ = 1) de los datos de composición por talla de todas las pesquerías palangreras (Pesquerías 12-19, triángulos rojos), o de las pesquerías palangreras central y del sur solamente (Pesquerías 14-17; cuadros verdes). t = toneladas métricas.

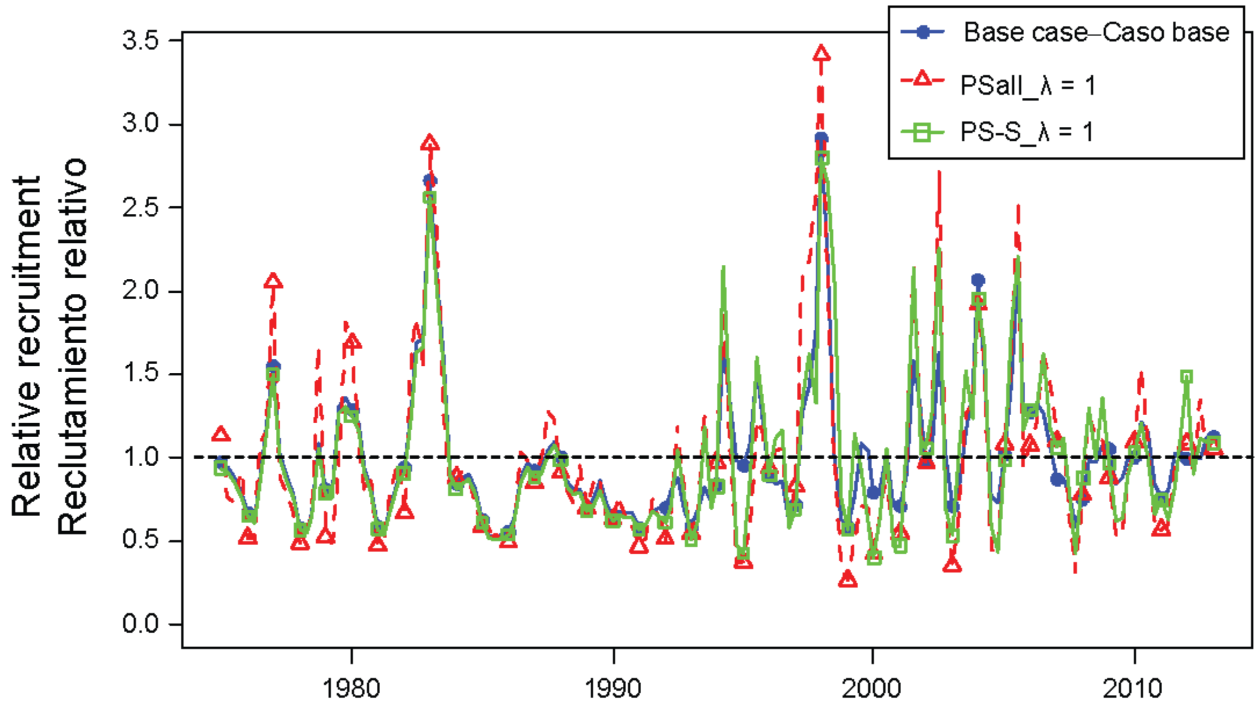

FIGURE C.3b. Comparison of estimates of relative recruitment of bigeye tuna from the base case analysis (blue dots; size composition λ for all fisheries = 0.05) and two sensitivity analyses which up-weight (λ = 1) the size-composition data of all purse-seine fisheries (Fisheries 1-11; red triangles), or the southern purse-seine fishery only (Fishery 2; green squares). t = metric tons.
FIGURA C.3b. Comparación de las estimaciones del reclutamiento relativo de atún patudo del análisis de caso base (puntos azules; λ de composición por talla de todas las pesquerías = 0,05) y de dos análisis de sensibilidad que incrementan la ponderación (λ = 1) de los datos de composición por talla de todas las pesquerías cerqueras (Pesquerías 1-11, triángulos rojos), o de la pesquería cerquera del sur solamente (Pesquería 2; cuadros verdes). t = toneladas métricas.

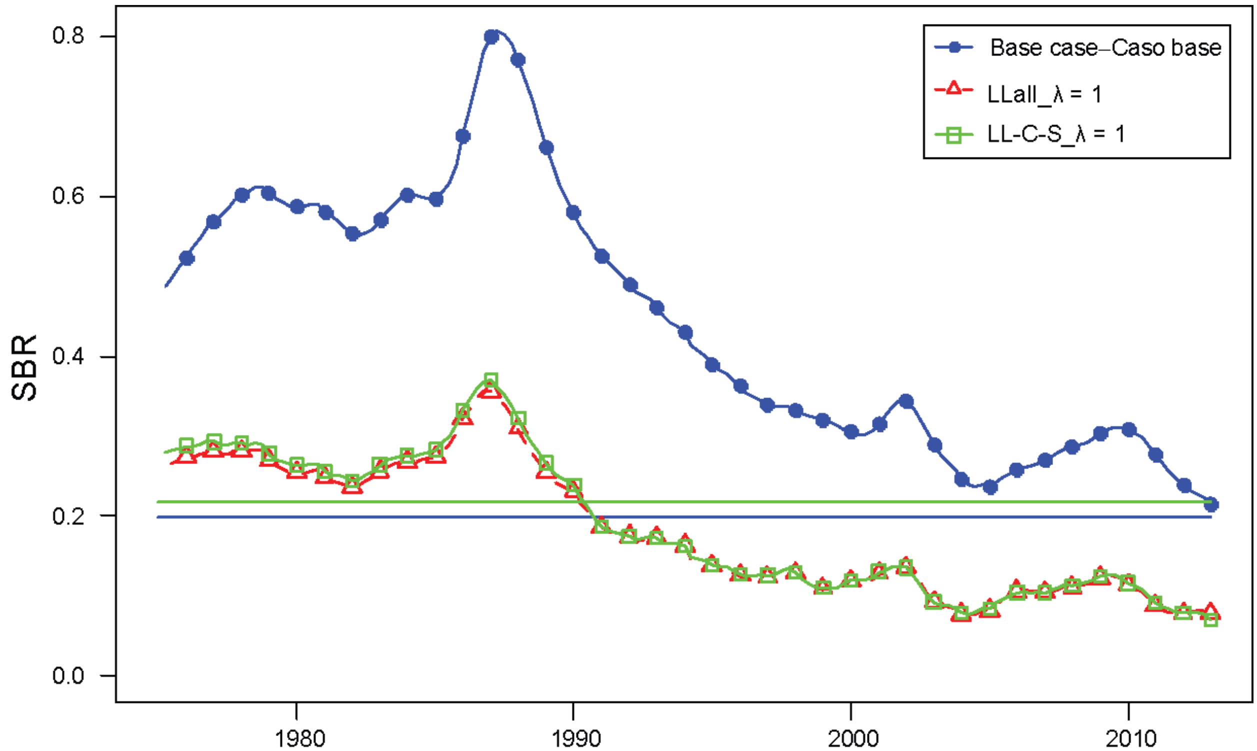

FIGURE C.4a. Comparison of estimates of the spawning biomass ratio (SBR) of bigeye tuna from the base case analysis (blue dots; size composition λ for all fisheries = 0.05) and two sensitivity analyses which up-weight (λ = 1) the size-composition data of all longline fisheries (Fisheries 12-19; red triangles), or the central and southern longline fisheries only (Fisheries 14-17; green squares). t = metric tons.

FIGURA C.4a. Comparación de las estimaciones del cociente de biomasa reproductora (SBR) de atún patudo del análisis de caso base (puntos azules; λ de composición por talla de todas las pesquerías = 0,05) y de dos análisis de sensibilidad que incrementan la ponderación (λ = 1) de los datos de composición por talla de todas las pesquerías palangreras (Pesquerías 12-19, triángulos rojos), o de las pesquerías palangreras central y del sur solamente (Pesquerías 14-17; cuadros verdes). t = toneladas métricas.

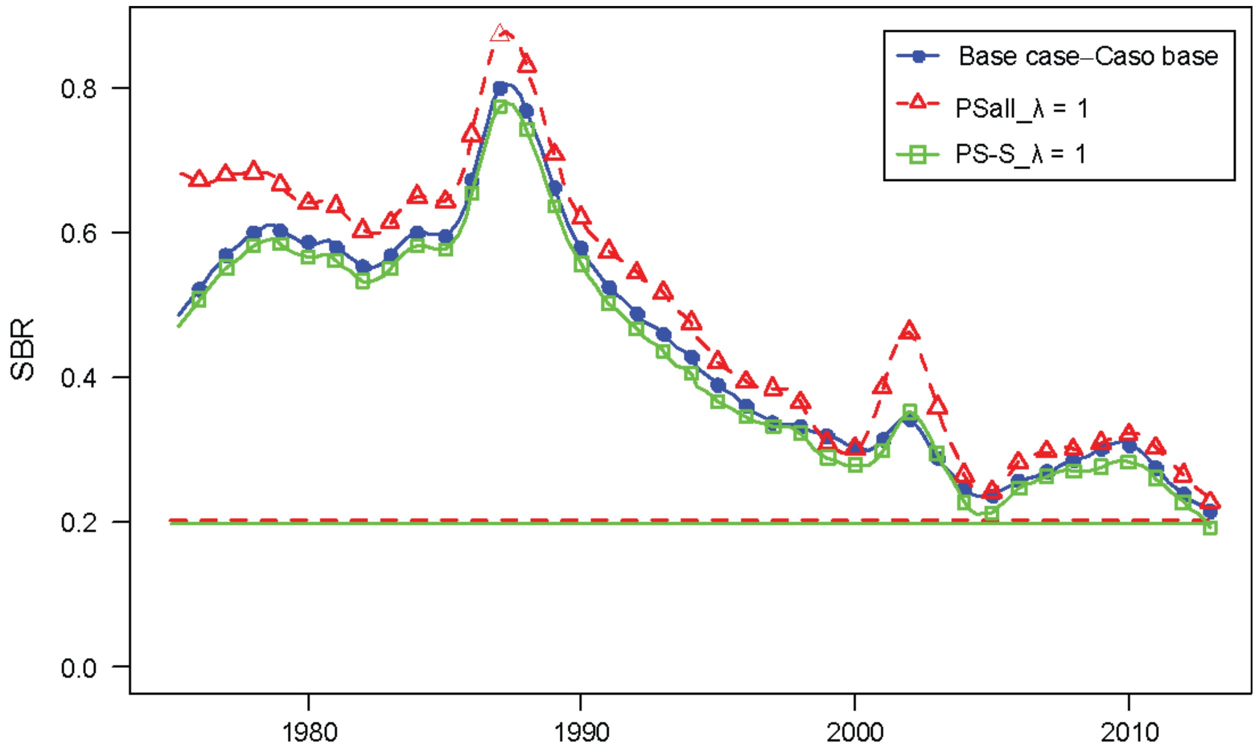

FIGURE C.4b. Comparison of estimates of the spawning biomass ratio (SBR) of bigeye tuna from the base case analysis (blue dots; size composition λ for all fisheries = 0.05) and two sensitivity analyses which up-weight (λ = 1) the size-composition data of all purse-seine fisheries (Fisheries 1-11; red triangles), or the southern purse-seine fishery only (Fishery 2; green squares). t = metric tons.
FIGURA C.4b. Comparación de las estimaciones del cociente de biomasa reproductora (SBR) de atún patudo del análisis de caso base (puntos azules; λ de composición por talla de todas las pesquerías = 0,05) y de dos análisis de sensibilidad que incrementan la ponderación (λ = 1) de los datos de composición por talla de todas las pesquerías cerqueras (Pesquerías 1-11, triángulos rojos), o de la pesquería cerquera del sur solamente (Pesquería 2; cuadros verdes). t = toneladas métricas.

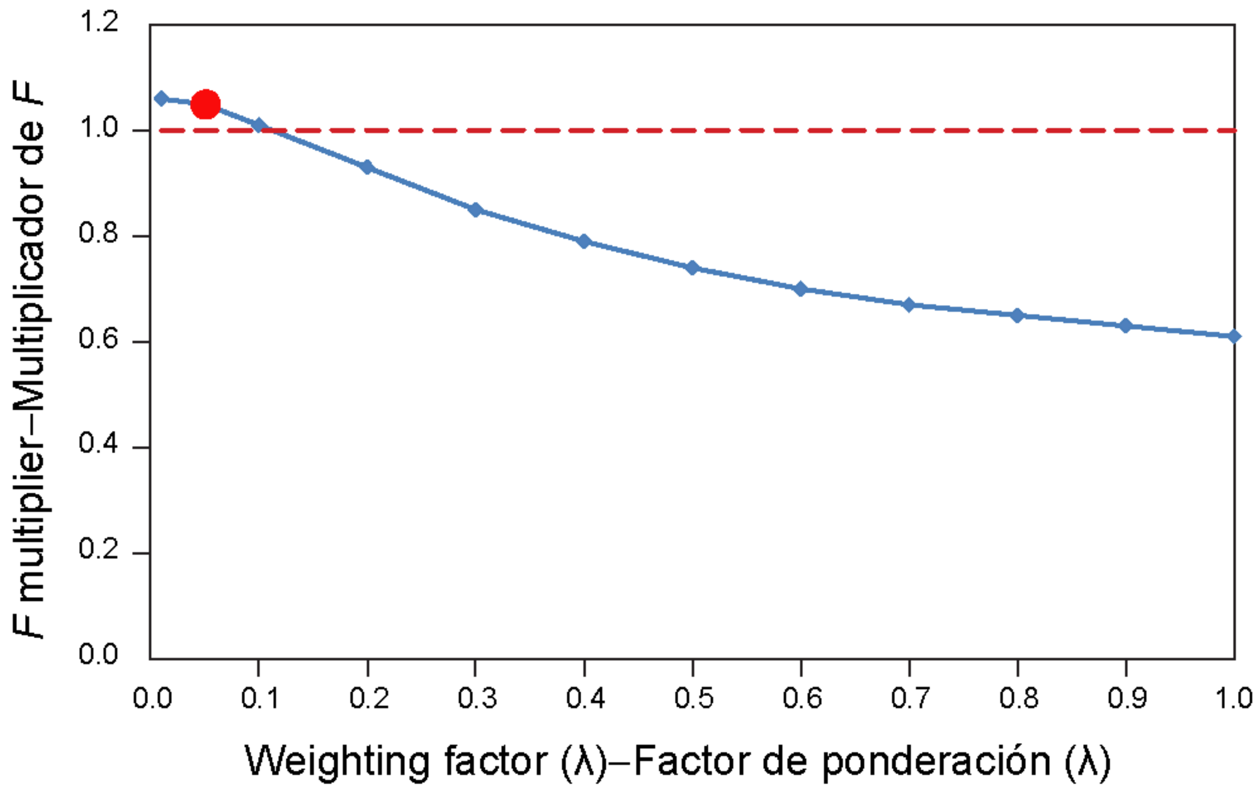

FIGURE C.5. Relationship between the *F* multiplier and different levels (λ) of weighting of the size composition data. The large dot indicates the λ assumed in the base case model (0.05). The horizontal dashed line indicates F_{MSY}.

FIGURA C.5. Relación entre el multiplicador de *F* y distintos niveles (λ) de ponderación de los datos de composición por talla. El punto grande indica el λ supuesto en el modelo de caso base (0.05). La línea de trazos horizontal indica F_{MSY}.

TABLE C.1. Estimates of management-related quantities for bigeye tuna for the base case and for sensitivity analyses to assigning different weighting factors (λ) to the size-composition data for various fisheries (Table 2.1). LL: longline; PS: purse-seine.

TABLA C.1. Estimaciones de cantidades relacionadas con la ordenación del atún patudo del caso base y de los análisis de sensibilidad que asignan distintos factores de ponderación (λ) a los datos de composición por talla de varias pesquerías (Tabla 2.1). LL: palangre; PS: red de cerco; all: todas.

	Base case	**PS-all λ = 0.05**		**LL-all λ = 0.05**	
	All λ = 0.05	**LL-all λ = 1**	**LL 14-17 λ = 1**	**PS-all λ = 1**	**LL 2 λ = 1**
MSY-RMS	106,706	99,124	98,180	97,018	95,334
B_{MSY}- B_{RMS}	418,468	312,484	313,793	409,722	388,362
S_{MSY}- S_{RMS}	105,969	71,818	72,708	106,472	99,877
B_{MSY}/B_0- B_{RMS}/B_0	0.24	0.29	0.29	0.24	0.24
S_{MSY}/S_0- S_{RMS}/S_0	0.20	0.22	0.22	0.20	0.20
C_{recent}/MSY- C_{recent}/RMS	0.97	1.04	1.05	1.06	1.08
B_{recent}/B_{MSY}- B_{recent}/B_{RMS}	1.02	0.47	0.41	1.01	0.86
S_{recent}/S_{MSY}-S_{recent}/S_{RMS}	1.08	0.36	0.32	1.12	0.97
F multiplier- Multiplicador de *F*	1.05	0.54	0.51	0.95	0.85

APPENDIX D: CORRELATION WITH ENVIRONMENTAL VARIABLES

ANEXO D: CORRELACIÓN CON VARIABLES AMBIENTALES

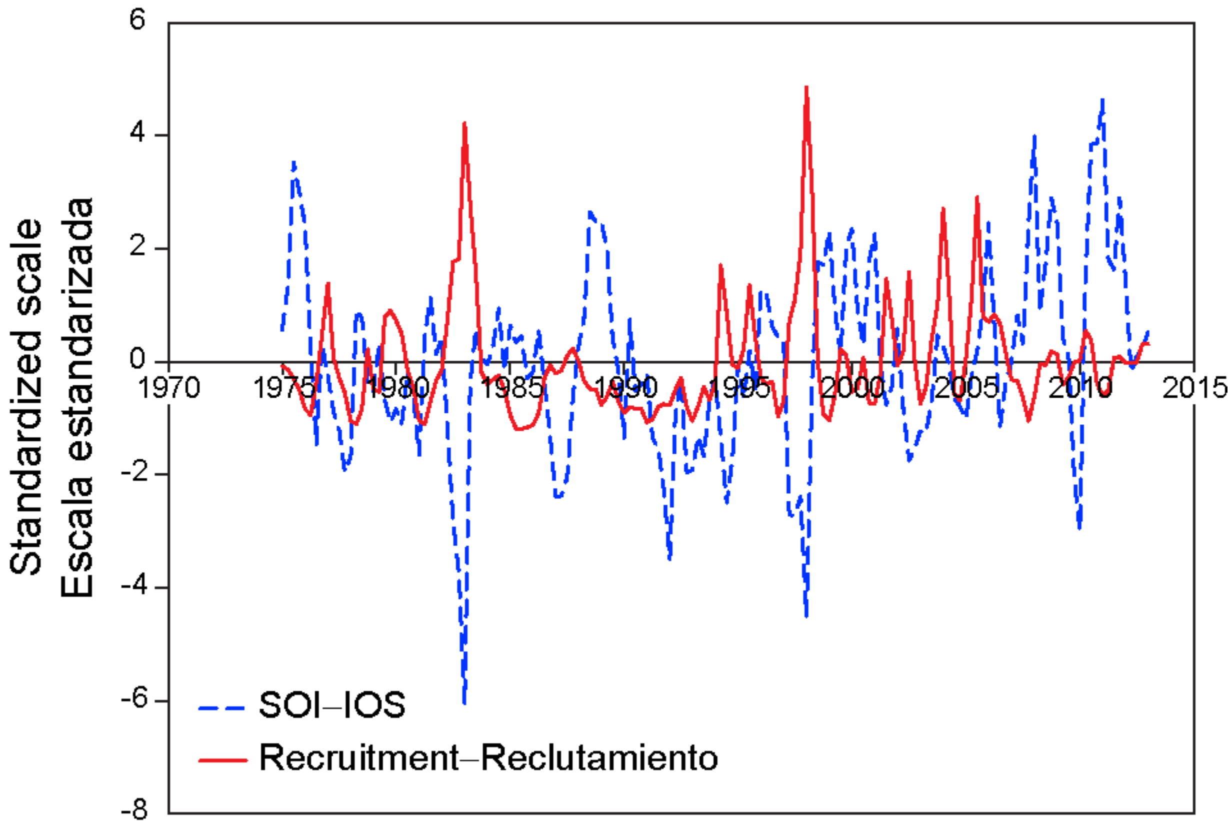

FIGURE D.1. Quarterly time series of bigeye standardized recruitments and the Southern Oscillation Index (SOI).

FIGURA D.1. Series de tiempo trimestrales de reclutamiento estandarizado de patudo y el Índice de Oscilación del Sur (IOS).

APPENDIX E: ADDITIONAL RESULTS FROM THE BASE CASE ASSESSMENT

This appendix contains additional results from the base case assessment of bigeye tuna in the EPO. These results are total fishing mortality rates.

ANEXO E: RESULTADOS ADICIONALES DE LA EVALUACIÓN DEL CASO BASE

Este anexo contiene resultados adicionales de la evaluación de caso base del atún patudo en el OPO. Estos resultados son tasas de mortalidad por pesca total.

TABLE E.1. Average annual fishing mortality rates for bigeye in the EPO for the base case assessment.

TABLA E.1. Tasas medias de mortalidad anual por pesca de patudo en el OPO para la evaluación del caso base.

	Age (quarters) - Edad (trimestres)				
	1-4	**5-8**	**9-12**	**13-19**	**20+**
1975	0.01	0.09	0.08	0.06	0.01
1976	0.01	0.05	0.11	0.09	0.01
1977	0.01	0.04	0.13	0.11	0.02
1978	0.01	0.05	0.15	0.11	0.02
1979	0.01	0.06	0.14	0.11	0.02
1980	0.01	0.05	0.15	0.12	0.02
1981	0.01	0.06	0.13	0.10	0.02
1982	0.01	0.04	0.10	0.09	0.01
1983	0.01	0.03	0.11	0.09	0.01
1984	0.01	0.03	0.10	0.08	0.01
1985	0.00	0.03	0.09	0.08	0.01
1986	0.00	0.03	0.12	0.11	0.02
1987	0.00	0.03	0.14	0.14	0.02
1988	0.00	0.03	0.13	0.13	0.02
1989	0.00	0.03	0.14	0.12	0.02
1990	0.01	0.03	0.13	0.17	0.12
1991	0.01	0.03	0.14	0.19	0.15
1992	0.01	0.03	0.13	0.16	0.12
1993	0.04	0.04	0.13	0.15	0.12
1994	0.15	0.14	0.23	0.19	0.13
1995	0.25	0.24	0.22	0.18	0.11
1996	0.37	0.29	0.24	0.16	0.10
1997	0.37	0.32	0.28	0.16	0.10
1998	0.27	0.27	0.21	0.17	0.12
1999	0.18	0.23	0.20	0.14	0.08
2000	0.33	0.40	0.30	0.17	0.10
2001	0.34	0.31	0.27	0.20	0.15
2002	0.35	0.40	0.35	0.28	0.22
2003	0.31	0.29	0.28	0.23	0.18
2004	0.33	0.33	0.28	0.20	0.14
2005	0.38	0.41	0.27	0.15	0.09
2006	0.41	0.44	0.28	0.15	0.09
2007	0.32	0.35	0.20	0.11	0.08
2008	0.35	0.42	0.28	0.12	0.05
2009	0.48	0.50	0.31	0.14	0.07
2010	0.47	0.47	0.25	0.15	0.10
2011	0.41	0.46	0.28	0.16	0.10
2012	0.49	0.48	0.33	0.17	0.16

REFERENCES—REFERENCIAS

Aires-da-Silva, A. and M.N. Maunder. 2007. Status of bigeye tuna in the eastern Pacific Ocean in 2006 and outlook. Inter-Amer. Trop. Tuna Comm., Stock Assess. Rep. 8: 105-203.

Aires-da-Silva, A. and M.N. Maunder. 2009. Status of bigeye tuna in the eastern Pacific Ocean in 2007 and outlook for the future. Inter-Amer. Trop. Tuna Comm., Stock Assess. Rep. 9: 101-202.

Aires-da-Silva, A. and M.N. Maunder. 2010a. Status of bigeye tuna in the eastern Pacific Ocean in 2009 and outlook for the future. Inter-Amer. Trop. Tuna Comm., Stock Assess. Rep. 10: 116-228.

Aires-da-Silva, A. and M.N. Maunder. 2010b. An evaluation of spatial structure in the stock assessment of bigeye tuna in the eastern Pacific Ocean. Document BET-01-02b, External review of IATTC bigeye tuna assessment. La Jolla, California, USA; 3-7 May 2010.

Aires-da-Silva, A. and M.N. Maunder. 2010c. Sensitivity analysis of bigeye stock assessment to alternative growth assumptions. Document BET-01-03, External review of IATTC bigeye tuna assessment. La Jolla, California, USA; 3-7 May 2010.

Aires-da-Silva, A., M.N. Maunder and C.E. Lennert-Cody. 2010. An investigation of the longline fishery length-frequency residual pattern in the stock assessment of bigeye tuna in the eastern Pacific Ocean. Document BET-01-05, External review of IATTC bigeye tuna assessment. La Jolla, California, USA; 3-7 May 2010.

Aires-da-Silva, A., M.N. Maunder and P.K. Tomlinson. 2010. An investigation of the trend in the estimated recruitment for bigeye tuna in the eastern Pacific Ocean. Document BET-01-06, External review of IATTC bigeye tuna assessment. La Jolla, California, USA; 3-7 May 2010.

Anonymous. 2006. Report of the Albacore Working Group Meeting (November 28-December 2, 2005, La Jolla, CA, U.S.A.)**:** 30 p. (http://isc.ac.affrc.go.jp/isc6/ISC06_Annex%206_ISC- ALBWG _Report_Final.pdf)

Beddington, J.R. and D.B. Taylor. 1973. Optimum age specific harvesting of a population. Biometrics 29: 801-809.

Beverton, R.J.H. and S.J. Holt. 1957. On the dynamics of exploited fish populations. Minis. Agri. Fish. Food Inves., Ser. 2, 19: 533 p.

Bigelow, K., J. Hampton, and N. Miyabe. 2002. Application of a habitat-based model to estimate effective longline fishing effort and relative abundance of Pacific bigeye tuna (*Thunnus obesus*). Fish. Ocean. 11: 143-155.

Clark, W.G. 1991. Groundfish exploitation rates based on life history parameters. Can. J. Fish. Aquat. Sci. 48: 734-750.

Eveson, J. P., Laslett, G. M., and Polacheck, T. 2004. An integrated model for growth incorporating tag-recapture, length-frequency, and direct aging data. Canadian Journal of Fisheries and Aquatic Sciences, 61: 292-306.

Francis, R.I.C.C. 1993. Monte Carlo evaluation of risks for biological reference points used in New Zealand fishery assessments. Can. Spec. Publ. Fish. Aquat. Sci. 120: 221-230.

Francis, R.I.C. 2011. Data weighting in statisitical fisheries stock assessment models. Can. J. Fish. Aquat. Sci. 68: 1124:1138.

Getz, W.M. 1980. The ultimate sustainable yield problem in nonlinear age structured populations. Mathematical Bioscience 48: 279-292.

Hampton J. 2000. Natural mortality rates in tropical tunas: size really does matter. Can. J. Fish. Aquat. Sci. 57: 1002-1010.

Hampton, J. 2002. Stock assessment of bigeye tuna in the western and central Pacific Ocean. Sec. Pacif. Comm., Oceanic Fish. Prog., 15th meeting, Stand. Comm. Tuna Billfish, BET-1: 37 p. (http://www.spc.int/oceanfish/Html/SCTB/SCTB15/BET-1.pdf)

Hampton, J., K. Bigelow, and M. Labelle. 1998. A summary of current information on the biology, fisheries and stock assessment of bigeye tuna (*Thunnus obesus*) in the Pacific Ocean, with recommendations for data requirements and future research. Sec. Pacif. Comm., Oceanic Fish. Prog,, Tech. Rep. 36: 46 p.

Hampton, J. and D.A. Fournier. 2001a. A spatially disaggregated, length-based, age-structured population model of yellowfin tuna (*Thunnus albacares*) in the western and central Pacific Ocean. Mar. Fresh. Res. 52: 937-963.

Hampton, J. and D.A. Fournier. 2001b. A preliminary stock assessment model for bigeye tuna in the Pacific Ocean. Sec. Pacif. Comm., Oceanic Fish. Prog., 14th meeting, Stand. Comm. Tuna Billfish. BET-1: 31 p. (http://www.spc.org.int/OceanFish/Html/SCTB/SCTB14/bet1.pdf)

Hampton, J., P. Kleiber, Y. Takeuchi, H. Kurota, and M. Maunder. 2003. Stock assessment of bigeye tuna in the western and central Pacific Ocean, with comparisons to the entire Pacific Ocean. Sec. Pacif. Comm., Oceanic Fish. Prog., 16th meeting, Stand. Comm. Tuna Billfish, BET-1: 80 p. (http://www.spc.org.int/OceanFish/Html/SCTB/SCTB16/bet1.pdf)

Hampton, J. and M.N. Maunder. 2005. Comparison of Pacific-wide, western and central Pacific, and eastern Pacific assessments of bigeye tuna. WCPFC–SC1 SA WP–2−SUP, 19p. (http://www.spc.int/oceanfish/Html/WCPFC/SC1/pdf/SC1_SA_WP_2_SUP.pdf

Hampton, J. and M.N. Maunder. 2006. An update of Pacific-wide assessment of bigeye tuna with comparisons with eastern Pacific assessment results.(http://www.iattc.org/PDFFiles2/SAR-7-07c.ii-Pacific-wide-BET-assessment.pdf)

Harley, S. J. and M. N. Maunder. 2003. Recommended diagnostics for large statistical stock assessment models. Sec. Pacif. Comm., Oceanic Fish. Prog., 16th meeting, Stand. Comm. Tuna Billfish, MWG-3: 34 p. (http://www.spc.org.int/OceanFish/Html/SCTB/SCTB16/mwg3.pdf)

Harley, S.J. and M.N. Maunder. 2004. Status of bigeye tuna in the eastern Pacific Ocean in 2002 and outlook for 2003. Inter-Amer. Trop. Tuna Comm., Stock Asses. Rep. 4: 120-286.

Harley, S.J. and M.N. Maunder. 2005. Status of bigeye tuna in the eastern Pacific Ocean in 2003 and outlook for 2004. Inter-Amer. Trop. Tuna Comm., Stock Asses. Rep. 5: 168-290.

Hinton, M.G. and H. Nakano. 1996. Standardizing catch and effort statistics using physiological, ecological, or behavioral constraints and environmental data, with an application to blue marlin (*Makaira nigrican*s) catch and effort data from Japanese longline fisheries in the Pacific. Inter-Amer. Trop. Tuna Comm., Bull. 20: 169-200.

Hoyle, S.D. and M.N. Maunder. 2006 Standardization of yellowfin and bigeye CPUE data from Japanese longliners, 1975-2004. IATTC Working Group on Stock Assessments, 7th Meeting, SAR-7-07. (http://www.iattc.org/PDFFiles2/SAR-7-07-LL-CPUE-standardization.pdf)

Kume, S. 1967. Distribution and migration of bigeye tuna in the Pacific Ocean. Rep. Nankai Reg. Fish. Res. Lab. 25: 75-80.

Laslett, G. M., Eveson, J. P., and Polacheck, T. 2002. A flexible maximum likelihood approach for fitting growth curves to tag-recapture data. Canadian Journal of Fisheries and Aquatic Sciences, 59: 976-986.

Langley, A., J. Hampton, P. Kleiber and S. Hoyle. 2008. Stock assessment of bigeye tuna in the western and central Pacific Ocean, including an analysis of management options. WCPFC-SC4-2008/SA-WP-1 Rev.1, Port Moresby, Papua New Guinea, 11−22 August 2008.

Lehodey, P., J. Hampton, and B. Leroy. 1999. Preliminary results on age and growth of bigeye tuna (*Thunnus obesus*) from the western and central Pacific Ocean as indicated by daily growth increments and tagging data. Sec. Pacif. Comm., Oceanic Fish. Prog., 12th meeting, Stand. Comm. Tuna Billfish, BET-2: 18 p. (http://www.spc.org.nc/OceanFish/Html/SCTB/SCTB12/WP/SCTB99_WPBET-2.pdf)

Lennert-Cody, C.E., J.J. Roberts, and R.J. Stephenson. 2008. Effects of gear characteristics on the presence of bigeye tuna (*Thunnus obsesus*) in the catches of the purse-seine fishery of the eastern Pacific Ocean. ICES Jour. Mar. Sci., 65: 970-978.

Lennert-Cody, C.E., M.N. Maunder and A. Aires-da-Silva. 2010. Preliminary analysis of spatial-temporal pattern in bigeye tuna length-frequency distributions and catch-per-unit effort trends. Document BET-01-02a, External review of IATTC bigeye tuna assessment. La Jolla, California, USA; 3-7 May 2010.

Lennert-Cody, C.E. M. N. Maunder, A. Alexandre Aires-da-Silva and M. Minami. 2012. Defining population spatial units: simultaneous analysis of frequency distributions and time series. Fisheries Reseach 139: 85-92.

Mace, P.M. 1994. Relationships between common biological reference points used as thresholds and targets of fisheries management strategies. Can. J. Fish. Aquat. Sci. 51: 110-122.

Matsumoto, T. and W.H. Bayliff. 2008. A review of the Japanese longline fishery for tunas and billfishes in the eastern Pacific Ocean, 1998-2003. Inter-Amer. Trop. Tuna Comm., Bull. 24: 1-187.

Maunder, M.N. 2002a. Status of yellowfin tuna in the eastern Pacific Ocean. Inter-Amer. Trop. Tuna Comm., Stock Assess. Rep. 3: 47-134.

Maunder, M.N. 2002b. The relationship between fishing methods, fisheries management and the estimation of MSY. Fish and Fisheries 3: 251-260.

Maunder, M.N. 2004. Status of yellowfin tuna in the eastern Pacific Ocean in 2002 and outlook for 2003. Inter-Amer. Trop. Tuna Comm., Stock Assess. Rep. 4: 5-119.

Maunder, M.N. (compiler) 2006. Report from the workshop on stock assessment methods, IATTC, La Jolla, California (USA), 7-11 November 2005. (http://www.iattc.org/PDFFiles2/Assessment-methods-WS-Nov05-ReportENG.pdf)

Maunder, M.N. (compiler) 2007. Report from the workshop on management strategies, IATTC, La Jolla, California (USA), 17-20 October 2006. (http://www.iattc.org/PDFFiles2/Management-strategies-WS-Oct-06-ReportENG.pdf)

Maunder, M.N. and A. Aires-da-Silva. 2010. Investigation of catch-per-unit-of-effort data used in the eastern Pacific Ocean bigeye assessment model. Document BET-01-04, External review of IATTC bigeye tuna assessment. La Jolla, California, USA; 3-7 May 2010.

Maunder, M.N., A. Aires-da-Silva, R. Deriso, K. Schaefer, and D. Fuller. 2010. Preliminary estimation of age- and sex-specific natural mortality of bigeye tuna in the eastern Pacific Ocean by applying a cohort analysis with auxiliary information to tagging data. Inter-Amer. Trop. Tuna Comm., Stock Assess. Rep. 10: 253-278.

Maunder, M.N. and Deriso, R.B. (in press) A stock-recruitment model for highly fecund species based on temporal and spatial extent of spawning. Fisheries Research.

Maunder, M.N. and S.J. Harley. 2002. Status of bigeye tuna in the eastern Pacific Ocean in 2001 and outlook for 2002. Inter-Amer. Trop. Tuna Comm., Stock Assess. Rep. 3: 201-311.

Maunder, M. N. and S. J. Harley. 2003. Methodological improvements to the EPO tuna stock assessments. Sec. Pacif. Comm., Oceanic Fish. Prog., 16th meeting, Stand. Comm. Tuna Billfish, MWG-2: 26 p. (http://www.spc.org.int/OceanFish/Html/SCTB/SCTB16/mwg2.pdf)

Maunder M.N., S.J. Harley, and J. Hampton. 2006. Including parameter uncertainty in forward projections of computationally intensive statistical population dynamic models. ICES Jour. Mar. Sci. 63 (6): 969-979.

Maunder M.N. and S.D. Hoyle. 2006. Status of bigeye tuna in the eastern Pacific Ocean in 2004 and outlook for 2005. Inter-Amer. Trop. Tuna Comm., Stock Assess. Rep. 6: 103-206.

Maunder, M.N. and S.D. Hoyle. 2007. Status of bigeye tuna in the eastern Pacific Ocean in 2005 and outlook for 2006. Inter-Amer. Trop. Tuna Comm., Stock Assessment Report, 7: 117-248.

Maunder, M.N. and G.M. Watters. 2001. Status of yellowfin tuna in the eastern Pacific Ocean. Inter-Amer. Trop. Tuna Comm., Stock Assess. Rep. 1: 5-86.

Maunder, M.N. and G.M. Watters. 2003. A-SCALA: an age-structured statistical catch-at-length analysis for assessing tuna stocks in the eastern Pacific Ocean. Inter-Amer. Trop. Tuna Comm., Bull. 22: 433-582.

Methot, R. D. 2005. Technical description of the Stock Synthesis II assessment program. NOAA Fisheries. http://www.sefsc.noaa.gov/sedar/download/S16_AW_04.pdf?id=DOCUMENT

Methot, R. D. 2009. User manual for Stock Synthesis. Model Version 3.04b. NOAA Fisheries.

Methot, R.D., Wetzel, C.R. 2013. Stock synthesis: providing a biological and statistical framework for fishery management forecasts across a data-poor to data-rich continuum. Fish. Res. 142: 86-99.

Nakamura, E.L. and J.H. Uchiyama. 1966. Length-weight relations of Pacific tunas. *In* Manar, T.A. (editor), Proc., Governor's [Hawaii] Conf. Cent. Pacif. Fish. Resources: 197-201.

Okamoto, H. and W.H. Bayliff. 2003. A review of the Japanese longline fishery for tunas and billfishes in the eastern Pacific Ocean, 1993-1997. Inter-Amer. Trop. Tuna Comm., Bull. 22: 219-431.

Philander, S. G. 1990. El Niño, La Niña, and the Southern Oscillation. Academic Press, Inc. 293 pp.Reed, W.J. 1980. Age-specific harvesting in a nonlinear population model. Biometrics 36: 579-593.

Richards, F.J. 1959. A flexible growth function for empirical use. Jour. Exper. Botany, 10: 290-300.

Schaefer, K.M. 2009. Stock structure of bigeye, yellowfin, and skipjack tunas in the eastern Pacific Ocean. Inter-Amer. Trop. Tuna Comm., Stock Assess. Rep. 9. 203-221.

Schaefer, K.M. and D.W. Fuller. 2006. Estimates of age and growth of bigeye tuna (*Thunnus obesus*) in the eastern Pacific Ocean, based on otolith increments and tagging data. Inter-Amer. Trop. Tuna Comm., Bull. 23: 33-76.

Schaefer, K. M., and D. W. Fuller. 2009. Horizontal movements of bigeye tuna (*Thunnus obesus*) in the eastern Pacific Ocean, as determined from conventional and archival tagging experiments initiated during 2000-2005. Inter-Am. Trop. Tuna Comm., Bull., 24: 189-248.

Schaefer, K. M., D. W. Fuller, and B. A. Block. 2009. Vertical movements and habitat utilization of skipjack (*Katsuwonus pelamis*), yellowfin (*Thunnus albacares*), and bigeye (*Thunnus obesus*) tunas in the equatorial eastern Pacific Ocean, ascertained through archival tag data. *In* Nielsen, Jennifer L., Haritz Arrizabalaga, Nuno Fragoso, Alistair Hobday, Molly Lutcavage, and John Sibert (editors), 2009, Tagging and Tracking of Marine Animals with Electronic Devices. Springer: 121-144.

Schaefer, K.M., D.W. Fuller, and N. Miyabe. 2005. Reproductive biology of bigeye tuna (*Thunnus obesus*) in the eastern and central Pacific Ocean. Inter-Amer. Trop. Tuna Comm., Bull. 23: 1-32.

Schnute, J. 1981. A versatile growth-model with statistically stable parameters. Canadian Journal of Fisheries and Aquatic Sciences, 38: 1128-1140.

Stocker, M. (editor). 2005. Report of the Ninteenth North Pacific Albacore Workshop. Nanaimo, B.C. Canada, Pacific Biological Station, Nanaimo, B.C.: 127 p. (http://www.dfompo.gc.ca/Library/315833.pdf)

Suda, A. and S. Kume. 1967. Survival and recruitment of bigeye tuna in the Pacific Ocean, estimated by the data of tuna longline catch. Nankai Reg. Fish. Res. Lab, Rep. 25: 91-104.

Sun, C, C. Huang, and S. Yeh. 2001. Age and growth of the bigeye tuna, *Thunnus obesus*, in the western Pacific Ocean. Fish. Bull. 99: 502-509.

Thompson, G.G. 1993. A proposal for a threshold stock size and maximum fishing mortality rate. Can. Spec. Publ. Fish. Aquat. Sci. 120: 303-320.

Tomlinson, P. 2002. Progress on sampling the eastern Pacific Ocean tuna catch for species composition and length-frequency distributions. Inter-Amer. Trop. Tuna Comm., Stock Assess. Rep. 2: 339-365.

von Bertalanffy, L. 1938. A quantitative theory of organic growth. Human Biology, 19(2):181-213.

Wang, S-P., M. Maunder and A. Aires-da-Silva. 2009. Implications of model and data assumptions: an illustration including data for the Taiwanese longline fishery into the eastern Pacific Ocean bigeye tuna (*Thunnus obesus*). Fish. Res. 99 (1-2): 118-126.

Watters, G.M. 1999. Geographical distributions of effort and catches of tunas by purse-seine vessels in the eastern Pacific Ocean. Inter-Amer. Trop. Tuna Comm., Data Rep. 10: 100 p.

Watters, G.M. and R. Deriso. 2000. Catch per unit of effort of bigeye tuna: a new analysis with regression trees and simulated annealing. Inter-Amer. Trop. Tuna Comm., Bull. 21: 527-571.

Watters, G.M. and M.N. Maunder. 2001. Status of bigeye tuna in the eastern Pacific Ocean. Inter-Amer. Trop. Tuna Comm., Stock Assess. Rep. 1: 109-210.

Watters, G.M. and M.N. Maunder. 2002. Status of bigeye tuna in the eastern Pacific Ocean. Inter-Amer. Trop. Tuna Comm., Stock Assess. Rep. 2: 147-246.

Zhou, J., Chen, Y., Dai, X., Harley, S.J., Hoyle, S.D., Maunder, M.N. and Aires-da-Silva, A. 2012. Implications of uncertainty in the spawner-recrtuiment relationship for fisheries management: An illustration using bigeye tuna (Thunnus obesus) in the eastern Pacific Ocean. Fisheries Research 119-120: 89-93.